Fate, accumulation and impact of metallic nanomaterials in the terrestrial environment

Wu, J.

Fate, accumulation and impact of metallic nanomaterials in the terrestrial environment

Juan Wu

Fate, accumulation and impact of metallic nanomaterials in the terrestrial environment

PhD Thesis at Leiden University, The Netherlands

The research described in this thesis was conducted at the Institute of Environmental Sciences (CML), Leiden University, the Netherlands.

ISBN: 978-90-5191-998-1

Cover design: Juan Wu

Photograph: Juan Wu

Printing: GVO printers & designers B.V., Ede, The Netherlands

Fate, accumulation and impact of metallic nanomaterials in the terrestrial environment

Proefschrift

ter verkrijging van

de graad van doctor aan de Universiteit Leiden,

op gezag van rector magnificus prof.dr.ir. H. Bijl,

volgens besluit van het college voor promoties

te verdedigen op donderdag 16 december 2021

klokke 10.00 uur

door

Juan Wu

Geboren te Yingtan city, Jiangxi province, China

In 1991

Promotoren: Prof.dr.ir. W.J.G.M. Peijnenburg

Prof.dr.ing. M.G. Vijver

Copromotor: Dr.ir. T. Bosker

Promotiecommissie:

Prof.dr. A. Tukker (Universiteit Leiden) - Voorzitter

Prof.dr. N.J. de Voogd (Universiteit Leiden) – Secretaris

Overige commissieleden:

Prof. dr. ir. C.A.M. van Gestel (Vrije Universiteit Amsterdam)

Dr. Y. Zhai (Technical Universiteit Delft)

Prof.dr. S.A. Bonnet (Universiteit Leiden)

Dr. K.B. Trimbos (Universiteit Leiden)

Contents

Leiden, The Netherlands, 2017

Chapter 1

General Introduction

1.1 State of science of nanomaterials

The concept of nanotechnology was initiated by Richard P. Feynman in the lecture entitled "There's Plenty of Room at the Bottom" in 1959[1,2], whereas the term "nanotechnology" was firstly created by Norio Taniguchi in 1974[3,4]. Over the years, nanotechnology has emerged as a cutting-edge field of science with the potential to revolutionize the technology of the 21st century as it enables design, characterization and production of devices or materials at a nanometer scale. Nanotechnology is generally defined as "a science, engineering, and technology conducted at the nanoscale (1 to 100 nm in at least one dimension)[5]. In the last decades, a large number of research projects in the field of nanoscience and nanotechnology were funded by both industry and government over the world[6], which makes nanotechnology become one of the most rapidly growing markets worldwide. Already, nanotechnology is changing the world in many ways and is applied in almost every field of science and household products[7]. The latest data reported that there are more than 5,169 nano-related products in the worldwide market[8] and the estimated global market of nanotechnology will exceed US$ 125 billion by 2024[9].

The rapid development of nanotechnology extends the production and application of manufactured nanomaterials. The definition of nanomaterial according to European Commission Regulation (2011/696/EU) is "A natural, incidental or manufactured material containing particles, in an unbound state or as an aggregate or as an agglomerate and where, for 50 % or more of the particles in the number size distribution, one or more external dimensions is in the size range 1–100 nm". With the advancement of nanotechnology, nanomaterials/nanoproducts have experienced several generations. The first generation of nanomaterials (2000-2005) usually refers to "passive nanostructures" that comprise relatively simple carbon-based and inorganic materials[10,11,12]. These particles were used in products such as automobile tires (carbon and silica), cement (calcium silicate hydrate nanoplatelets), sunscreen (titanium dioxide) and antibacterial textiles (silver)[11,12]. From 2005 to 2010, the second generation of active nanomaterials appeared on the market. These materials were characterized by nanoscale elements that serve as the functional ingredient in electronics, sensors and medicines et al[10,11,12]. Examples of use are gold-silica

nanoparticles for cancer treatment, silver nanowires for the transparent conductive film of displays, surface-functionalized superparamagnetic iron oxide nanoparticles for the treatment of iron deficiency anemia in adult chronic kidney disease patients and brain tumors, and as contrast agents in magnetic resonance imaging[12]. The third generation of nanomaterials (2010-2020) are constructed multifunctional nanosystems, in which the integration between organic and inorganic nanomaterials was increased. These combined nanomaterials/nanodevices were integrated into other systems[10,11,12]. They can assemble or disassemble themselves, to some extent, to react to the environment[11]. For example, the third generation of nanomaterials has been developed to deliver drugs to a targeted pharmacological site, thus reducing the amounts of the drug and potential adverse side effects[11]. From 2020 onwards, the fourth generation of nanomaterials intends to build up molecular nanosystems that allow each nanomolecule in the system to have a specific structure and function[10,11,12].

The nanoscale size can transfer the classical physics to quantum effects in nanoparticles (NPs)[6], and as a result NPs exhibit novel and unique properties, as compared to the individual molecules or their bulk counterpart. These include a high surface area to volume ratio, high chemical and catalytic properties, extraordinary electrical, optical, thermal and magnetic properties, easy functionalization et al.[2,13,14]. These properties make that NPs are applied in a large number of fields, in particular cosmetics, textiles, electronics, energy, environment, agriculture, biology, pharmacy, healthcare and medicine[7,13,15] (**Figure 1.1**). Among numerous NPs which have been produced, metals (e.g. silver, copper) and metal oxides (e.g. titanium dioxide, zinc oxide) are produced most commonly for diverse applications. These NPs have been categorized as metal-based NPs. With the increase in the manufacture and use of metal-based NPs, there is the likelihood of increased emissions of metal-based NPs to the environment[14,16,17]. As a result, the metal-based NPs have been detected in a range of environments, including air, surface water, sediments, sludge and soil. Therefore there is a great necessity to improve the understanding of the impacts and potential risks of metallic NPs to the environment. In this thesis, I focus on the potential environmental risk of the most widely utilized metallic nanoparticles (NPs): silver nanoparticles (AgNPs) and titanium dioxide nanoparticles (TiO_2NPs)[18,19]. The particles are of the 1st generation NPs and have an estimated global annual

production of 135-420 and 60,000-150,000 tons, respectively[20].

1.2 The application of nanomaterials in agriculture

Recent research has claimed that nanotechnology can potentially revolutionize the agriculture sector by producing a variety of nano-agrochemicals and nanosensors to enhance crop productivity and quality[21]. To date, metallic NPs such as CaNPs, MgNPs, ZnONPs, ZnNPs, CuNPs, Magnetite (Fe_2O_3)NPs and manganese zinc ferrite NPs have been applied as nanofertilizers[21]. These nanofertilizers can improve the accessibility of nutrients to the plant parts, prevent the loss of nutrients, and enhance the fertility of soil. Additionally, the application of metallic NPs with antimicrobial and insecticidal properties such as ZnONPs, AgNPs, CuNPs, TiO_2NPs and Al_2O_3NPs as nanopesticides against pests and plant pathogens has been documented[15,21]. These nanoparticles can work as the active ingredients of pesticides or as a carrier for targeted pesticides delivery. Compared to traditional agrochemicals, nano-agrochemicals can significantly increase their efficiency and reduce the application dose, which is good for sustainable agriculture[15,21]. However, the ecological and environmental risks associated with these new nano-agrochemicals must be carefully addressed before their wide applications.

1.3 Current understanding of nanoecotoxicology and risk assessment of nanomaterials

1.3.1 The development of nanotoxicology

The expected increase in emissions of nanomaterials into the environment will enhance the interactions between NPs and organisms, and this will possibly lead to unknown biological effects. This encouraged global scientific and governmental attention on assessing the safety of manufactured nanomaterials, resulting in the rapid development of the discipline of nanoecotoxicology. Nanoecotoxicology, a sub-discipline of ecotoxicology, is emerged to address the toxic effects of nano-scaled substances on organisms and the constituents of ecosystems[22]. Nanoecotoxicology aims to identify and predict the behavior, fate and adverse effects of NPs in/on the ecosystems, and hence to provide data and knowledge about making regulations on nanosafety. Three basic strategies for evaluating the toxicity of NPs have been

proposed by Oberdörster et al.: (1) physicochemical characterization (size, surface area, shape, solubility, aggregation), (2) elucidation of the biological effects from *in vitro* studies, (3) confirmation of the effects through *in vivo* studies[23]. Based on these strategies, nanotoxicity tests have been performed using a range of aquatic and terrestrial organisms[14,24]. Generally, negative impacts of NPs on bacteria have been reported. These impacts include cell membrane damage, inhibition of bacterial growth and biomass, alterations of bacterial community composition, structure and functions[25,26]. The impacts of NPs on the survival, growth and reproduction of animals have been widely reported[27,28]. Adverse responses on plants induced by NPs include the inhibition of seed germination and plant growth, reduction of biomass, and alterations in the photosynthesis of plants[14,29]. Nowadays, investigations of the impacts of NPs on organisms are extenuatingly moving to the scale from the single laboratory-reared species to the natural communities. For example, microcosm studies of AgNPs and TiO_2NPs have been widely assessed to impact on soil microbial communities[30]; Geitner et al.[31] investigated the impact of the size of cerium oxide (CeO_2) NPs on their uptake, transport and distribution in a wetland mesocosm. The adverse effects of NPs are determined by a variety of parameters such as the physicochemical properties of NPs, the dynamic behaviour of NPs in the exposure medium, and the exposure route and dosage. Any modification of these parameters might change the biological fate of NPs, resulting in the risks of NPs being assessable only on a case-by-case basis[32]. Therefore, the full-scale understanding of the ecotoxicity of NPs is still a challenging task for environmental and ecotoxicological scientists. Evaluation of the characteristics and the fate of NPs in complex matrixes such as soil and organisms and the combined effects of different NPs in aquatic and terrestrial (eco)systems, are the major subject of ongoing research in the field of nanoecotoxicology[33]. Moreover, research into the bioavailability, fate and mechanisms of action of NPs in organisms are largely lagging behind the knowledge about their observed adverse effects on organisms. Further, the trophic transfer of NPs within some simple aquatic and microbial food chains has been reported, but there is little known about the potential bioaccumulation and biomagnification of NPs in complex terrestrial food chains[34]. These gaps call for more efforts on the ecotoxicity studies of NPs.

1.3.2 The toxicity mechanisms of metallic nanoparticles

Oxidative damage is the most frequently suggested pathway for many adverse effects induced by NPs. The physical interaction between living organisms and NPs can induce the generation of excess reactive oxygen species inside organisms, which can cause lipid peroxidation, cell membrane damage, cell structure alteration, protein and DNA damage, and inhibit the growth of organisms[35,33]. Moreover, the formation of biologically active NPs-protein corona complexes is also considered as a possible mechanism for the toxicity of NPs[36]. Once NPs are in contact with protein-containing biological fluids like plasma, the NPs–protein corona complexes will be formed on the surface of NPs[36]. This can govern the fate and functions of NPs in an organism as the NPs–protein corona complexes rather than the "bare" NPs are 'seen' as the effective unit by cells in the cell–nanoparticle interactions processes[36,37]. Additionally, the accumulation and internalization of NPs in organisms has been suggested as the major determinant driving their toxicological effects[38]. The cellular uptake of NPs can occur by means of attachment of the NPs to cell membranes or clog the pores and barriers of cells wall/membranes, thereby causing mechanical damage and inhibiting nutrient uptake and transport[35,38].

1.3.3 Regulations and policies of nanosafety

Undoubtedly, the environmental risk assessment of NPs is a worldwide issue, and therefore global efforts have been taken in assessing nanosafety. For example, the EU incorporated the risk assessment of NPs into the generic EU-policies such as the REACH (Registration, Evaluation, Authorisation and Restriction of Chemicals) and the CLP (Classification, Labelling and Packaging) regulations[11]. Further, the European Commission is funding numerous research projects about the potential impacts of NPs and NPs-containing products on environmental health[11]. Similar, in the United States, the Environmental Protection Agency (EPA) administered a special regulation for NPs in the Toxic Substances Control Act (TSCA) and created the US National Nanotechnology Initiative (NNI)[39]. As the biggest developing country, China also takes many actions in nanosafety assessment. For instance, some regulations related to nanosafety have been created by China, such as Occupational risk management applied to engineered nanomaterials (GB/T 38091.2-2019),

Nanomaterial risk evaluation (GB/T 37129-2018), Guidance on toxicological screening methods for nanomaterials (GB/Z 39262-2020). Also, the National Natural Science Foundation of China (NSFC) has launched numerous research projects with aims ranging from the methodology of NPs characterization, assessment of the hazards of NPs to the environment and to human beings, to recommendations regarding the regulation of nanosafety to the Chinese government. China has founded many institutions that are dedicated to fundamental and applied researches in the field of nanoscience and technology, such as "The National Center for Nanoscience and Technology" and the "Key Laboratory for Biomedical Effects of Nanomaterials and Nanosafety, Chinese Academy of Sciences (CAS)". Global financial support in nanosafety speeds up the development of the risk assessment of NPs. Generally, the current existing frameworks and tools for risk assessment of NPs are modified from the risk assessment paradigm for chemicals (**Figure 1.1**)[40]. Basically, the risk assessment of chemicals is composed of a four-step workflow including problem formulation, exposure assessment, hazard assessment and identification, and risk characterization[40]. The MARINA risk assessment framework is for instance suggested as a flexible approach for efficient information collection and risk assessment of NPs[41]. This framework is composed of two phases: phase 1 is the problem framing with the specific goal to identify relevant exposure scenarios throughout the life cycle of NPs; phase 2 is the iterative risk assessment, consisting of four steps[11,41]. The four steps of phase 2 are risk characterization, defining data needs, data gathering, and data evaluation[11,41]. Risk assessment of NPs can help policymakers and managers to make regulations about managing the safe production and use of NPs in the industry by integrating risk considerations with scientific and socioeconomic information.

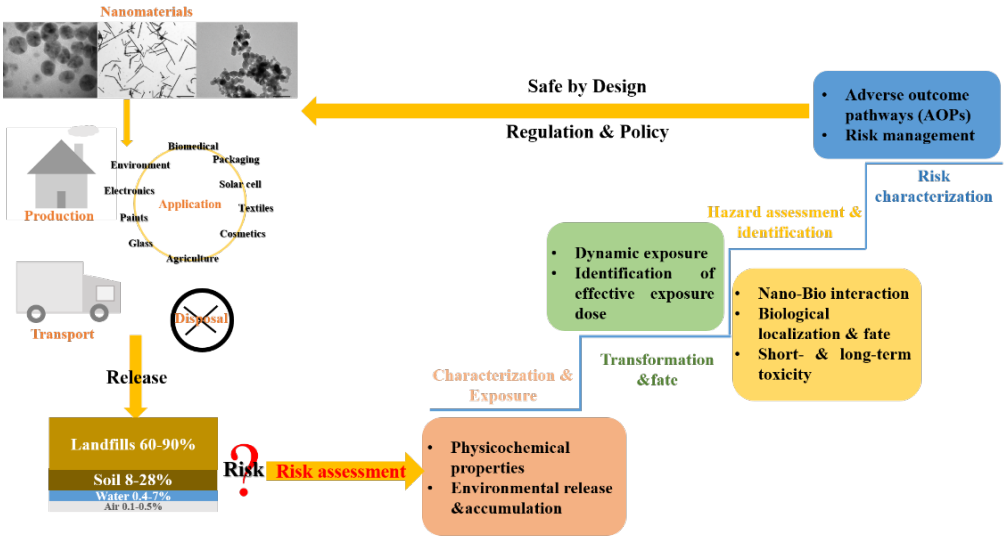

Figure 1.1 Schematic diagram showing the applications and emissions of NPs in environment and risk assessment paradigm for NPs.

1.4 The fate of metallic nanoparticles in the terrestrial environment

The release of metallic nanoparticles into the environment can occur intentionally or unintentionally throughout the lifespan of NPs-containing products, during synthesis, production, transport, usage and disposal[19,42,43,44] (**Figure 1.1**). A large part of the released NPs is excepted to end up and accumulate in soil [45]. NPs can be introduced into soil directly by the application of NPs for soil remediation and the application of nano-agrochemicals such as nano-pesticides, nano-fertilizers and nano-amendments to agricultural fields[46,47,48,30]. In addition, the discharge of sewage or biosolids from wastewater treatments to soil and the runoff from nano-agrochemicals are important indirect major pathways for NPs to enter soil[42,30,49,50]. It is still a challenging task to quantify the concentrations of metallic NPs in soil due to analytical limitations. Several studies have predicted the concentrations of NPs in the environmental compartments using mathematical modeling. The concentration of TiO_2NPs and AgNPs in soil has been estimated to be in the range of 1-10 μg/kg and 0.01-0.1μg/kg[51]. Sun et al.[52] predicted that the concentration of TiO_2NPs and AgNPs increases in the range of 0.09-0.24 μg/kg/y and 0.9-1.8 ng/kg/y for natural and urban

soil, and 940-3600 μg/kg/y and 0.09-0.65 μg/kg/y for sludge treated soil. Given the growing commercial applications of these nanoparticles and hence increasing emission of NPs into the soil, there is an emergent need to evaluate their fate, ecotoxicity and environmental risks in soil.

After being released into soil, NPs will undergo a series of transformation processes including physical, chemical and biological transformations[49,53,24,54] (**Figure 1.2**). Physical transformations of NPs usually refer to their aggregation, agglomeration, sedimentation in soil, and ad/de-sorption to/from the soil matrix[11]. Dissolution, oxidation, sulfidation, chlorination, precipitation and changes of surface properties are the main chemical transformations of NPs in soil[11]. Biological transformations are the processes mediated by the interaction with organisms, such as biological oxidation, complexation with the exudates/excretes by organisms to form a new surface coating[11]. These transformation processes of NPs in soils can be affected by both environmental conditions such as soil pH, the content of soil organic matter, and the intrinsic physicochemical properties of NPs including size, shape, surface charge and coating[17,24,55]. The dynamic transformations of NPs in soil may alter their behavior, fate, bioavailability, and hence their cellular uptake and toxicity on organisms[17,24]. For instance, the dissolution of the soluble metallic NPs (e.g. AgNPs, CuNPs, CuONPs and ZnONPs) plays a vital role in governing the toxicological effects. When exposed to soluble NPs, both the particulate form and the metal ions released from the NPs may contribute to the overall toxicity as the tested organisms always interact with both of them. But whether the nanoparticles themselves or the released metal ions dominate the observed toxicity of soluble metallic NPs is still under investigation and can differ between species and type of NPs. For example, the dominant role or sole role of dissolved ions to the toxicity have been reported for AgNPs in maize (*Zea mays*)[56], Onion (*Allium cepa*), alga *Chlamydomonas reinhardtii*[29] and *Euglena gracilis*[57,58], and bacteria *Escherichia coli*[59], CuONPs in wheat (*Triticum aestivum L.*)[60] and ZnONPs in maize (*Zea mays L.*) and cabbage (*Brassica oleracea var. capitata L.*)[56]. In contrast, particle-dominant toxicity has also been reported for AgNPs in *Lolium multiflorum*[61], ZnONPs in *Scenedesmus obliquus*[28] and CeO_2NPs in *Arabidopsis thaliana*[62]. The inconsistent results require more effort in exploring the relative contribution of particulate and ionic forms to the overall

toxicity of metallic NPs. The relative contribution of particulate and ionic forms of NPs suspensions to the overall toxicity of the suspension of the NPs, is most likely attributable to the fate of the particles in the exposure medium and the processes occurring at the exposure – bio interface. It hence is crucial to determine both fate as well as responses of NPs in organisms when performing exposure experiments.

Similarly, the processes of aggregation/agglomeration and sedimentation also play the main role in affecting the state of NPs in the dispersion medium and hence impact the bioavailability and toxicity of NPs to biota[63]. Based on the classic Derjaguin-Landau-Verwey-Overbeek (DLVO) theory, the aggregation of NPs occurs once the electrostatic repulsive forces were lower than the van der Waals attractive forces between particles[64]. Aggregation of NPs in exposure medium results in larger size of NPs and affects the sedimentation rate of NPs. Both of the aggregation and sedimentation processes may ultimately lead to the changes of the effective exposure dose and uptake rates of NPs, and hence affect the biological impacts of NPs[65]. Several studies have reported that the size of NPs agglomerates instead of the primary size of NPs plays the predominant role in the cytotoxic of NPs[66,67]. Therefore, it is critical to consider the dynamic transformations of NPs into their environmental risk assessment, which enables to more accurately capture the actual effective exposure of organisms to NPs and offer a better and more comprehensive assessment of their impacts on the ecosystem and environment.

1.5 Consideration of factors affecting the impacts of nanoparticles on biota

In addition to the impacts of the dynamic transformations (dissolution aggregation and sedimentation) of NPs on their toxicity, the physicochemical characteristics of the NPs and the exposure duration may influence the responses of organisms to NP . Further, it should be pointed out that the NPs co-exist with numerous pollutants including other nanoparticles once they entered the environment. This may result in modulation of the effects of individual NPs. The observed toxicity of NPs is the outcome of the combined effects exerted by the characteristics of NPs, the exposure route, the dynamic behavior of NPs in the exposure medium, and the intrinsic toxicity of the NPs (**Figure 1.2**). In this section, how these factors can affect the

impacts of NPs on biota will be documented.

1.5.1 Physicochemical characteristics of nanoparticles

The physicochemical properties of NPs including shape, size and coating are crucial factors influencing their impacts on organisms. The size of NPs is one of the determinant factors affecting the uptake, translocation and phytotoxicity in organisms as the barriers that inhibited the entrance of NPs into organisms have a certain size-exclusion limit[68,55,69]. This size-exclusion limit results in the plants being inclined to take up NPs with smaller sizes[55,69] and hence induce higher phytotoxicity. For example, AuNPs with a size of 3.5 nm can be taken up by tobacco, whereas AuNPs with an average diameter of 18 nm remained on the outer surfaces of the root of tobacco plants[70]. Smaller sizes NPs were found to be more phytotoxic as exemplified for AgNPs in *Allium Cepa*[71], *Spirodela Polyrhiza*[72] and Arabidopsis[73], ZnONPs in broad bean (*Vicia faba*)[74], maize (*Zea mays*)[75], Chinese cabbage (*Brassica rapa var. pekinensis*)[76] and CuONPs in soybean (*Glycine max cv. Kowsar*)[77]. However, contradictory results about the impacts of size on plants have been reported, such as size-independent toxicity[78] or larger size inducing more intense adverse effects[79,80]. The inconsistent results suggest that the impacts of NPs on organisms are not only related to their size.

Next to the size, the surface modification of NPs, for example by using citrate, tannic acid, or polyvinyl alcohol (PVP) as coating, can affect their impacts on organisms[55,69]. These coatings can change the toxicity of NPs by affecting their dispersion, stability and agglomeration of NPs in the exposure medium[55,69]. For example, Navarro et al.[29] comprehensively assessed the effects of nine different coated AgNPs on the photosynthesis of the algae *Chlamydomonas reinhardtii* and demonstrated that the role of different coatings in affecting the toxicity of AgNPs to algae was related to their complexation with the released Ag ions. Similarly, the stability, uptake, translocation and biological responses of soybean to cadmium sulfide quantum dots were also found to be dependent on their surface coatings[81]. Nevertheless, no generic coating-dependent impact of NPs can be concluded. Reports of coated NPs inducing comparable, lower or higher toxicity than uncoated NPs have been published[82,81,83]. How the coatings change the interactions between NPs and biota and the associated

(eco)toxicological effects depends also on the other physicochemical properties of the NPs and on the testing conditions. Therefore, investigating the joint effects of coating and other characteristics of NPs is important in order to comprehensive understand their bioavailability and toxicity on biota.

In addition to the size- and coating-dependent toxicity of NPs, the shape-dependent impacts of NPs on organisms have also been investigated. For example, shape-dependent transformation and translocation of CeO_2NPs in Cucumber plants have been demonstrated[84]. To date, Ag nanospheres have been reported to induce higher toxicity in Arabidopsis plants[73], ryegrass *Lolium multiflorum*[85,86], alga *Raphidocelis subcapitata*[87,88] as compared to other shapes, including triangular, decahedral, nanocubes, and nanowires composed of Ag. However, some contradictory results about the shape-dependent toxicity have been obtained as well. For instance, Ag nanoplates and Ag nanowires were found to be more toxic to the algae *Chlorococcum infusionum* as compared to Ag nanospheres[89], and no obvious shape-related impacts of AgNPs were observed on bacteria (E*shericlia coli*[59], *Bacillus cereus*, and *Pseudomonas aeruginosa*) after exposure to Ag nanospheres, Ag nanowires and Ag nanocubes[86]. These results indicate that the test species plays an important role in affecting the shape-dependent impacts of NPs. Even though the results regarding the effects of physicochemical characteristics of NPs on their bioavailability and toxicity are growing, the picture of the ecotoxicity of NPs is still far from clear. This thesis compared the uptake, translocation and phytotoxicity of Ag nanospheres and Ag nanowires in lettuce, and investigated how the joint effects of size, length and coating of Ag nanowires influence the uptake and phytotoxicity of nanowires in plants.

1.5.2 Long-term exposure

The impacts of NPs on organisms are highly related to the variability of exposure time. For example, Ag_2SNPs had no adverse effects on cowpea (*Vigna unguiculata L.* Walp.) and wheat (*Triticum aestivum* L.) during 24h exposure, but reduced the root biomass of these plants by more than 30 % after 2 weeks of exposure[90]. Zhai et al.[91] also observed that the soil bacterial composition was significantly altered by TiO_2NPs after exposure of 1 and 60 days, but no obvious shifts were observed after 15 days of exposure. Similarly, the impacts of NPs on plants and soil microbes vary over time

have been reported for CuNPs[92], CuONPs[93,94], ZnONPs[93,95,96,97], AgNPs[92,98], and Fe_2O_3[99]. These results highlight that assessing the toxicity of NPs using a single timepoint should be done with caution and short-term assessment may not fully reveal the potential toxicity of NPs. Ecotoxicological study of NPs over a longer exposure period is needed. Additionally, the dynamics of both exposure and biological responses should be considered for a better understanding of the interactions between NPs and biota. Therefore, this thesis investigated the long-term impacts of AgNPs on plants and the soil bacterial community with a series of different exposure times.

1.5.3 Co-existing contaminants

Importantly, after entering the environment, NPs inevitably come to contact with other contaminants, including NPs of different composition and/or of different morphology that are also present in the environment. Therefore, in the natural environment, biota are rarely exposed to single NPs but rather to a mixture of NPs. The interactions between different NPs can influence their bioavailability and toxicity to biota by forming NPs-NPs complexes through electrostatic interaction and/or surface complexation/adsorption[100,101,102], and/or by affecting their respective transformations such as dissolution, aggregation/agglomeration and sedimentation[101,103,104]. This may result in the impacts of mixtures of NPs on biota being completely different from the summed impacts of the single NPs. For example, antagonistic effects have been found for TiO_2NPs and CeO_2NPs in *Nitrosomonas europaea*[101], AgNPs and hematite nanoparticles in *E. coli*[104], TiO_2NPs and ZnONPs in *E. coli* and *A. hydrophila*[102]. Jośko et al. compared the toxicity of each combination of binary mixtures of NPs including ZnONPs, CuONPs TiO_2NPs, Cr_2O_3NPs and Fe_2O_3NPs to the toxicity of the individual NPs using the cress *Lepidium sativum*, flax *Linum usitatissimum*, wheat *Triticum aestivum* and cucumber *Cucumis sativus* as test species[105]. These authors also found that all of the binary mixtures induced significantly lower toxicity to the plants in comparison to the summed toxicity of the individual NPs[105]. However, some research indicated synergistic effects, which is contradictory to the above results. For instance, the co-exposure of CuONPs and ZnONPs caused severe inhibition of the growth and photosynthesis of spinach

Spinach oleracea as compared to the exposure of single NPs[106]. The mixture of ZnONPs and CeO_2NPs had synergistic effects in *Nitrosomonas europaea*[101]. Understanding the interactions between different NPs and how the interactions affect their mixture toxicity can provide a more complete picture for the risk assessment of NPs in the natural environment. However, current understanding of the mixture toxicity of multiple NPs is largely lacking. Even less is understood regarding the impacts on plants and the trophic transfer. It is therefore demonstrated in this thesis how a mixture of NPs will affect the transfer of NPs along a terrestrial food chain and the associated impacts on consumers. This advances the current understanding of the fate of NPs and their possible risks in/to terrrestrial ecosystems.

1.6 Interactions of metallic nanoparticles with terrestrial biota

Soil organisms including plants and soil microbes are exposed to NPs, producing the associated nano-bio interface that plays a dominant role in determining the adverse effects of NPs. The interactions occurring at the nano-bio interfaces are greatly influenced by the physicochemical properties of NPs, the exposure conditions, and the tested species[107] (**Figure 1.2**). For example, the dynamic nano-bio interactions result in the formation of protein coronas, particles wrapping, cellular uptake and internalization of NPs. These phenomena will affect the biological fate of NPs and hence potentially influence whether or not adverse biological effects of NPs are observed[108,107]. Therefore, a good understanding of the interactions between NPs and terrestrial organisms is paramount for their environmental risk assessment.

1.6.1 Uptake, translocation and impacts of nanoparticles in plants

Plants, being primary producers, form the foundation of the terrestrial ecosystem. They play a vital role in regulating nutrient cycling, maintaining the functioning and stability of ecosystems, and supplying food within food webs. Given the potential adverse effects of NPs and the importance of plants, it is therefore necessary to comprehensively understand the uptake, translocation and phytotoxicity of NPs in plants.

After exposure, NPs are first adsorbed/absorbed onto the surface of the plant root. For the uptake of NPs by plants, the adsorbed/absorbed NPs need to penetrate a

series of physiological barriers from the root surface to vascular tissues (xylem). These barriers include the root surface cuticle, cell wall, epidermis, cortex, endodermis and Casparian strip. For example, Ma et al.[109]observed La_2O_3 NPs (22 nm) and their aggregates in the intercellular spaces, middle lamellas, cytoplasm and vacuoles of cucumber roots using TEM-EDS. Geisler-Lee et al.[110] confirmed the presence of 20-40 nm AgNPs in the cell walls and plasmodesmata of *Arabidopsis thaliana* roots. Theoretically, only the NPs smaller than 20 nm can be taken up via the pores of the cell wall of plant roots as the estimated pore diameters are in between 5 and 20 nm[111]. However, many studies have reported the presence of NPs larger than 20 nm inside the plant roots[110,111]. The possible explanations for the uptake of NPs larger than 20 nm by plants are 1) the NPs might enlarge the pore size by inducing the destruction of the cell wall[112]; 2) the NPs might enter the intercellular spaces or even the xylem using a crack-entry pathway[113]. Also, NPs can be taken up by plant roots through endocytosis and intercellular plasmodesmata[111,114,115].

Once inside the plant roots, NPs can be translocated via the vascular system to the other organs like stems, leaves, and fruits[55,69]. Even though a large number of studies have reported the uptake and translocation of metallic NPs in plants, the majority of them focused on the total metal concentrations in plant shoots[11682117]. Knowledge of whether the NPs taken up by plant roots will translocate upwards in the form of particles or ions is thus still scarce. In fact, both particles and the released ions can be taken up by plant roots, have a different biodistribution, and will therefore end up in different parts of the plant and in different biochemical forms, and will subsequently contribute differently to the adverse effects induced by exposure to metallic NPs. It is therefore important to differentiate the relative contributions of the particulate form and dissolved ionic forms to the overall toxicity of suspensions of metallic NPs.

After being taken up in plants, metallic NPs can induce adverse impacts on plants at the morphological, physiological and biochemical levels. Morphological damages caused by metallic NPs were not only observed at the contact zone of the roots but also in other organs including stem and leaves. Morphological changes including the inhibition of the formation of the lateral root and root elongation, the reduction of biomass and leaf surface area and chlorosis were observed in a range of plants

exposed to metallic NPs[35,118,60]. Metallic NPs can also affect the transpiration rate, the fluidity and permeability of the membrane, the production of chlorophyll and the photosynthetic activity in plants[35,114,119,120]. Moreover, exposure to metallic NPs can induce excess production of reactive oxidative species including singlet oxygen, superoxide anion, hydrogen peroxide and hydroxyl radicals inside plant cells[119,120]. This can cause oxidative stress and hence activate the antioxidative defense mechanism of plants[119,120]. Further, the phytotoxicity of metallic NPs at the genomic level including DNA damage, the increase of chromosome aberration and micronuclei was also observed for various NPs[121,122]. In contrast to the negative impacts on plants, metallic NPs were also reported to have positive effects on plants growth, including the increase of biomass, protein content and the photosynthesis rate in plants[123]. For example, Kaveh et al.[124] observed a significant increase in biomass of *Arabidopsis thaliana* after exposure to low concentrations of AgNPs (below 2.5 mg/L) for 10 days, whereas a significant decrease in plant biomass at a higher concentration of AgNPs (from 5-20mg/L). Similar positive impacts on the growth of plants were also observed for Cu, CuO, ZnO, TiO_2 NPs[125]. These contradictory results indicate that assessment of the impacts of NPs on plants needs to consider the properties of NPs, the experimental methodology, and the plant species.

Aside from root exposure, plants also can be exposed to metallic NPs through their leaves. Nowadays, more and more metallic NPs are being applied in agriculture directly as fertilizers[48,126], pesticides[48], plant protectors[127] and growth regulators[21] or as a carrier[128] to increase the efficiency of traditional agrochemicals. Foliar application of nano-enabled agrochemicals is considered to be a more promising tool than soil application[129]. Foliar application of nano-agrochemicals may improve their bioavailability and efficiency, hence reducing their application doses and rates and lowering the associated environmental risks of nano-enabled agrochemicals[129]. The foliar application of nano-agrochemicals is expected to increase in the future[127]. This enhances the opportunities for plants to get in contact with NPs through leave exposure. However, studies carried out so far with the foliar exposure pathway are quite rare, even though this information has important implications for the safety application and risk assessment of NPs. Additionally, studies also demonstrated that

plants respond differently to NPs under hydroponic and soil cultivation. TiO_2NPs had for instance no effects on the growth of tomatoes under hydroponic cultivation[130] but enhanced the growth of tomatoes upon soil cultivation[131]. Therefore, the differences in uptake, translocation and phytotoxicity of AgNPs in lettuce exposed via different pathways (foliar versus root exposure, hydroponics versus soil cultivation) were investigated in this thesis.

1.6.2 Effects of nanoparticles on soil microbial communities

Next to plants, research also demonstrated the impacts of NPs on soil microbes. Soil microbes play critical roles in maintaining the health of both soil and plants by governing soil biological processes including nutrient transformation and cycling, energy flow, and degradation/detoxification of contaminants. Investigating the NPs-microbe interactions is therefore critical for the risk assessment of NPs in the terrestrial ecosystem, given the increasing emissions of NPs into the soil. So far, the majority of the research investigating the impacts of NPs on soil microbes was conducted with single cultured species. Tripathi et al.[114] documented the available data about the impacts of AgNPs on soil heterotrophic microbes and found that *Escherichia coli* was the most investigated species, followed by *Staphylococcus aureus*, *Pseudomonas*, *Salmonella typhi* and *Bacillus subtilis*. The effects of AgNPs on these bacteria include the inhibition of their growth, the decline of respiration, the disintegration of the plasma membrane, the damage of cell membranes, and even cell death[114]. Recently, two reviews summarized the nanotoxicity of metallic NPs to beneficial soil bacteria[132,133]. The authors reported that exposure to TiO_2, CuO and ZnO NPs also induced bacterial toxicity, for example causing growth inhibition, inhibition of cell viability, inhibition of metabolism, inactivation of enzymes and proteins, mitochondrial dysfunction, cell membrane damage, and DNA damage[132,133]. It also highlighted that the responses of microbial communities to NPs are poorly understood[133].

Investigating the impacts of NPs on the natural soil microbial community rather than on single cultures is needed as exposure of NPs to natural soil microbial communities represents a more environmentally realistic exposure scenario. To date, NPs have been reported to affect microbial growth[93], biomass[134], abundance[135], activity[93,135] and

metabolic profiles[136] of soil microbial communities as well as the activity of soil enzymes[93,134]. The impacts of NPs on soil microbial communities are highly dependent on the type of NPs tested, the exposure duration, and the actual dosage[135]. For example, the application of a low concentration of 10 mg/kg of ZnO and CuONPs stimulated the enzymatic activity and population size of soil microbial community[93]. In contrast, Xu et al.[134] found that CuONPs applied at concentrations of in between 100 and 1000 mg/kg inhibited the soil microbial biomass and the activity of soil enzymes, whereas the impacts induced by CuONPs were stronger than in the case of TiO_2NPs. Samarajeewa et al.[137] demonstrated that microbial growth and activity in a sandy loam soil were inhibited by AgNPs and the effects were more pronounced upon increasing exposure time. Recently, research regarding the impacts of NPs on soil microbial communities is developing from morphological and physiological endpoints (including microbial growth and biomass of soil microbial communities and soil enzyme activities) to the changes in structure and composition of the soil community (from domain to species levels) with the help of high-throughput sequencing technologies. For example, $Cu(OH)_2$ nanopesticides significantly shifted the composition of a soil bacterial community and the changes in the composition of the bacterial community varied over time[138]. Meier et al.[139] found that AgNPs induced both taxonomic and functional changes in the structure of a soil bacterial community by 16S and metatranscriptomic sequencing. These authors also identified the specific taxa that were tolerant (eg. *Sphingomonas* and *Bradyrhizobium*) or sensitive (eg. *Terrimonas*) to AgNPs exposure[139]. However, the above studies were performed with bare soil and the information about how the effects of NPs on soil microbial communities are affected by the cultivation of plants is limited.

Importantly, soil microbes always co-exist with plant roots in the rhizosphere and they can be connected by a number of pathways[140,141]. Plant roots can release root exudates into the rhizosphere, which provide the primary carbon source for supporting the growth of soil microbes[142,143]. Meanwhile, plants rely upon these soil microbes like plant growth-promoting bacteria (PGPB) for nutrient uptake and cycling, and for protection of the plants against environmental stressors[141,144,145]. NPs with antimicrobial properties may ultimately disrupt the interactions between plants

and soil microbes, resulting in either detrimental or beneficial impacts on soil microbial communities and/or plant growth[146]. On the other hand, plant roots may affect the transformations of NPs in soil and hence change the impacts of NPs on the rhizosphere bacterial community. However, very limited research conducted so far about the in-depth understanding of the NPs-microbe-plant interactions.

1.6.3 Terrestrial trophic transfer of nanoparticles

As mentioned in section 1.4.1, a large number of studies have evidenced the uptake, translocation and accumulation of NPs in plants. As plants are at the basis of many food-webs, there is a great potential for NPs of being transferred from plants to consumers. Although there has been some progress in understanding the trophic transfer of NPs in freshwater and marine food chains, limited information is available on the trophic transfer and bioaccumulation of NPs along terrestrial food chains. As far as I am aware, so far less than 15 publications have investigated the transfer and biomagnification of metallic nanoparticles with terrestrial food chains. Even though all of the studies confirmed the trophic transfer of NPs, 1) the extent of transfer and biomagnification of the NPs to the subsequent trophic level was inconsistent across the food chains and tested NPs; 2) the majority of the current studies was performed with the nonactive NPs, AuNPs and CeO_2NPs, only one paper reported the similar data on soluble NPs CuONPs and AgNPs; 3) no research described in the literature determined the combined effects of different NPs on their trophic transfer via food chains; 4) no research of the publications investigated the impacts of trophic transfer of nanoparticles on alterations of the behaviour of the consumers. To date, extensive research has already demonstrated the accumulation of NPs in animals via direct exposure to NPs, which can cause toxic impacts, including inhibition of growth, activity and reproduction, for a range of animals[14]. Therefore, it is reasonable to ask whether the food chain transfer of NPs can also result in unintended adverse effects on consumers. Although the interest is emerging, the trophic transfer of NPs along terrestrial food chains is still a poorly understood field of research and deserves careful investigations for a comprehensive understanding of the fate, behavior, and hazards of NPs in the environment.

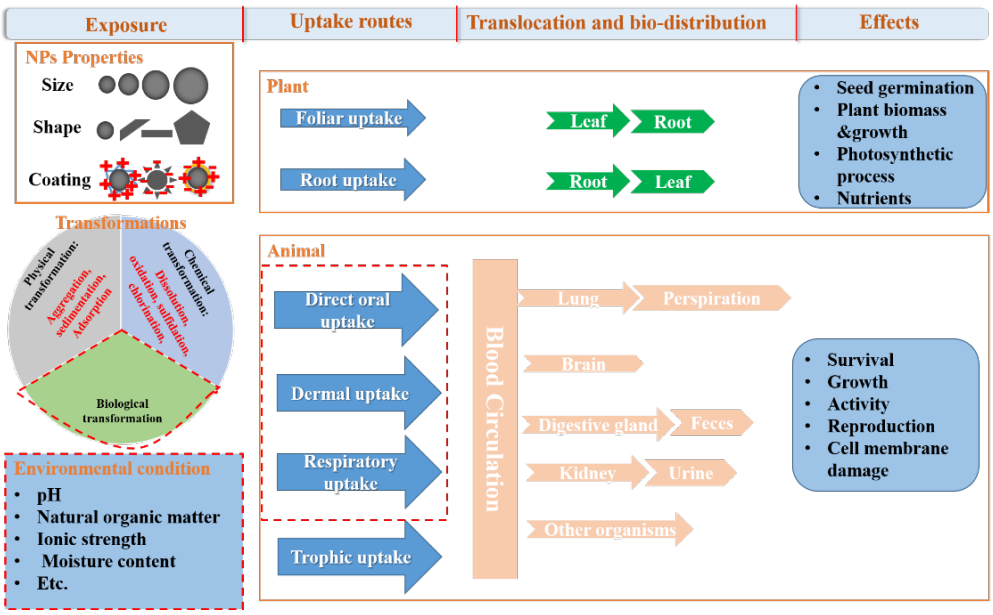

Figure 1.2 Schematic illustration of the interactions between NPs and organisms (modified from Vijver et al. Environ. Sci.: Nano, 2018, 5, 2473). The red dashed line indicates the factors that were not investigated in this thesis. The exposure scenarios of NPs to organisms were influenced by physico-chemical properties of NPs, the dynamic fate of NPs and the environmental conditions. At the nano-bio interface, the bioavailability of NPs depends on exposure route and tested organisms, and hence changes the subsequent translocation, biodistribution and effects of NPs in organisms.

1.6.4 Selected species in this thesis

This thesis focuses on investigating the impacts of metallic NPs on the terrestrial ecosystem. Therefore, plants and soil bacterial communities were chosen as the test organisms. Lettuce is a worldwide cultivated leafy vegetable crop with an estimated annual production of around 27 million tons globally and an annual consumption of 25 pounds per person[147]. It is a typical leafy vegetable that is suited for evaluating the ecotoxicity of chemicals and soil amendments to higher terrestrial plants, as recommended by various regulations (ASTM (American Society for Testing and Materials), 2003, US EPA (1996), ISO (International Organization for Standardization), 2005, OECD/OCDE, 2006a, OECD/OCDE, 2006b). Additionally, lettuce is an easily available plant that can comfortably be cultivated hydroponically.

Further, previous studies demonstrated that lettuce was well able to take up NPs. Therefore, lettuce (*Lactuca sativa*) was chosen as the model species in this thesis for investigating the uptake, translocation, accumulation and toxicity of metallic NPs in plants.

The rhizosphere is a highly biologically active zone where soil, plant roots and microbes interact.[148] These interactions are critical for ecosystem functioning and nutrient cycling in terrestrial ecosystems[148,149]. Also, rhizosphere bacteria provide many functions in supporting the growth of host plants, including enhancing the tolerance to abiotic stress and protection against pathogens[148,149]. It should be highlighted that the rhizosphere is also a critical place where the adsorption/absorption of toxic substances to/from plant roots occurs[148]. The nano-bio interface inevitably influences the composition and structure of the rhizosphere bacterial community, which may disrupt the associated microbial functions and hence affect the growth of plants. Therefore, in this thesis the rhizosphere bacterial community was chosen as another terrestrial biota to better assess the impacts of NPs on the terrestrial ecosystem.

Gastropods have widely been used to monitor environmental pollution[150]. Among them, terrestrial snails are recognized as excellent ecological and biological indicators for assessing the ecotoxicity of NPs[150,151]. This is because of the ease of collection and sampling, their global distribution, short life cycle, small size, high reproductivity, high adaption to various environmental conditions, and ease of culture under laboratory conditions[150,152]. They are also susceptible to stress and able to accumulate diverse pollutants including metallic trace elements[150,152]. Further, snails can serve as a link for supplying food and energy between primary producers (e.g. plants) and secondary consumers (e.g. birds). Therefore, the land snail *Cornu aspersum* was selected as the primary consumer in this thesis to explore the potential trophic transfer and the consequent toxicity of AgNPs and TiO_2NPs along with the lettuce-snail food chain.

1.7 Objectives and research aims of this thesis

The research described in this thesis was performed with the objective to enhance the knowledge on the fate, accumulation and toxicity of NPs in terrestrial plant and food

chains (**Figure 1.3**), and is subsequently aimed at providing suggestions for improvements of the ecotoxicological risk assessment of NPs in terrestrial systems and more specifically for the application of NPs in agriculture. This thesis aimed to:

1. investigate the uptake, translocation and phytotoxicity of AgNPs (a typical metallic NP) in lettuce upon different exposure scenarios;

2. investigate the dynamics of metal ions dissolving from the NPs and their impacts on metal accumulation in plants and effects on a soil rhizosphere bacterial community;

3. investigate the trophic transfer, biomagnification and toxicity of metallic NPs in a terrestrial food chain.

The key research questions of this thesis can be summarized as follows:

1. How does the exposure pathway affect the uptake, translocation, and phytotoxicity of AgNPs in plants? (Chapter 2 and 4)

2. How do the shape, size and coating of NPs affect the uptake, translocation, and phytotoxicity of AgNPs? (Chapter 3)

3. What is the relative contribution of the nanoparticulate and the released ionic form to the overall toxicity of suspensions of NPs and on metal accumulation in plants? (Chapter 2 and 3)

4. How and to what magnitude does the dynamic dissolution of AgNPs in soil affect their bioavailability to plants? (Chapter 4)

5. How does the soil rhizosphere bacterial community respond to exposure to AgNPs, and does this response change over time? (Chapter 4)

6. How does a mixture of AgNPs and TiO_2NPs affect the transfer of the individual NPs along a terrestrial food chain of lettuce-snails and the associated impacts on the consumer? (Chapter 5)

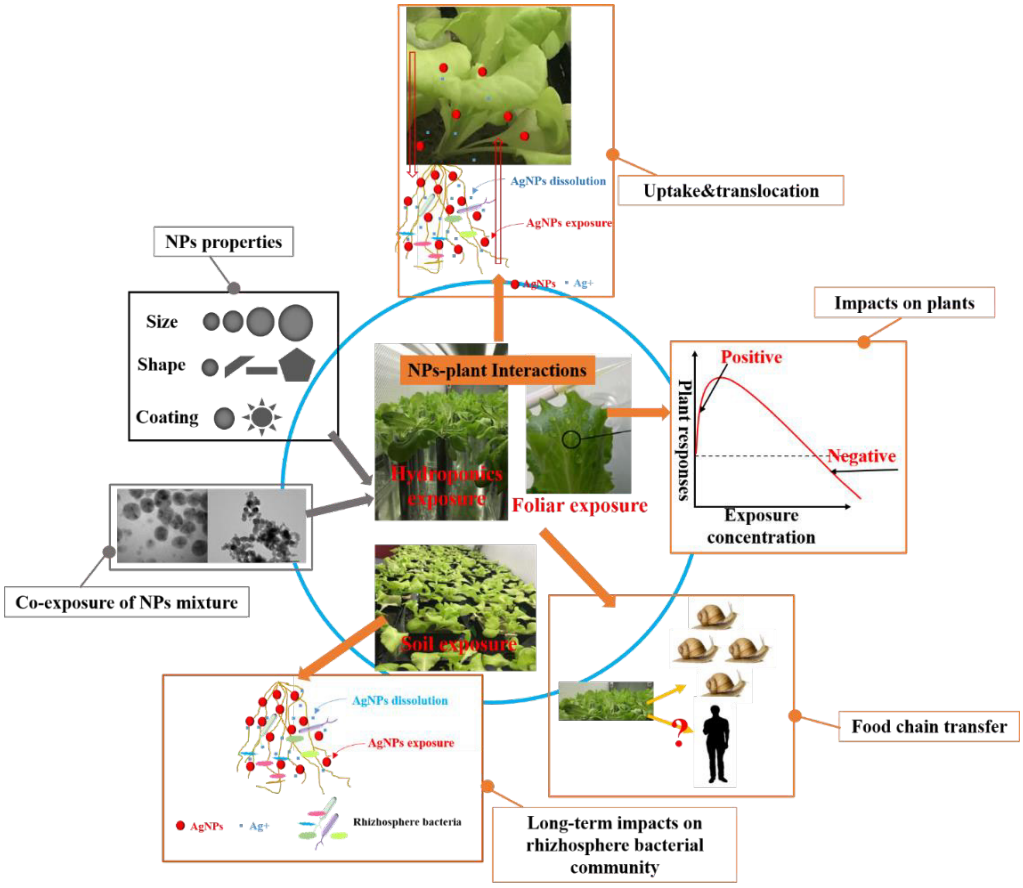

Figure 1.3 An overall graphic illustration of the experimental set-up and the main focuses of this thesis.

1.8 Outline of this thesis

Chapter 1. General introduction regarding metallic nanoparticles, their fate, uptake and effects on terrestrial species. Also, food chain transfer is discussed and a summary of the objectives of this thesis is provided.

Chapter 2. In this chapter we investigated how the exposure route of AgNPs affects their accumulation, toxicity and anti-oxidant responses in lettuce. In addition, we determined the relative contribution of ionic and particulate Ag to the observed toxicity and Ag accumulation in lettuce.

Chapter 3. In this chapter, we determined how the size-aspect ratio and coating of silver nanowires affect the contributions of dissolved and particulate Ag to the overall phytotoxicity of these particles on lettuce. Additionally, we quantified the toxicokinetic rate constants of particulate and ionic Ag in lettuce exposed to different types of silver nanowires.

Chapter 4. In this chapter, we determined the dissolution of AgNPs amended to soil at different exposure doses and at different exposure times in the presence and absence of plants. Concomitantly, the associated impacts on soil pH, Ag accumulation in plants, and the alterations of the rhizosphere bacterial community were investigated.

Chapter 5. In this chapter, we investigated the trophic transfer of single AgNPs and TiO_2NPs as well as the trophic transfer of a mixture of AgNPs and TiO2-NP from lettuce to snails and their distribution in snails. Furthermore, the adverse effects of single NPs and the mixture of AgNPs and TiO_2NPs on snails associated with food chain transfer were compared over time.

Chapter 6. The main findings of the thesis are summarized; the challenges and future perspectives towards nanoecotoxicology and risk assessment are discussed.

Luxembourg, Luxembourg, 2017

Photo by Cherry


Paris, France, 2018

Chapter 2

Foliar versus root exposure of AgNPs to lettuce: Phytotoxicity, antioxidant responses and internal translocation

Juan Wu, Guiyin Wang, Martina G. Vijver, Thijs Bosker, Willie J. G. M. Peijnenburg

Published in Environmental Pollution
261 (2020) 114117

Abstract: Whether toxicity of silver nanoparticles (AgNPs) to organisms originates from the nanoparticles themselves or from the dissolved Ag-ions is still debated, with the majority of studies claiming that extracellular release of Ag-ions is the main cause of toxicity. The objective of this study was to determine to contribution of both particles and dissolved ions to toxic responses, and to better understand the underlying mechanisms of toxicity. In addition, the pathways of AgNPs exposure to plants might play an important role and therefore are explicitly studied as well. We systematically assessed the phytotoxicity, internalization, biodistribution, and antioxidant responses in lettuce (*Lactuca sativa*) following root or foliar exposure to AgNPs and ionic Ag at various concentrations. For each endpoint the relative contribution of the particle-specific versus the ionic form was quantified. The results reveal particle-specific toxicity and uptake of AgNPs in lettuce as the relative contribution of particulate Ag accounted for more than 65% to the overall toxicity and the Ag accumulation in whole plant tissues. In addition, particle toxicity is shown to originate from the accumulation of Ag in plants by blocking nutrient transport, while ion toxicity is likely due to the induction of excess ROS production. Root exposure induced higher toxicity than foliar exposure at comparable exposure levels. Ag was found to be taken up and subsequently translocated from the exposed parts of plants to other portions regardless of the exposure pathway. These findings suggest particle-related toxicity, and demonstrate that the accumulation and translocation of silver nanoparticles need to be considered in assessment of environmental risks and of food safety following consumption of plants exposed to AgNPs by humans.

2.1 Introduction

Due to their excellent catalytic and superconducting properties and their strong antibacterial activity, engineered silver nanoparticles (AgNPs) are present in a large variety of consumer, agricultural and medical products and are produced in large amounts[137,153]. However, with the accelerating production and application, there is the likelihood of release into the environment with emissions expected to increase[154,155]. The released AgNPs are expected to end up and accumulate in soil due to biosolids fertilization application, sewage disposal, irrigation, and waste landfills[156,157,158]. Likewise, AgNPs also can be disproportionately emitted into the

atmosphere and adsorbed onto fine atmospheric dust as a consequence of industrial activities, waste incineration, spray application by households (e.g. disinfection and anti-odor sprays) and the application of agricultural products[156,159,160]. Plants are in direct interaction with air, soil and water, and as primary producers are vital for the functioning of ecosystems, supplying food to different consumer levels. It is therefore needed to properly understand how enhanced exposure to synthetic AgNPs induces their uptake and subsequent translocation in plants as originating from the soil based uptake routes as well as from the air-borne route. This knowledge will allow to provide relevant information for the evaluation of the potential risks of AgNPs to plants, being of great importance given their position within ecosystems as well as being a food source for humans.

After root exposure, the uptake and translocation from roots to leaves were reported, as well as adverse responses on plants. These responses include inhibition of seed germination and root elongation, reduction of biomass, and impacts on the photosynthetic system of plants[35]. However, the current understanding of the impacts of foliar exposure on i) plant growth, and ii) AgNPs uptake and translocation from leaves to roots is rather limited. This information may carry important implications regarding the effect of atmospheric deposition on pollutant concentrations in above-ground plant segments as well as on the safety of AgNPs-added agricultural products applications. Based on the limitedly available studies, there have been contradictory reports where foliar exposure induced more metal accumulation but less toxicity[161], or more metal accumulation and higher toxicity[118], or less metal accumulation and less toxicity in plants[162] as compared to root exposure. These apparent inconsistencies regarding the relationship between the toxicity and metal accumulation in plants highlight that the interactions of plants and nanoparticles involved in different exposure pathways should be investigated in greater detail.

In addition, it remains controversial whether the toxicity of a AgNPs suspension is specifically caused by nanoparticles itself or is due to the released ionic Ag. Although Ag-ions released from the AgNPs are often seen as the main cause of observed toxicity[29,57,163,164,165], the particle-specific toxicity has been reported and was in some

cases shown to be important[61,166]. Moreover, plants are known to take up particles/ions through cuticular pores and stomata in case of foliar exposure[167,168], and through the root epidermis in case of root exposure[169]. These different exposure routes change the ratio of ions versus particles that are taken up by plants. Whether this would lead to differences in Ag-ions /NPs biodistribution across the plant organs remains unclear. Furthermore, Ag-ions have a different mode of action and bioavailability compared to the particulate form[170]. However, differentiating the contribution of particulate Ag versus dissolved Ag-ions on the overall toxicity of AgNPs suspensions is challenging due to their common co-occurrence. This type of comparative toxicity assessment of AgNPs suspensions and Ag-ions is mostly performed with freshwater species in parallel experiments using identical concentrations of total Ag[61,164,166]. However, it should be noted that the dissolution of Ag-ions from the particulate Ag in AgNPs suspension is a dynamic process, and the ratio of occurrence of particle forms versus ionic forms alters over time and is influenced by the concentration of AgNPs suspension as well as by water chemistry and/or soil properties[171,172]. To address this issue, time weighted average concentrations and standardized aqueous test media instead of soil were used in this study.

In the present study, we exposed lettuce (*Lactuca sativa*) which is a widely cultivated vegetable having a large foliar surface, to different concentrations of AgNPs and/or Ag-ions following root or foliar exposure. The aims of the study were to: 1) investigate the relative contribution to toxicity and accumulation of dissolved Ag versus particulate Ag of AgNPs suspension, and 2) determine the difference in uptake, translation and phytotoxic responses of lettuce in both exposure pathways. Knowledge on uptake routes and toxic species provides building blocks to generate a mechanistic-based effect assessment for the plants, which is of great importance given their position within ecosystems as well as being a food source for humans.

2.2 Materials and methods

2.2.1 Characterization of AgNPs suspensions and quantification of dissolved Ag-ions

Suspensions of spherical AgNPs (RAS AG, Regensburg, Germany) with a nominal size of 20 nm were obtained at a concentration of 100 g/L Ag in water under nitrogen gas. $AgNO_3$ was purchased from Sigma–Aldrich (Zwijndrecht, Netherlands). Stock suspensions were freshly prepared in 1/4 Hoagland solution (pH 6.0 ± 0.1; without EDTA or chloride to avoid Ag chelation or precipitation, Hoagland solution compositions are described in **Table S2.1**, Supplementary material) after 5 min sonication at 60 Hz (USC200T, VWR, Amsterdam, The Netherlands). The size distribution and zeta potential of the nanoparticle suspensions at the exposure concentrations were analysed at 1, 24, 48 and 72 h after incubation in 1/4 Hoagland solution using a zetasizer Nano-ZS instrument (Malvern, Instruments Ltd., Royston, UK).

The dissolution kinetics of AgNPs suspension at 0.1, 0.5 and 1 mg/L in 1/4 Hoagland solution over 72 h were investigated to obtain the actual exposure concentrations of soluble Ag. After being exposed to 1/4 Hoagland solution for 0, 6, 16, 24, 48 and 72 h, the suspensions (defined as $AgNPs_{(total)}$) were taken from the tube (top 10 cm) and centrifuged at 30,392 g for 30 min at 4 °C (Sorvall RC5Bplus centrifuge, Bleiswijk, Netherlands) to remove the particulate Ag remaining in suspension. The supernatants obtained in this step were used as the corresponding dissolved Ag suspension (defined as $AgNPs_{(ion)}$). Next, the concentrations of $AgNPs_{(total)}$ and $AgNPs_{(ion)}$ were measured by Atomic Absorption Spectroscopy (AAS, Perkin Elmer 1100B, Waltham, MA, USA) after adding a drop of 65% HNO_3 into the solution. Accordingly, the concentration of $AgNPs_{(particle)}$ is the difference between the Ag measured as $AgNPs_{(total)}$ and $AgNPs_{(ion)}$[136]. All experiments were run in triplicate.

2.2.2 Plant growth and experimental design

Lactuca sativa seeds were sterilized for 15 min with NaClO (0.5% w/v), rinsed three times with tap water, and then immersed in deionized water for 24 h. The seeds were germinated in a rolled paper towel suspended in deionized water. After 3 d, the

seedlings were placed in Petri dishes (10 seedlings/dish) with 50 mL of 1/8 Hoagland solution for one week and then the young plants were transferred to 22 mL tubes (one seedling per tube) containing 1/4 Hoagland solution for a further week of growth. The seed germination and growth were kept in a climate room at a 20/16 °C day/night temperature and 60% relative humidity set to a 16 h photoperiod.

The plants were exposed to $AgNPs_{(total)}$ and $AgNPs_{(ion)}$ for 15 days via the root or leaves (see below for details). The exposure procedure was modified from a previous study[161]. In all cases, the tubes that contained exposure medium and the control treatments with 1/4 Hoagland solution had lids with a small hole and were covered with aluminum foil to minimize the impact of light-induced transformations of AgNPs and to avoid evaporation of water. Plants were placed with their roots within the tubes, and the upper parts such as leaves were placed above the foil. All exposure tests were performed under the same conditions as described above for seeds growth.

Root exposure. Uniform pre-grown lettuce plants were selected and were exposed through the roots to either $AgNPs_{(total)}$ suspensions at nominal concentrations of 0.1, 0.5 and 1 mg/L, or the corresponding dissolved concentration of Ag ($AgNPs_{(ion)}$) released from the above concentrations of $AgNPs_{(total)}$ using $AgNO_3$ (12 replicates per treatment). The AgNPs suspensions were prepared by mixing different volumes of the AgNPs stock suspension into 1/4 Hoagland solution and sonicating for 10 min at 60 Hz to facilitate dispersion prior to application. The $AgNPs_{(total)}$ concentrations were chosen based on our preliminary tests which showed that the highest concentration (1 mg/L) reduced the fresh biomass of lettuce by *ca.* 40% after one week, and $AgNPs_{(ion)}$ concentrations were selected according to the dissolution kinetics of AgNPs suspensions. The exposure media were renewed every 3 d.

Foliar exposure. No significant effects on biomass production were found during preliminary tests in which lettuce leaves were exposed to AgNPs suspensions at the same concentrations as used for root exposure, and roots were exposed to AgNPs continually. Thus, uniformly grown lettuce plants were divided into two groups for foliar exposure. In one group (defined as *foliar exposure*), which is mainly used to study the effects of foliar application of AgNPs, the freshly prepared $AgNPs_{(total)}$ suspensions with nominal concentrations of 1, 10, and 50 mg/L (fresh biomass

decreased by around 40% after one week preliminary exposure under the highest concentration) were carefully dropped onto lettuce leaves. A volume of 0.5 mL of the AgNPs suspensions was applied to each plant seven times per day (every two hours during daytime). The small volume and high application frequency ensured effective exposure of the leaves to AgNPs suspensions and minimal Ag loss due to dripping off the leaves. To avoid Ag contamination of the hydroponic medium, dry cellulose tissues were added to the small hole in the lids. The Ag content in the 1/4 Hoagland solution was below the detection limit, indicating that the foliar applied Ag was the only source for the plants.

In the other group (defined as *single-leaf immersed exposure*), which is only used for comparison with the uptake and accumulation of Ag via root exposure, one of the lettuce leaves was immersed in AgNPs suspensions at nominal concentrations of 0.1, 0.5 and 1 mg/L (same as root exposure).

2.2.3 Biomass and Ag accumulation measurement

All treated plants were harvested after 15 d of exposure and subsequently thoroughly washed with flowing deionized water and rinsed with ultrapure water three times. Next, the plants were separated into the root and shoot. For the leaf immersed exposure treatments, plants were separated into three parts: root, unexposed leaves (shoot) and exposed leaf. After measuring the fresh biomass, half of the samples were flash-frozen in liquid nitrogen and stored at -80 °C for further biochemical analysis.

To determine the total Ag content in plant tissues, the attached AgNPs/ Ag-ions were removed by immersing the whole plant for 20 min in 10 mM HNO_3, followed by immersion for 20 min in 10 mM EDTA, and finally thoroughly rinsing with Milli-Q water[161,173]. Samples were oven-dried for 72h at 70°C and weighed to determine dry weight. The weighed root and shoot samples were digested by adding 3 mL of HNO_3 (65%) at 120 °C for 40 min on a hotplate and then 1.5 mL of H_2O_2 (30%) was added and heated at 120 °C for another 20 min[174]. Following digestion, the samples were diluted with deionized water to 3 mL and analysed on their metal content by using AAS (Perkin Elmer 1100B, Waltham, MA, USA). Ten blanks were used to calculate the detection limit of Ag for AAS. Standard Ag solutions of 0.5 mg/L and 1 µg /L were measured every 20 samples to monitor the stability of AAS. Recoveries were found

to be in between 95% and110% for AAS. Blanks and Ag standard solutions were included in the digestion procedure for quality control purposes.

2.2.4 Biochemical analysis of plant tissue

The variations in chlorophyll pigment could affect plant growth as chlorophyll has an important role in photosynthesis. In addition, NPs toxicity to plants has been related to oxidative stress as a result of increased reactive oxygen species (ROS) productions and disturbance in defense mechanisms[35]. Therefore, chlorophyll pigment, ROS production and the related antioxidants were measured as follows.

Photosynthetic Pigment Measurement. Fresh leaves (0.1~0.2 g) were homogenized in liquid nitrogen and extracted with 80% acetone for 24 h at 4 °C in the dark followed by centrifuging for 10 min at 4500 g at 4 °C. Chlorophyll a and b, and carotenoids were determined by using a UV–vis spectrophotometer at 663, 646 and 470 nm respectively[175].

ROS production analysis. The superoxide anion ($O_2^{\cdot -}$) assay in root and shoot tissues of different treatments were performed according to the method of Wang and Lou[176] with a modification by oxidizing hydroxylamine hydrochloride. This procedure yields nitrite which can react with sulphanilamide and a-naphthylamine to form a red azo dye with a maximum absorbance at 530 nm. Hydrogen peroxide (H_2O_2) was quantified according to Mosa et al.[177] by incubating the plant extracts with potassium iodide and reading the absorbance at 390 nm. The content of H_2O_2 was obtained based on a H_2O_2 standard curve (R^2=0.99). Malondialdehyde (MDA) was measured to analyse lipid peroxidation following the method of Mosa et al.[177] using a UV–vis spectrophotometer.

Enzymatic antioxidants. Fresh roots or leaves tissues (0.1~0.2 g) were separately homogenized in ice cold extraction buffer. After centrifugation at 10,000 g for 20 min at 4 °C, the supernatants were used for superoxide dismutase (SOD), ascorbate peroxidase (APX), catalase (CAT) and peroxidase (POD) activities analysis following the protocols as described by Ma et al.[174].

Non-enzymatic antioxidants. The ascorbate (ASA) content in plant tissues was estimated spectrophotometrically at 525 nm according to the method of Kampfenkel

et al.[178] by quantifying on the basis of a standard curve of L-ascorbic acid (Sigma-Aldrich, Zwijndrecht, Netherlands). The extracts were obtained by grinding 0.1 g leaf tissues in 0.8 mL 6% (v/v) trichloroacetic (ice cold) and centrifuging at 15,600 g for 10 min at 4 °C. The reduced glutathione (GSH) level was assayed by the method modified from Xia et al.[179] based on the fact that the sulfhydryl groups present in the tissue homogenates react with 5,5'-dithiobis (2-nitrobenzoic acid) (DTNB) to form a yellow dye with maximum absorbance and read at 412 nm.

More detailed information about the biochemical parameters methodology and quantifications can be found in the supplementary material.

2.2.5 Data analysis

The behavior of AgNPs during the exposure period involves dynamic processes, especially in the root exposure. Time weighted average concentrations (C_{TWA}) were therefore used to assess the actual exposure concentration of $AgNPs_{(total)}$, $AgNPs_{(particle)}$ and $AgNPs_{(ion)}$ over each 3 d refreshment period. The TWA concentration was calculated based on the following equation[136]:

$$C_{TWA} = \frac{\sum_{n=0}^{N}\left(\Delta t_n \frac{C_{n-1}+C_n}{2}\right)}{\sum_{n=1}^{N}\Delta t_n} \qquad (1)$$

Where Δt is the time interval, n is the time interval number, N is the total number of intervals (N=5), C is the concentration at the end of the time interval.

To calculate the relative contribution of $AgNPs_{(partices)}$ and $AgNPs_{(ion)}$ to the effects induced by the suspensions of AgNPs, the decrease of biomass as compared to the control was chosen as the endpoint of assessment. Based on the previous literature[180], it is widely believed that the modes of actions of $nanoparticle_{(particle)}$ and $nanoparticle_{(ion)}$ are likely to be independent, which is in line with the assumption of the response addition model:

$$E_{(total)} = 1 - \left(\left(1 - E_{(particle)}\right)\left(1 - E_{(ion)}\right)\right) \qquad (2)$$

where $E_{(total)}$ and $E_{(ion)}$ represent the effects caused by the nanoparticle suspensions and their corresponding released ions, which were quantified experimentally. This makes $E_{(particle)}$ as the only unknown, allowing for direct calculation of the effects

caused by the $AgNPs_{(particle)}$.

The Ag enrichment factor (EF), defined to evaluate the ability of plants to accumulate Ag, was calculated using the following equation:

$$EF = \frac{M_{plant}}{M_{medium}} \quad (3)$$

The Ag content in plants (M_{plant}) was calculated as follows:

$$M_{Plant} = C_{leaves} \times DW_{leaves} + C_{roots} \times DW_{root} \quad (4)$$

Where C_{leaves} and C_{roots} represent the Ag concentration in leaves and roots, in units of milligrams per kilogram.

The Ag content in the medium (M_{medium}) was calculated as follows:

Root exposure: $$M_{medium} = C_{TWA} \times V_{exposure} \quad (5)$$

Foliar exposure: $$M_{medium} = \frac{\sum_{n=0}^{N}\left(\Delta t_n \times (C_{exposure} \times V_{exposure})\right)}{\sum_{n=1}^{N} \Delta t_n} \quad (6)$$

Where Δt is the time interval between each drop, n is the time interval number, N is the total number of intervals (N=104), C is the exposure concentration of AgNPs suspensions (mg/L), V is the exposure volume dropped onto the leaves each time (L).

The Ag translocation factor (TF), defined to evaluate the capacity of plants to transfer Ag from specific parts to the remainder of the plant, was calculated as follows:

$$TF = \frac{C_{shoots}}{C_{roots}} \text{ for root exposure; } TF = \frac{C_{roots}}{C_{shoots}} \text{ for foliar exposure.} \quad (7)$$

Statistically significant differences among different concentrations in the same group were analysed by one-way ANOVA followed by Turkey's honestly significant difference tests at $\alpha < 0.05$ using IBM SPSS Statistics 25 (Data were tested for normal distribution and homogeneity of variance with Shapiro-Wilk test and Bartlett test prior to running the ANOVA, with no deviations from both found). The T-test was performed to analyse the significance between $AgNPs_{(ion)}$ and $AgNPs_{(total)}$ ($p<0.05$). Results are expressed as mean ± standard error of 12 replicates for biomass and 4 replicates for biochemical parameters and Ag bioaccumulation. All test statistics (p-

values) are presented in **Table S2.2**, supplementary material.

2.3 Results

2.3.1 AgNPs suspension characterization

The DLS results showed that the AgNPs aggregated rapidly in the 1/4 Hoagland solution as the hydrodynamic diameter increased over time (**Table S2.3**). The Zeta-potential of the AgNPs suspensions of all concentrations ranged between -9.5 to -15.4 mV and their changes were slight over the test period (**Table S2.3**). The ionic Ag concentration increased gradually over time while the concentration of total and particulate Ag decreased over time (**Figure 2.1**). The extent of ionic Ag released was found to be related to the concentrations of the AgNPs suspensions as the percentage of $AgNPs_{(ion)}$ increased by 38%, 29% and 24% after 72 h of incubation in the exposure medium at nominal concentrations of 0.1, 0.5 and 1 mg/L, respectively. Based on the dynamic dissolution behaviors of $AgNPs_{(total)}$, TWA concentrations of $AgNPs_{(ion)}$ were chosen as the exposure concentration of ionic Ag (corresponding dissolved Ag released from AgNPs) to plants, that is: 6.3, 36.6 and 85.0 μg/L are the average Ag-ions concentrations present in AgNPs suspensions of nominal concentrations of 0.1, 0.5 and 1 mg/L, respectively (**Table S2.4**).

2.3.2 Impacts on growth of lettuce

Shoot and root biomass of the lettuce plants were significantly reduced for the $AgNPs_{(total)}$ and $Ag_{(ion)}$ treatments with a dose-dependent effect regardless of exposure pathway (**Figure 2.2**; **Table S2.2**). Following root exposure to 0.1, 0.5 and 1 mg/L of $AgNPs_{(total)}$, the biomass of lettuce significantly decreased by 24, 48 and 78% for the roots and 27, 52 and 70% for the shoots relative to the controls, respectively. For the corresponding concentrations of dissolved $AgNPs_{(ion)}$, only the highest exposure concentration caused significant effects on root/shoot biomass with a reduction of 26/20 % compared to the control, respectively. The results indicated a particle-specific toxicity to plants, in addition to the particles being a potential source of Ag-ions. Following foliar exposure, a significant decrease on root/shoot biomass (42/28%) was observed at the highest exposure concentration of $AgNPs_{(total)}$, while a significant increase was observed only in root biomass (34%) at 1 mg/L. On the other

hand, the highest actual amount of $AgNPs_{(total)}$ based on the TWA method in case of foliar exposure was 1.12 mg, which was 10 times higher than the highest amount (0.048 mg) in case of root exposure. However, the corresponding effects on biomass reduction were much lower in case of foliar exposure than in case of root exposure. This indicated higher $AgNPs_{(total)}$ toxicity following root exposure when considering exposure on the basis of a similar dose expression.

The chlorophyll content in leaves was measured as an indicator of the photosynthetic performance of the plants. AgNPs had no significant impacts on total chlorophyll content of lettuce (**Table S2.2**), regardless of Ag forms or exposure pathways, although a trend toward a decreasing chlorophyll content with increasing dose was noted (**Figure S2.1** Supplementary).

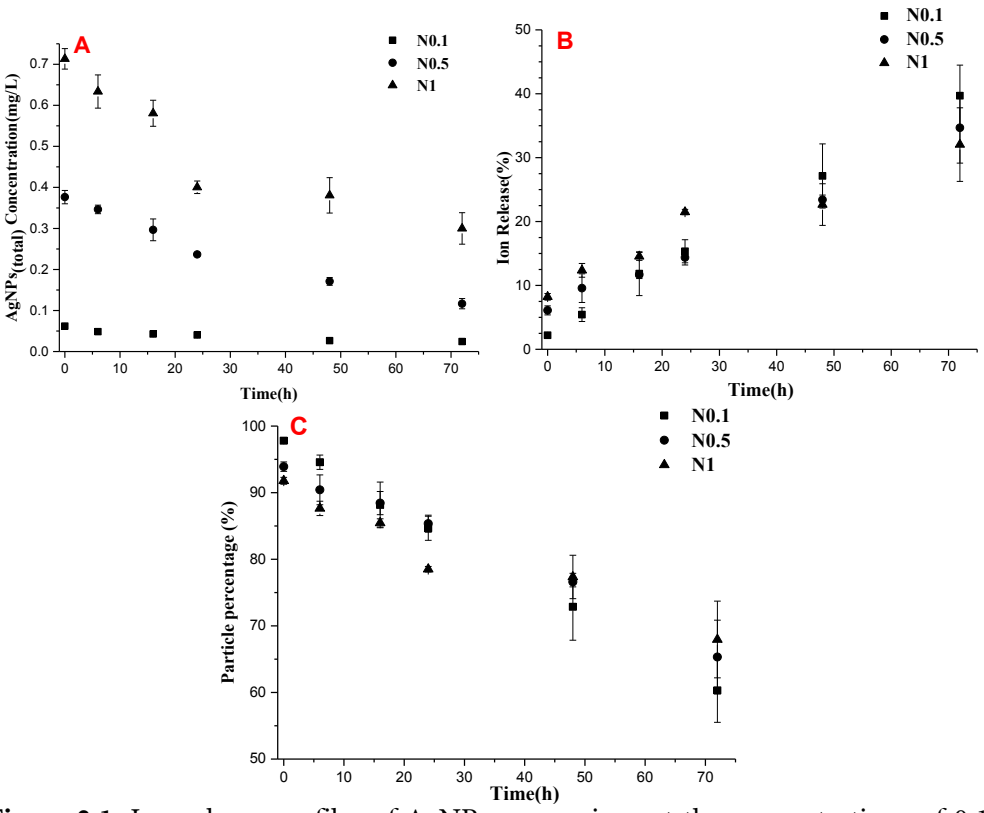

Figure 2.1. Ion release profiles of AgNPs suspensions at the concentrations of 0.1 mg/L, 0.5 mg/L and 1 mg/L(N0.1, N0.5, N1) in the exposure medium over time. (A) Total Ag concentrations in the AgNPs suspension. (B) Percentages of dissolved Ag released in the AgNPs suspension. (C) Percentages of particulate Ag present in the AgNPs suspensions. Data are the mean ± SE (n = 3).

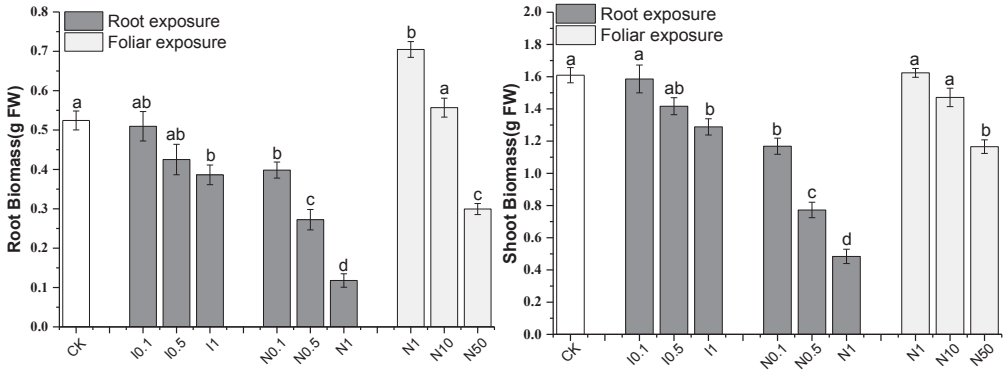

Figure 2.2. Root and shoot fresh biomass of lettuce (*Lactuca sativa*) exposed to different concentrations of $AgNPs_{(total)}$ and $AgNPs_{(ion)}$ after 15 days of exposure. Data are the mean ± SE (n = 12). Different letters in the same group indicate statistically significant differences between treatments at $p<0.05$. I0.1, 0.5 and 1 represent *Lactuca sativa* exposed to the $AgNPs_{(ion)}$ concentrations as released from AgNPs suspensions with nominal concentrations of 0.1,0.5 and 1 mg/L; N0.1, 0.5, 1, 10 and 50 represent *Lactuca sativa* exposed to nominal $AgNPs_{(total)}$ concentrations of 0.1, 0.5, 1, 10 and 50 mg/L.

2.3.3 Analysis of oxidative stress

Exposure to increasing concentrations of $AgNPs_{(ion)}$ under root exposure significantly increased the accumulation of $O_2^{\bullet -}$, H_2O_2 and MDA in lettuce roots and shoots (**Figure 2.3**; **Table S2.2**). For root exposure to $AgNPs_{(total)}$, the content of $O_2^{\bullet -}$ and MDA in shoots, and the content of H_2O_2 in roots were significantly increased upon increasing exposure concentrations. Even though not significant, a slight increase of $O_2^{\bullet -}$ and MDA in roots and of the H_2O_2 contents in shoots in comparison with control also should be noted following root exposure to $AgNPs_{(total)}$ (**Figure 2.3** and **Table S2.5**).

For foliar exposure, no significant differences (**Figure 2.3**; **Table S2.2**) in the contents of $O_2^{\bullet -}$, H_2O_2 and MDA were found in roots and shoots of lettuce exposed to $AgNPs_{(total)}$, the exception being the $O_2^{\bullet -}$ contents in the group of root tissues (ANOVA, P=0.01; **Figure 2.3**), as the $O_2^{\bullet -}$ content was significantly increased by 68% at the highest exposure concentration compared to the control (**Table S2.5**).

In general, the accumulation of ROS in roots/shoots following root exposure to

$AgNPs_{(ion)}$ was higher or equal to the ROS production in case of exposure to the corresponding concentration of $AgNPs_{(total)}$ (**Figure 2.3**). This finding suggests that $AgNPs_{(particle)}$ contributed only to a limited extent to the induction of oxidative stress and/or its effects are being efficiently counteracted by the antioxidants system. There was an exposure pathway-dependent pattern for the alterations of the ROS production in plants, with an increasing tendency for root exposure to $AgNPs_{(total)}$, whereas a slight decrease of H_2O_2 and MDA contents in roots via leaf exposure to $AgNPs_{(total)}$ was observed (**Figure 2.3** and **Table S2.5**).

2.3.4 Antioxidants responses

A clear dose-dependent effect on the activity of enzymatic antioxidants activities was observed following root exposure. Compared to the control, the changes of the enzymatic antioxidants activity were significantly increased upon increasing exposure concentrations in plant roots and shoots regardless of the form of Ag (**Table 2.1**), except for the APX activity in plant roots ($P>0.1$, **Table S2.2**). In addition, the alterations of SOD, CAT and POD activities in plants exposed to $AgNPs_{(total)}$ were comparable to, or slightly higher than the changes in case of exposure to the corresponding concentration of $AgNPs_{(ion)}$, with the exception of APX activity (**Table 2.1**). This suggests that the alterations of the enzymatic antioxidants activity triggered by the $AgNPs_{(ion)}$ was stronger than in case of corresponding $AgNPs_{(particle)}$.

For foliar exposure, significant differences were found for APX and CAT activity (**Table 2.1**; **Table S2.2**). Interestingly, there was no consistent concentration dependent pattern with regard to enzyme type and plants organ. For instance, the APX and CAT activities decreased in shoots and increased in roots as the exposure concentration increased. The SOD and POD activity decreased in roots with increasing exposure concentrations, but their changes are irregular in shoots.

The contents of the non-enzymatic antioxidants ascorbic acid (ASA), reduced glutathione (GSH) and the carotenoids did not change significantly following any of the exposure modalities (**Table 2.1**; **Table S2.2**).

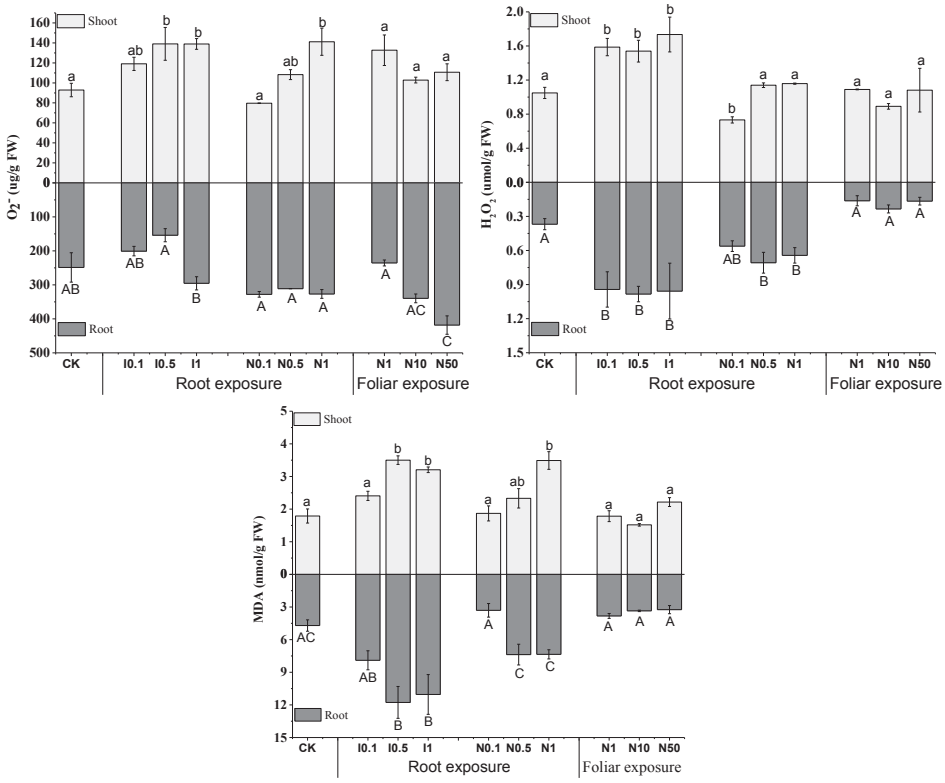

Figure 2.3. $O_2^{\cdot-}$, H_2O_2 and MDA production in *Lactuca sativa* exposed to different concentrations of $AgNPs_{(total)}$ and $AgNPs_{(ion)}$ after 15 days of exposure. Data are mean ± SE (n = 4). Within the same plant tissue, the different letters in the same group indicate statistically significant differences between treatments at $p<0.05$. I0.1, 0.5 and 1 represent *Lactuca sativa* exposed to the $AgNPs_{(ion)}$ concentrations as released from AgNPs suspensions with nominal concentrations of 0.1,0.5 and 1 mg/L; N0.1, 0.5, 1, 10 and 50 represent *Lactuca sativa* exposed to nominal $AgNPs_{(total)}$ concentrations of 0.1, 0.5, 1, 10 and 50 mg/L

2.3.5 Accumulation and translocation of silver in lettuce tissue

Significant differences (**Figure 2.4**; **Table S2.2**) were found in Ag accumulation in roots/shoots of lettuce after 15 d of exposure for all exposure scenarios with a general concentration-dependent increase. An exposure pathway- and a particle-specific effect on the accumulation were observed as well. For instance, the Ag accumulation in whole plants (root+shoot) for $AgNPs_{(total)}$ was much higher than the accumulation for the corresponding $AgNPs_{(ion)}$ concentration and differed by a factor of 2.7 - 17.4 times for root exposure and 2.9 - 4.1 times for single leaf exposure. In addition, at

equivalent exposure concentrations, more Ag accumulated in lettuce plants following root exposure than following foliar exposure (**Figure 2.4** A and B), with a significant difference observed in N0.5 and N1 treatments (t-test, $p<0.05$).

Regarding Ag enrichment factors (EFs), significant differences (**Table 2.2**; **Table S2.2**) among different exposure concentrations were observed for all groups with the exception of the group of root exposure to $AgNPs_{(total)}$ (ANOVA, $p=0.285$). The EFs of $AgNPs_{(total)}$ were higher than the EFs for the corresponding $AgNPs_{(ion)}$ for root exposure (t-test, $p<0.05$; **Table 2.2**) with the treatment at the lowest concentration of 0.1 mg/L as the exception, while the corresponding concentration of $AgNPs_{(ion)}$ was higher than the concentration of $AgNPs_{(total)}$ for single leaf exposure (t-test, $p<0.05$; **Table 2.2**). This suggests that $AgNPs_{(particle)}$ are more inclined to be taken up by root exposure whereas $AgNPs_{(ion)}$ was more inclined to be taken up via leaf exposure. This indicates a Ag form-dependent uptake for different exposure ways. The EFs of $AgNPs_{(total)}$ in lettuce via different exposure routes follow the order: root exposure > foliar exposure > exposure via single leaf immersion. This suggests an exposure pathway-specific impact on Ag accumulation in lettuce plants.

Likewise, significant differences (**Table 2.2**; **Table S2.2**) among the translocation factors (TFs) for different exposure concentrations were only observed in the $AgNPs_{(total)}$ exposure groups via root exposure and foliar exposure, with a decreasing tendency upon increasing exposure concentration. In addition, the TFs of the $AgNPs_{(ion)}$ were higher than the corresponding $AgNPs_{(total)}$ for root exposure at all concentrations (t-test, $p<0.05$; **Table 2.2**) while no significant differences were observed between $AgNPs_{(total)}$ and $AgNPs_{(ion)}$ for single leaf exposure (t-test, $p>0.05$; **Table 2.2**). For $AgNPs_{(total)}$ exposure, the TFs decreased in the following order for different exposure pathways: foliar exposure > single leaf immersion exposure > root exposure. This order indicates that Ag is more inclined to be transmitted from the shoots to the roots instead of being translocated from the roots to the shoots.

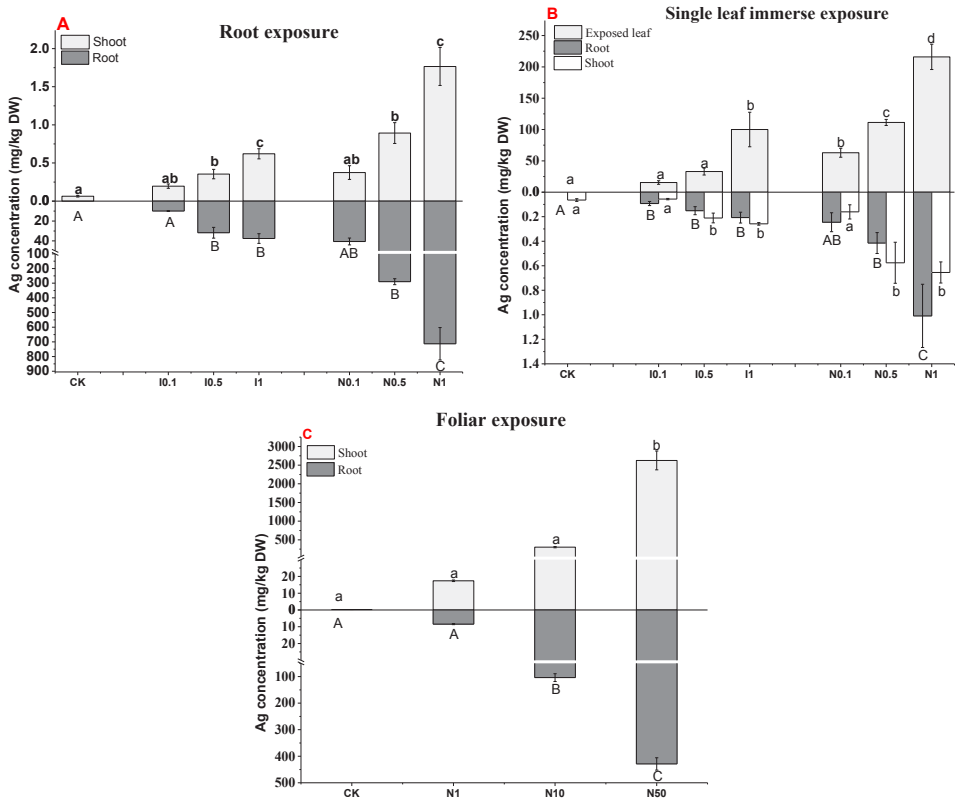

Figure 2.4. Ag concentration in lettuces after exposure to different concentrations of AgNPs and corresponding dissolved Ag^{+} for 15 days. Data are mean ± SE (n = 4). Within the same plant tissue, the different letters in the same group represent statistically significant differences between the treatments at $p< 0.05$. I0.1, 0.5 and 1 represent *Lactuca sativa* exposed to the $AgNPs_{(ion)}$ concentrations as released from AgNPs suspensions with nominal concentrations of 0.1,0.5 and 1 mg/L; N0.1, 0.5, 1, 10 and 50 represent *Lactuca sativa* exposed to nominal $AgNPs_{(total)}$ concentrations of 0.1, 0.5, 1, 10 and 50 mg/L.

Table 2.1. Variations enzymatic antioxidants (SOD, CAT, APX and POD) and non-enzymatic antioxidants activity (ASA, GSH and Carotenoid) in *Lactuca sativa* exposed to different concentrations of AgNPs(total) and AgNPs(ion) after 15 days of exposure. Data are mean ± SE (n = 4). Within the same plant tissue, the different letters in the same group indicate significant differences between treatments at $p<0.05$.

	Treatments		Enzymatic antioxidants				Non-enzymatic antioxidants[a]		
			SOD	APX	CAT	POD	ASA	GSH	Carotenoid
Root tissues		CK	107.1±16.8a	99.8±27.1a	128.8±12.1a	460.9±41.8a			
	Root exposure	I0.1	144.8±22.5a	200.8±33.2a	136.3 ±8.4a	183.3±19.2b			
		I0.5	237.8±28.6ab	120.7±7.5a	137.1±12.9a	198.1 ±12.3b			
		I1	341.9±46.8b	129.8±12.7a	287.5±16.4b	313.9±39.2b			
		N0.1	285.0±9.4ab	137.3±16.0a	140.9±8.0a	268.1±19.7b			
		N0.5	330.7±84.4bc	142.4±13.6a	189.2±18.6a	232.9±26.9b			
		N1	494.6±35.6c	78.1±10.0a	304.1±18.3b	307.5±6.15b			
	Foliar exposure	N1	93.0±9.7a	72.2±2.3a	229.0±17.9ab	438.6±55.7a			
		N10	74.2±13.4a	85.8±2.4a	245.3±18.5b	375.5±37.8a			
		N50	52.9±11.2a	181.8±1.2b	395.3±49.9c	377.0±33.5a			
Shoot tissues		CK	82.8±18.8a	112.0±20.6a	18.7±7.9a	123.3±21.1a	331.9±25.6ab	0.70±0.03a	0.19±0.02a
	Root exposure	I0.1	138.8±11.7a	118.5±12.4a	51.1±5.1ab	139.3±27.9a	370±18.1b	0.63±0.03a	0.18±0.01a
		I0.5	169.1±9.5a	165.2±34.3ab	97.1±18.0bc	204.4±15.5ab	270.3±23.3a	0.74±0.07a	0.16±0.01a
		I1	312.5±23.2b	257.1±19.7b	134.7±21.6c	284.7±28.0b	228.6±37.7a	0.75±0.04a	0.15±0.01a
		N0.1	294.5±25.6b	52.9±5.7a	24.4±4.0a	124.1±8.2a	260.6±18.3a	0.66±0.01a	0.16±0.01a
		N0.5	375.6±13.6b	49.2±2.6a	74.4±11.9a	201.8±18.4ab	256.0±45.5a	0.70±0.01a	0.13±0.01b
		N1	371.7±27.8b	191.7±31.0b	140.3±18.8b	257.01±27.7b	280.0±54.2a	0.74±0.03a	0.13±0.01b
	Foliar exposure	N1	99.0±25.3a	154.7±6.1a	41.9±4.1a	135.0±12.9a	296.9±31.5a	0.70±0.08a	0.18±0.01a
		N10	25.7±4.5a	23.9±6.9b	23.8±4.8a	117.8±6.1a	359.5±18.5a	0.81±0.02a	0.17±0.02a
		N50	56.6±12.2a	20.7±5.8b	23.1±3.7a	141.7±9.6a	347.5±31.8a	0.83±0.07a	0.14±0.01a

[a] Non-enzymatic antioxidants only analysed for shoot tissue

Table 2.2. Enrichment (EF) and transfer (TF) factors of Ag for lettuces exposed to the indicated concentrations of $AgNPs_{(total)}$ or corresponding dissolved $AgNPs_{(ion)}$. The data represent the mean ± SE (n =4). The different letters in the same group indicate statistically significant differences between treatments at $p<0.05$. * represent statistically significant differences for EFs or TFs between $AgNPs_{(total)}$ and $AgNPs_{(ion)}$ in same row(t-test, $p<0.05$).

Nominal exposure concentrations of AgNPs		EFs		TFs	
		$AgNPs_{(ion)}$	$AgNPs_{(total)}$	$AgNPs_{(ion)}$	$AgNPs_{(total)}$
Root exposure	0.1 mg/L	0.915±0.093a	0.554±0.036a*	0.072±0.008a	0.037±0.006a*
	0.5 mg/L	0.403±0.032b	0.639±0.035a*	0.043±0.007a	0.014±0.002b*
	1 mg/L	0.253±0.019b	0.614±0.025a*	0.042±0.005a	0.009±0.002b*
Single leaf immerse	0.1 mg/L	0.130±0.049a	0.084±nd a	0.078±0.018a	0.045±0.012a
	0.5 mg/L	0.051±0.006b	0.027±0.003b*	0.047±0.006a	0.043±0.007a
	1 mg/L	0.055±0.008b	0.027±0.001b*	0.029±0.007a	0.047±0.013a
Foliar exposure	1 mg/L		0.188±0.005a		0.174±0.017a
	10 mg/L		0.193±0.020ab		0.092±0.006b
	50 mg/L		0.271±0.024a		0.036±0.006c

2.3.6 Relative contribution of $AgNPs_{(particle)}$ and $AgNPs_{(ion)}$ to toxicity and accumulation

As can be seen from **Table 2.3**, in the case of root exposure, the $AgNPs_{(particle)}$ contributed more to toxicity than $AgNPs_{(ion)}$ regardless of the plant tissue (root, shoot, or the whole plant). The $AgNPs_{(particle)}$ accounted for more than 65% of the overall toxicity. The contributions of the $AgNPs_{(particle)}$ to the overall toxicity show a decreasing tendency upon increasing exposure concentration. Similarly, the ratio of particles versus ions in the AgNPs suspensions decreased from 5.0 to 4.1 when the exposure concentrations increased from 0.1 to 1 mg/L. Additionally, the relative contribution of the particulate Ag to the overall Ag accumulation in plants was much higher than the contribution of the corresponding $AgNPs_{(ion)}$ as well, accounting for about 67 - 95% for root exposure and 78 - 63% for leaf exposure in whole plant at all exposure concentrations. In summary, exposed plants to $AgNPs_{(total)}$ following different exposure pathways caused differences in the phytotoxicity and total Ag accumulation in plants, but the dominant role of $AgNPs_{(particle)}$ in the contribution of Ag accumulation was similar for the two exposure pathways. In addition, when the exposure concentrations of $AgNPs_{(total)}$ increased, the relative contribution of

$AgNPs_{(ion)}$ to the overall Ag accumulation decreased for root exposure whereas the $AgNPs_{(ion)}$ contributions increased in the case of foliar exposure (**Table 2.3**).

Table 2.3. Relative contribution (%) of AgNPs(particle) and AgNPs(ion) to toxicity and accumulation at different concentrations of AgNPs suspensions.

	AgNPs suspension	Root exposure				Single leaf immerse exposure	
		Relative contribution to biomass decrease		Relative contribution to accumulation		Relative contribution to accumulation	
		$AgNPs_{(particle)}$	$AgNPs_{(ion)}$	$AgNPs_{(particle)}$	$AgNPs_{(ion)}$	$AgNPs_{(particle)}$	$AgNPs_{(ion)}$
Root	0.1 mg/L	88.5	11.5	75.5	24.5	62.2	37.8
	0.5 mg/L	65.5	34.5	89.0	11.0	63.7	36.3
	1 mg/L	72.5	27.5	94.7	5.3	79.5	20.5
Shoot	0.1 mg/L	94.8	5.2	47.6	52.4	65.0	35.0
	0.5 mg/L	79.2	20.8	60.3	39.7	63.5	36.5
	1 mg/L	75.8	24.2	64.8	35.2	60.5	39.5
Whole plant	0.1 mg/L	93.4	6.6	67.3	32.7	77.6	22.4
	0.5 mg/L	76.0	24.0	87.4	12.6	68.9	31.1
	1 mg/L	74.8	25.2	94.5	5.5	63.2	36.8

2.4 Discussion

In this study, the uptake, translocation and various response endpoints in lettuce after 15 days of exposure to AgNPs suspensions and dissolved Ag-ions following foliar versus root pathway were compared. Explicitly the effects induced by ionic Ag released from AgNPs versus the particle-related effects of $AgNPs_{(particle)}$ on phytotoxicity and ROS in lettuce were differentiated. This is one of the first studies focusing on higher plants in which the exposure pathways of foliar or root exposure are considered. AgNPs are one of the most commercialized nanoparticles available[181,182] and (unwanted) impacts on primary producers have been studied intensively, but the focus has been mostly on aquatic primary producers, such as algae and duckweed[61,164,166,183].

The results of this study demonstrate that both the released ions and particulate Ag cause adverse impacts on the growth of lettuce in a dose-dependent manner when

using biomass as the endpoint of effect assessment (**Figure 2.2**). Importantly, the results of assessment of the relative contribution to biomass reduction revealed that particulate Ag was found to dominate the toxicity of AgNPs suspensions, although the contribution of particulate Ag to the overall toxicity decreased slightly with increasing exposure concentrations (**Table 2.3**). Similarly, previous studies also reported that particulate Ag outperforms the corresponding dissolved ions with regard to the overall toxicity to other vascular plants species, including *Arabidopsis thaliana*[166] and *Lolium multiflorum*[61].

Internalization of AgNPs was reported, with their bioavailability comparable to[184], lower than[185], or even higher[110] than that of Ag-ions depending on experimental conditions and plant species. In present study, the relative contributions of $AgNPs_{(particle)}$ to the overall Ag accumulation were higher than that of the corresponding $AgNPs_{(ions)}$ regardless of exposure concentrations and pathways. Moreover, the EFs of $AgNPs_{(total)}$ were slightly higher than in case of the corresponding $AgNPs_{(ions)}$ via root exposure. Taken together, these observations confirmed that $AgNPs_{(particle)}$ play a dominant role in the accumulation of Ag in lettuce exposed to $AgNPs_{(total)}$. The results obtained in this study are not in line with the understanding of other researchers of uptake, as Ag-ions are thought to be more readily internalized than particulate Ag in plant tissues[186] because the cell wall and the cell membrane constitute a barrier for particle internalization[185]. The findings of present study could be in part caused by the large proportion of the $AgNPs_{(particle)}$ in AgNPs suspensions, as exposure concentrations of $AgNPs_{(particle)}$ were approximately 5 times higher than the exposure concentrations of $AgNPs_{(ions)}$ in the AgNPs suspensions. This is in line with other studies, where the accumulation of Ag in plants was found to be positively correlated with the amount of AgNPs in the medium[161,165,173]. Similarly, previous studies have also discovered that the accumulation of Ag in the AgNPs treatments was much higher than in the case of Ag-ions treatments[57], even at the same exposure level[187]. Yang et al.[187]confirmed the direct uptake of Ag particles; and nanoparticulate Ag was the main Ag species accumulated in plants. The reason they suggested for this finding is that Ag-ions bind easily to hard and soft ligand residues on the cell wall (e.g., hydroxyl, carboxyl, amino, and thiol groups), which could immobilize Ag-ions on the root surface and limit

their internalization[187].

The uptake and accumulation of Ag in organisms have been reported to be responsible for the toxicity of AgNPs in many cases. Our results also agree with this general finding as upon increased Ag accumulation in plants, increased reduction in biomass was found. The pattern of $AgNPs_{(particle)}$ contribution to the overall Ag accumulation is consistent with the contribution of $AgNPs_{(particle)}$ to the overall toxicity. This suggests that the toxicity induced by the uptake and accumulation of Ag was mainly due to the intracellular uptake and accumulation of particulate Ag. After uptake and accumulation of $AgNPs_{(total)}$, particles can deposit and/or aggregate in plasmodesmata and in the cell wall[110], which might cause mechanical damage[188] and/or the blockage of intercellular communication. This could affect nutrient uptake and translocation, and the regulation of plasma membrane receptors, as well as plasma membrane recycling and signaling[189] in plants. Additionally, once AgNPs accumulate in plants, small amounts of Ag-ions could be released *in vivo* from the particles[90,161,190]. The released Ag-ions would in-place biological transform to secondary particles (e.g. AgNPs, Ag_2S, AgCl-NPs and others Ag-species)[90,161,187]. It was reported that in general the newly formed particles were about 2-3 times larger than the originally dosed AgNPs[161]. Both the dissolution from the accumulated AgNPs and the progress of forming secondary particles *in vivo* could also partially inhibit the plant growth[90,190].

Based on previous literature assessing the overall toxicity of nanoparticle suspensions, the main mechanism driving the phytotoxicity of nanoparticles is the production of excess reactive oxygen species and/or the cellular uptake of metallic Ag[38,190]. It was reported that induced oxidative stress levels in plants can lead to lipid peroxidation and damaged cell membrane permeability, eventually resulting in growth inhibition in plants[191]. This study confirmed that oxidative stress expressed as $O_2^{\cdot -}$, H_2O_2 and MDA contents was enhanced in roots and/or shoots at higher exposure concentrations of $AgNPs_{(total)}$ relative to the control in case of root exposure. Interestingly, the ROS production in ionic treatments was higher or not significantly different from the ROS production in the corresponding $AgNPs_{(total)}$ treatments. This can be explained by the activation of the antioxidant system to counteract the

elevated ROS production and maintain the redox status. For instance, following root exposure, the SOD activity in plant roots/shoots of $AgNPs_{(total)}$ treatments was higher than for the corresponding $AgNPs_{(ion)}$ treatments, suggesting that more $O_2^{\cdot -}$ in $AgNPs_{(total)}$ treatments can be catalyzed to less toxic species by SOD[174]. As a result, the $O_2^{\cdot -}$ contents in plant roots/shoots of $AgNPs_{(total)}$ treatments were similar to/lower than the corresponding $AgNPs_{(ion)}$ treatments. A concentration-dependent influence on the enzymatic antioxidants can be noted because higher $AgNPs_{(total)}$ and $AgNPs_{(ion)}$ exposure concentrations induced higher enzymes activity when compared to control plants. However, following root exposure, APX activity in plant roots decreased with increasing exposure concentration and POD activity was lower than in the control. This implied that when the stresses exceed the tolerance threshold of plants, the antioxidant enzyme activity is depleted. Similar results were reported by Zhang et al.[60], who found that exposure to copper nanoparticles and ionic copper significantly decreased the antioxidant enzyme activities in wheat (*Triticum aestivum* L.) as compared to the control. Considering the results of the $AgNPs_{(total)}$ and $AgNPs_{(ion)}$ treated plants, the SOD, CAT and POD activities in $AgNPs_{(total)}$ treated plant roots/shoots were just slightly higher than/similar to the corresponding $AgNPs_{(ion)}$ treatments, and hence an ionic-specific influence on enzymatic antioxidant activities became obvious. This means that the toxicity of $AgNPs_{(total)}$ caused by oxidative damage was predominantly from the Ag-ions.

The impact of exposure pathways on toxicity and uptake of NPs in plants is still an open question. The observations from this study clearly demonstrated that root exposure to AgNPs had a stronger negative effect on plants than foliar exposure when biomass was selected as the endpoint of assessment, even though the exposure amount of total Ag (0.048 mg) was 10 times lower than the amount (1.12mg) in case of foliar exposure. Although an irregular trend was observed for antioxidants for foliar exposure, the MDA in different treatments also indicated that root exposure induced more toxicity than foliar exposure to some extent as MDA is indicative of the extent of lipid peroxidation content. The accumulation and translocation of AgNPs depending on the exposure pathways were also observed in present study. The plants accumulated more Ag following root exposure, but the translocation of Ag inside the plants from the exposed part to the unexposed part is more efficient in

case of foliar exposure (**Table 2.2**). Not only leaf-root translocation but also leaf-leaf translocation of Ag was observed for foliar exposure. This difference is likely due to the different pathways/mechanisms involved in Ag uptake and translocation between root exposure and foliar exposure. The entrance of AgNPs into plants by foliar exposure is most likely through stomatal openings, and across the cuticles via hydrophilic pores and/or via cuticle diffusion and direct disruption[129]. After foliar uptake, ions or particles are transported to other parts of plant (unexposed leaves, roots) through the phloem system[167,168,192]. It is reported that the pressure gradient or the mass flow of photosynthate in leaves drive the flow stream of nanoparticles and assist them to move in the phloem through phloem loading mechanisms[69,167,193,]. For root uptake of NPs, the most accepted mode is that NPs are adsorbed onto the root surface firstly and then penetrate the cell walls and the plasma membranes of the epidermal layers in the roots. The ions and particles inside plants are transported from the root to the aerial part via xylem loading by either the apoplastic pathway or the symplastic pathway, which in turn are driven by the transpiration stream[193]. As reported[194,195], root exposure to AgNPs suspensions can significantly reduce the water transpiration, thus the upwards movement of Ag could be inhibited. This pathway likely occurred as particles trafficked through the plant organs and induced biomass reduction were reported.

The results obtained from present study have implications for food safety as the fate of AgNPs in plants was affected by the exposure concentrations and the mode of application. Moreover, since NPs are not fully removed by washing with water, AgNPs in and on crops may potentially be transferred to humans. Strategies to limit human consumption of metallic NPs originating from soil fertilizer, atmospheric deposits and agricultural foliar sprays should therefore raise more attention. In addition, the results of this study provide information on the effects of environmental transfer of nanoformulated agricultural products that are applied intentionally to roots or leaves. Furthermore, the understanding of the mechanisms of AgNPs entrance and translocation to all the plant parts via foliar or root pathway are not well-developed. Studies at subcellular levels are thus required to explore this issue in detail. Finally, literature suggests that different NPs will present different solubility and plant homeostasis and regulation. Thus, more studies involving a

wider range of NPs, exposure conditions, plant species and plant growth stages should be conducted to investigate the toxicity and internalization of NPs in the future.

2.5 Conclusions

This research has revealed the response chains within the plants for different forms of Ag in AgNPs suspensions following different exposure routes. The action chain of toxicity of particulate Ag was induced by the penetration of AgNPs into cells, followed by the translocation to various organs and by suggested blocking of internal trafficking, thus resulting in biomass reduction. The toxicity caused by the ions in AgNPs suspension was mainly due to the generation of oxidative stress, whether induced by extracellularly adherence of ions to the plants or by the accumulation of Ag in the plants. In addition, the relative contributions of $AgNPs_{(particle)}$ to the overall toxicity and the Ag accumulation in plants of AgNPs suspensions were 75-93% and 63%-95%, respectively, regardless of exposure pathway, indicating that the $AgNPs_{(particle)}$ dominated the toxicity of AgNPs suspensions to plants rather than $AgNPs_{(ion)}$. The exposure pathway significantly affects AgNPs uptake and phytotoxicity in lettuce, with the biomass decreasing and Ag accumulation via root exposure being much higher. Although particulate Ag contributed more to the accumulation of Ag in plants, the ionic Ag was more inclined to be transported to other parts of the plant as the TFs of $AgNPs_{(ion)}$ were higher than the TFs of $AgNPs_{(total)}$. Overall, our observations, together with mechanistic explanations, will improve the understanding of the interaction of AgNPs and terrestrial plants, as well as the hazard evaluation AgNPs exposures either being intentionally added applications in agriculture as well as unintentionally exposures from air-born emissions and soil emissions.

2.6 Supplementary Information

ROS production analysis.

Superoxide radical ($O_2\cdot^-$). 0.5 mL of the supernatant, 0.90 mL of 50 mM potassium phosphate buffer (pH 7.8), and 0.10 mL of 10 mM hydroxylamine hydrochloride were mixed together and incubated at 25 °C for 30 min. After incubation, 0.6 mL of the above reaction mixture was removed, and 0.6 mL of 17 mM sulphanilamide and 0.6 mL of 7mM a-naphthylamine were added in order, and the mixture was further kept at 25°C for 20 min. The absorbance of the supernatant was read at 530 nm and a standard curve was used to calculate the generation rate of $O_2\cdot^-$.[196]

H_2O_2 Content. After extraction, the homogenate was centrifuged at 12,000 g for 15 min. 0.5 ml of the supernatant was mixed with 0.5 ml of potassium phosphate buffer (10 mM, pH 7) and 1 ml of 1 M potassium iodide (KI) was added and checked their absorbance at 390 nm. The content of H_2O_2 was given on a standard curve. [177]

Malondialdehyde (MDA).0.2g fresh shoots samples were homogenized with 2 ml of pre-cooled 0.1% (w/v) trichloroacetic acid (TCA). After they were ground in an ice bath, the solid phase was centrifuged at 10,000 × g for 15 min at 4 °C. next, 1 ml of the supernatant was added to 1/(2) ml 0.5% (w:v) TBA in 20% TCA and then boiled for 30min at 95 °C, then quickly cooled in an ice bath and centrifuged at 10000g for 15 min and finally were measured by a multi-well spectrophotometer at 450, 532 and 600 nm. [177]

Antioxidant enzyme assays

Enzyme Extraction. The tissue samples were homogenized in ice cold 50 mM sodium phosphate buffer (pH 7.8) containing 1 mM EDTA and 1% (w/v) polyvinylpyrrolidone (PVPP) at a 1:9 w/v ratio and using a pre-cooled ball mill. The extract was obtained after centrifugation (10,000 rpm, 20 min, 4 °C). The supernatant was used for enzyme activity assay.

Superoxide dismutase (SOD). 50 µL the supernatants(enzyme extract) and 2.95ml 0.05M phosphate buffer (pH 7.8) containing 13 mM L-methionine, 100 nM EDTA-Na_2, 75 µM NBT and 2 µM riboflavin were mixed in cuvette and placed in the plant growth chamber with light intensity 250 µmol $m^{-2}s^{-1}$ (4000 lux) for 20 min. Blank A consisted of the assay mixture plus the enzyme extract, and was placed in dark while

Blank B that included all components of the assay mixture except the enzyme extract was placed in light. The reaction stopped when the lamp was switched off and the tubes were placed in darkness. Reduction of NBT was recorded at 560 nm. One unit of the enzyme activity was defined as the amount of enzyme required to result in a 50% inhibition of the rate of NBT reduction at 560 nm.[197]

Peroxidase (POD). 50 µL of enzyme extract was mixed with reaction buffer containing 2.75 mL/(1.75mL)of 50 mM sodium phosphate buffer (pH 7.0) and 0.1 mL of 4% guaiacol in cuvette and 0.1 mL of 1% H_2O_2 was used to initiate the reaction. Increased absorbance was recorded at 470 nm for 2 min. One unit of enzyme activity was defined as the amount of the enzyme which caused a change of 0.001 in absorbance per minute. [174]

Catalase (CAT). 100 µL of enzyme extract was placed in a quartz cuvette with 1.9 mL/(2.9mL) of 15 mM H_2O_2 in phosphate buffer(50mM,pH=7), and the absorbance was recorded at 240 nm for 3min. The H_2O_2 extinction coefficient was 23.148 mM^{-1} cm^{-1}. [174]

Ascorbate peroxidase (APX). 100 µL of enzyme extract was placed in a quartz cuvette with 886 µL of 0.1M phosphate buffer at pH=7.4 and 4 µL of 25 mM ascorbate were placed in a quartz cuvette. Decreased absorbance was monitored at 290 nm over a period of 4min at 30-s intervals after initiating the reaction with 10 µL of 17 mM H_2O_2 at 290 nm. The activity was calculated using an extinction coefficient of $2.8 mM^{-1} \cdot cm^{-1}$.[198]

Non-enzymatic antioxidants.

Ascorbate content. The ascorbic acid (µM/g Fresh weight) content was estimated spectrophotometrically at 525 nm following Kampfenkel et al.[178] comparing it with the standard curve of L-ascorbic acid. 0.1g of frozen tissue was ground with 0.8 ml 6% (v/v) TCA with a mortar and pestle in liquid nitrogen. The homogenate was centrifuged at 15,600 g for 5 min at 4 °C. Total ascorbate was determined in a reaction mixture consisting of 200 µL of supernatant, 200 µL of 150 mM phosphate buffer (pH 7.4) containing 5 mM EDTA and 100 µL of 10 mM dithiothreitol (DTT) to reduce DAsA to AsA. After 15 min at 25°C, 100 µL of 0.5% (w/v) N-ethylmaieimide

was added to remove excess DTT. AsA was assayed in a similar manner except that 200 µL of deionized H_2O was substituted for DTT and N-ethylmaleimide. Colour was developed in both series of reaction mixtures with the addition of 400 µL of 10% (w/ v) TCA, 400 µL of 44% (v/v) H_3PO4, 400 µL of 4% a,a'-dipyridyl in 70% (v/v) ethanol and 200 µL of 3% $FeCl_3$. The reaction mixtures were incubated at 40°C for 60 min; the absorbance was then recorded at 525 nm. The amount of ascorbate (µM g−1 FW) was estimated with a standard curve of ascorbic acid (10–100 µM).[199]

GSH. Reduced glutathione level was assayed by the method of Beutler et al.[200] based on the fact that the sulfhydryl groups present in the tissue homogenates react with 5,5'-dithiobis (2-nitrobenzoic acid) (DTNB) to form a yellow dye with maximum absorbance and read at 412 nm. Briefly, 0.1 g of tissues was homogenized in 12% TCA or 5 mM EDTA sodium in 10% TCA (1:10) and centrifuged at 5000g for 5 min at 4°C. 0.5 ml of supernatant was added to 2.5 mM DTNB in 0.2 M sodium phosphate buffer pH 8.0, and the formation of the thiolate anion was immediately measured at 412 nm. Determinations were expressed in µmol g^{-1}.[201]

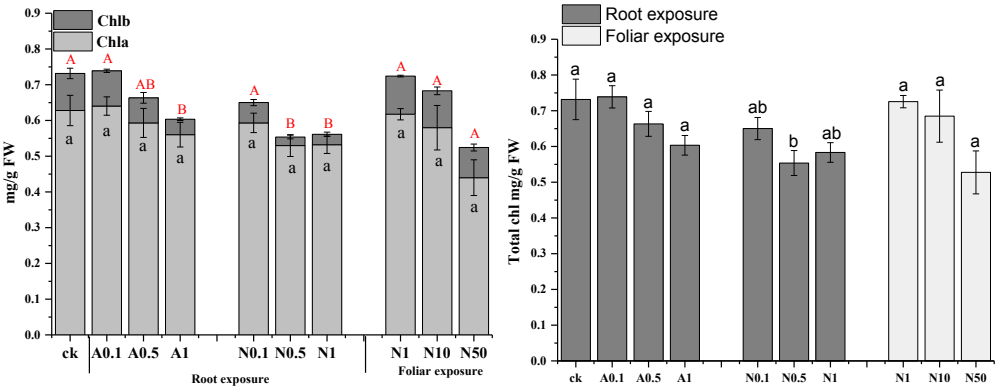

Figure S2.1. Effects of $AgNPs_{(total)}$ and ionic Ag on chlorophyll contents in the leaves after 15 days of exposure. Data are mean ± SE (n = 4). Within the same plant tissue, the different letters in the same group indicate statistically significant differences between treatments at $p<0.05$. I0.1, 0.5 and 1 represent Lactuca sativa exposed to the AgNPs(ion) concentrations as released from AgNPs suspensions with nominal concentrations of 0.1,0.5 and 1 mg/L; N0.1, 0.5, 1, 10 and 50 represent Lactuca sativa exposed to nominal AgNPs(total) concentrations of 0.1, 0.5, 1, 10 and 50 mg/L.

Table S2.1. Composition of the Hoagland's nutrient solution.

Chemicals	Concentration (mg/L)
$Ca(NO_3)_2{\cdot}4H_2O$	945
KNO_3	607
$MgSO_4{\cdot}7H_2O$	493
$NH_4H_2PO_4$	115
H_2BO_3	1.48
$Mn(NO_3)_2{\cdot}4H_2O$	1
$Zn(NO_3)_2{\cdot}6H_2O$	1.19
$CuSO_4{\cdot}5H_2O$	0.05
Mo $Na_2O_4.2\ H_2O$	0.02
$FeSO_4.7\ H_2O$	11.1

¼ Hoagland solution (pH is measured and adjusted at 6) is obtained after 4 times dilution of the Hoagland's solution with MilliQ water

Table S2.2. Results of statistical analysis of variance (ANOVA) of various endpoints in *Lactuca sativa* exposed to different concentrations of $AgNPs_{(total)}$ and $AgNPs_{(ion)}$ for 15d.

Exposure pathway	Type of tissues	End points	P value	
			$AgNPs_{(total)}$	$AgNPs_{(ion)}$
Root exposure	Root tissues	Biomass	<0.0001	0.004
		Ag concentration in plants	<0.0001	<0.0001
		$O_2^{-}\cdot$	0.134	0.041
		H_2O_2	0.037	0.021
		MDA	0.004	0.006
		SOD	0.001	0.006
		APX	0.219	0.126
		CAT	<0.0001	<0.0001
		POD	0.001	<0.0005
	Shoot tissues	Biomass	<0.0001	0.001
		Ag concentration in plants	<0.0001	<0.0001
		$O_2^{-}\cdot$	0.009	0.004
		H_2O_2	<0.0005	0.023
		MDA	0.005	0.001
		SOD	<0.0001	<0.0001
		APX	0.002	0.007
		CAT	0.0001	0.001
		POD	0.002	0.003
		ASA	0.514	0.028
		GSH	0.077	0.260
		Carotenoid	0.005	0.169
		Chlorophyll a	0.195	0.433
		Chlorophyll b	<0.0005	0.007
		EFs	0.285	<0.0001
		TFs	0.003	0.063

Single leaf immerse exposure	Exposed leaf	Ag concentration in plants	<0.0001	0.001
	Root tissues	Ag concentration in plants	0.001	<0.0001
	Shoot tissues	Ag concentration in plants	0.002	0.0001
		EFs	<0.0001	0.011
		TFs	0.975	0.067
Foliar exposure	Root tissues	Biomass	<0.0001	
		Ag concentration in plants	<0.0001	
		$O_2^{-}\cdot$	0.011	
		H_2O_2	0.042	
		MDA	0.097	
		SOD	0.066	
		APX	0.024	
		CAT	<0.0005	
		POD	0.434	
	Shoot tissues	Biomass	<0.0001	
		Ag concentration in plants	<0.0001	
		$O_2^{-}\cdot$	0.077	
		H_2O_2	0.673	
		MDA	0.150	
		SOD	0.127	
		APX	0.0002	
		CAT	0.090	
		POD	0.781	
		ASA	0.434	
		GSH	0.292	
		Carotenoid	0.146	
		Chlorophyll a	0.063	
		Chlorophyll b	0.554	
		EFs	0.031	
		TFs	<0.0005	

Table S2.3. Hydrodynamic Diameter and Zeta-Potential of AgNPs Suspensions in 1/4 Hoagland solution

Nominal concentration	Hydrodynamic diameter (nm)			Zeta-potential (mV)		
	1 h	24 h	48 h	1 h	24 h	48 h
0.1 mg/L	469±31	1263±38	1781±230	-16±0.5	-15.4±0.6	-14.6±0.6
0.5 mg/L	256±27	578±67	1090±102	-14.7±3.7	-13.5±3.5	-10.9±5.4
1 mg/L	246±26	692 ±64	1190±262	-16±0.4	-15.1±0.6	-15.3±0.5
10 mg/L	43±1	62±23	71.1±27	-15.2±0.5	-14.8±0.4	-12.1±0.4
50 mg/L	35±7	35±2	37±1	-12.0±0.7	-10.3±0.3	-9.5±0.5

Table S2.4. The actual exposure concentrations of AgNPs(total) and AgNPs(ion) in terms of initial concentrations or time weighted average concentration

Nominal concentration (mg/L)	Initial measured concentration (mg/L)			TWA measured concentration (mg/L)			Total amount of Ag for Root/single leaf immerse exposure (mg)	Total amount of Ag for Foliar exposure amount (mg)
	$AgNPs_{(total)}$	$AgNPs_{(ion)}$	$AgNPs_{(particle)}$	$AgNPs_{(total)}$	$AgNPs_{(ion)}$	$AgNPs_{(particle)}$	$AgNPs_{(total)}$	$AgNPs_{(total)}$
0.1	0.0620	0.0014	0.0606	0.0351	0.0063	0.0288	0.004	
0.5	0.3763	0.0230	0.3533	0.2203	0.0366	0.1837	0.0242	
1	0.7133	0.0587	0.6547	0.4386	0.0850	0.3536	0.0482	0.0185
10	8.3467	1.1400	7.2067					0.2160
50	43.3500	6.8233	36.7433					1.1217

Table S2.5. Variations to control(%) of the parameters related to oxidative stress in lettuces exposed to the indicated concentrations of $AgNPs_{(total)}$ or corresponding $AgNPs_{(ion)}$.

			Oxidative stress			Enzymatic antioxidants				Non-enzymatic antioxidants		
			$O_2^{\cdot -}$	H2O2	MDA	SOD	APX	CAT	POD	ASA	GSH	Carotenoid
Root tissues	Root exposure	I0.1	-19.3	155.8	67.9	35.2	101.1	5.8	-60.2			
		I0.5	-38.2	166.8	150.2	122.1	20.9	6.5	-57.0			
		I1	18.1	159.7	134.6	219.3	30	123.2	-31.9			
		N0.1	31.8	52.3	-29.7	166.1	37.5	-23.1	-59.8			
		N0.5	25.0	92	56.7	208.8	42.6	-55.9	-49.5			
		N1	31.3	74.5	53.8	361.9	-21.8	147.5	-50			
	Foliar exposure	N1	-5.3	-55.8	-18.8	-13.1	-27.7	77.7	-4.8			
		N10	36.5	-36.4	-28.7	-30.7	-14	90.4	-25.6			
		N50	68.1	-55	-31	-50.6	82.1	206.8	-18.2			
Shoot tissues	Root exposure	I0.1	28.2	51.3	34.5	58	5.8	173.2	15.9	11.5	-9.4	-3.1
		I0.5	49.7	46.7	95.7	92.5	47.5	418.9	70.1	-18.5	6.2	-13.4
		I1	49.6	65.4	79.2	255.8	129.6	619.8	136.9	-31.1	7.5	-19.8
		N0.1	-14.2	-30.2	15.8	235.3	-52.7	30.4	3.3	-21.5	-6.1	-16.7
		N0.5	16.6	8.6	30.3	327.7	-56	297.6	67.9	-22.9	-0.7	-31.2
		N1	52.0	10.4	95	323.2	98.8	649.6	113.9	-15.6	6.6	-32.7
	Foliar exposure	N1	42.9	3.9	-0.3	12.7	38.1	123.6	12.3	-10.5	-0.2	-3.2
		N10	10.7	-15	-15.1	-70.7	-78.7	27.1	-2	17.5	15.8	-10
		N50	19.2	3.1	23.9	-35.5	-81.5	23.3	17.9	14	19.9	-26.5


Camp Nou,Barcelona, Spain, 2018


Porto, Portugal, 2018

Chapter 3

Quantifying the relative contribution of particulate versus dissolved silver to toxicity and uptake kinetics of silver nanowires in lettuce: impact of size and coating

Juan Wu, Qi Yu, Thijs Bosker, Martina G. Vijver, Willie J. G. M. Peijnenburg

Published in Nanotoxicology 14 (2020) 1399-1414

Abstract: Functionalized high-aspect-ratio silver nanowires (AgNWs) have been recognized as one of the most promising alternatives for fabricating products, with their use ranging from electronic devices to biomedical fields. Given concerns on the safety of AgNWs, there is an urgent need to investigate the relation between intrinsic properties of AgNWs and their toxicity. In this study, lettuce was exposed for either 6 or 18 days to different AgNWs to determine how the size/aspect ratio and coating of AgNWs affect the contributions of the dissolved and particulate Ag to the overall phytotoxicity and uptake kinetics. We found that the uncoated AgNW (39 nm diameter×8.4 μm length) dissolved fastest of all AgNWs investigated. The phytotoxicity, uptake rate constants and bioaccumulation factors of the PVP-coated AgNW (43 nm diameter×1.8 μm length) and the uncoated AgNW (39 nm diameter×8.4 μm length) were similar, and both were higher than that of the PVP-coated AgNW with the larger diameter(65 nm diameter×4.4 μm length). These results showed that the diameter of the AgNWs predominantly affected toxicity and Ag accumulation in plants. Particulate Ag was found to be the predominant driver/descriptor of overall toxicity and Ag accumulation in the plants rather than dissolved Ag for all AgNWs tested. The relative contribution of dissolved versus particulate Ag to the overall effects was influenced by the exposure concentration and the extent of dissolution of AgNWs. This work highlights inherent particulate-dependent effects of AgNWs in plants, and suggests that toxicokinetics should explicitly be considered for more nanoparticles and organisms, consequently providing more realistic input information for their environmental risk assessment.

3.1. Introduction

The widespread use of silver nanoparticles in products and applications has raised concerns about their potential side-effects on environmental and human health[41,57,62,202,203]. Numerous investigations have reported adverse impacts on a range of endpoints of spherical-shaped silver nanoparticles to both aquatic and terrestrial organisms, including impacts on growth or reproductive inhibition, generation of ROS, alteration of enzyme expression, DNA damage and genotoxicity[35,69, 204]. High aspect ratio silver nanowires and silver nanotubes are also an active area for commercialization and nanotechnology research, given their superior electrical,

plasmonic, optical and antibacterial properties[205,206,207,208].

To date, a very limited number of studies have discussed the biological effects of wire-shaped metallic nanoparticles on aquatic and terrestrial organisms. From those papers, morphological comparison studies of nanoparticles showed that the dissolution behavior and the biological effects of wire-shaped nanoparticles are distinctly different from the dissolution behavior and adverse effects of nanosphere or nanoplate analogues[87,89,209,210]. Intrinsic properties such as size, surface chemistry and charge of nanowires could play a key role in controlling their adverse effects to organisms, as has been widely confirmed by studies on spherical nanoparticles[81,89,211]. To the best of our knowledge, less than 15 studies have been published in which the impact of physicochemical properties of nanowires on their toxic effects were examined. Based on these studies, aspect ratio and length seem to play a dominant role in regulating the adverse effects of nanowires. However, four contradictory patterns of toxicity have been reported;

1) higher aspect ratio and longer nanowires induced increased cytotoxic[212,213,214,215] or;
2) lower aspect ratio and shorter nanowires induced higher toxicity to daphnia[208,216] or;
3) shorter nanowires presented more cytotoxicity than the longer nanowires without a consistent aspect ratio dependent pattern [217] or;
4) the length and aspect ratio do not affect toxicity[218,219,220].

Moreover, surface coating can affect the dissolution and the stability or aggregation of nanoparticles, which in turn may modulate the adverse effects of nanoparticles to organisms [29]. So far, most studies on nanowires concentrated on *in vitro* cytotoxicity and no studies on the effects of size/aspect ratio and coating of nanowires on plants are available. In addition, numerous studies suggested that the toxicity of silver nanospheres to aquatic and terrestrial organisms can be attributed to the release of ions from NPs[29,57]. However, our previous results showed that particulate Ag dominates phytotoxicity[221]. Given the importance of shape, it is therefore key to better understand whether the toxicity of silver nanowires suspension is exerted by nano-particulate Ag or by the released ionic Ag.

Extensive research on Ag nanospheres suggests that bioaccumulation of AgNPs is a determinant for their toxicological effects[38]. Importantly, previous studies showed that the cellular uptake of gold nanowires by mammalian cells[220,222] and silver nanowires by daphnids[216,223] were affected by their aspect ratio and length. To the best of our knowledge, there is currently no data is available on the bioaccumulation and phytotoxicity of AgNWs in terrestrial plants. Moreover, toxicokinetic and toxicodynamic models for nanoparticles have placed considerable emphasis on tracing metal accumulation in organisms in order to interpret their toxicological effects. Some studies have reported on parameters associated with uptake biokinetics of metal nanoparticles (e.g. uptake and elimination rate constant, as well as bioaccumulation factor)[224,225,226]. However, in most cases the measurements performed within these studies focused on total metal concentrations of metallic nanoparticles (particulate plus dissolved form), which prevents differentiating between the relative contributions of dissolved and particulate Ag to the phytotoxicity and toxicokinetics of AgNWs. It is critical to collect this data, as distinguishing the dissolved metal concentration and particulate concentration could increase the accuracy of quantification of kinetics parameters of soluble metallic nanoparticles[227]. This would help to provide a more accurate understanding of the particle-specific accumulation of nanoparticles in plants. However, currently it remains unclear whether the inherent properties of AgNWs not only influence dissolution, but also the uptake kinetics of AgNWs in plants. Plants, which play a vital role in providing ecosystems services and form the base of most food webs, are likely exposed to silver nanoparticles via air, soil and water[221]. Therefore, much more efforts in exploring the adverse impacts of silver nanowires on plants are necessary.

This study therefore aims to i) investigate the importance of the physicochemical properties of AgNWs on their toxicity and on the uptake of Ag in higher plants, and ii) to distinguish the corresponding relative contribution to suspension toxicity and Ag accumulation of ionic and particulate Ag present in suspensions. To this end, the widely cultivated vegetable lettuce (*Lactuca sativa*) was exposed to a series of concentrations of different types of silver nanowires and ionic Ag in hydroponic systems for 6 days to generate dose-toxic response curves. Subsequently, the EC_{25} level for each of the AgNWs was selected as the exposure concentration to quantify

the biokinetics parameters of Ag uptake in plants after 18 days of exposure. Since there are limited data available on the uptake and toxicity of Ag nanowires in higher plants, this study facilitates the establishment of toxicokinetic models to describe the accumulation of silver nanowires in higher plants.

3.2. Materials and methods

3.2.1 AgNW suspensions: preparation and characterization

$AgNO_3$ was obtained from Sigma-Aldrich (Zwijndrecht, the Netherlands). Original stock suspensions of polyvinylpyrrolidone (PVP) coated low aspect ratio AgNW (LAR-AgNW:43 nm diameter×1.8 μm length) and medium aspect ratio AgNW (MAR-AgNW: 65 nm diameter×4.4 μm length) were purchased from Nanogap (Milladoiro, Spain). Noteworthily, the PVP used in the two PVP-coated AgNWs was of the same composition and the same method and the same materials were used to coat the two nanowires. This means that there are no differences in the nature and the thickness of the PVP-coating between the two tested PVP-coated AgNWs. The uncoated high aspect ratio AgNWs (HAR-AgNW: 39 nm diameter×8.4 μm length) were purchased from Ras-Ag (Regensburg, Germany). All original stock suspensions of AgNWs were stored at 4 °C in the dark. The actual silver concentrations of the original stock AgNWs suspensions were measured in triplicate by means of Atomic Absorption Spectroscopy (AAS, PerkinElmer 1100 B, Waltham, MA, USA). Taking aliquots from the original stock AgNWs suspensions was always performed under a nitrogen atmosphere. Suspensions of AgNWs dispersed in 1/4 Hoagland solution (pH 6.0 ± 0.1) with a concentration of 50 mg/L were used to determine the actual size and shape by Transmission Electron Microscopy (TEM, JEOL 1010, JEOL Ltd., Tokyo, Japan) after sonication for 10 min. The composition of the Hoagland solution is described in **Table S2.1**, Supplementary material. The surface area and volume of the AgNWs were calculated assuming that the AgNWs possessed a perfect cylindrical structure. The basic physico-chemical data of the three AgNWs are presented in **Table S3.1**. The results discussed in this study are based on actual measured data and all data obtained from the TEM excluded the PVP coating.

3.2.2 AgNWs dissolution testing

The dissolution kinetics of suspensions of the AgNWs were monitored over 72 hours at the concentrations equaling the EC_{25} level of each AgNW. The dissolution experiments were conducted under the same conditions as used in the toxicity and uptake experiments but without plants to avoid underestimation due to the uptake of dissolved Ag by plants. For each AgNW suspension, 6 mL aliquots dispersed in 1/4 Hoagland solution for 1, 6, 12, 24, 48 and 72 h were collected in duplicate from the top 8 cm of the tubes. One of these samples was digested for at least 3 d at room temperature by addition of a few drops of concentrated nitric acid (65%) to determine the total concentration of AgNWs in the suspension (defined as $AgNWs_{(total)}$ hereafter). The other aliquot was centrifuged at 30,392 g for 30 min at 4 °C (Sorvall RC5Bplus centrifuge, Bleiswijk, Netherlands) and subsequently the supernatants were filtered via a syringe filter of 0.02 μm pore diameter (Anotop 25, Whatman, Eindhoven, The Netherlands). The obtained solutions represented the concentration of dissolved Ag in the suspensions (defined as $AgNWs_{(dissolved)}$), as determined using AAS after addition of a few drops of concentrated HNO_3. The particulate Ag concentrations were obtained as a function of exposure time by calculating the difference between $AgNWs_{(total)}$ and $AgNWs_{(dissolved)}$ at each timepoint. The assessments of the dissolution of each AgNW at each timepoint were performed in triplicate.

3.2.3 Plant pre-culture and toxicity assay

Lactuca sativa seeds obtained from Floveg GmbH (Kall, Germany) were sterilized with NaClO (0.5% w/v) for 15 min and cleaned with deionized tap water. After immersion in deionized water for 24 h, 15 seeds were germinated and grown in a Petri-dish containing 1/8 Hoagland solution for 2 weeks. The young seedlings were then transferred to tubes (one seedling per tube) with 22 mL of 1/4 Hoagland solution, and left to grow 7 d before being exposed to AgNWs. All experiments were performed in a climate room with 16 /8 h of light/darkness and 60 % relative humidity at a 20 /16 °C day/night temperature regime.

The toxicity tests in this study were carried out to establish the dose-response curves

of the AgNWs. The EC_{50} and EC_{25} values were calculated to compare the toxicity of the three AgNWs. Briefly, a series of actual exposure concentrations ranging from 0.006 to 3.94 (LAR-$AgNW_{(total)}$), 3.92 (MAR-$AgNW_{(total)}$) or 4.48 mg/L (HAR-$AgNW_{(total)}$) were prepared in 1/4 Hoagland solution of exposure groups containing uniform pre-grown seedlings. Exposure concentrations of Ag-ions (ranging from 0.005 to 0.80 mg/L) were used as a reference to obtain the dose-response curve of the ions ($AgNWs_{(dissolved)}$) released from the AgNWs in suspension. After exposure for 6 days, the biomass of the plants was recorded after the plants were washed thoroughly with deionized tap water and air-dried for 4 hours. The tubes used in this study were covered with aluminum foil and the medium was refreshed every 3 d. All treatments, including the control, were exposed for 6 days in quadruplicate at the same conditions of plants pre-growth.

3.2.4 Uptake experiments of AgNWs and dissolved Ag in plants

The EC_{25} level of each $AgNW_{(total)}$ based on the toxicity experiments described above, was selected to perform the uptake experiments of AgNWs in plants over 18 d. Dispersing the AgNWs into 1/4 Hoagland solution results in a mixture of particulate Ag and dissolved Ag ions which changes over time due to sedimentation of particle agglomerates and continuous dissolution of Ag-ions. Thus, in addition to exposure experiments with AgNWs suspensions, dissolved Ag exposure experiments using $AgNO_3$ were performed separately to obtain the relevant toxicity and uptake information about the dissolved ionic Ag. To study this, time weighted average (TWA) concentrations of ionic Ag at corresponding exposure time points obtained from the dissolution kinetic experiments of AgNWs, were selected as the exposure concentrations. The exposure experiments were performed using the same protocol as in the above mentioned toxicity experiments. One tube contained one plant, with three replicates per treatment. Ag-spiked 1/4 Hoagland solutions were refreshed every 3 d for a total of 18 d. At each exposure time point of 0.25, 0.5 1, 2, 3, 6, 9, 12 and 18 d, plants were collected to determine the Ag content in plant tissues.

After harvesting the plants from each exposure period, the whole plants were immersed in 10 mM HNO_3 for 30 min, transferred into 10 mM EDTA (Ethylenediaminetetraacetic acid) for 30 min, and finally thoroughly rinsed with

Milli-Q water to remove the strongly attached AgNWs/Ag-ions. Subsequently, the plants were divided into the root and shoot and oven-dried for at least 72 h at 70 °C. After determining the dry biomass of roots and shoots, the samples were digested by adding 6 mL of concentrated HNO_3 for 1 h at 120 °C, followed by adding 2 mL of H_2O_2 at 120 °C until the solutions were clear. Finally, the digest solutions were diluted by adding deionized water to a final volume of 3 mL and the concentrations of Ag were subsequently analysed using AAS. For quality control, blanks containing a Ag standard solution were digested with the same digestion procedure as used for the plants. Standard solutions of Ag at 0.5 mg/L were monitored every 20 samples to examine the stability of the machine. The exposure concentrations of each refreshed batch were determined and the standard deviations were less than 5%.

3.2.5 Data analysis

As Ag-ions are continuously released from AgNWs and the particulate Ag will sediment into the bottom of tubes, the exposure concentration of each AgNW and of the corresponding dissolved ions changes over time. The TWA method can catch the dynamic changes of NPs associated with exposure conditions and offers a more accurate and naturally relevant expression of the actual effective exposure of organisms to NPs than when using the static initial exposure concentrations [228]. Therefore, the expression of the exposure concentrations of $AgNWs_{(total)}$, $AgNWs_{(particulate)}$ and $AgNWs_{(dissolved)}$ was based on the time weighted average (TWA) concentration for each exposure period instead of expressing the exposure concentration by means of the initially measured concentrations. The TWA concentrations can be calculated according to the following equation:

$$C_{TWA} = \frac{\sum_{n=0}^{N}\left(\Delta t_n \frac{C_{n-1}+C_n}{2}\right)}{\sum_{n=1}^{N}\Delta t_n} \qquad (1)$$

Where n is the time interval number, N is the total number of intervals, Δt is the time interval, C is the concentration at the end of the time interval.

A first order kinetics equation was used to model the sedimentation process of AgNWs:

$$[Ag_{NW}]_t = ([Ag_{NP}]_0 - P_2) \times exp^{-K_S t} + P_1 \qquad (2)$$

The increase of the concentration of dissolved Ag released from each AgNW in 1/4 Hoagland solution followed first order kinetics:

$$[Ag^+]_t = (P_1 - [Ag^+]_0) \times exp^{-K_d t} + P_2 \quad (3)$$

Incorporation of the size and length of AgNWs, the dissolution of each AgNW in 1/4 Hoagland solution can be described as follows:

$$\frac{d[Ag^+]_t}{dt} = N_0 \rho \frac{dV}{dt} = N_0 KA = N_0 K_D (2\pi R^2 + 2\pi RL) \quad (4)$$

Where $[Ag^+]_t$ and $[Ag_{NW}]_t$ are the concentration of dissolved Ag-ions and particulate Ag at a given point in time with the units of mg/L, P_1 and P_2 are the concentration of particulate Ag and dissolved Ag-ions at equilibrium; K_d and K_S is the first-order rate constants of dissolution and sedimentation (d^{-1}), respectively. N_0 is the number of AgNWs present in one liter of suspension at t = 0 (1/L, $N_0 = \frac{C_{NP(0)}}{\rho V_{(0)}}$). V is the volume of AgNWs (μm^3). A is the area of the AgNWs (μm^2). R is the mean radius of AgNWs (nm). L is the mean length of the AgNWs (μm). K_D is the dissolution rate constant of AgNWs (ng/cm²/h). $[Ag^+]_t$, $[Ag_{NW}]_t$, $[Ag^+]_0$, $[Ag_{NW}]_0$ and time t were measured experimentally. Thus the rate constants can be calculated by fitting equations (2), (3) and (4).

The decrease of biomass of plants exposed to each AgNW suspension is induced by particulate and dissolved Ag together, with the modes of action widely believed to be independent. The response addition model is therefore used to calculate the relative contributions of particulate Ag and dissolved Ag in AgNWs suspensions to the observed toxicity[136,180]:

$$E_{(total)} = 1 - \left(\left(1 - E_{(particulate)}\right)\left(1 - E_{(dissolved)}\right)\right) \quad (5)$$

where $E_{(total)}$ represents the biomass decrease caused by the suspension of AgNWs as quantified experimentally. $E_{(dissolved)}$ is the decrease of biomass induced by ionic Ag present in the AgNWs suspension as calculated based on the dose-response curve of $AgNO_3$ towards lettuce biomass decrease. The biomass decrease caused by the particulate Ag in AgNWs can be calculated directly as $E_{(particulate)}$ is the only unknown

in the equation.

The concentrations of EC_{25} and EC_{50} for biomass decrease of plants exposed to three kinds of $AgNWs_{(total)}$, $AgNWs_{(particulate)}$ and ionic Ag were calculated with the dose-response-inhibition model in GraphPad using TWA and initial exposure concentrations, respectively.

The mass of Ag accumulated in plants tissues exposed to each AgNW and the corresponding dissolved Ag-ions over time can be described by equation (6):

$$\frac{d[Ag]_{plant}}{dt} = K_u[Ag]_{exposure} - K_e[Ag]_{plant} \quad (6)$$

Where K_u and K_e are the uptake rate constant (d^{-1}) and elimination rate constant (d^{-1}) of Ag from $AgNWs_{(total)}$, $AgNWs_{(particulate)}$ and the corresponding dissolved Ag, respectively.

Since at the initial phase of the accumulation process the uptake rate is expected to be much faster than the elimination rate, the elimination of Ag was assumed to be negligible, and equation (6) was simplified into

$$\frac{d[Ag]_{plant}}{dt} = K_u[Ag]_{exposure} \quad (7)$$

Integration of this differential equation leads to equation (8):

$$[Ag]_{plant}(t) = K_u[Ag]_{exposure}(t) \times t \quad (8)$$

Where $[Ag]_{plant}(t)$ is the mass of Ag accumulated in plant tissues (μg/plant), $[Ag]_{exposure}(t)$ is the exposure content of $AgNWs_{(total)}$, $AgNWs_{(particulate)}$ and the corresponding dissolved Ag-ions (μg), respectively. K_u is the uptake rate constant. The dynamic changes of exposure concentrations of $AgNWs_{(total)}$, $AgNWs_{(particulate)}$ and $AgNWs_{(dissolved)}$ should be considered when fitting this model. Thus, the uptake rate constant of $AgNWs_{(total)}$, $AgNWs_{(particulate)}$ and $AgNWs_{(dissolved)}$ from each AgNW were obtained by fitting equation (8) to the measured Ag content in plants and TWA exposure content of $AgNWs_{(total)}$, $AgNWs_{(particulate)}$ and $AgNWs_{(dissolved)}$ at each time point ranging from 1 h to 3 d.

The Ag bioaccumulation factor (BAF) was calculated using the following equation:

$$BAF = \frac{[Ag]_{plant}}{[Ag]_{medium}} \quad (9)$$

Where $[Ag]_{plant}$, the content of Ag in the plants (μg/plant), and $[Ag]_{medium}$, the content of Ag in the exposure medium (μg), were obtained experimentally.

The Ag translocation factor (TF), defined to evaluate the capacity of plants to transfer Ag from roots to the shoots, was calculated as follows:

$$\mathrm{TF} = \frac{[Ag]_{shoots}}{[Ag]_{roots}} \quad (10)$$

Where $[Ag]_{shoots}$ and $[Ag]_{root}$ represent the Ag content in plant shoot tissues and root tissues (μg/plant), respectively.

The differences for EC_{25}, EC_{50} and toxicokinetic parameters of accumulation of Ag among the different AgNWs were analysed for significance using one-way ANOVA followed by Turkey's honestly significant difference tests at $\alpha < 0.05$ using IBM SPSS Statistics 25. The Shapiro-Wilk test was used to check for normality and the Bartlett test for homogeneity of the variance of the data, with no deviations found for both. All results are expressed as mean ± standard error, based on 4 replicates for biomass decrease and 3 replicates for Ag bioaccumulation

3.3.Results

3.3.1 TEM characterization and dissolution behavior of AgNWs

The TEM pictures confirmed that the shapes of the three types of Ag nanoparticles used in this study were wire-like and that the diameters were in agreement with the information provided by the producer (**Table S3.1**, **Figure 3.1**). However, the length of MAR-AgNW and HAR-AgNW, as determined by TEM, was much shorter than indicated by the producer. Based on these values, the surface area of three AgNWs followed the order of HAR-AgNW > MAR-AgNW > LAR-AgNW (**Table S3.1**). No obvious aggregation was observed for the three types of freshly prepared AgNWs in the exposure medium based on at least 10 TEM images for each AgNW.

As shown in **Figure 3.2**, the dissolution behavior of the NWs over time was different across the different types of AgNW. The percentage of $AgNW_{(dissolved)}$ (calculated by

using $[Ag]_{dissolved}/[Ag]_{total}$) increased by 4.2%, 3.9% and 8.5% for LAR-AgNW, MAR-AgNW and HAR-AgNW respectively, after incubation in 1/4 Hoagland solution from 1 h to 72 h. The dissolution extent of HAR-AgNW was 8% higher than that of LAR-AgNW and MAR-AgNW (**Figure 3.2B**). Similarly, the dissolution rate constant, K_d, of uncoated HAR-AgNW was slightly higher than the dissolution rate constant of PVP-coated LAR-AgNW and MAR-AgNW (**Table S3.2**). However, once incorporated the surface area of AgNWs to model the dissolution rate constant, the K_D of HAR-AgNW was the lowest (**Table S3.2**). Even though the initial exposure concentration of MAR-AgNW was a bit higher than that of LAR-AgNW, their sedimentation rate constants were similar (**Table S3.2**).

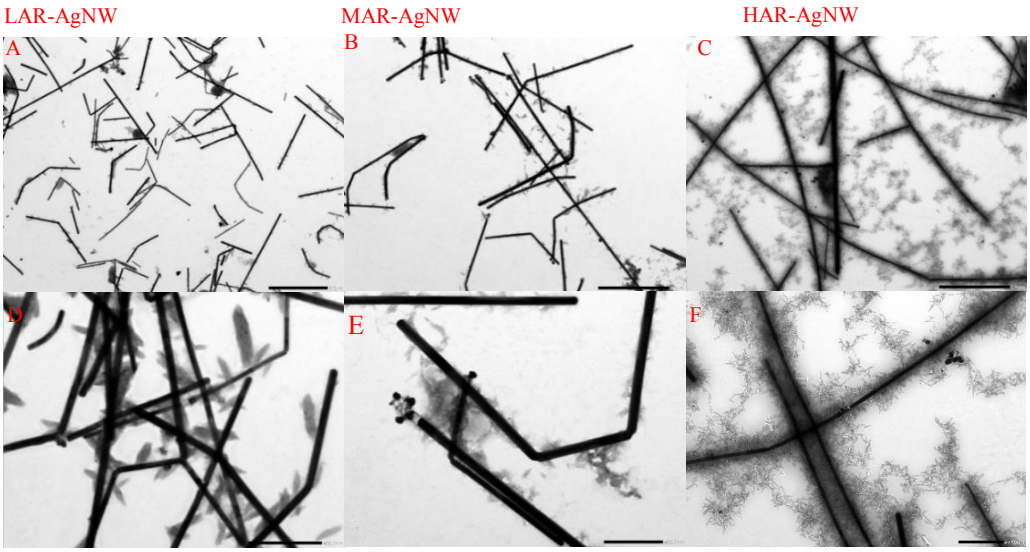

Figure 3.1. TEM images of AgNWs after 1 h of incubation in the exposure medium (scale bar for A, B and C: 200 μm; scale bar for D, E and F: 500 nm). LAR-AgNW: 43 nm diameter×1.8 μm, PVP-coated, MAR-AgNW: 65 nm diameter×4.4 μm, PVP coated, HAR-AgNW: 39 nm diameter×8.4 μm, uncoated.

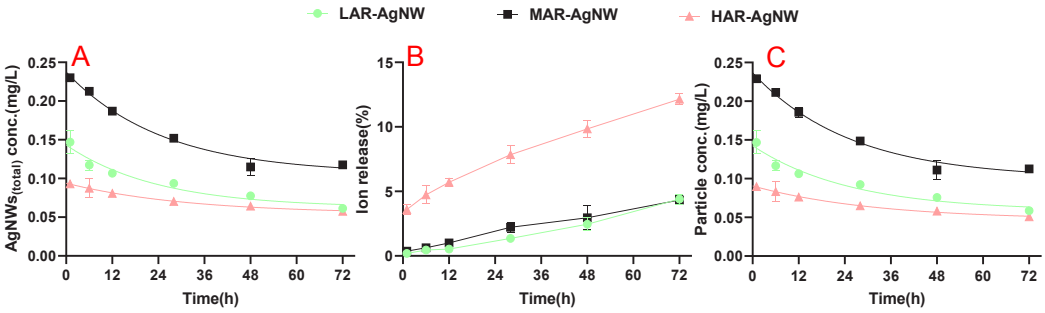

Figure 3.2. Ion release profiles of AgNWs suspensions at the EC_{25} level in the exposure medium over time. (A) Total Ag concentrations in the AgNW suspensions. (B) Percentage of dissolved Ag released in the AgNW suspensions, (C) particulate Ag concentrations in AgNWs suspensions. Data are mean ± SE (N=3). (LAR-AgNW: 43 nm diameter×1.8 μm, PVP-coated, MAR-AgNW: 65 nm diameter×4.4 μm, PVP coated, HAR-AgNW: 39 nm diameter×8.4 μm, uncoated).

3.3.2 Acute toxicity of AgNWs and AgNO3 to Lactuca sativa

The dose-response curves of plants exposed to the different kinds of AgNWs and ionic Ag for 6 d show that both AgNWs and ionic Ag can induce significant toxicity to plants, decreasing the biomass of plants as a function of increasing exposure concentrations of suspensions of Ag-species (**Figure 3.3**, **Figure S3.1**). Based on the dose-response curves, the effect concentrations (EC) of $AgNWs_{(total)}$ and their corresponding $AgNWs_{(particulate)}$ causing 25% (EC_{25}) and 50% (EC_{50}) inhibition of plant growth were calculated. The EC_{25} (0.07 mg/L) and EC_{50} (0.15 mg/L) values based on TWA exposure concentrations of Ag-ions were about 1.3-2.4 fold and 2.1-3.3 fold lower than the corresponding effect levels of the AgNWs tested, respectively, indicating that Ag-ions were the most toxic to lettuce.

We also investigated differences in toxicity among different kinds of AgNWs to plants on the basis of total Ag. The relative EC_{50} values based on $AgNWs_{(total)}$ was significantly higher for MAR-AgNW compared to LAR-AgNW and HAR-AgNW, which had a comparable EC_{50} value to each other (LAR-AgNW≈HAR-AgNW<MAR-AgNW), regardless of the way in which EC_{50} was expressed (ANOVA, C_{TWA} *vs* C_I, P=0.008 *vs* 0.016, **Table 3.1**). This suggests that the suspensions of LAR-AgNW and HAR-AgNW induced higher toxicity than suspensions of MAR-AgNW. Importantly,

when expressed as $AgNWs_{(particulate)}$, no significant differences were observed for the EC_{50} values among the three AgNWs tested (ANOVA, P=0.135 for C_{TWA} and P=0.287 for C_I, **Table 3.1**). In addition, the EC_{25} values of $AgNW_{(total)}$ (ANOVA, P=0.003) and $AgNW_{(particulate)}$ (ANOVA, P=0.022) for both LAR-AgNW and HAR-AgNW were significantly lower than the corresponding values of MAR-AgNW regardless of the way in which EC_{25} was expressed. This indicates that the effects of aspect ratio and coating of AgNWs on the phytotoxicity were more obvious at low effective concentration levels.

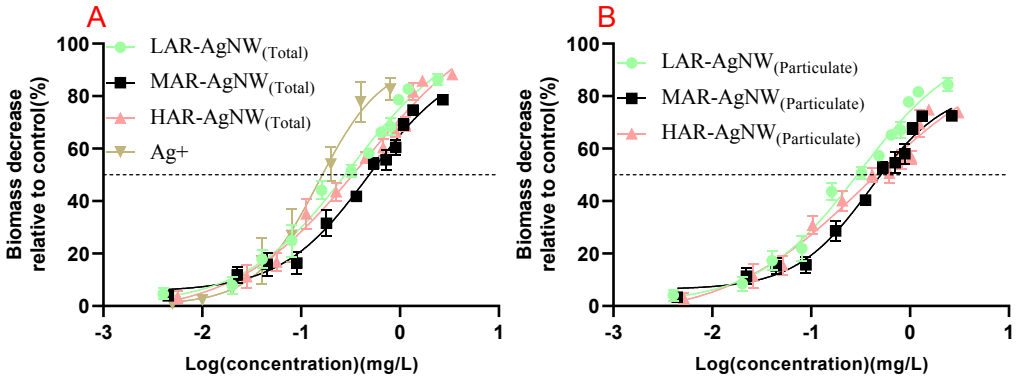

Figure 3.3. Dose–response curves of biomass decrease of *Lactuca sativa* exposed to different concentrations of (A)$AgNWs_{(total)}$ and $AgNO_3$, and (B) $AgNWs_{(particulate)}$ expressed as time weighted concentrations. Data are mean ± SE (N=3).(LAR-AgNW: 43 nm diameter×1.8 μm, PVP-coated, MAR-AgNW: 65 nm diameter×4.4 μm, PVP coated, HAR-AgNW: 39 nm diameter×8.4 μm, uncoated).

3.3.3 Bioaccumulation kinetics and translocation of AgNWs and dissolved Ag in plant tissues

After 18 d the Ag content in control plants was below the detection limit. The mass of silver accumulated in plants was positively correlated with exposure time regardless of AgNW type or Ag-form. After exposure to the suspensions of LAR-AgNW, MAR-AgNW and HAR-AgNW at the EC_{25} level for 18 d, the content of Ag in the plants increased to 7.5, 11.1 and 6.5 μg/plant, which was respectively 50, 33 and 11 times higher compared to the corresponding amount of dissolved Ag released from the AgNWs at the EC_{25} value (**Figure 3.4**A and 4B). This suggests particulate-

specific uptake of Ag for all three AgNWs tested. According to **Table S3.3**, exposure time had no significant effect on the BAFs values of $AgNWs_{(total)}$, $AgNWs_{(particulate)}$ and $AgNWs_{(dissolved)}$ for all AgNWs after exposure for more than 9 d (ANOVA, $P>0.25$, **Table S3.3**).

Meanwhile, the type of AgNW was found to have a significant effect on the bioaccumulation process as the K_u and BAF values of $MAR\text{-}AgNW_{(particulate)}$ were much lower compared to $LAR\text{-}AgNW_{(particulate)}$ and $HAR\text{-}AgNW_{(particulate)}$ (ANOVA, $P<0.05$). Furthermore, the Ag content in plant shoots was only detectable for the $AgNWs_{(total)}$ groups exposed for more than 9 d. However, the transfer factors for all treatments were less than 0.02, suggesting that a major portion of the Ag remained in the plant roots. In addition, all type of AgNWs (ANOVA, $P=0.055$, **Table 3.2**) and exposure time (ANOVA, $P=0.117$, **Table 3.2**) did not significantly influence the Ag translocation from roots to shoots.

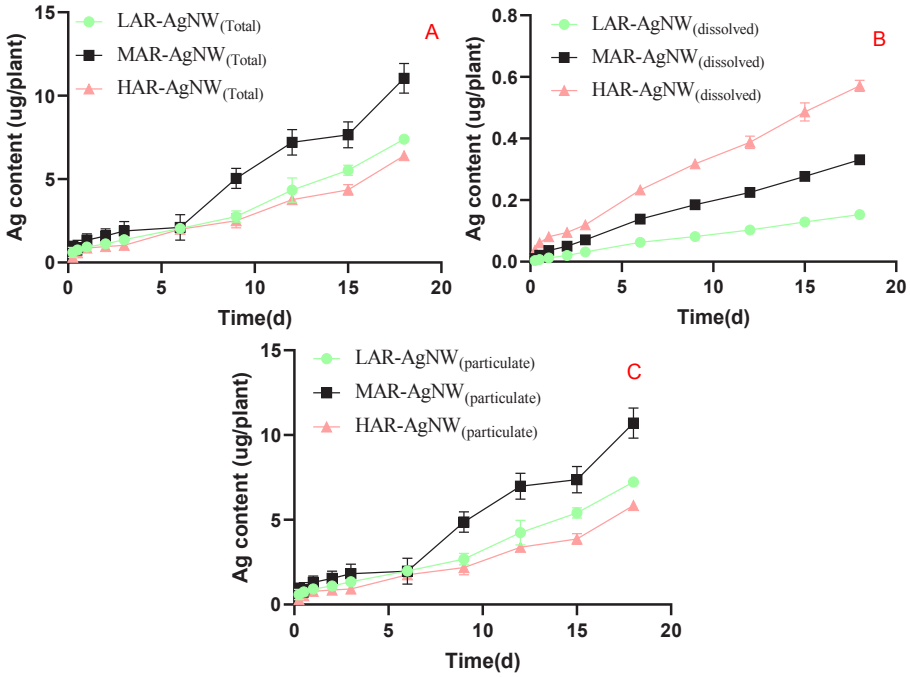

Figure 3.4. Measured Ag uptake in *Lactuca sativa* exposed to different (A) AgNWs suspension, (B) the particulate Ag and (C) the corresponding concentrations of dissolved Ag at EC_{25} level over 18 days. Data are mean ± SE (N=3). (LAR-AgNW: 43 nm diameter×1.8 μm, PVP-coated, MAR-AgNW: 65 nm diameter×4.4 μm, PVP coated, HAR-AgNW: 39 nm diameter×8.4 μm, uncoated)

3.3.4 Relative contribution of dissolved Ag and particulate Ag to toxicity and Ag uptake in plants

In general, the dominant role of $AgNWs_{(particulate)}$ to the overall toxicity relative to the corresponding dissolved Ag was observed in all exposure cases (**Figure 3.5**). In addition, exposure concentration was found to have a significant impact on the relative contribution of $AgNWs_{(particulate)}$ to the overall toxicity regardless of the type of AgNWs exposed. For instance, the relative contributions of $AgNWs_{(dissolved)}$ to the overall suspension toxicity were found to increase by 11.1%, 17.2% and 41.5% for LAR-AgNW, MAR-AgNW and HAR-AgNW when the exposure concentrations increased from 0.04, 0.02 and 0.03 to 2.42, 2.71 and 3.39 mg/L, respectively. Therefore the relative contribution of $HAR\text{-}AgNW_{(dissolved)}$ to toxicity at high concentrations was much higher than that of $LAR\text{-}AgNW_{(dissolved)}$ and $MAR\text{-}AgNW_{(dissolved)}$ (ANOVA, $P<0.001$, **Figure 3.5**). Similarly, uptake of $AgNWs_{(particulate)}$ dominated the contribution to overall Ag accumulation in plants compared to the uptake of $AgNWs_{(dissolved)}$ for all AgNWs tested as the contribution of the NWs accounted for more than 85% of the Ag accumulation in the plants. Additionally, the relative contributions of $AgNWs_{(dissolved)}$ increased significantly after exposure from 0.25 d to 3 d and then tended to be stable for LAR-AgNW and MAR-AgNW ($P<0.001$, **Figure 3.5**D). Among the three types of AgNWs, the $HAR\text{-}AgNW_{(dissolved)}$ contributed most to the overall Ag accumulation in plants with a contribution of about 10% at the EC_{25} exposure level for 18 d, which was much higher than that of $LAR\text{-}AgNW_{(dissolved)}$ (2%) and $HAR\text{-}AgNW_{(dissolved)}$ (3%) (ANOVA, $P<0.001$, **Figure 3.5**D).

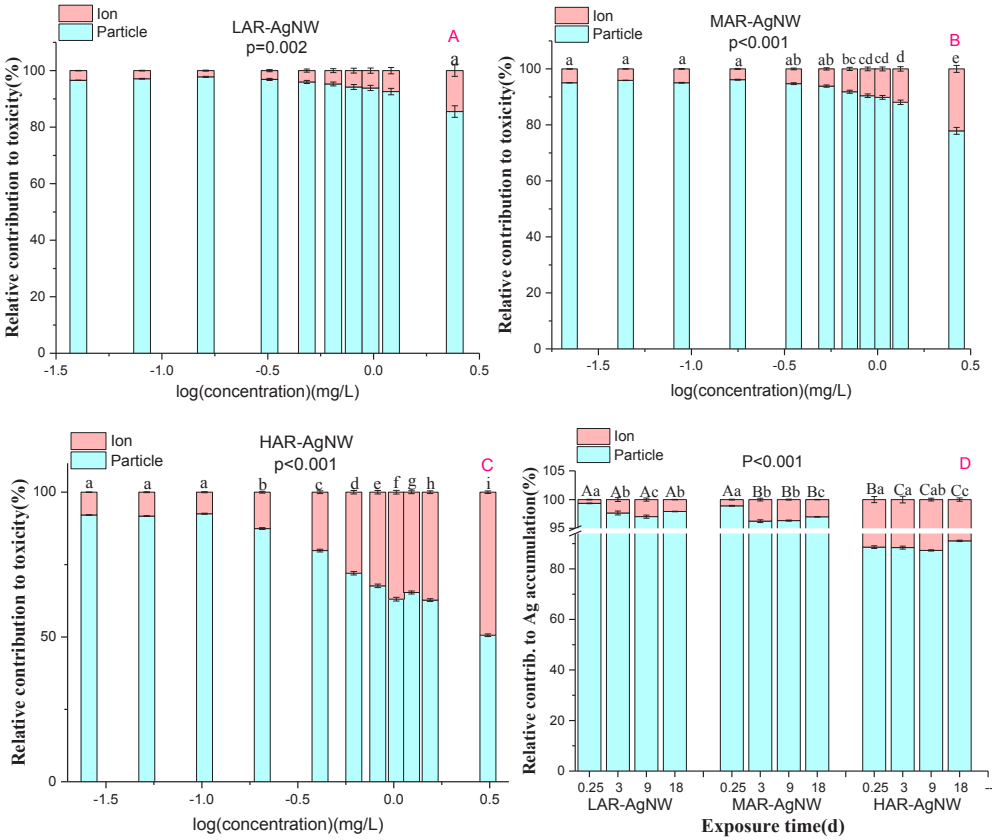

Figure 3.5. Relative contribution (%) of different $AgNWs_{(particle)}$ and $AgNWs_{(ion)}$ to toxicity at different concentrations (A, B and C), and to Ag accumulation at EC25 concentrations for different exposure time (D). The data represent the mean ± SE (n = 3). The different letters in the same group indicate statistically significant differences between treatments at $p < 0.05$. (LAR-AgNW: 43 nm diameter×1.8 μm, PVP-coated, MAR-AgNW: 65 nm diameter×4.4 μm, PVP coated, HAR-AgNW: 39 nm diameter×8.4 μm, uncoated)

Table 3.1. The EC_{25} and EC_{50} values of AgNWs(total) and AgNWs(particulate) expressed as initial concentrations and expressed as time weighted average concentrations. The data represent the mean ± SE (n = 4). The different letters of the same Ag form in the same column indicate statistically significant differences between treatments among three AgNWs at $p < 0.05$.

		EC_{25}(mg/L)		**EC_{50}(mg/L)**	
		C_I (95% confidence Interval)	C_{TWA} (95% confidence Interval)	C_I (95% confidence Interval)	C_{TWA} (95% confidence Interval)
$AgNWs_{(total)}$	LAR-AgNW	0.137a (0.098-0.175)	0.084a (0.060-0.107)	0.513a (0.387-0.800)	0.315a (0.238-0.491)
	MAR-AgNW	0.237b (0.179-0.290)	0.164b (0.124-0.200)	0.718b (0.549-1.045)	0.497b (0.380-0.724)
	HAR-AgNW	0.116a (0.071-0.164)	0.088a (0.054-0.124)	0.528ab (0.366-1.174)	0.417ab (0.286-0.965)
	Ag+	0.057c (0.047-0.088)	/	0.150c	/
$AgNW_{(particulate)}$	LAR-AgNW	0.144a (0.102-0.191)	0.086a (0.060-0.115)	0.542a (0.385-0.866)	0.318a (0.226-0.503)
	MAR-AgNW	0.246b (0.184-0.300)	0.157b (0.114-0.197)	0.701a (0.520-0.910)	0.422a (0.317-0.546)
	HAR-AgNW	0.105a (0.057-0.178)	0.061a (0.022-0.096)	0.616a (0.351-1.117)	0.382a (0.201-0.902)

Table 3.2. Uptake rate constants, BAFs and TFs for *Lactuca sativa* exposed to different AgNWs at EC_{25} level over 18 d. The data represent the mean ± SE (n = 3). The different letters in the same column indicate statistically significant differences between treatments at $p < 0.05$. Asterisks indicate statistically differences between different Ag forms of each AgNW for the same row at $p < 0.05$.

Type of AgNWs	K_{uptake} (d^{-1})			BAFs			TFs
	Total Ag	Particulate Ag	Dissolved ions	Total Ag	Particulate Ag	Dissolved ions	Total Ag
LAR-AgNW	0.139±0.007a	0.136±0.006a	0.245±0.021a*	0.630±0.006a	0.621±0.006a	0.758±0.018a*	0.010±0.001a
MAR-AgNW	0.105±0.008b	0.098±0.008b	0.244±0.014a*	0.531±0.026b	0.507±0.024b	0.745±0.009a*	0.010±0.002a
HAR-AgNW	0.153±0.013a	0.149±0.015a	0.229±0.009a*	0.700±0.011c	0.684±0.011c	0.759±0.014a*	0.015±0.001a

LAR-AgNW: 43 nm diameter×1.8 μm, PVP-coated, MAR-AgNW: 65 nm diameter×4.4 μm, PVP coated, HAR-AgNW: 39 nm diameter×8.4 μm, uncoated

3.4. Discussion

3.4.1 Dissolution behavior of AgNWs

Our results showed that the dissolution of uncoated HAR-AgNW was much higher compared to PVP-coated AgNWs with lower aspect ratio values (LAR-AgNW and MAR-AgNW). The dissolution rate constant (h^{-1}) of AgNWs was observed to follow the order of HAR-AgNW > MAR-AgNW > LAR-AgNW. Scanlan et al.[216] made the generic statement that dissolution increases for short AgNWs with a low aspect ratio compared to longer AgNWs with a higher aspect ratio in EPA media. The discrepancy with our results suggests that restricting or placing too much focus on aspect ratio for toxicity assessment is not giving the full picture. A larger surface area of nanoparticles can increase the contact between NPs and the oxidant, thereby accelerating the dissolution[87]. Although the surface area of HAR-AgNW was larger compared to LAR-AgNW and MAR-AgNW, the dissolution rate constant ($ng/cm^2/h$) which incorporated the surface area of AgNWs was lowest for HAR-AgNW (LAR-AgNW≈MAR-AgNW > HAR-AgNW, **Table S3.2**). This indicates that the dissolution behaviors of AgNWs in this study cannot be explained by the larger surface area only. Therefore, we postulate that the differences in dissolution kinetics of HAR-AgNW compared to LAR-AgNW and MAR-AgNW were due to the absence of PVP-coating on HAR-AgNW. This suggests that a PVP-coating largely played a role with regard to the dissolution behaviors in the current study, and was more important than the dimensions of AgNWs. In addition, the dissolution of AgNWs in the present study was found to be less than 15%, which was much lower than the extent of Ag released from Ag nanospheres (about 30%) obtained by our previous study under similar exposure conditions[221]. This was consistent with the findings that spherical AgNPs displayed the highest dissolution, followed by Ag nanocubes and AgNWs[85], confirming that the dissolution of AgNPs is shape-dependent.

3.4.2 Coating related factors cannot fully explain toxicity differences among AgNWs

All three AgNWs suspensions tested in this study inhibited the growth of plants significantly with the EC_{50} values ranging from 0.32 to 0.49 mg/L expressed on TWA

basis (compared to 0.52 to 0.71 mg/L expressed as the initial concentrations). Comparison of the toxicity levels deduced for the three AgNWs tested suggests that a low aspect ratio and a lack of coating of AgNWs are slightly more toxic than high aspect ratio and PVP-coated AgNWs. This finding is consistent with the results of Scanlan et al[216], who concluded that short AgNWs with low aspect ratio exhibited higher toxicity compared to long AgNWs with high aspect ratio. However, Chae et al.[223] reported that larger and longer PVP-coated AgNWs dispersed in TAP medium exhibited greater toxicity to algae than the smaller and shorter ones. These apparent contradictions indicate that the impacts of AgNWs characteristics on their toxicity can also depend on the test species and/or the chemistry of the exposure medium. An important goal of PVP-coating is to promote the dispersion and to reduce the agglomeration of nanoparticles[82,229,230], which in turn affects their toxicity as sedimentation and aggregation can contribute to reduced toxicity[231,232]. However, in the current study we found that the sedimentation of PVP-coated LAR-AgNW and MAR-AgNW was similar, and both sedimentation rate constants were higher than the sedimentation rate constants of uncoated HAR-AgNW (**Figure 3.2** and **Table S3.2**), whereas the toxicity of MAR-AgNW was lowest. In addition, the higher toxicity of uncoated nanoparticles has been commonly attributed to their faster dissolution[231,233,234]. However, the toxicity of LAR-AgNW and HAR-AgNW was comparable, while the dissolution of HAR-AgNW was significantly increased compared to LAR-AgNW. Our results indicate that the sedimentation and dissolution of AgNWs associated with the lack of coating may not be indicative of their phytotoxicity.

3.4.3 Accumulation kinetics of AgNWs and dissolved Ag

All three AgNWs suspensions induced Ag uptake in plants roots. Contaminants can be taken up by plant roots via apoplastic transport through the intracellular spaces of adjacent cells along cell walls and via symplastic/transmembrane pathway through plasmodesmata/cell membranes between cells[235,236]. In this study, Ag uptake via the plant roots was rapid and equilibrium was reached quickly. In addition, the data of AgNWs accumulation in plant roots fitted the one-compartment kinetic model well (R^2>0.9). Taken together, these results indicate that in our study apoplastic transport

was likely the major pathway for the uptake of Ag by plant roots after AgNWs adhere to the root epidermis. The limited translocation of Ag from roots to shoots in all AgNWs exposure treatments further confirmed this, as it is difficult for materials taken up by the apoplastic pathway to cross the Casparian strip (a barrier limits the entrance of substances to xylem or phloem) and thus cannot be transported into the above-ground parts. Wang et al.[192] also confirmed that CuO NPs pass through the epidermis into root tissues via the apoplastic route. All toxicokinetic parameters of dissolved Ag were much higher than those of $AgNWs_{(particulate)}$, demonstrating that the accumulation of Ag-ions in plants proceeds much faster than the accumulation of particulate Ag. This implies that dissolved Ag is more bioavailable than particulate Ag.

Among the three types of AgNWs tested, the uptake rate constants and BAFs of both $AgNWs_{(total)}$ and $AgNWs_{(particulate)}$ followed the order of LAR-AgNW (PVP-coated) ≈ HAR-AgNW (uncoated) > MAR-AgNW (PVP-coated). As the LAR-AgNW and HAR-AgNW have a similar diameter but different length and coating, this result suggests that the dimension, more specifically, the diameter of AgNWs is the dominant factor related to their cellular uptake. The AgNPs with smaller diameter might easier pass through the pores in/between cell walls due to the size exclusion limit of cell walls and/or apoplast[68]. Torrent et al.[82] showed that silver nanospheres accumulated in lettuces, and that accumulation was diameter (size) dependent, but coating independent, which is in line with our findings. Previous studies of wire-shaped nanoparticles are shown to behave totally different compared to the results found in our study – but it should be noted that those were all conducted on non-flora species. For example, the cellular uptake of Au nanowires in MCF-7[220] and HeLa[222] cells, of Ag nanowires in daphnids[216], and of Fe nanowires in HeLa cell[237] and NIH/3T3 fibroblast cells[218] was length dependent: shorter NWs are more likely to be taken up compared with longer ones in general. However, from our results, no definite dependency on length-specific uptake of AgNWs in plants can be concluded. Our results highlight that interaction between metal-based NPs and plants should consider the combined effects of diameter, length, shape and surface chemistry.

3.4.4 Particulate Ag-dominant effects

Ionic Ag was more toxic in comparison to all AgNWs (see EC_{50} values) when plants were exposed to an equal dose of total Ag. A great number of studies (based on silver, zinc, copper, gold, iron and nickel-based nanoparticles) suggested that the toxicity of metal-based nanoparticles is mainly driven by the dissolved ions shed from the particulate form. However, following exposure to the specific amount of Ag-ions which corresponded to the amount released from metallic NPs, toxicity originating from the nanoform rather than from the ionic Ag present in suspension has also been confirmed [85]. The dominant contribution of particulate Ag to the overall toxicity of AgNWs was also found in this study on the basis of assessing the relative contributions of particulate Ag and the corresponding dissolved Ag to the reduction of plants biomass. The almost similar EC_{50} values of $AgNWs_{(total)}$ and $AgNWs_{(particulate)}$ also revealed that the particulate Ag was the major source of toxicity of AgNWs. Similar particulate-originated toxicity was observed following exposure of algae to PVP-AgNWs as the dissolved concentration of Ag, as released from the AgNWs, was below 0.05 ppm [223]. In addition, our previous study in which we exposed lettuce to spherical AgNPs at similar conditions as employed in the current study, also verified the particle-ruling toxicity [221]. Gorka and Liu[85] also suggested that the toxicity observed for *Lolium multiflorum* cannot be explained by ionic silver solely when the plants are exposed to AgNWs, AgNPs and Ag nanocubes. The similar contribution of particulate Ag among different shapes of Ag nanoparticles confirms that the dominant role of particles in suspension toxicity of Ag materials to higher plants is shape-independent.

For the accumulation experiments, the exposure concentrations of dissolved Ag at each time point were comparable to the TWA concentrations of dissolved Ag released from each AgNWs at the EC_{25} level at the same exposure time. The dominant contribution patterns of $AgNWs_{(particulate)}$ to the total Ag accumulation in plants were similar to the contribution of $AgNWs_{(particulate)}$ to the overall toxicity. The similar patterns strongly indicate that a relationship between the phytotoxicity of AgNWs and the Ag accumulation in plants exists. This potentially indicates that the accumulation originates from particulate Ag, which is also responsible for the

phytotoxicity of AgNWs. Once the AgNWs are taken up by plants, the *in-vivo* dissolution of AgNWs and in-place biological transformation of new particles can occur to some extent[85,90]. These processes could also affect the plant growth partly[90,190]. Dang et al.[227] also reported that particulate Ag dominates the overall Ag accumulation in wheat (*Triticum aestivum*) exposed to suspensions of AgNPs. In addition, the relative importance of ions versus particles of AgNPs are highly dependent on the dissolution extent of AgNPs. This observation is consistent with our findings that the particulate Ag contribution to the overall Ag accumulation of HAR-AgNW (which displayed the highest dissolution ability) was higher than that of LAR-AgNW and MAR-AgNW. Our results showed furthermore the relative contribution of ion versus particulate to the overall adverse effects depends on the exposure concentration (**Figure 3.5**).

3.5. Conclusions

To the best of our knowledge, this is the first investigation that explored the effects of PVP-coated and uncoated AgNWs with different dimensions on their phytotoxicity and toxicokinetics of the dissolved and particulate Ag in terrestrial plants. Our results showed that PVP-coating affected the dissolution behaviors of AgNWs. This coating associated dissolution behavior was found not to affect the phytotoxicity of the AgNWs studied. The toxicity and the toxicokinetics parameters of the three AgNWs followed the order of LAR-AgNW≈HAR-AgNW>MAR-AgNW. This indicates that the diameter of the AgNWs plays a crucial role in determining the toxicity and Ag accumulation of AgNWs. In addition, the particulate Ag dominates the overall toxicity and Ag accumulation in plants of AgNWs suspensions compared to dissolved Ag. Overall, the results of this study highlighted that the toxicokinetics and toxicodynamics of AgNWs associated with different dimension and coating should be taken into account when studying the interactions between NPs and biological systems. Our findings provide in depth understanding of nanosafety to plants as well as can contribute to further developing knowledge regarding their safe design to mitigate the side effects of nanowires. Furthermore, the established EC_{50}-values and the toxicokinetic parameters of AgNWs can be incorporated into predictive models for assessing risk NWs for environmental health and safety

3.6 Supplementary Information

Table S3.1. The nominal and actual values of the characteristics of the AgNWs used in this study.

	Nominal Mean values					Actual Mean values					
AgNWs type	Diameter (nm)	Length (μm)	Aspect ratio	SA (μm^2)	Volume (μm^3)	Diameter (nm)	Length (μm)	Aspect ratio	SA (μm^2)	Volume (μm^3)	coating
LAR-AgNW	40	3	75	3.80	0.004	43.1	1.8	42	0.247	0.003	PVP
MAR-AgNW	70	30	428	6.61	0.115	64.5	4.4	68	0.898	0.144	PVP
HAR-AgNW	40	25	625	3.14	0.031	38.6	8.4	218	1.021	0.010	uncoated

LAR-AgNW: 43 nm diameter×1.8 μm, PVP-coated, MAR-AgNW: 65 nm diameter×4.4 μm, PVP coated, HARAgNW: 39 nm diameter×8.4 μm, uncoated; All data obtained from the TEM excluded the PVP coating

Table S3.2. Dissolution rate constants of $AgNWs_{(dissolved)}$ and sedimentation rate constant of $AgNWs_{(particulate)}$ for each AgNWs at EC25 level over 72 h

Type of AgNWs	K_D ($ng.cm^{-2}.h^{-1}$)		K_d(h^{-1})		K_S((h^{-1})	
	K value	R^2	K value	R^2	K value	R^2
LAR-AgNW	0.031	0.99	0.011	0.95	0.039	0.92
MAR-AgNW	0.039	0.99	0.021	0.95	0.039	0.98
HAR-AgNW	0.016	0.97	0.027	0.94	0.031	0.90

LAR-AgNW: 43 nm diameter×1.8 μm, PVP-coated, MAR-AgNW: 65 nm diameter×4.4 μm, PVP coated, HARAgNW: 39 nm diameter×8.4 μm, uncoated

Table S3.3. Bioaccumulation (BAFs) and transfer (TF) factors of Ag for *Lactuca sativa* exposed at the EC25 concentrations of AgNWs over 3, 9, 15 and 18 d.

Type of AgNW	Exposure duration (d)	Applied dose (μg)	BAFs			TFs
		total	Total Ag	Particulate	Dissolved ions	Total Ag
LAR-AgNW	3	1.98	0.70±0.05a	0.69±0.05a	0.95±0.08a*	/
	9	5.93	0.47±0.03b	0.46±0.03b	0.81±0.04a*	0.015±0.003a
	15	9.90	0.56±0.02ab	0.56±0.02ab	0.77±0.02a	/
	18	11.85	0.63±0.01a	0.62±0.01a	0.76±0.02a*	0.010±0.001a
MAR-AgNW	3	3.50	0.54±0.09a	0.52±0.09a	0.96±0.04a*	/
	9	10.50	0.49±0.03a	0.46±0.03a	0.83±0.01b*	0.012±0.0002a
	15	17.5	0.44±0.03a	0.42±0.03a	0.75±0.01b	/
	18	21.00	0.53±0.03a	0.51±0.02a	0.75±0.01b*	0.010±0.002a
HAR-AgNW	3	1.55	0.67±0.10a	0.64±0.11a	0.96±0.03a*	/
	9	4.64	0.55±0.05a	0.51±0.06a	0.85±0.01b*	0.018±0.002 a
	15	7.75	0.56±0.02a	0.54±0.03a	0.78±0.03b	/
	18	9.29	0.70±0.01a	0.68±0.01a	0.76±0.01b*	0.015±0.001 a

The data represent the mean ± SE (n = 3). The different lower-case letters in the same column of each AgNW indicate statistically significant differences among exposure time at $p < 0.05$. (LAR-AgNW: 43 nm diameter×1.8 μm, PVP-coated; MAR-AgNW: 65 nm diameter×4.4 μm, PVP coated; HARAgNW: 39 nm diameter×8.4 μm, uncoated.)

Table S3.4. Goodness of fit of uptake rate constants for *Lactuca sativa* exposed to different AgNWs at EC_{25} level over 18 d.

Type of AgNWs	K_{uptake} (d^{-1})		
	Total Ag	Particulate Ag	Dissolved ions
LAR-AgNW	0.98	0.98	0.97
MAR-AgNW	0.95	0.94	0.87
HAR-AgNW	0.80	0.78	0.87

d^{-1} = per day

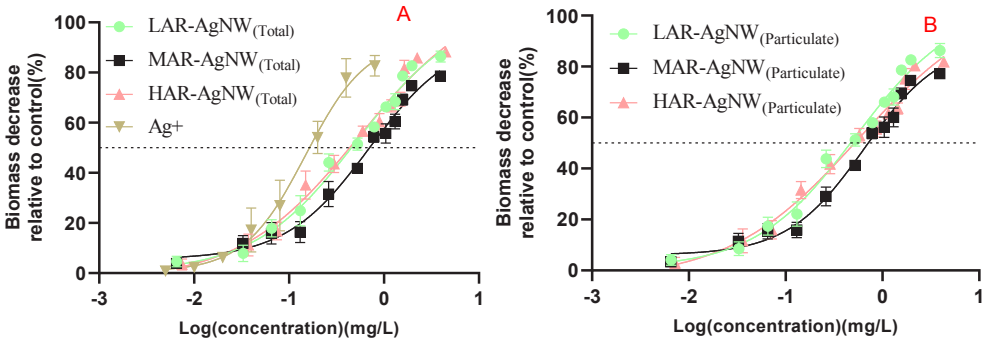

Figure S3.1. Dose–response curves of biomass decrease of *Lactuca sativa* exposed to different concentrations of (A)$AgNWs_{(total)}$ and AgNO3, and (B) $AgNWs_{(particulate)}$ expressed as initial exposure concentrations. Data are mean ± SE (N=3).(LAR-AgNW: 43 nm diameter×1.8 μm, PVP-coated, MAR-AgNW: 65 nm diameter×4.4 μm, PVP coated, HARAgNW: 39 nm diameter×8.4 μm, uncoated


Chefchaouen, Morocco, 2018
Photo by Yupeng
yupeng

Chapter 4

The dissolution dynamics and accumulation of AgNPs in a microcosm consisting of soil -lettuce - rhizosphere bacterial community

Juan Wu, Yujia Zhai, Gang Liu, Thijs Bosker, Martina G. Vijver, Willie J. G. M. Peijnenburg

Submitted ACS sustainable chemistry & engineering

(2021), Accepted

Abstract: Assessment of chronic impact of metallic nanoparticles (NPs) in soil ecosystems is a necessity for ensuring safe and sustainable application. NPs affect plants and their associated microbial life, whilst the plants and their associated microbiota affect nanoparticles fate. Here, we measured the available Ag pool (determined as the DTPA-extractable Ag) in AgNPs amended sandy-loam soil (1, 10 and 50 mg Ag per kg soil) over a period of 63d, with and without lettuce. The associated impacts on soil pH, Ag accumulation in lettuce and the responses of the rhizosphere bacterial community were determined. We found that the addition of AgNPs significantly increased the soil pH after short-term (7d) incubation. Noteworthy, the extractability of Ag in AgNPs amended soil was concentration-dependent and changed over time because of their continuous dissolution and uptake by plants. Ag uptake and upwards translocation in lettuce was positively correlated with the extractable Ag content in soil. Furthermore, long-term (63d) exposure to 50 mg/kg of AgNPs altered the structure and composition of the rhizosphere bacterial community potentially by regulation of bacterial groups associated to element (e.g., N and S) cycling and stress tolerance. In conclusion, our results demonstrated that the dynamic dissolution of AgNPs in sandy-loamy soil plays an important role in influencing the overall Ag bioavailability of the NPs in plants. The enhanced effects of AgNPs on the alterations in the rhizosphere bacterial community highlight that the long time-resolved dynamics of NPs exposure should be taken into consideration for accurate ecological risk assessment of NPs in the soil ecosystem.

4.1. Introduction

The rapid development of nanotechnology over the past two decades has inspired the production and application of nano-agrochemicals, and claims have been made that these nano-agrochemicals can improve the sustainability of agriculture[21,238]. As more and more nano-agrochemicals are introduced in agriculture as fertilizers or pesticides, agricultural soil is inevitably becoming an important sink for nanomaterials[15]. Silver nanoparticles (AgNPs) are one of the most extensively used commercialized nanomaterials worldwide, and the global production of AgNPs will reach a value of USD 2.45 billion by 2022[239,240]. Given their excellent antimicrobial

properties, they have shown great potential in crop protection as insecticidal agrochemicals and against plant pathogens (phytopathogenic fungi, bacteria, and viruses)[21]. This makes the impact assessment of AgNPs in soil ecosystems a necessity for the safe and sustainable usage of nanoscale products.

The impacts of metallic nanoparticles on soil ecosystems have been reported to largely depend on their bioavailable fractions[241]. For instance, Pu et al.[241] reported that the toxicity of CuO nanoparticles in maize plants and microbes was mainly modulated by the gradually released bioavailable Cu concentration. Soil properties are known to be a key factor affecting the bioavailability of metallic nanoparticles in nature soil[242,243]. An important property is soil pH, which modulates the bioavailability of metallic nanoparticles by affecting the oxidation, aggregation, transformation and dissolution processes of metallic nanoparticles in soil[24,244]. Importantly, plants, a key component of soil ecosystems[221], can alter the soil properties directly by themselves or indirectly by the interaction with nanoparticles. For instance, the amount of soil organic material in soil can be influenced by the presence of plants as nearly 5-40% of the photosynthetically fixed carbon is transported to the rhizosphere by plant root exudates[142]. Moreover, the interaction between plant roots and metallic nanoparticles can alter the abundance and composition of root exudates as well as soil pH[142,245,246]. Soil organic matter and the root secreted chelators (such as phytosiderophores) can immobilize/sequester NPs and the released metal ions[247,158]. These changes in soil environment may modify the available pool of Ag derived from AgNPs and in turn influence the plant responses[146,245].

However, to our knowledge, the information regarding how plant roots influence the labile pool of Ag in a AgNPs amended rhizosphere and the consequent relationship with the Ag accumulation in plant is scarce. Recently, Del Real et al.[49] used DTPA and $CaCl_2$ extractions to assess the lability of Ag in soil mixed with AgNPs-containing sludges (18 -400 mg/kg) at a single-time point (4 weeks). The authors demonstrated that the low Ag content in wheat is consistent with the low lability of Ag in soil[49]. However, it should be noted that plant growth over time can dynamically change the soil environment and thus the dynamic particle dissolution, which may make the

bioavailable concentration of Ag time-dependent[248,249]. To capture these dynamics and their impacts on ecosystems, experiments of longer time scales need to be performed in which a series of time points are included at which the bioavailability of Ag in soil is assessed in a toxicity assay.

Similar to plants, soil bacteria also plays important role in soil ecosystem by reflecting soil fertility and governing soil biological processes like nutrient transformation and cycling, and energy flow[137,250]. The impacts of AgNPs on bacterial communities of unplanted soil have been extensively reported with inconclusive findings[137,139,250,251,252]. It is suggested that the responses of soil microbial community to AgNPs depend on the soil properties, exposure concentration, exposure duration as well as the behaviours of AgNPs in soil[251,252]. Therefore, the alterations in the soil environment induced by plants may modify the AgNPs effects on the rhizosphere soil bacteria behaviours[253], which may result in either detrimental or beneficial impacts on the soil ecosystem[141,146,247]. To date, little information is available about how AgNPs alter rhizosphere soil bacterial communities[149,246,254]. This is surprising, because it is known that soil rhizosphere bacteria play a crucial role in supporting the host plant growth by regulating nutrient uptake and to some extent by supporting against environmental stressors[141,145]. Thus, long-term impact of AgNPs on rhizosphere soil bacterial community deserves more investigation.

In this study, lettuce plants, a popular representative of the leafy vegetables worldwide, were exposed to 0, 1, 10 and 50 mg/kg of AgNPs over a period of 63 days. The objectives of this study are a) to investigate if and to what extent the plants and AgNPs affect the soil pH and how this impacts the (potentially) available Ag concentrations shedding from AgNPs, b) to quantify Ag accumulation and translocation in a soil-plant system, and c) to determine the alterations of the rhizosphere soil bacterial community structure in response to exposure to AgNPs, as a function of exposure concentration and exposure time. This study provides useful information to correlate the time-related changes of bioavailable Ag from AgNPs amended soil with the plant growth and soil microbial communities. Such information is important for risk assessment of nanomaterials in soil ecosystems and for safely and sustainably applying nano-enabled agrichemicals.

4.2. Materials and Methods

4.2.1 Silver nanoparticles

Stock suspensions of spherical AgNPs (NM-300K) with a nominal diameter of 15 nm and a concentration of 100 g/L were provided by RAS AG (Regensburg, Germany). Physico-chemical properties and information on the characterization of the AgNPs are summarized in JCR Reports[255]. AgNPs suspensions at 1, 10 and 50 mg/L were prepared by diluting the AgNPs stock in 1/4 Hoagland solution (pH 6.0 ± 0.1). The composition of the Hoagland solution is described in **Table S2.1** (Supplementary material). The suspensions were sonicated for 5 min at 60 Hz (USC200T, VWR, Amsterdam, The Netherlands). The freshly prepared suspensions were used to determine the size distribution and zeta potential with a Zetasizer Nano-ZS instrument (Malvern, Instruments Ltd., Royston, UK) at 1, 24 and 48 h of incubation. The data is published in our previous publication[221] and provided in **Table S4.1**. The TEM picture of the AgNPs is also provided in **Figure S4.1** (Supplementary material).

4.2.2 Soil preparation

Surface agricultural soil (0-20 cm) was collected from a non-polluted site (52°10'16.8"N 4°26'58.9"E, Leiden, Netherlands), mixed thoroughly, sieved to 2 mm after being air-dried, and stored at 4 °C before use. The soil is sandy-loam with pH of 8.4 in water and 7.4 in KCl solution, containing 2.2 % of organic carbon, with clay content of 18.4% and cation exchange capacity of 0.39 $cmol^{(+)}\ kg^{-1}$. No Ag (< detection limit) was detected in the untreated soil. The exchangeable cations content and the content of various metals were determined, and these properties are reported in **Table S4.2**.

4.2.3 Plant growth and exposure assay

Lactuca sativa seeds (Floveg GmbH, Kall, Germany) were firstly sterilized for 5 min in 0.5% (w/v) NaClO, followed by rinsing three times with tap water and immersing for 24 h in tap water. Afterwards, the seeds were germinated in Petri dishes filled with a wet filter paper (15 seedlings/dish). After 3 d, 1/4 Hoagland solution was added into the Petri dishes to supply nutrients for seedling growth. After pre-growing in Petri dishes for one week, the young seedlings were transferred to bottles (one seedling per

bottle) with a height of 15 cm containing Hoagland solution for a further two weeks of growth. The suspensions in the Petri dishes and bottles were refreshed every 3d.

The AgNPs suspensions were prepared in 1/4 Hoagland solution and sonicated at 60 Hz for 15 min before application to soil. Afterwards, the AgNPs suspensions were added to soil to achieve the nominal concentration of 1, 10 and 50 mg Ag per kg soil. The exposure concentrations of AgNPs were chosen based on the predicted and measured concentration of AgNPs in sludge/biosolid[49]. The soil was mechanically stirred with a mixer for 15 min to homogenize the AgNPs. Control treatment was treated the same as the AgNPs treatments with the addition of same volume of 1/4 Hoagland solution. Next, two uniform pre-grown seedlings were transferred into one plastic pots (9 cm length, 9 cm wide, 9.5 cm high) containing 0.5 kg of AgNPs amended soil or clean soil. Treatments containing 1, 10 or 50 mg Ag per kg soil but without plants were also performed under the same conditions. In brief, this experiment consisted by 3 components: a) AgNPs applications dose (0, 1, 10 and 50 mg/kg), b) exposure time (3-63 d), and c) the presence or absence of plants, for a total of 17 treatments in triplicate as described in **Table S4.3**. The pots were watered every two days and all pots were placed in a climate room under the conditions of day/night temperature at 20/16 °C and the light/dark cycle of 16/8 h with 60 % relative humidity until harvest. After each exposure time point, the plants in each pot were harvested, and subsequently the non-rhizosphere (further referred to as bulk soil) and soils with rhizospheres (further referred to as rhizosphere soil) were collected.

4.2.4 Plant harvesting and soil sample collection

At each selected sampling date, pots were picked up randomly and sacrificed for collecting plant samples and soil samples. Plants were carefully removed from the pots, and the soil which was left in the pots was defined as bulk soil where the influence by plant roots is negligible[245]. The collected bulk soil was mixed thoroughly for further use. The soil that was loosely attached to the roots was firstly removed by shaking the plants (discarded) and then the soil that closely adhered to the roots was collected as rhizosphere soil (<1 mm away from the root) following the method reported by Guan et al.[146]. The collected rhizosphere soil was mixed thoroughly for

further use. For Ag extraction and pH measurement, the bulk soil and rhizosphere soil samples were air-dried. The rhizosphere soil samples used for the soil DNA extraction, were stored at 4 °C.

After collecting the soil samples, plants were thoroughly washed with flowing tap water and rinsed in deionized water for 10 min, which was repeated three times. Subsequently, plants were divided into root and shoot and after air-drying, the biomass of plant roots and shoots was recorded. To determine the Ag content in plants, plants were firstly washed with 10mM HNO_3, 10mM EDTA and Milli-Q water to remove the attached AgNPs/Ag^+ ions as described previously[221]. Next, plants were oven-dried, weighed and digested with HNO_3 (65%) and H_2O_2 (30%) at 120 °C [221]. Finally, the digests were diluted, and Ag concentrations were analysed by means of a Graphite furnace atomic absorption spectrometer (AAS, PerkinElmer 1100 B, Waltham, MA, USA). The bioaccumulation factor (BAF) of Ag from soil to plant roots and the translocation factor (TF) of Ag from roots to shoots were calculated as follows[221]:

$$BAF = \frac{[Ag]_{root}}{[Ag]_{soil}}; \mathrm{TF} = \frac{[Ag]_{shoots}}{[Ag]_{roots}}$$

Where $[Ag]_{root}$ represents the concentrations of Ag in the plants (mg/kg), and $[Ag]_{soil}$ represents the exposure concentration of AgNPs in the soil (mg/kg), $[Ag]_{shoots}$ represent the Ag concentrations in plant shoot tissues (mg/kg), respectively.

4.2.5 Labile Ag extraction from AgNPs amended soil and soil pH measurement

At each sampling date, ~2.0 g of air-dried soil samples were extracted with 20 mL of $CaCl_2$ extractant or 4 mL of DTPA extractant[245]. $CaCl_2$ can extract the metals from the soil making use of cation competition processes, which has been considered to be "readily available" to plants/soil organisms. DTPA extraction is used for extracting the "readily available" fraction as well as the "potentially available" fraction that is reversibly bound to the soil solid matrix, which has been suggested to be an indication for metallic nanoparticle dissolution in soil[245]. The $CaCl_2$ extractant was prepared by dissolving $CaCl_2$ salt in Milli-Q water to reach the final concentration of

0.01M. The DTPA extractant was a mixture of 0.005 M DTPA, 0.01 M $CaCl_2$, and 0.1 M triethanolamine (TEA). All extractions were conducted using a reciprocal shaker for 2 h at 180 rpm. After extraction, the samples were centrifuged at 4500 rpm for 30 min and the supernatants were filtered using 0.22 μm filter. Afterwards, the filter samples were acidified with concentrated HNO_3 (the final HNO_3 concentrations were less than 2 %) and stored at 4 °C before performing ICP-MS measurements. Standard Ag solutions of 0.5 mg/L (AAS) and 10 ng/L (for ICP-MS) was measured every 20 samples to monitor the stability of the machines. Blanks and Ag standard solutions were included in the digestion procedure for the purposes of quality control. The average recovery of Ag for the digestion procedure was 91% with the standard deviation of 7% and the recovery for the machines was from 99% to 101%. The detection limits for AAS and ICP-MS were 1 μg/L and 1 ng/L respectively. The RSDs for all samples measurement were below 5%.

Within all samples treatments and times, pH was measured within the original supernatants (without centrifugation, filter and acidifying) from the $CaCl_2$ extracts representing soil pH of soil extractable available fraction[248].

4.2.6 Rhizosphere soil DNA extraction and Illumina Miseq sequencing

The DNA from the soil rhizosphere was extracted using Qiagen DNeasy PowerSoil Kit (Hilden, Germany). After quality control checking, a universal bacterial primer set (515F: 5'-GTGCCAGCMGCCGCGGTAA-3' and 909R: 5'-CCCGTCAATTCMTTTRAGT-3') was used for PCR amplification by targeting the variable V4-V5 regions of bacterial 16S rRNA genes. Paired-end sequencing was done using 2 × 300 bp Illumina Miseq platform (Illumina, Inc., San Diego, CA, USA) by BaseClear (Leiden, the Netherlands). The obtained sequences are deposited into the National Center for Biotechnology Information (NCBI) database (Project number: PRJNA732000). Quantitative Insights Into Microbial Ecology (QIIME2) pipeline was used to process the sequences. Sequences quality control was performed using the software package DADA2. Qualified sequences were processed to construct the Feature Table that was collapsed at the genus level (i.e., level 6 of the Greengenes taxonomy). The q2-phylogeny plugin was used to build the phylogenetic tree (**Figure S4.2**), and the q2-diversity plugin was conducted to compute alpha and beta diversity

metrics. The sampling depth was rarefied to remove the heterogeneity (**Figure S4.3**). The q2-feature-classifier plugin was conducted for taxonomic assignment.

4.2.7 Statistical analysis

Statistically significant differences regarding the $CaCl_2$ extractable Ag, DTPA extractable Ag, plant biomass, Ag content in plants among treatments were analysed by means of one-way ANOVA followed by Duncan's honestly significant difference tests at $\alpha < 0.05$ using IBM SPSS Statistics 25 (no deviations of data were found for normal distribution and homogeneity of variance with Shapiro-Wilk test and Bartlett test prior to running the ANOVA). The t-test was performed to determine the differences of the tested endpoints between bulk soil and rhizosphere soil ($\alpha < 0.05$). Results are expressed as mean ± standard error of 3 replicates. The QIIME2 diversity alpha-group-significance plugin was used to test the significance of Shannon index across the different treatments. The principal coordinates analysis (PCoA) based on the weighted UniFrac distance matrices was applied to compare community dissimilarities, and the Permutational multivariate analysis of variance (PERMANOVA) was used for significance test. The featured taxa that are differentially abundant in each treatment was identified using analysis of composition of microbiomes (ANCOM). The FDR test was used to correct the p-values from false positives in the multi-comparison tests. Spearman correlations between the tested endpoints were carried out in R with the package of "ggcorrplot" and were considered significant when $p<0.05$.

4.3. Results

4.3.1 Soil pH changes in bulk and rhizosphere soil after AgNPs amendment

Results showed that the addition of AgNPs significantly increased the soil pH of both unplanted (from 7.70 to 7.82) and planted soil (from 7.70 to 7.87) after 7 d of incubation (**Figure 4.1**A). However, the significant differences between control treatment and AgNPs treatments disappeared after long-term exposure (63d). Additionally, the soil pH of all treatments deceased after long-term exposure as compared to short-term exposure (7d). Noteworthy, no significant difference in soil

pH was observed between 10 mg/kg AgNPs planted and unplanted soil regardless of exposure duration (p=0.184 for 7d and p=0.956 for 63d). In addition, the soil pH did not differ between the treatments amended with different concentrations of AgNPs regardless of exposure duration (**Figure 4.1**).

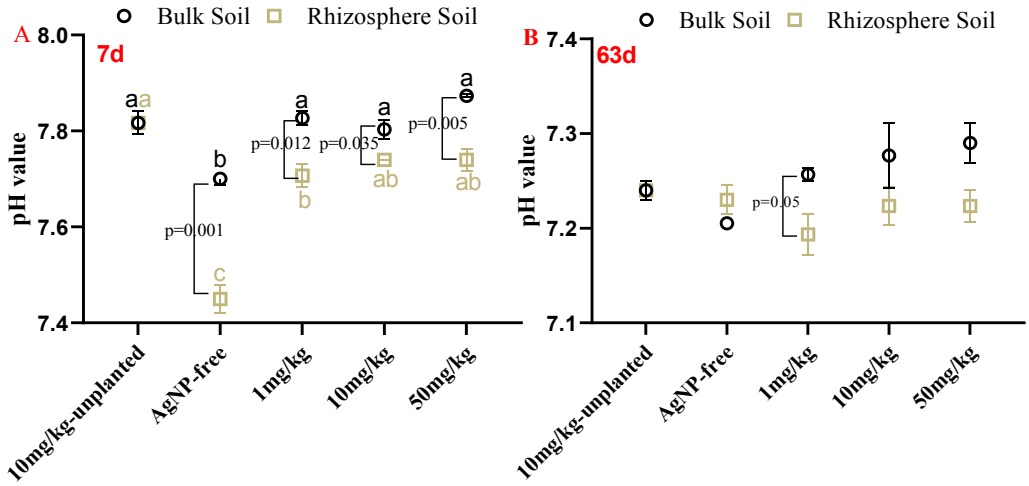

Figure 4.1. Soil pH in rhizosphere soil and bulk soil exposed to AgNPs with or without plant for 7 d (A) and 63 d (B). Different letters indicate the significant difference among the treatments in same soil ($p<0.05$). The numbers indicate the significant differences between the bulk soil and rhizosphere soil under same treatment($p<0.05$). Data expressed as mean ± SEM of triplicate samples.

4.3.2 Changes of extractability of Ag in bulk and rhizosphere soil

For the freshly prepared 1 mg/kg AgNPs amended soil (day 0-referred to transplanting date), the $CaCl_2$-extractable amount of Ag was below the detection limit, while the corresponding DTPA-extractable amount of Ag was 7 ± 2 µg/kg. Similarly, the $CaCl_2$-extractable amounts of Ag were 3.3 ± 0.8 µg/kg and 29 ± 5 µg/kg for 10 mg/kg and 50mg/kg AgNPs amended soil; while the DTPA-extractable amounts of Ag were 28 ± 3 µg/kg, 142 ± 4 µg/kg for 10 mg/kg and 50mg/kg AgNPs amended soil, respectively. Upon increasing incubation time, the extractable amount of Ag in both unplanted and planted soil decreased (**Figure 4.2**A). For example, for the 10 mg/kg AgNPs unplanted soil, the DTPA- extractable amount of Ag decreased from 28 ± 3 to 9.7 ± 0.5 µg/kg (incubation for 7 d) and to 2.9 ± 0.1 µg/kg (incubation for 63 d). Regarding the extractability of Ag in unplanted and planted soil at the same

cultivation time, the DTPA-extractable amount of Ag in bulk soil and rhizosphere soil was similar to (7 d) or significantly higher than (63 d, ANOVA, $p=0.01$) unplanted soil, while the $CaCl_2$ extractable amount of Ag in both cultivation time followed the order of unplanted soil > bulk soil > rhizosphere soil.

The differences of $CaCl_2$ extractable Ag and DTPA extractable Ag for AgNPs amended soil with different concentrations of AgNPs in bulk soil and rhizosphere soil are shown in **Figure 4.2**. A clear concentration-dependent impact on the extractable amount of Ag was observed for both bulk soil and rhizosphere soil regardless of $CaCl_2$ extractant or DTPA extractant. For the low AgNPs concentration (1 mg/kg), the amount of Ag extracted by the $CaCl_2$ extraction was below the detection limit, while the DTPA-extractable amount of Ag was less than 0.5 μg/kg soil. Compared to the concentration of 10 mg/kg AgNPs amended soil, the extractable amount of Ag in soil amended with 50 mg/kg AgNPs was significantly increased by a factor of 19 ~ 61 for $CaCl_2$ extraction and 7 ~ 14 for DTPA extraction under different conditions, respectively. Between bulk soil and rhizosphere soil, no significant differences were observed for the $CaCl_2$ extractable Ag regardless of exposure concentration or time. For DTPA extractable Ag, significant difference between bulk and rhizosphere soil was only observed for the soil to which 50 mg/kg AgNPs were added (t-test, $p<0.005$).

We also investigated the changes of the extractability of AgNPs in rhizosphere soil (10 mg/kg AgNPs) over time by DTPA extraction, as shown in **Figure 4.3**A. An interesting tendency was observed as the DTPA extractable Ag in the rhizosphere soil decreased rapidly in the first 3 d of cultivation and then increased gradually after 7 and 15 d of cultivation but decreased again from 15 to 63 d of cultivation. In addition, the extractable amount of Ag in planted soil after 7 d of cultivation was slightly higher when compared to the extractable amount of Ag after 63 d of cultivation in all experimental scenarios. However, statistically significant differences were only observed in 50 mg/kg AgNPs amended bulk soil for DTPA extraction ($p<0.005$, t-test).

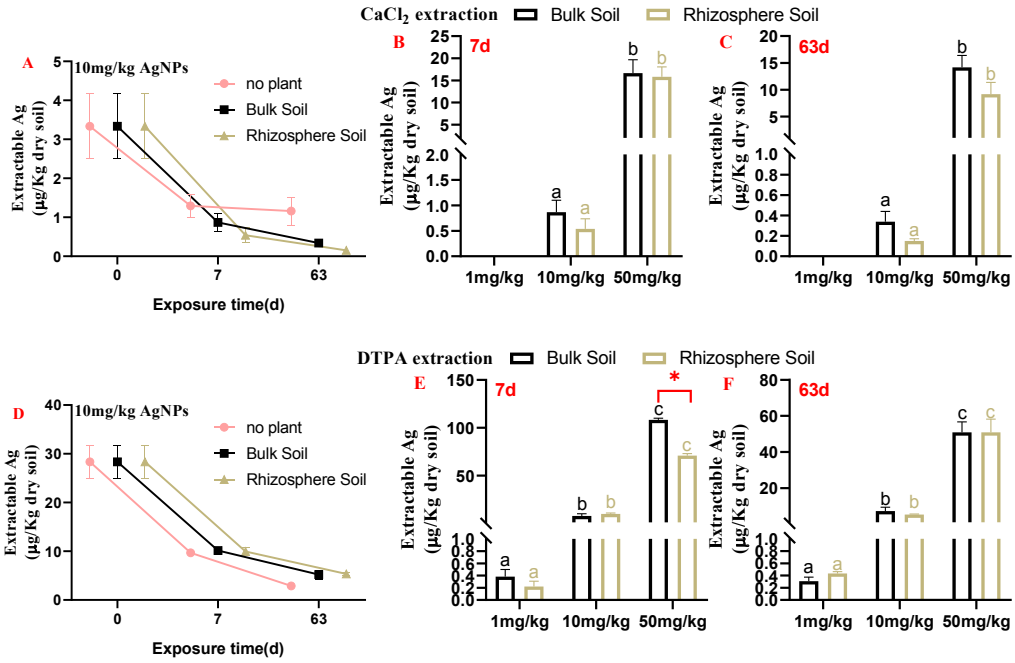

Figure 4.2. $CaCl_2$ and DTPA extractable Ag in AgNPs amended soil. A and D: Changes in response to the presence of plants for 10 mg/kg AgNPs treatment over time. B and E: Changes in bulk and rhizosphere soil with different concentration of AgNPs after 7 d of exposure. C and F: Changes in bulk and rhizosphere soil with different concentrations of AgNPs after 63 d of exposure. Different letters indicate statistically significant differences among the treatments in the same soil ($p<0.05$). The * indicates the significant differences between the bulk soil and the rhizosphere soil under the same treatment ($p<0.05$). Data are expressed as mean ± SEM of triplicate samples.

4.3.3 Ag accumulation and translocation in the soil-plant system

At the same exposure duration (7d or 63d), no significant differences in plant biomass were observed between control treatment and AgNPs treatments regardless of the exposure concentration ($p = 0.858$ for 7d and $p=0.541$ for 63d, **Figure S4.4**).

The change of Ag concentration in plant roots in 10 mg/kg AgNPs treatment over time is shown in **Figure 4.3**D. The Ag concentrations in the plant roots increased after 3, 7, and 15d of cultivation and then decreased in the cultivation period of 15 d to 63 d, which followed the same pattern of the DTPA extractable Ag in the corresponding rhizosphere soil over time. Interestingly, when comparing the Ag

concentrations in plants upon 7 d cultivation to 63 d cultivation at the same applied AgNPs dose, no significant difference was observed (**Figure 4.3**B, t-test, $p>0.05$). **Figure 4.3** also shows the accumulation and translocation of Ag in plant tissues after cultivation for 7 and 63 d in soil to which different amounts of AgNPs were added. The Ag concentrations in plant roots were more than 10 times higher than the Ag concentration in the corresponding shoots upon the same exposure concentration and time. Moreover, Ag was taken up by plant roots and translocated into plant shoots in all AgNPs amended treatments with a general concentration-dependent increase. For example, the Ag concentrations in lettuce shoots were around 1.6 mg Ag/kg plant for the treatment of 50 mg/kg AgNPs, which is 10 ~ 13 times higher than found in the shoots of plants exposed to 1 mg/kg AgNPs amended soils (0.16 mg/kg for 7 d and 0.13 mg/kg for 63 d).

In addition, the BAFs of Ag in all exposure treatments were higher than 1. The high Ag concentrations in plant roots and the high BAFs of Ag indicated the potential biomagnification of Ag from soil to plant. The presence of Ag in plant shoots shows the translocation ability of Ag from plant roots to shoots, even though the TFs of Ag in all treatments were lower than 0.1.

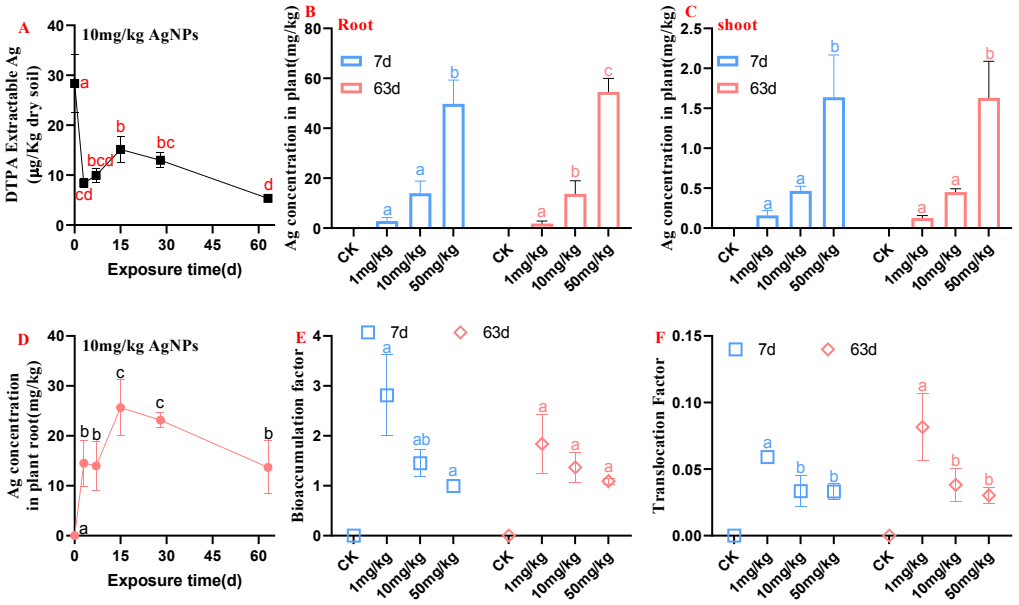

Figure 4.3. DTPA extractable Ag in rhizosphere soil (A) and Ag accumulation in plant root (D) in 10 mg/kg AgNPs treatment over time. Ag accumulation in plant root (B), plant shoot (C), and the BAFs (E) and TFs (F) among different AgNPs concentrations after 7 and 63 d of exposure. The concentration of Ag in plant roots and shoots for the control treatment were considered as 0 as they were below the detection limit. Different letters indicate a statistically significant difference among the treatments at the same exposure duration ($p<0.05$). Data are expressed as mean ± SEM of triplicate samples. CK means the control treatment.

4.3.4 Response of Soil Microbial Communities to AgNPs in rhizosphere soil

The alterations of the bacterial community in the rhizosphere in response to AgNPs exposure were further investigated. The Shannon index, which reflects the species richness, was used to evaluate the Alpha diversities of the rhizosphere bacteria in control soil and in AgNPs-amended soil. For 7 d of incubation, the changes of Shannon indices among the control and the soil amended with different concentrations of AgNPs were irregular (**Figure 4.4**A). However, after increasing the incubation duration to 63 d, a clear tendency we observed was that the Shannon index decreased with the increasing exposure concentration of AgNPs.

The shifts in the rhizosphere bacterial community structure induced by AgNPs

treatments over time were further analysed by principal coordinate analysis (PCoA) (**Figure 4.4**B). After an incubation of 7 d, the bacterial communities in control and different AgNPs treatments clustered together with each other. However, when the incubation time increased to 63 d, the bacterial communities exposed to 10 mg/kg AgNPs and 50 mg/kg AgNPs were clearly separated from the control. Moreover, the bacterial communities in 10 and 50 mg/kg AgNPs amended soil separated from each other. This indicates that the impacts of AgNPs on the bacterial community structure are time dependent.

Additionally, the community composition at the phylum level in response to different treatments is provided in **Figure S4.3**. Proteobacteria (with the average relative abundance of 29%-34%), Actinobacteria (27%-31%), Bacteroidetes (9%-14%) and Acidobacteria (9%-11%) were the dominant bacterial phyla in both control soil and AgNPs-amended soil after 7d of incubation. By increasing the incubation period from 7 d to 63 d, the average relative abundance of Actinobacteria decreased from 27 – 31 % to 16 – 20 %, again indicating that the effect of AgNPs on the bacterial composition is time-dependent. The featured taxa that are differentially abundant between the different treatments, were identified using ANCOM analysis (**Figure 4.4**C). In general, no featured taxa were found in the AgNPs treatments after 7d incubation. After incubation for 63d, a total of 16 featured taxa were observed, which greatly contributed to the observed differences between 50 mg/kg Ag amended soil and the control soil. From those featured taxa, 8 taxa (including the phyla of Acidobacteria and Gemmatimonadetes, the class of Holophagae, the order of Microtrichales, the family of Fimbriimonadaceae, Nitrososphaeraceae and Desulfarculaceae) were down-regulated and 8 taxa (including the order of Rhodospirillales, the family of vermiphilaceae, sphingobacteriaceae, Holosporaceae and Methylophilaceae, and the genus of *Pontibacter*, *Mesorhizobium* and *Sphingorhabdus*) were up-regulated in 50 mg/kg AgNPs when compared with the control. These results further confirmed a long-term impact of a high concentration of AgNPs on the rhizosphere bacterial community composition.

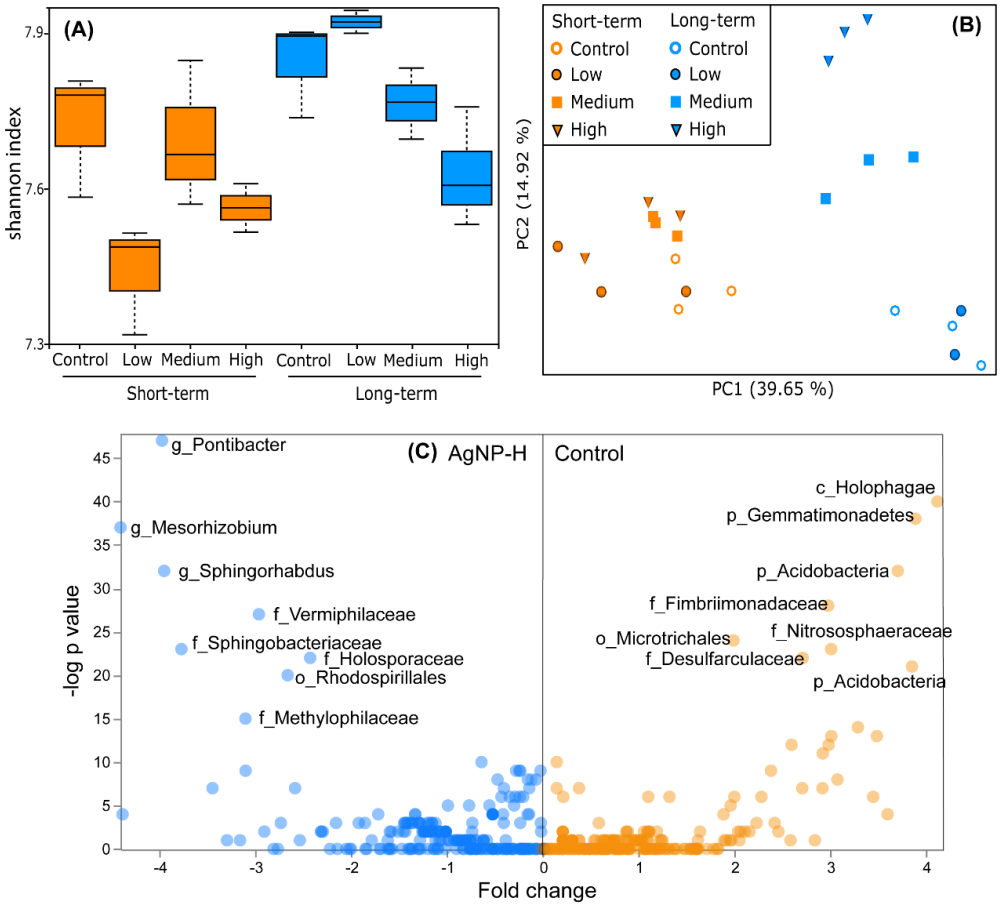

Figure 4.4. (A) Changes in the within community (α) diversity shown as the Shannon index; (B) Principal coordinate analysis (PCoA) of the bacterial community structure. (C) Featured taxa identified between the control and soil amended with 50 mg/kg AgNPs upon 63 d of incubation.

4.3.5 Correlation analysis of exposure conditions, soil pH, extractable Ag in soil, plant parameters, and soil bacteria communities

As shown from the map of Spearman's correlations (**Figure 4.5**), the soil pH was negatively correlated with exposure time but had no significant relationship with exposure concentration. The amount of DTPA-extracted Ag in both bulk and rhizosphere soil was significantly and positively correlated with the exposure concentration of AgNPs since all correlation coefficients were higher than 0.9. In

addition, the amount of Ag accumulated in the plant root and the shoots was correlated positively with DTPA-extracted Ag in the soil. Root and shoot concentrations were highly related because of the translocation of Ag from root to shoot. No relationships were observed between exposure time or soil pH and extractable Ag in soil as well as Ag content in plants. On the contrary, the Shannon index of the soil bacterial community was positively correlated with exposure time but negatively correlated with soil pH and the BAFs of Ag in plants.

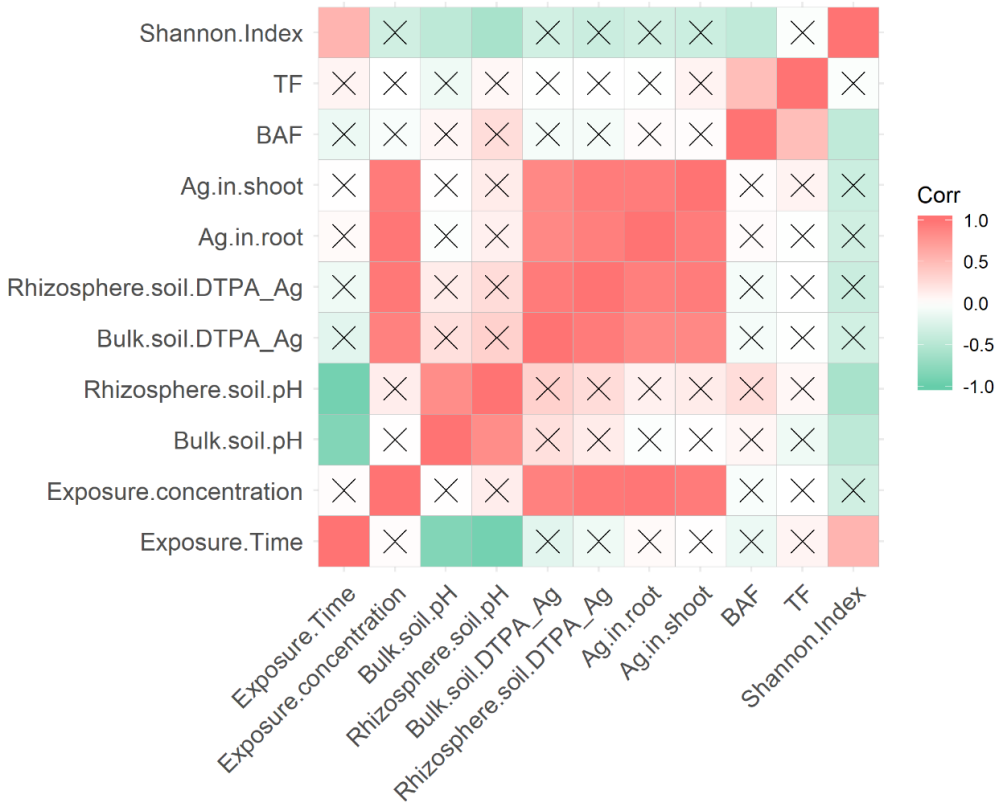

Figure 4.5. Spearman correlation map between the tested parameters including exposure conditions, soil pH, extractable Ag in soil, plant related parameters and Shannon index of soil bacterial community. Correlations with $p > 0.05$ fill with ×. Significant negative correlations (corr < 0) are given in gradations of green. Positive correlations (corr > 0) are given in gradations of red.

4.4. Discussion

Overall this study enhanced the understanding of how the dynamic dissolution of AgNPs in soil affects their bioavailability in the rhizosphere-lettuce interface and of long-term impacts of AgNPs on rhizosphere soil bacterial community. Our results revealed that the addition of AgNPs significantly increased the soil pH after 7 d of incubation regardless of the presence of lettuce plants (**Figure 4.1**A). This statistically significant increase is in line with the results of previous studies observing an increase of soil pH after amending soil with metallic nanoparticles[138,246]. The alterations of the soil metabolite profiles as well as the abundance and composition of root exudates can change soil pH[245,246]. For example, Zhang et al.[246] suggested that the increase of soil pH might be attributed to the decrease of the concentrations of several fatty acids in metabolites of the soil induced by exposure to AgNPs. Additionally, the dissolution of AgNPs can also contribute to higher pH[248] as it can consume the H^+ in the system or release OH^- into soil following the stoichiometry below:

$2\ Ag(s) + 1/2\ O_2 + 2H^+ \rightarrow 2\ Ag^+ + 2\ H_2O$[256]

or:

Ag_2O (oxide layer formed on the surface of AgNPs) + $H_2O \rightarrow 2\ Ag^+ + 2\ OH^-$ [231].

However, the soil pH decreased after increasing the incubation time to 63d and no significant differences were observed between treatments after 63d of incubation. This pattern was similar to the findings of Das et al.[257], who also reported the soil pH increased at the initial exposure period but decreased after long-term exposure. The findings suggest that the aging of AgNPs in soil neutralized the pH changes between treatments.

The dissolution of metallic nanoparticles is known to be the dominant process governing the availability of metals derived from metallic nanoparticles[248]. Thus, the dissolution of AgNPs in soil over time was investigated using DTPA extraction. The DTPA extractable Ag was less than 0.3% for all experimental scenarios, suggesting that the dissolution of AgNPs in soil was very limited, even in the rhizosphere. This was in line with the previous studies[49,258], which also revealed the very low lability/release of Ag from AgNPs amended soil. Interestingly, a gradual increase of

DTPA extractable Ag in rhizosphere soil was observed during the cultivation period from 3 to 15 d (**Figure 4.3**A), indicating the gradual dissolution of AgNPs in soil. However, the extractable Ag in rhizosphere soil decreased as the cultivation period increased from 15 to 63 d. Also, the Ag concentration extracted from the AgNPs amended soil after 63 d of cultivation was slightly lower than that after 3 d and 7 d of cultivation. There are several possible explanations for this observation of declining Ag concentrations. Firstly, the dissolution of AgNPs might have become slower after 15 d of cultivation, or the AgNPs dissolution reached saturation over a longer exposure duration. There is a plethora of information revealing the two-phase dissolution behaviour of AgNPs, containing a short but rapid initial release phase and a longer but slower second release phase[259,260]. Secondly, the uptake of Ag by plant roots was much faster than the dissolution process of AgNPs in soil as indicated by comparing the extractable Ag from AgNPs and the Ag uptake by plant roots over time (**Figure 4.3**A and D). This led to a relative decrease of Ag accumulation in the plants for the cultivation period from 15 to 63 d. Finally, this decline might be a result of the combination of Ag precipitation, irreversible binding of Ag^+/AgNPs to the soil solid matrix, as well as the transformation of AgNPs in soil[24]. After long-term exposure in soil, AgNPs have a large potential of being transformed to silver sulphide or other sulphur-bound Ag forms[49,261], which will reduce the solubility and extractability of AgNPs. A previous study also found that the concentration of labile Ag in soil was significantly decreased by increasing the incubation time to two weeks and to six months, and evidenced S groups-bound Ag was the predominant form after the soil was amended with soluble Ag[262], so-called aging processes. The changes of extractable concentration of Ag over time suggest that the single or fixed exposure duration cannot capture the actual dissolution and accumulation process of AgNPs in soil[245], which may result in inaccurate assessment of the bioavailability or toxicity of AgNPs.

Our results demonstrated that the DTPA extractable Ag concentration in unplanted soil, bulk soil and rhizosphere soil was almost equal (**Figure 4.2**D), suggesting that the effect of lettuce on the dissolution of AgNPs was limited. The $CaCl_2$-extractable amount of Ag followed the order of unplanted soil > bulk soil > rhizosphere soil (**Figure 4.2**A). This indicates that $CaCl_2$-extractable Ag is a better predictor of Ag

uptake by plants as it better represents the more "readily available" Ag form. Gao et al.[245] also suggested that DTPA-extraction is a better indication for metallic nanoparticle dissolution in soil while $CaCl_2$ extraction provides a more accurate prediction of the uptake of nanoparticles by plants. The observed Ag in plant shoot tissues shows the translocation of Ag from root to shoot. In addition, the Ag accumulation and translocation were positively correlated with the extractable amount of Ag in soil (**Figure 4.5**) and the trend of Ag accumulation in the plants over time was similar to the dissolution of AgNP in soil (**Figure 4.3**). These results indicate that the dissolution of AgNPs is the predominant process related to the Ag uptake by plant roots.

For the rhizosphere bacterial community, we did not observe any significant impact of AgNP in short-term exposure (7d) regardless of exposure concentration. However, after long-term exposure (63 d), the Shannon index decreased, and the bacterial communities separated from control with increasing exposure concentration. This suggests that the effects of AgNPs concentration on the diversity and composition of the rhizosphere bacterial community varied over time. Moreover, 8 upregulated bacterial taxa and 8 downregulated featured taxa were observed in the treatment of 50 mg/kg AgNPs after 63 d of exposure, which contributed the most in inducing the differences between AgNPs treatment and the control. Previous research stated that the soil microbiome can shift its composition by increasing the Ag-tolerant taxa in response to AgNPs stress[137,263]. Similarly, the abundance of Ag resistant and sensitive genus *Mesorhizobium*[264] was found to be increased in the soil amended with high concentration of AgNPs in our study. In addition, several bacterial groups associated with the removal/degradation of a number of contaminants were stimulated in response to AgNPs, including the genus *Pontibacter* that is able to remove metals[264,265], and *Sphingorhabdus* and *Sphingobacteriaceae* that are related with the degradation of a variety of recalcitrant organic compounds[247,246,266]. In addition, *Pontibacter* (strongly associated with the N fixation gene nifH)[146], *Mesorhizobium*[261] and *Rhodospirillales* (containing free-living N_2-fixing bacteria)[247,263] were also promoted, indicating that long-term exposure of AgNPs stimulate the bacterial taxa related to nitrogen cycling. Besides these upregulated bacterial taxa, several bacteria were significantly inhibited upon long-term exposure to high concentration of AgNPs such as Acidobacteria and

Desulfarculaceae[246,267,268]. These bacteria are involved in carbon usage, sulphur reduction, and iron reduction. The alterations of the identified featured taxa highlight the potential disruption of agricultural systems because of AgNPs exposure by affecting the functional bacterial groups associated with nutrient acquisition, stress tolerance and biogeochemical elements cycling (such as C, N and S). Moreover, the changes of the diversity and structure of the rhizosphere soil bacterial community over time also emphasize the importance of investigating the dynamic impacts of nanoparticles on the rhizosphere bacterial communities.

4.5. Conclusions

Overall, the presence of the lettuce played a limited role in affecting AgNPs dissolution in soil as the extractability of Ag in unplanted and planted soil was similar at the same exposure conditions. We found that the dissolution of AgNPs in soil is the dominant process influencing Ag uptake via the roots and translocation to the shoots. The Ag extractability from AgNPs amended soil and accumulation of Ag in the plants changed over time. The diversity and composition of the rhizosphere soil bacterial community were altered after long-term exposure to high concentration of AgNPs. These results highlight the importance of taking in consideration time-resolved dynamics of the soil-plant system in response to nanoparticle exposure. The slow but continuing dissolution of AgNPs in soil can provide a sustaining antimicrobial effect against plant pathogens (phytopathogenic fungi, bacteria, and viruses). This implies that the repetitive applications of AgNPs are not needed, which likely diminishes the total Ag concentration applied. This is an important potential benefit of using AgNPs containing agrochemicals compared to applying ionic Ag-solutions. However, attention should still be paid to control the potential negative effects of AgNPs in soil-plant systems as high amounts of Ag in plant roots and the long-term alterations of the composition of the rhizosphere bacterial community were observed.

4.6 Supplementary Information

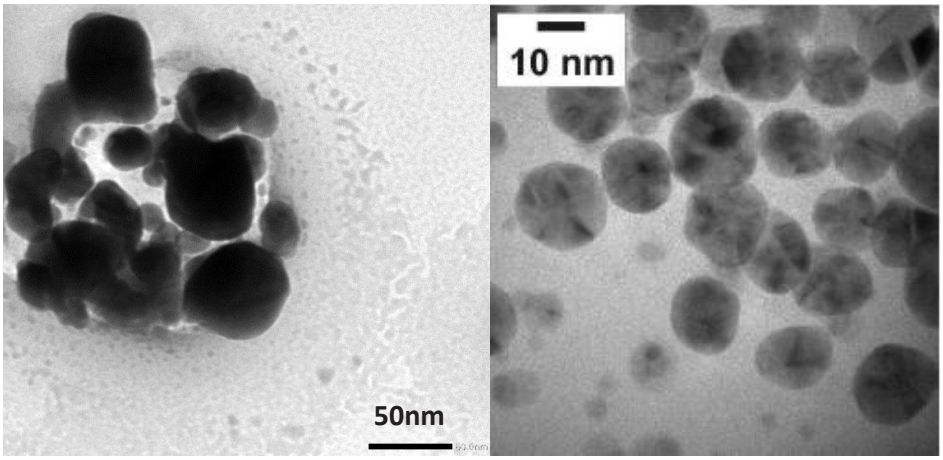

Figure S4.1 TEM picture of AgNP

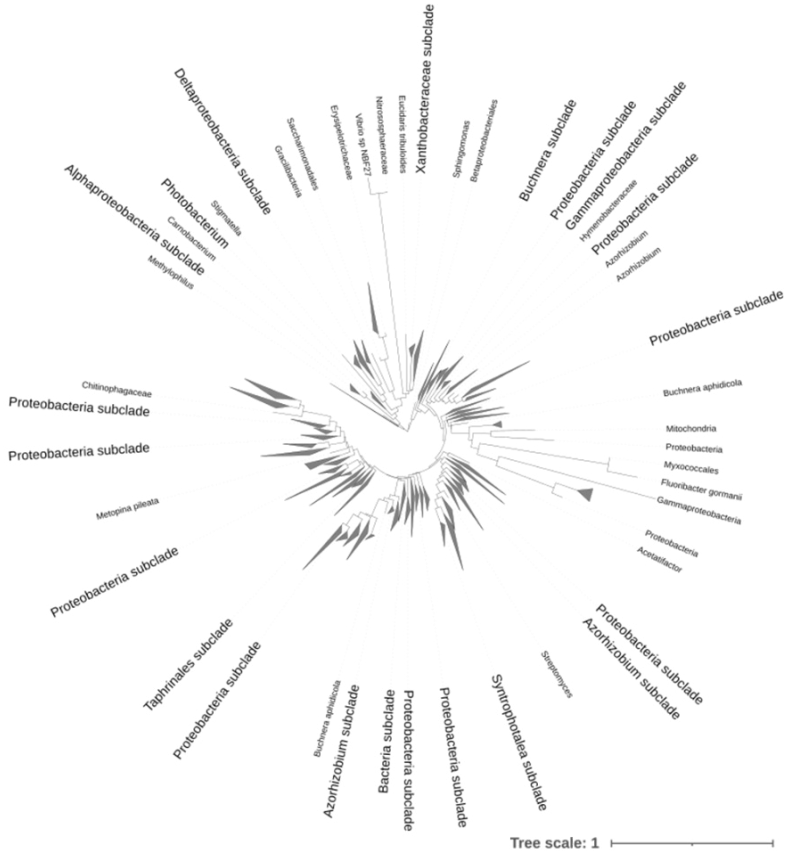

Figure S4.2 Phylogenetic tree of the rhizosphere bacterial community generated using align-to-tree-mafft-fasttree pipeline from the q2-phylogeny plugin.

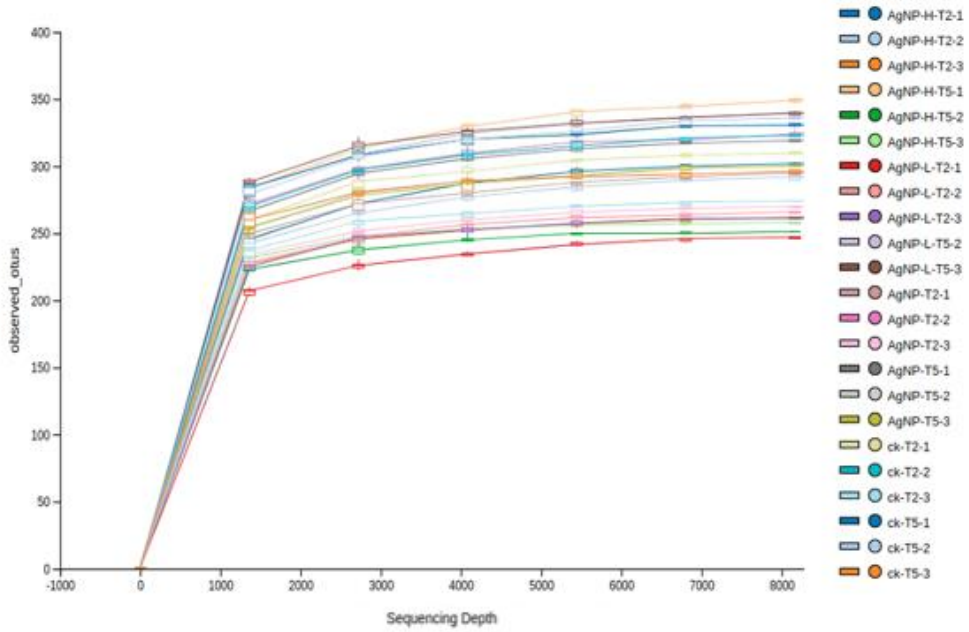

Figure S4.3 Rarefaction curves of rhizosphere bacterial communities in the soil samples of control and different AgNPs treatments.

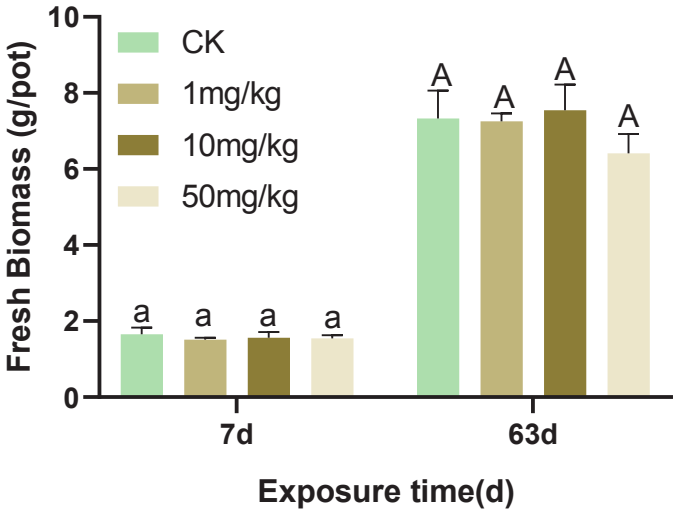

Figure S4.4 The biomass of lettuce exposed to different concentrations of AgNPs upon 7d or 63 cultivation.

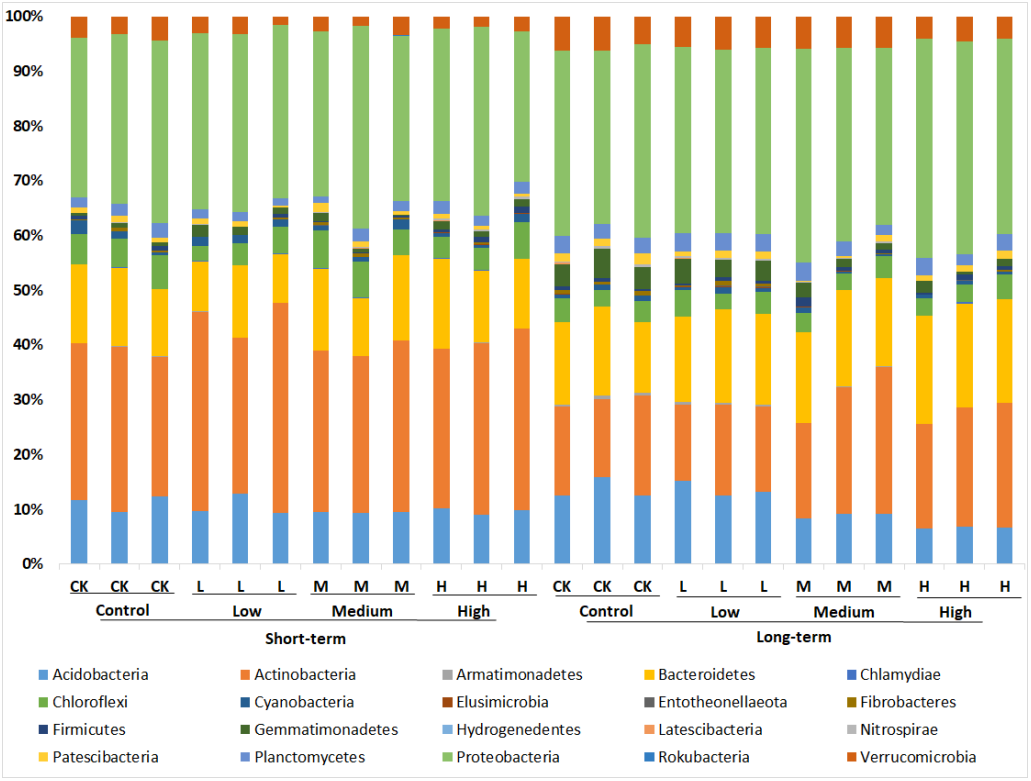

4

Figure S4.5 The composition of the rhizosphere soil bacterial communities at the phylum/class levels.

Table S4.1. Hydrodynamic Diameter and Zeta-Potential of AgNPs Suspensions in 1/4 Hoagland solution

Nominal concentration	Hydrodynamic diameter (nm)			Zeta-potential (mV)		
	1 h	24 h	48 h	1 h	24 h	48 h
1 mg/L	246±26	692 ±64	1190±262	-16±0.4	-15.1±0.6	-15.3±0.5
10 mg/L	43±1	62±23	71.1±27	-15.2±0.5	-14.8±0.4	-12.1±0.4
50 mg/L	35±7	35±2	37±1	-12.0±0.7	-10.3±0.3	-9.5±0.5

Physicochemical properties of the soil used in this study[269]

The physicochemical properties of the soil used in this study are reported in **Table S4.2**.

• The pH was determined according to the method reported by Slattery et al. (1999)[270]. The soil: water and soil: KCl ratio was 1:2.5 for both measurements.

• Organic carbon was analysed according to the method reported by Walkley and Black (1934)[271].

• The cation exchange capacity (CEC) and exchangeable cation content were determined according to the method reported by Hendershot and Duquette (1986)[272]. Al, Ca, K, Mg and Na were extracted with 0.1 M $BaCl_2$, and the concentrations were determined by Inductively Coupled Plasma Optical Emission Spectrometry (ICP-OES) (PerkinElmer Optima 4300 DV, PerkinElmer, Waltham, MA, USA).

• The total metal contents were extracted with a mixture of HNO_3 and HCl (1:3 v/v) in Teflon reactors under 10 bar, 180 °C and 35 min as operational conditions of the microwave oven. The concentration in the extracts was determined by ICP-OES as above.

Table S4.2. Soil characteristics (standard error)

	Units	Soil
pH_{H2O}	-	8.35 (0.04)
pH_{KCl}	-	7.43 (0.04)
Organic C	%	2.16 (0.09)
CEC	$cmol^{(+)}\ kg^{-1}$	0.386 (0.009)
Na^{+}		0.054 (0.001)
K^{+}		0.032 (0.001)
Ca^{2+}		0.062 (0.001)
Mg^{2+}		0.102 (0.002)
Al^{3+}		0.137 (0.003)
Element		**Total concentration***
Ag	$mg\ kg^{-1}$	udl
As		udl [76]
Cd		udl [13]
Co		udl [190]
Cr		1.41 (0.24) [180 (Cr^{3+}) – 78 (Cr^{6+})]
Cu		2.24 (0.03) [190]
Fe		8284 (435) [niv]
Mn		172.91 (5.84) [niv]
Ni		30.53 (10.61) [niv]
Pb		udl [530]
Ti		357.7 (23.6) [niv]
Zn		8.97 (1.48) [720]

CEC: Cation Exchange Capacity, udl: under detection limit. []: Intervention values for soil remediation in Netherlands (niv: no intervention value). (1.VROM - Ministry of Housing, Spatial Planning and the Environment (2013) Circular on target values and intervention values for soil remediation. The Netherlands).

Table S4.3. Experimental design

Exposure time	Treatment	plant	Concentration ($mg\ L^{-1}$)
0d	AgNPs1	planted	1
	AgNPs10	planted	10
	AgNPs10	unplanted	10
	AgNPs50	planted	50
7d	AgNPs0 (ck)	planted	0
	AgNPs1	planted	1
	AgNPs10	planted	10
	AgNPs10	unplanted	10
	AgNPs50	planted	50
63d	AgNPs0(ck)	planted	0
	AgNPs1	planted	1
	AgNPs10	planted	10
	AgNPs10	unplanted	10
	AgNPs50	planted	50
3d	AgNPs10	Planted	10
15d	AgNPs10	Planted	10
28d	AgNPs10	Planted	10

Iceland, 2018

Photo by Beilun

Chapter 5

Trophic transfer and toxicity of (mixtures of) Ag and TiO_2 nanoparticles in the lettuce - terrestrial snails food chain

Juan Wu, Thijs Bosker, Martina G. Vijver, Willie J. G. M. Peijnenburg

Submitted in Environmental Science & Technology

(2021), In revision

Abstract: The increasing application of biosolids and agrochemicals containing silver nanoparticles (AgNPs) and titanium dioxide nanoparticles (TiO_2NPs) results in their inevitable accumulation in soil, with unknown implications along terrestrial food chains. Here, the trophic transfer of single NPs and a mixture of AgNPs and TiO_2NPs from lettuce to snails and their associated impacts on snails were investigated. Both AgNPs and TiO_2NPs were transferred from lettuce to snails with trophic transfer factors (defined as the ratio of the Ag/Ti concentration in snail tissues to the Ag/Ti concentration in the lettuce leaves) of 0.2 to 1.1 for Ag and 3.8 to 47 for Ti. Moreover, the majority of Ag captured by snails in the AgNPs-containing treatments was excreted via faeces, whereas more than 70% of Ti was distributed in the digestive gland of snails in the TiO_2NPs-containing treatments. Additionally, AgNPs-containing treatments significantly inhibited the activity of snails, while TiO_2NPs-containing treatments significantly reduced faeces excretion of snails. Furthermore, the concurrent application of AgNPs and TiO_2NPs did not affect the biomagnification and distribution patterns of Ag and Ti in snails, whereas their co-existence exhibited more severe inhibition of the growth and activity of snails than in the case of applying AgNPs or TiO_2NPs alone. This highlights the possibility of nanoparticle transfer to organisms of higher trophic levels via food chains and the associated risks to ecosystem health.

5.1. Introduction

The release of silver and titanium dioxide nanoparticles into agricultural soil is expected to increase through the expanding application of nano-containing biosolids and agrochemicals[55,273]. This raises concerns about their potential adverse side-effects on soil ecosystems and the potential risk to plants and animals. To date, extensive studies have been performed to understand the interactions between metallic nanoparticles and plants because of the crucial role of plants in the terrestrial food chain. Emerging evidence suggests that AgNPs and TiO_2NPs can be taken up by plant roots and subsequently be translocated to leaves[82,187,274,275,276], and even to the fruits/grains[240,277,278] of certain plant species. For example, the uptake and translocation of Ag/AgNPs were observed in rice (*Oryza sativa L.*) with measured translocation factors of 0.11 to 0.21[187], and in lettuce (*Lactuca sativa*) with

translocation factors of 0.002 to 0.01[82], as well as with translocation factors of 0.1 to 0.6 in ryegrass (*Lolium multiflorum*)[61]. Similarly, the accumulation of TiO_2NPs in lettuce[274,275], wheat (*Triticum aestivum*)[279,280] and cucumber (*Cucumis sativus*)[276,278] was confirmed. The considerable evidence of the accumulation of AgNPs and TiO_2NPs in edible parts of plants makes it reasonable to assume the likelihood of their transfer and potential biomagnification to higher-level consumers via the food chain. In contrast to the studies on the trophic transfer of AgNPs/TiO_2NP in aquatic food webs (mostly focused on algae to daphnia[281,282] or daphnia to zebrafish[283]), limited attention has been paid to the trophic transfer of AgNPs/TiO_2NPs within terrestrial food chains, especially for the transfer from plants to animals.

Currently, there are few publications addressing the trophic transfer of metallic nanoparticles from terrestrial plants to primary consumers and the subsequent bioaccumulation in these primary consumers. Judy et al.[284,285] reported the bioaccumulation of gold NPs from tobacco (*Nicotiana tabacum* L. cv *Xanthi*) and tomato (*Lycopersicon esculentum*) to the tobacco hornworm (*Manduca sexta*). CeO_2 NPs have been reported to transfer along several food chains, including: lettuce - snail (*Achatina fulica*)[286], lettuce - hornworm (*Spodoptera litura* F.) - chicken (*Gallus gallus domesticus*)[287], zucchini (*Cucurbita pepo* L.) - cricket (*Acheta domesticus*) - spider (family Lycosidae)[288] and kidney bean (*Phaseolus vulgaris* var. red hawk) - Mexican bean beetles (*Epilachna varivestis*) - spined soldier bugs (*Podisus maculiventris*)[289]. Previous studies also reported on the trophic transfer of La_2O_3 NPs through the lettuce - cricket - mantid (*Tenodera aridifolia sinensis* and *Sphodromantis centralis*)[290] food chain and of CuO NPs via the lettuce - cricket - lizard (*Anolis carolinensis*) food chain[291]. Even though those studies provided evidence of the trophic transfer of NPs via terrestrial food chains, the extent of transfer and biomagnification of NPs to the subsequent trophic level was inconsistent across the food chains. For example, the transfer of AuNPs from tobacco to tobacco hornworm occurred with trophic transfer factors of 6.2 to 11.6[284], while CeO_2-NPs were not magnified at all from lettuce to snail (trophic transfer factor =0.037)[286]. However, in none of the mentioned publications the impacts of trophic transfer of NPs on the behavioural alterations of the consumers was investigated. This information is valuable for assessing their possible risks to the environment and

ecosystem health.

Additionally, another area that is in lack of knowledge is related to the biomagnification and the effects of mixtures of nanoparticles on herbivores that feed on exposed plants. Importantly, once entered into the natural environment, nanoparticles always co-exist with numerous pollutants[292,293] including other nanoparticles[105]. This might result in interactions between the particles. TiO_2NPs are known to have a large specific surface and a strong adsorption ability, which are among the key reasons why TiO_2NPs can affect the biological effects of co-existing pollutants. For example, TiO_2NPs have been reported to decrease the toxicity of ZnO nanoparticles and CuO particles in cress (*Lepidium sativum*), wheat and cucumber[105]. To our knowledge, up till now only one study focused on soil ecosystems concerning the impacts of a mixture of TiO_2 and AgNPs. Specifically, Liu et al.[294] found that TiO_2NPs mitigate the inhibition by AgNPs of the growth of the plant *Arabidopsis thaliana* and the earthworm *Eisenia fetida* as well as the reduction of soil microbial biomass. The mixture of TiO_2NPs and AgNPs significantly decreased the Ag concentration but increased the Ti concentration in plants in comparison with the individual nanoparticles. The differences in Ag/Ti accumulation in plants induced by mixtures of NPs may affect the subsequent trophic transfer of the particles. However, to date, no study is available about the trophic transfer of a mixture of TiO_2NPs and AgNPs along a terrestrial food chain. In addition, the lack of published studies on this topic and the inconsistent biomagnification results highlight the need for further studies on the trophic transfer of nanoparticles in terrestrial food webs. This is especially true for mixtures of NPs, which constitutes a representative environmentally realistic exposure scenario.

In this study, lettuce and garden snails (*Cornu aspersum*) were used to study the trophic transfer of AgNPs and TiO_2NPs and the associated effects on snails. Lettuce is a worldwide cultivated leafy vegetable crop that is suited for evaluating the ecotoxicity of chemicals and soil amendments to higher terrestrial plants, as recommended by various regulations[295]. Similarly, terrestrial snails are recognized as excellent ecological and biological indicators for assessing the ecotoxicity of NPs[150,151]. This is because of the ease of collection and sampling, their global distribution, short

life-cycle, small size, high reproductivity, high adaption to various environmental conditions, and ease of culture under laboratory conditions[150,152]. The lettuce roots were firstly exposed to Ag^+, AgNPs, TiO_2NPs or to a mixture of these NPs, and then the leaves containing internalized Ag/Ti were fed to the snails. Afterwards, the growth and behavior of the snails were monitored over a period of 22 days and the metal accumulation and metal distribution in the snails was determined. The objectives of this study are to investigate 1) the trophic transfer of AgNPs and TiO_2NPs from lettuce leaves to snails, focusing on the biomagnification and biodistribution of Ag/Ti in snails; 2) the effects on snail behavior associated with trophic transfer of AgNPs and TiO_2NPs; 3) the effects of a mixture of AgNPs and TiO_2NPs on the trophic transfer and the behavior of snails. The findings of this study will help to improve the understanding of the trophic transfer of nanoparticles along a terrestrial food chain and the subsequent effects on higher-level consumers. This will provide important information about the potential risk of nanomaterials in ecosystems.

5.2.Materials and Methods

5.2.1 Nanoparticles preparation and characterization

Suspensions of spherical AgNPs (NM-300K, 100 g/L) with a nominal size of 15 nm were obtained from RAS AG (Regensburg, Germany), which is a standard reference of nanosilver for commercial and industrial application as recommended by OECD. TiO_2NPs powder of series NM-105 (mixture of anatase (80%) and rutile (20%) crystal structure, 99.5% purity), with a diameter around 25 nm were purchased from the European Commission's Joint Research Centre (Ispra, Italy). $AgNO_3$ was purchased from Sigma–Aldrich (Zwijndrecht, Netherlands). The size and shape of both AgNPs and TiO_2NPs were characterized by Transmission Electron Microscopy (TEM, JEOL 1010, JEOL Ltd., Tokyo, Japan). The hydrodynamic size and zeta potential of AgNPs and TiO_2NPs suspensions were measured after incubation in 1/4 Hoagland solution for 1 h using a zetasizer Nano-ZS instrument (Malvern, Instruments Ltd., Royston, UK). More details of the physico-chemical properties of the AgNPs and TiO_2NPs are summarized in Reports of the European Commission's Joint Research Centre [255,296].

Suspensions of nominal 0.75 mg/L AgNPs and 200 mg/LTiO_2NPs (based on EC_{25} concentrations for lettuce[274,221]) were freshly prepared in 1/4 Hoagland solution (pH 6.0 ± 0.1; the composition of the Hoagland solution is described in **Table S2.1**) after sonication for 15 min at 60 Hz (USC200T, VWR, Amsterdam, The Netherlands). A mixture containing 0.75 mg/L AgNPs and 200 mg/L TiO_2NPs was prepared by adding a specific amount of AgNPs and TiO_2NPs into 1/4 Hoagland solution and sonicating for 15 min at 60 Hz. The exposure concentration of $AgNO_3$ (used as a reference salt for dissolved Ag ions) was 0.05 mg/L, based on the range of Ag-ion concentrations obtained upon dissolution of AgNPs at the test concentrations indicated above.

5.2.2 Plant cultivation and nanoparticles exposure

Lettuce seeds (*Lactuca sativa*) purchased from Floveg GmbH (Kall, Germany) were sterilized with NaClO (0.5% w/v) for 5 min. After immersing in deionized water for 24 h, the seeds were germinated and allowed to grow in Petri dishes containing wet filter papers (15 seeds per dish). Subsequently, the seedlings were hydroponically grown in tubes (one seedling per tube) containing 1/4 Hoagland solution for three weeks as described by Dang et al.[297] to harvest sufficient leave biomass for feeding the snails. Next, the uniformly pre-grown seedlings were selected and exposed to either Ag^+, AgNPs, TiO_2NPs, the mixture of AgNPs and TiO_2NPs, or the Hoagland solution alone (as negative control) via the roots for 28 days[286]. Each treatment had 30 seedlings/replicates. All the tubes containing a seedling and exposure medium were covered with aluminum foil in order to minimize the impact of light-induced transformations of AgNPs and TiO_2NPs. The exposure media of all tubes were renewed every two days and refilled to a volume of 22 mL on the day in between the days of refreshment of the suspensions. All experiments were performed in a climate room at a 25/20 °C day/night temperature regime with a 16 h light cycle and 60 % relative humidity[287]

After harvesting, the plants were removed from the exposure suspensions and washed with tap water for 10 mins. Afterwards, the plants were kept at 4 °C until they were used to feed the snails. A small portion of the plant tissues (roots and shoots) were immersed into 10 mM HNO_3, 10 mM EDTA for 1 hour each and finally rinsed

with Milli-Q water to remove the attached nanoparticles/metal ions[297,298]. The washed samples were oven-dried at 70 °C for 72 h and digested with *aqua regia* (HNO_3 (65%): HCl (37%) = 1:3)[299]. The total Ag/Ti contents in the plant roots/shoots of each treatment were measured by inductively coupled plasma-mass-spectrometry (ICP-MS, PerkinElmer NexION 300D). The translocation factor (TF) of Ag/Ti from roots to shoots was calculated as follows[298,300]:

$$\mathrm{TF} = \frac{[Ag/Ti]_{shoots}}{[Ag/Ti]_{roots}}$$

Where $[Ag/Ti]_{root}$ represents the concentrations of Ag/Ti in the plants root tissues (mg/kg) and $[Ag]_{shoots}$ represents the Ag/Ti concentrations in plant shoot tissues (mg/kg), respectively.

5.2.3 Snail exposure

The feeding experiments were performed based on the method reported by Ma et al. with a small modification[286]. Specifically, the Juvenile snails (*Cornu asperum*) were collected from a biologically handled garden (52°09'39.4"N 4°28'36.8"E, Leiden, Netherlands) and acclimated for 6 weeks in the laboratory, whilst feeding clean lettuce. Prior to the experiments in which NPs-contaminated lettuce leaves were fed to snails, the acclimated snails were not fed for 48h to ensure their maximum consumption of leaves. The pre-selected snails with the diameter of ~1.1 cm and weight of ~0.4 g were randomly assigned to five treatments cultured in glass bottles and fed with either unexposed leaves (control) or Ag^+, AgNPs, TiO_2NPs, AgNPs+TiO_2NPs (mixture) contaminated leaves. Each treatment had three replicates (bottles) and each replicate contained 3 snails. Immediately before feeding, the fresh leaves were cut into small pieces, weighed, thoroughly mixed and introduced to the bottles as diet (around 1 g per bottle) every two days for a period of 22 days. At each feeding interval, the unconsumed leaves in each bottle were removed and weighed to calculate the leaf consumption rate. During the 22 days of feeding period, faeces produced by snails in one bottle were collected, weighed every two days, and stored cumulatively at 4 °C in order to measure the Ag/Ti contents. After 22 d of feeding, the snails were fed with untreated (clean) leaves for 48 h to depurate the Ag/Ti from the gut before harvest.

5.2.4 Measurement of snail growth and behaviour

During the feeding period, the weight and diameter (the instruction of diameter measurement is given in **Figure S5.1**) of the snails were measured every two days at the same time during the day to monitor their growth. The mobility of snails was analysed by recording the movement of snails in a cylinder glass, and distance was tracked with video using an iPhone 7. The behavioural activity of snails was assessed using the behavioural state score (BSS) system as described previously[301] with some modification. Specifically, snails' activity was scored at 5 levels ranging from 0 to 4 (**Table S5.1**): 0 point for full retraction into its shell; 1 point for being withdrawn without head visible, 2 point for a protruding head without movement, 3 point for an extended foot and head with slight movement, 4 point for full extended with active movement. The feeding and excretion speeds of snails were determined by weighing the consumption of leaves and the production of faeces.

After sacrificing the snails, the shell was removed and snails were divided into the digestive gland (which included the digestive gland, stomach and intestine) and soft tissue (including foot, head, eyes, tail, hermaphroditic duct and mantle) according to the methods provided by University of Florida & United States Department of Agriculture (http://idtools.org/id/mollusc/dissection_snail.php). Thereafter, the dissected snails were stored at -80 °C separately for further analysis. The snail tissues and faeces were oven-dried at 70 °C for 3 days and weighed. The dried and weighed body, digestive gland and faeces were digested with HNO_3 (65%) at room temperature overnight. Subsequently, the pre-treated solutions were further digested with an appropriate volume of *aqua regia* by sonicating for 2 h in an ultrasonic bath at 60 °C and further kept in a water bath at 80 °C for 3-5h. Afterwards, the solutions were diluted and Ag/Ti contents were measured with an ICP-MS.

Trophic transfer factors (TTFs)[286], defined as the ratio of the concentration of Ag/Ti in snails body, digestive gland or faeces (mg/kg) to the concentration of Ag/Ti in lettuce leaves, were calculated with the following formula:

$$\mathrm{TTF} = \frac{[Ag/Ti]_{Snail}}{[Ag/Ti]_{shoot}}$$

5.2.5 Statistical analysis

Statistically significant differences regarding the tested endpoints among treatments at the same time point were analysed by means of one-way ANOVA followed by Duncan's honestly significant difference tests at $\alpha < 0.05$ using IBM SPSS Statistics 25. The Shapiro-Wilk test was used to check for normality and the Bartlett test for homogeneity of the variance of the data. If either of these assumptions were not met, data were log10 transformed to improve their fit. Results are expressed as mean ± standard error of 3 replicates. Besides, the results of prior-calculation of sample size by defining the critical effect size at 25% and the post-hoc calculation of power are provided in **Table S5.2**.

5.3. Results

5.3.1 Characterisation of AgNPs and TiO_2NPs

TEM micrographs showed that both AgNPs and TiO_2NPs formed agglomerates after being dispersed in water (**Figure S5.2**). Both spherical and slightly elongated shape of AgNPs with the diameter ranging from 6 to 45 nm (average 22.6 ± 0.79 nm, n=15) were observed from the TEM images. And the primary TiO_2NPs exhibited a more angular shape having a diameter ranging from 11 to 37 nm (average 21.5 ± 0.57 nm, n=15). The average hydrodynamic diameter of 0.75 mg/L AgNPs and 200 mg/L TiO_2NPs after dispersing in 1/4 Hoagland solution was 239 ± 14 nm and 978 ± 218 nm with the corresponding Zeta potential of -14.5 ± 0.75 mV and -14.4 ± 0.71, respectively. As measured by ICP-MS, the actual exposure concentration of Ag in the AgNPs treatment and the mixture treatment was 0.57 ± 0.05 mg/L and 0.55 ± 0.05 mg/L; the actual exposure concentration of Ti in the TiO_2NPs treatment and the mixture treatment was 103 ± 4 mg/L and 111 ± 8 mg/L, respectively.

5.3.2 Accumulation of Ag or Ti in plants

No significant inhibition of plant growth was observed for all treatments at the selected exposure concentrations when using biomass as the endpoint (data are provided in **Figure S5.3**). As shown in **Figure 5.1**, Ag or Ti were taken up by plant roots and subsequently translocated into plant shoots after exposure to Ag^+, AgNPs,

TiO_2NPs or the mixture for 28 days. The Ag concentration in plants of the Ag^+ treatment was much lower than the Ag concentration in plants of the AgNPs and mixture treatments (ANOVA, $p<0.005$). For example, the average Ag concentrations in plant shoots were 0.21, 1.01 and 1.08 mg/kg for Ag^+, AgNPs and mixture treatments, respectively. Interestingly, exposure to AgNPs alone resulted in a higher Ag concentration in plant roots in comparison to exposure to the mixture, while the differences of the Ag concentration between AgNPs and mixture treatments disappeared in the plant shoots. In contrast, significant differences of Ti concentration between TiO_2NPs and mixture treatments were only observed in the plant shoots (t-test, $p=0.036$) rather than in the plant roots (t-test, $p=0.667$). The average Ti concentrations in plant shoots were 6.15 and 9.07 mg/kg for TiO_2NPs and mixture treatments, respectively. Furthermore, the translocation factors of Ag and Ti in the mixture treatment were both higher than in the treatment of AgNPs or TiO_2NPs alone (**Table 5.1**, $p<0.05$).

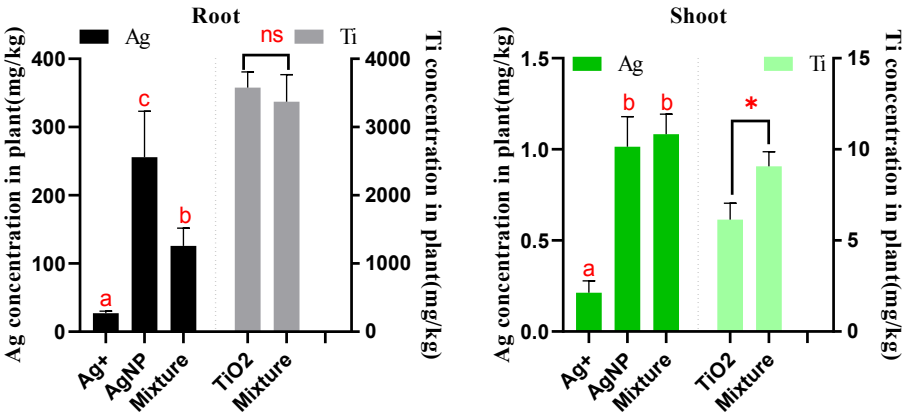

Figure 5.1. The Ag or Ti contents in lettuce root (A) and shoot (B) for different treatments after 28 d of exposure. Both Ag and Ti concentrations displayed in the figures were normalized with the concentrations of Ag/Ti in the control treatment. The different letters indicate significant differences among different treatments within the same tested metal at $p<0.05$.

5.3.3 Ag or Ti content in snails and trophic transfer

As shown in **Figure 5.2**A, either Ag or Ti was detected in the snails in the corresponding treatments. This suggests that both Ag and Ti could be transferred to snails from lettuce leaves when lettuce was exposed to either Ag^+/AgNPs or TiO_2NPs via the root. The Ag concentrations in the soft tissues of the snails in the Ag^+ treatment were higher than in the case of the AgNPs-containing treatments: AgNPs and mixture. The Ag concentration in the digestive gland and the faeces of snails consuming lettuce that were exposed to AgNPs and the mixture were much higher than the Ag-concentration in snails of the Ag^+ treatment (**Figure 5.2**A). In addition, no significant differences were observed for the Ag/Ti concentration in snails between the treatments of single NPs and the mixture regardless of the snail organs (ANOVA, $P>0.05$). This indicates that co-exposure to AgNPs and TiO_2NPs did not affect the trophic transfer of Ag or Ti compared to the trophic transfer following exposure to AgNPs or TiO_2NPs alone.

The Ag concentrations in snails followed the order of digestive gland ≈ faeces > soft tissues, regardless of the consumption of lettuce exposed to Ag^+, AgNPs, or to the mixture. More than 40% of the Ag captured by the snails remained in the digestive gland or was excreted into the faeces in all Ag-containing treatments, while the retention of Ag in snail soft tissues was only 9 – 16 % for any of the Ag-containing treatments (**Figure 5.2**B). The Ti concentration in snails organs and egestion of TiO_2NPs and mixture treatments both followed the order of digestive gland > faeces > soft tissues. More than 70% of Ti was found to be retained in the digestive gland of snails (**Figure 5.2**B).

Additionally, the TTFs of Ag/Ti from lettuce leaves to snails organs were calculated. The TTFs of Ag from lettuce leaves to snail soft tissues and the digestive gland in the Ag^+ treatment were higher than the TTFs calculated from the AgNPs exposure and as calculated from the mixture treatment (**Table 5.1**). The TTFs of Ag in snail organs of the Ag^+ treatment were well above 1, while the TTFs in snail organs of AgNPs or the mixture were below or similar to 1. This suggests that biomagnification of Ag occurred in snails of the Ag^+ treatment whilst it did not occur in the AgNPs and mixture treatments. Furthermore, the TTF of Ti from lettuce leaves to snail soft

tissues in the TiO_2NPs treatment was higher than the TTF in case of the mixture treatment. Finally, the TTFs of Ti from lettuce leaves to the digestive gland of the snails in the TiO_2NPs and the mixture treatments were higher than the TTFs from lettuce leaves to snail soft tissues. This is due to the observation that most of the Ti was accumulated in the snail digestive gland. All the TTFs of Ti from lettuce leaves to snail organs were higher than 4, regardless of the TiO_2NPs or mixture treatment. This suggests that Ti was biomagnified in snails via trophic transfer.

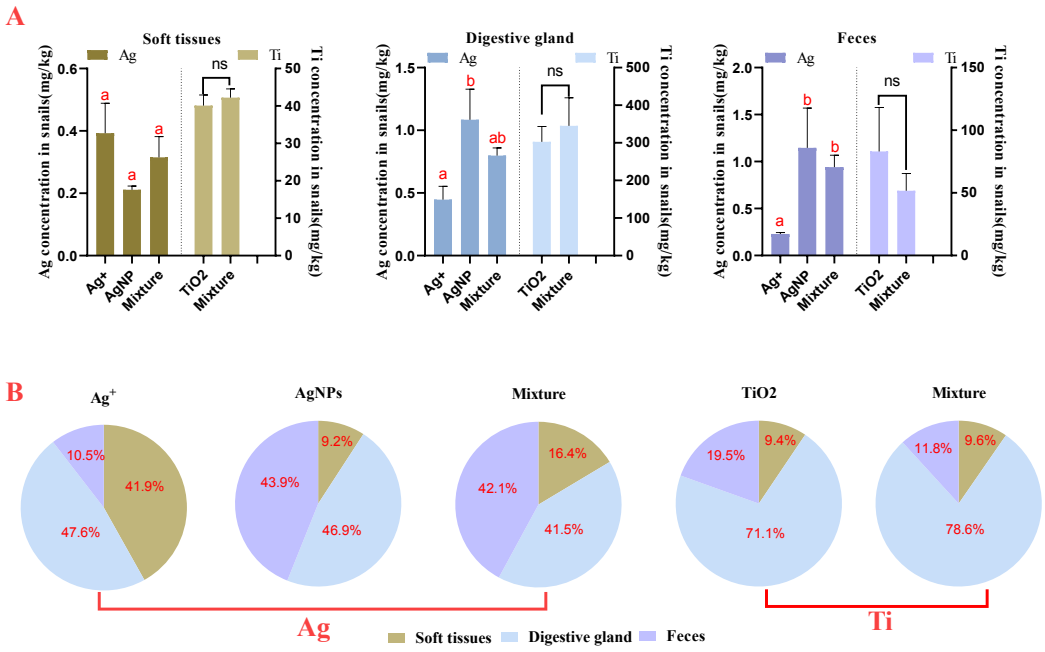

Figure 5.2. Ag and Ti concentrations (A) and distribution (B) in different organs and faeces of snails in different treatments along the food chain. Both Ag and Ti concentrations displayed in the figures were normalized with the concentrations of Ag/Ti in the control treatment. The different letters indicate significant differences of the same parameter among different treatments within the same organs at $p<0.05$.

Table 5.1. Translocation factors (TF) of Ag/Ti from lettuce roots to shoots and trophic transfer factor (TTF) of Ag/Ti from lettuce leaves to snail organs in different treatments. The different letters in the same column indicate statistically significant differences of same element between treatments at $p<0.05$.

Elements	Treatments	TFs (root to shoot)	TTFs (lettuce to snail soft tissues)	TTFs (lettuce to snail digestive gland)	TTFs (lettuce to snail faeces)
Ag	Ag+	0.008±0.001ab	1.8±0.5a	2.1±0.5a	1.1±0.07a
	AgNPs	0.004±0.001b	0.2±0.01b	1.1±0.2ab	1.1±0.15a
	Mixture	0.012±0.002a	0.2±0.05b	0.6±0.05b	0.7±0.10a
Ti	TiO2	0.002±0.0001a	5.3±0.5a	47±7a	11±6a
	Mixture	0.003±0.0004b	3.8±0.3a	37±8a	4.3±1.5a

5.3.4 Impact on snail growth

The impacts of nanoparticles on snails growth following exposure to lettuce leaves for 22 days were evaluated by monitoring the changes of their biomass or diameter (**Figure 5.3**). No snails died during the feeding and depuration period. Feeding with leaves contaminated with Ag^+, AgNPs, TiO_2NPs or the mixture did not result in a significant inhibition of snails biomass in comparison to the control (ANOVA, $p=0.173$). Even though the differences were not statistically significant, a 41.6% decrease in the biomass increase rate of snail in mixture treatment as compared to control treatment should be pointed out. This needs to be interpreted with care (low statistic power as stated in **Table S5.2**). In addition, compared to the control, significant inhibition of the snail diameter was observed for all treatments (ANOVA, $p<0.0001$), with average reductions of 56, 35, 68 and 90 % regarding the diameter increase rate of snail for the treatment with leaves exposed to Ag^+, AgNPs, TiO_2NPs and the mixture, respectively. When comparing the snails consuming leaves contaminated with the mixture to snails consuming leaves contaminated by single nanoparticles, significant differences in diameter increase rate were only observed between the treatments of lettuce with AgNPs and mixture ($p<0.005$).

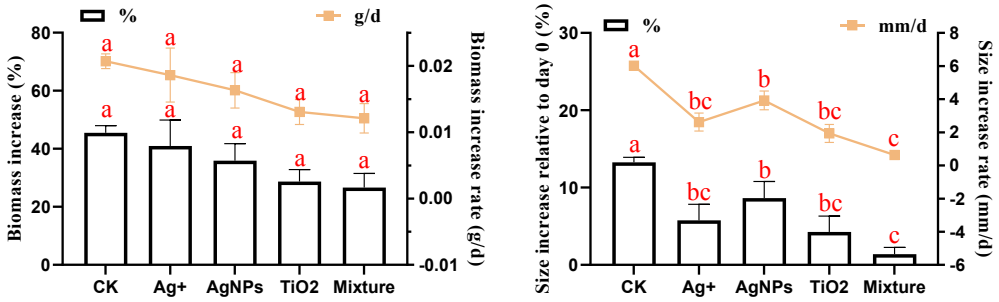

Figure 5.3. Effects of Ag^{+}, AgNPs, TiO_2NPs and mixture on snails growth through food chain transfer: (A) changes of biomass and (B) changes of diameter. CK treatment represents the snails were fed with unexposed lettuce leaves. The different letters indicate significant differences among different treatments within the same tested parameter at $p<0.05$.

5.3.5 Impact on food intake and excretion of snails

No significant differences in food intake were observed after the first two feeding periods (ANOVA, p=0.089 for 0-1 d and p=0.112 for 1-3 d, **Figure 5.4**A). After 6 d of feeding, the food intake rate of snails fed with the leaves exposed to the mixture of NPs was significantly reduced relative to control. By increasing the feeding duration to 10 and 16 d, the food intake rate of snails was significantly decreased for all treatments as compared to the control (ANOVA, p=0.007 for both feeding periods). Notably, although differences from control were observed, food intake did not differ significantly among the other treatments (Ag^{+}, AgNPs, TiO_2NPs and the mixture) regardless of the feeding periods.

Compared to control, excretion of faeces by the snails was significantly inhibited for all exposure scenarios in the first three feeding periods (ANOVA, p=0.018 for 0-1 d, p=0.006 for 1-3 d, p=0.004 for 3-6 d, **Figure 5.4**B). However, the effect on the excretion of snails in the AgNPs treatment disappeared after 10 d of feeding. In addition, a significant lower faeces excretion was observed and occurred in snails of TiO_2NPs treatments compared to AgNPs treatments after 6d of feeding. Nevertheless, no significant differences in snail excretion were observed among the treatments of Ag^{+}, AgNPs and the mixture regardless of feeding period, with the exception in the

period of 10-16 d that the excretion of snails in mixture was much lower than that of Ag^{+} and AgNPs.

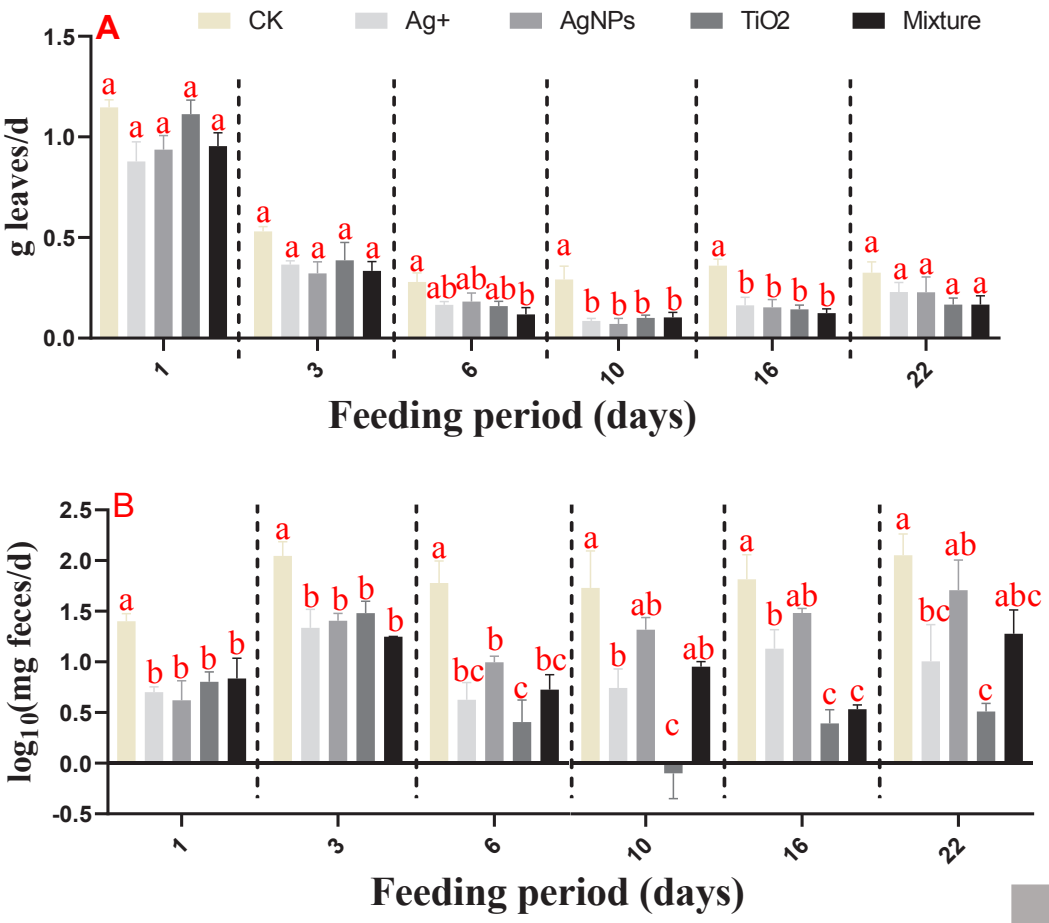

Figure 5.4. Effects of Ag^{+}, AgNPs, TiO_2NPs and mixture on snails food intake (A) and faeces excretion (B) upon trophic transfer. The different letters indicate significant differences between treatments within the same exposure period at $p<0.05$ (intragroup comparison).

5.3.6 Impact on snail activity

After 6d of feeding, significant differences of snail mobility were only detected in the mixture treatment when compared to the control group (**Figure 5.5**A). As the feeding duration was increased to 16 and 22 d, the moving speed of the snails in the TiO_2NPs and the mixture treatments was significantly decreased as compared to the control. In addition, no significant differences of snail moving speed were observed between the mixture and the single nanoparticles (AgNPs or TiO_2NPs) treatments regardless of the feeding period. Notably, the power analysis suggested that the required sample size for this endpoint ranged from 11 to 23 animals under different feeding duration when setting the critical effect size in comparison to the control at 25%. As we used 3 replicates only, our results are indicative only. Including more replicates is needed to properly uncover biological variation and to get more sturdy conclusions regarding this sublethal endpoint.

For the average behavioural state score, only the snails in the mixture treatment showed a reduction during the feeding period from 1 to 6 d. After 10 d of feeding, significant reductions of BSS were observed for the snails in all treatments except for the TiO_2NPs treatment when compared to control. This suggests that prolonged feeding of contaminated leaves induced more severe impacts on snails locomotion. Importantly, the BSS of snails in AgNPs and mixture treatments were similar after 10 d of feeding , but both lower than the BSS of snails in TiO_2NPs treatment.

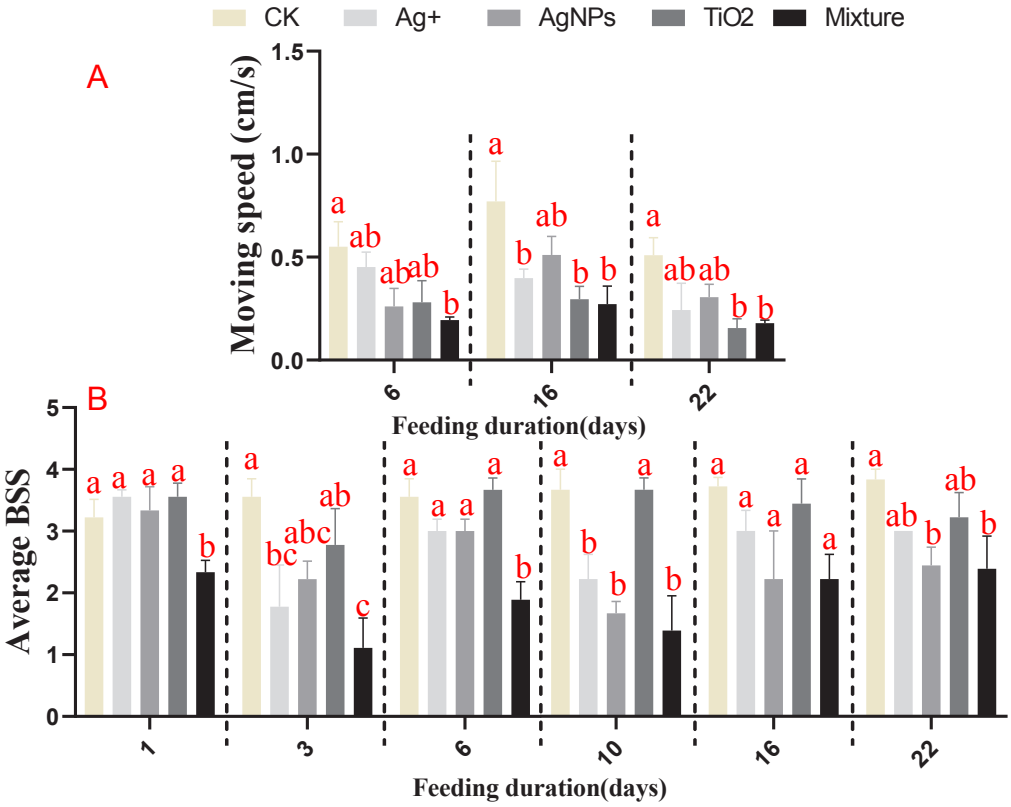

Figure 5.5. Effects of Ag^{+}, AgNPs, TiO_2NPs and mixture on snails moving speed (A) and average behavioural state score (B) upon food chain transfer. The different letters indicate significant differences between treatments within the same exposure period at $p<0.05$ (intragroup comparison).

5.4. Discussion

To our knowledge, this is the first study investigating the trophic transfer patterns of AgNPs, TiO_2NPs and their mixture from lettuce to land snails and the associated effects on various sublethal endpoints. Our results demonstrated that AgNPs, TiO_2NPs and their mixture were transferred along the food chain from the solution into the lettuce roots, to the leaves, and up into herbivorous snails, after which biodistribution occurs over different organs of the snails.

After being ingested into the gastro-intestinal tract of snails, xenobiotics will undergo extracellular and/or intracellular digestion in the digestive gland[302,303]. Subsequently,

size related translocation occurs inside snails[302,303]. Only nanoparticles that can cross the epithelium cell membranes in snails are able to be further transported into the foot, mantle and possibly even the brain and shell of the snails, while the larger nanoparticles will remain in the digestive gland or pass into the intestine for excretion[302,303]. This is why ionic Ag is more readily assimilated and translocated into other organs of snails than the particulate form. This hypothesis was supported by our findings that (1) more than 40 % of Ag was distributed in the soft tissues of snails consuming lettuce exposed to Ag^+, but less than 10 % of Ag or Ti was distributed in soft tissues of snails consuming lettuce exposed to AgNPs or TiO_2NPs; (2) the biomagnification of Ag occurred in the soft tissues and the digestive gland of snails of the Ag^+ treatment (TTFs >1), but no biomagnification was observed in snails organs of the AgNPs treatments (TTFs<1). In addition, as food ingestion was the only pathway for snails to take up Ag^+, AgNPs or TiO_2NPs in the current study, it was not surprising that a large fraction of Ag or Ti was detected in the digestive gland of the snails regardless of ionic or nanoparticles treatments after 2d of depuration. This finding is in agreement with previous studies in which the digestive system was the main site of accumulation of Ce in snails and chickens that were fed CeO_2 nanoparticle exposed plant leaves[286,287].

Importantly, more than 40% of the Ag that was captured by snails consuming the AgNPs-treated lettuce was excreted through their faeces. The same level of Ag excretion was found for snails in the mixture treatment. This results in a high excretion efficiency of Ag and low estimated values of the TTFs of Ag (below 1) in snails of the AgNPs-containing treatments. A conflicting result was reported by the group of Dang et al., who reported the biomagnification of AgNPs from lettuce to snails with TTFs of 2.0-5.9[304]. This discrepancy could be a reflection of differences in experimental conditions and the species, the growth stage and the life history traits of the snails involved[289,299,305]. On the contrary, only a small fraction of Ti (less than 10%) was excreted into the faeces of the snails in the TiO_2NPs or mixture treatments, and more than 70% of Ti was retained in the digestive gland. Additionally, biomagnification of Ti was observed in snails of TiO_2NPs containing treatments as the TTFs of Ti from lettuce to the digestive gland and soft tissue of snails were 38-49 and 4.7-6.5, respectively. The low excretion efficiency and the high estimated TTFs

of Ti in snails suggest that Ti exhibits a higher trophic availability to snails upon consumption of TiO_2NPs internalized lettuce leaves. Furthermore, the TTFs and biodistribution patterns of Ag or Ti in snails were similar between the single nanoparticle treatment and the mixture treatment. This indicates that the concurrent application of AgNPs and TiO_2NPs did not affect the trophic transfer and distribution pattern of Ag or Ti in snails when AgNPs or TiO_2NPs were applied singly.

We also observed that ingestion of leaves contaminated with AgNPs, TiO_2NPs, or their mixture induced adverse effects for the growth and activity (expressed as the average BSS) of snails. After ingestion of either Ag or Ti-containing leaves for 22 d, statistically significant inhibition of snails growth was only observed when using the diameter of the snails rather than the snails biomass as endpoint of assessment. Although not statistically significant, a reduction of 42 % of the biomass increase rate of the snails in the mixture treatment was observed in comparison with the snails in control. The combination of enhanced or reduced mucus secretion, food intake and faeces production could cause high variability in the weight of individual snail[306]. Similarly, up to 50% differences in moving speed of snails between AgNPs treatments and control were detected without statistical significance. We acknowledge that the small sample size of this study could be the reason for the absence of significant effects in terms of the endpoints of biomass and moving speed of snails, thus resulting in low statistical power. The high variability of the tested endpoints requires more replicates (e.g. 11-23 replicates for the endpoint of moving speed) to obtain effective data, thus biomass and moving speed of snails might not be practical indicators for assessing the growth and activity of *Cornu asperum*.

Despite the similar responses of snails to exposure to AgNPs and TiO_2NPs regarding the food intake, treatment of snails with TiO_2NPs contaminated leaves strongly affected their faeces excretion whereas AgNPs strongly affected the activity (expressed as the average BSS) of the snails. This indicates that the behavioural responses of snails to AgNPs and TiO_2NPs are different. The observed strong inhibition in faeces excretion for snails in the TiO_2NPs treatments can be attributed to the high retention of Ti observed in the digestive gland, which may disrupt the functioning of the digestive gland and thus reduce the metabolic activity of snails.

Data on trophic transfer effects of metallic nanoparticles on land snails are scarce, but several studies reported the ingestion of nanoplastics/microplastics, which are also to be considered as insoluble nanoparticles, by land snails[306,307]. These authors demonstrated that ingestion of nanoplastics/microplastics induced damage to the digestive organs of snails such as the digestive gland, intestine or stomach, and thus inhibited the growth and excretion of faeces by the snail *Achatina fulica*[306,307]. In contrast, the BSS of snails in AgNPs treatments was significantly inhibited. Such reduction observed in AgNPs treatments is similar to previous results which show that locomotive activities of springtails (*Lobella sokamensis)* were suppressed when fed with AgNPs exposed earthworms (*Eisenia andrei*)[308]. The energy reallocation or preservation in response to the stressors has been presumed as one explanation for the alterations of locomotion activity in animals[309,310]. Besides the costs of energy in respiration and growth, the snails in the AgNPs treatments may require higher energy for AgNPs excretion as a large fraction of Ag uptake by snails was excreted through their faeces[307], thus resulting in a reduction of the energy available for their locomotive activity. Alternatively, impairment of sensory and nervous system functions in organisms is also widely suggested to explain the alterations of locomotion activity[305,308,310].

Furthermore, the adverse effects were more severe in the snails of the mixture treatments compared to the effects caused by single AgNPs or TiO_2NPs in terms of growth and activity of snails, indicating additive/synergistic effects of AgNPs and TiO_2NPs. So far, knowledge on the mixture toxicity of AgNPs and TiO_2NPs is very limited for land gastropods, which makes the comparison of our results to other published studies difficult. There are two possible explanations for the enhanced toxicity after exposure to a mixture of nanoparticles: one explanation is related to the elevation of the cellular uptake of NPs. First, the presence of TiO_2NPs may change the bioavailability and uptake of Ag by affecting the dissolution and aggregation of the soluble Ag nanoparticles[103,311]. Secondly, TiO_2NPs can work as a carrier to facilitate the uptake of the co-existing nanoparticles[312,313] after the formation of TiO_2-AgNPs complexes, thus affecting the biological effects of co-existing AgNPs. Our results did not support this explanation as the Ag and Ti concentrations in snails were similar between the treatments of single nanoparticle and the mixture. Another

reason for the enhanced toxicity induced by the mixture is the possibility that the presence of TiO_2NPs and AgNPs induced higher oxidative stress, thus leading to more severe adverse effects[311,314]. Last but not least, although the patterns of behavioural changes of snails among different treatments over time are irregular, more severe adverse effects in terms of food intake and locomotion of snails were found at prolonged feeding durations. The observations call for research investigating the long-term effects of the mixture of nanoparticles in consumers through food chain transfer.

5.5. Environmental Implications

This study provided the first report about the trophic transfer and tissue-specific distribution of AgNPs, TiO_2NPs and their mixture along the lettuce-snail food chain, and the associated impacts on the growth and behaviours of snails. Given the increasing likelihood of application of nanoparticles in agriculture and soil remediation, the findings of this study emphasize the importance of considering trophic transfer as a potential pathway for exposure of terrestrial herbivorous to nanoparticles. The concurrent application of AgNPs and TiO_2NPs along the food chain induces additive/synergistic effects on the growth and activity of snails. Nevertheless, understanding the mechanistic underlying such effects remains challenging. More attention should therefore be paid to investigating the combined effects of NPs along the terrestrial food chain. Furthermore, prolonged feeding of contaminated leaves to snails enhanced the adverse effects. This finding highlights the importance of taking long-term application of nanoparticles into account in order to better understand the ecological risks of nanoparticles in terrestrial ecosystems.

5.6 Supplementary Information

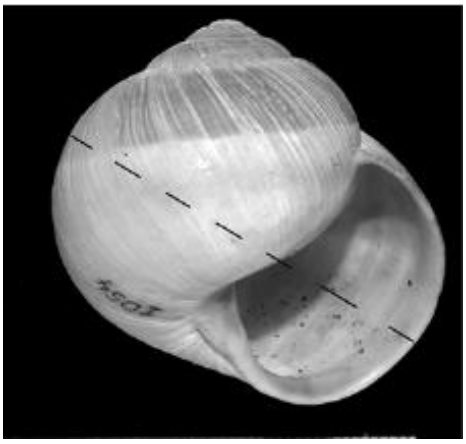

Figure S5.1. The broken line across the shell denotes the diameter measured in the present study[1].

1. Aydın Örstan. A method to measure snail shell. Triton, No 23 April 2011.

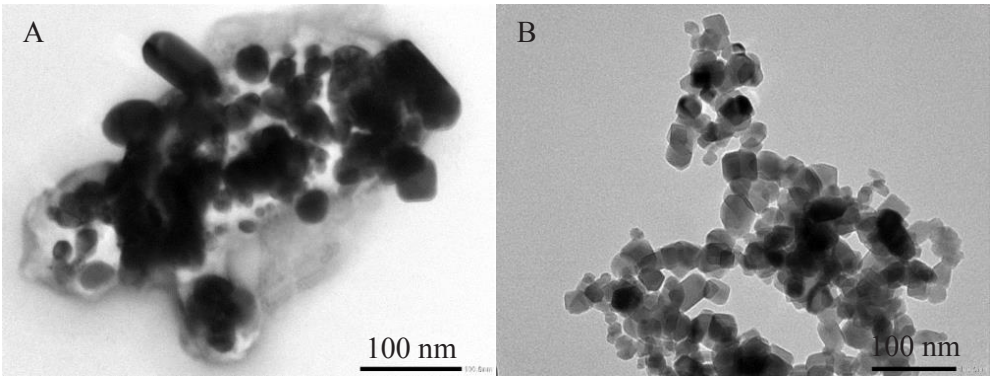

Figure S5.2. TEM picture of AgNPs (A) and TiO_2NPs (B)

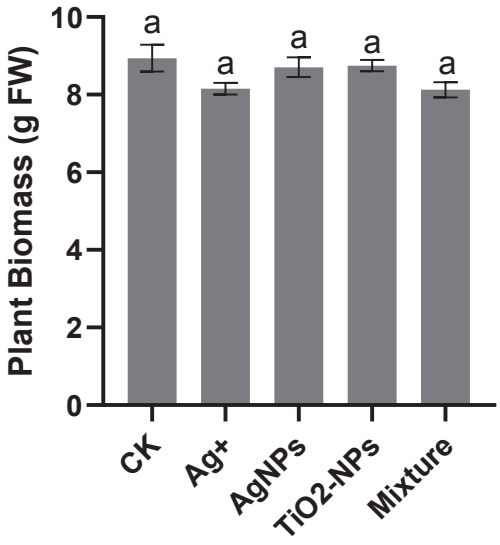

Figure S5.3. Fresh biomass of lettuce exposed to different treatments after 28 days of exposure. Data are the mean ± SE (N= 25). Different letters in the same group indicate statistically significant differences between treatments at $p < 0.05$.

Table S5.1. Summary of the Behavioral State Score (BSS) criteria.

Behavioral state score	Activity description	Picture indication
0	Body is retracted into its shell and operculum is closed	
1	snail withdrawal from the shell, no head visible	
2	protruding head without locomotion	
3	Snail exposes both head and foot but with a slight locomotion	
4	active locomotion of snail	

Table S5.2. Prior-calculation of sample size by defining the critical effect size at 25% and the post-hoc calculation of power

	Endpoints	Feeding duration (day)					
		1	3	6	10	16	22
Prior sample size calculation for each endpoint at power =0.8	Biomass increase (%)						4
	Size increase (%)						3
	Food intake (g leaves/d)	3	3	17	4	5	8
	Feces production (mg feces/d)	5	3	4	4	4	4
	Moving speed (cm/s)			20		11	23
	Behavioral state score	4	4	4	4	3	3
Post-hoc power calculation for each endpoint at n=3	Biomass increase (%)						0.64
	Size increase (%)						0.998
	Food intake (g leaves/d)	0.96	0.85	0.16	0.61	0.55	0.33
	Feces production (mg feces/d)	0.58	0.87	0.77	0.75	0.79	0.66
	Moving speed (cm/s)			0.14		0.23	0.13
	Behavioral state score	0.69	0.77	0.77	0.79	0.81	0.83

Jokulsarlon, Iceland, 2018


Nyhavn,Copenhagen, Denmark, 2019
HYTTEFADET

Chapter 6

General Discussion

The rapid increase in the manufacturing and application of engineered nanoparticles (NPs) is raising concerns on their release into the environment. A large part of the released NPs is expected to accumulate in soil, which results in an increasing concern about their negative impacts in soil ecosystems, especially in the soil-plant system[315,30,34]. Understanding the impacts of NPs on plants is of utmost importance for the ecotoxicity assessment of NPs, since plants can serve as a bridge to connect the underground components (e.g. soil bacteria) and higher-level consumers. Within this PhD I aimed to investigate the uptake, translocation and impacts of metallic NPs in plants and potentially in terrestrial food chains under different exposure scenarios. Within these studies there was a specific focus on distinguishing the relative contribution of the nanoparticulate versus the released ionic form from metallic NPs to the overall toxicity in plants. Importantly, the majority of studies on the NPs and plants are short term experiments. We conducted long(er) term exposures in order to partially fill up the associated knowledge gap on adverse effects after longer term exposure. Within these experiments we incorporated the exposure routes, exposure dynamics and physicochemical properties of NPs to study their fate, accumulation and phytotoxicity in plants. Finally, we investigated the long-term impacts of NPs on the rhizosphere soil bacterial community and their potential transfer and biomagnification into a terrestrial food chain.

In this final chapter I will first answer the research questions formulated in chapter 1, which have been addressed in Chapters 2-5:

1. How does the exposure pathway affect the uptake, translocation, and phytotoxicity of AgNPs in plants? (Chapter 2 and 4)

2. How do the shape, size and coating of NPs affect the fate, accumulation and phytotoxicity of AgNPs? (Chapter 2 and 3)

3. What is the relative contribution of the nanoparticulate and the released ionic form to the overall toxicity of suspensions of NPs and on metal accumulation in plants? (Chapter 2 and 3)

4. How and to what magnitude does the dynamic dissolution of AgNPs in soil affect their bioavailability to plants? (Chapter 4)

5. How does the soil rhizosphere bacterial community respond to exposure to AgNPs, and does this response change over time? (Chapter 4)

6. How does a mixture of AgNPs and TiO_2NPs affect the transfer of the individual NPs along a terrestrial food chain of lettuce-snails and the associated impacts on the consumer? (Chapter 5)

I will first briefly highlight the main findings of my thesis, and subsequently provide implications for environmental risk assessment and the agricultural application of NPs. I will also give an outlook and recommendations for future research here.

6.1 Answers to the research questions

6.1.1 How does the exposure pathway affect the uptake, translocation, and phytotoxicity of AgNPs in plants? (Chapter 2 and 4)

A higher reduction of the biomass of plants and stronger oxidative stress and alterations of the activities of enzymatic antioxidants in lettuce were observed following root exposure as compared to foliar exposure. This indicates that root exposure induced more phytotoxicity than foliar exposure at equal exposure concentrations. Additionally, exposure pathway-specific uptake and translocation of AgNPs was observed as well. The Ag uptake in the exposed tissue of plants for root exposure to AgNPs is higher than in the case of foliar exposure to AgNPs, whereas the translocation of Ag inside the plants from the exposed part to the unexposed part is more efficient following foliar exposure rather than following root exposure. Furthermore, soil exposure of AgNPs to plants was much less toxic compared to hydroponic exposure due to the lower bioavailability of AgNPs in soil.

6.1.2 How do the shape, size and coating of NPs affect the fate, accumulation and phytotoxicity of AgNPs? (Chapter 2 and 3)

The dissolution of AgNPs in Hoagland solution was found to be shape and coating–dependent but size-independent. The dissolution extent of silver nanospheres was higher than for the silver nanowires, and dissolution rates of uncoated silver nanowires were higher than dissolution rates of coated Ag nanowires. Additionally, the phytotoxicity and accumulation of AgNPs in plants were also shape-dependent.

Specifically, exposure to Ag nanospheres resulted in higher phytotoxicity in plants as compared to exposure to Ag nanowires. Further, the phytotoxicity and Ag accumulation in plants of the tested Ag nanowires was diameter (size) dependent, but coating independent. Exposure to the smaller sized silver nanowires induced more phytotoxicity and higher Ag accumulation in plants. This could be caused by the fact that AgNPs with smaller diameters might easier pass through the pores in/between cell walls due to the size exclusion limit of cell walls and/or apoplast, and hence induce higher toxicity[68].

6.1.3 What is the relative contribution of the nanoparticulate and the released ionic form to the overall toxicity of suspensions of NPs and on metal accumulation in plants? (Chapter 2 and 3)

According to the response addition model, we observed that nanoparticulate Ag ($NPs_{(particle)}$) was the predominant driver/descriptor of the overall toxicity and Ag accumulation in the plants rather than the released ionic Ag ($NPs_{(ion)}$) forms, as $NPs_{(particle)}$ accounted for more than 65% of the overall toxicity in all exposure scenarios. However, the relative contribution of $NPs_{(particle)}$ versus $NPs_{(ion)}$ to the overall effects was influenced by the exposure concentration and the extent of dissolution of the Ag nanowires. The contributions of dissolved ions to the overall toxicity of AgNPs suspensions showed an increasing tendency upon increasing exposure concentration. In addition, the contribution of $NPs_{(ion)}$ to the overall effects in AgNPs with a high dissolution ability was higher than in the cases of AgNWs with a low dissolution ability.

6.1.4 How and to what magnitude does the dynamic dissolution of metallic NPs in soil affect their bioavailability to plants? (Chapter 4)

Our results revealed that the extractable Ag from AgNPs amended soil increased with the increasing exposure concentration and changed over time as a result of the continuous dissolution and uptake of AgNPs by the plants. The pattern of Ag concentration in plant roots changing over time was similar to the change of the extractable Ag in the rhizosphere soil over time. Furthermore, the Spearman correlation demonstrated that the amount of Ag accumulated in the plant root and

the shoots were correlated positively with DTPA-extracted Ag in the soil. These results show the important role of the dissolution of AgNPs in soil in influencing their bioavailability.

6.1.5 How does the soil rhizosphere bacterial community respond to exposure to AgNPs, and does this response change over time? (Chapter 4)

We found that the alterations in the structure and composition of the rhizosphere soil bacterial community varied over time. For the short-term exposure (7d), we did not observe any significant impact of AgNPs on the rhizosphere bacterial community regardless of exposure concentration. However, after long-term exposure (63d) to 50 mg/kg AgNPs, the decrease of the Shannon index, the separation of the bacterial community from the control and a total of 16 significantly changed featured taxa were observed. The alterations in the rhizosphere soil bacterial community were potentially associated with the abundance changes in the bacterial groups related to element (e.g., N and S) cycling and stress tolerance.

6.1.6 How does a mixture of AgNPs and TiO_2NPs affect the NPs transfer of the individual NPs along a terrestrial food chain of lettuce-snails and the associated impacts on the consumer? (Chapter 5)

We found that both Ag and Ti could be transferred from lettuce leaves to snails with trophic transfer factors (TTFs) of 0.2 to 1.1 for Ag and 4.7 to 49 for Ti when lettuce was exposed to either AgNPs or TiO_2NPs via the root. Moreover, the majority of Ag captured by snails in the AgNPs-containing treatments was excreted via the feces, whereas more than 70 % of Ti was distributed in the digestive gland of snails in the TiO_2NPs-containing treatments. In addition, treatment of snails with TiO_2NPs contaminated leaves strongly affected their feces excretion whereas AgNPs strongly affected their activity (expressed as the average BSS). Furthermore, the concurrent application of AgNPs and TiO_2NPs induced more severe inhibition of the growth and activity of snails but did not affect the biomagnification and distribution patterns of Ag and Ti in snails as compared to the application of AgNPs or TiO_2NPs alone.

6.2 Implications for risk assessment

6.2.1 Implications for environmental risk assessment

In the public consultation "Towards a Strategic Nanotechnology Action Plan (SNAP) 2010-2015", the European Commission highlighted four priority thematic areas of nanosafety research in the near future: 1) material identification and classification; 2) exposure and transformation; 3) hazard mechanisms including both human toxicology and ecotoxicology; and 4) risk prediction tools including databases and ontologies[316]. The observations in this thesis improve the understanding of the second and third issues described above by 1) investigating the fate, accumulation and impacts of metallic NPs in soil-plant systems and food chain, and 2) differentiating the main driver of toxicity of the particulate and the dissolved ionic forms. Also, our results can partly contribute to set up the ecotoxicological database of NPs, which is associated with the fourth issue of risk prediction tools including databases and ontologies as proposed by SNAP.

Our findings advance the understanding of exposure and transformation of NPs by providing novel data on the interactions between metallic NPs and terrestrial biota. **First**, we found that root exposure of AgNPs induced higher toxicity and different biodistribution patterns of Ag in plants compared to foliar exposure. The results regarding the effects of exposure pathway on plants improve the risk evaluation of metallic NPs exposure related to intentionally added applications in agriculture as well as unintentionally exposures from air-born emissions and soil emissions.

Secondly, we incorporated the dynamic exposure processes including the time-dependent dissolution and sedimentation profiles of NPs in the exposure medium into the risk assessment of metallic NPs. The dissolution and sedimentation of NPs were found to largely and dynamically affect their effective exposure concentrations and hence affect their biological impacts. As a result we showed that the EC_{25} and EC_{50} values of AgNPs to lettuce based on the time-weighted exposure concentration (incorporating the dynamic exposure conditions) were lower than the EC_{25} and EC_{50} values based on the initial exposure concentration (considering exposure as being static and hence ignoring dissolution and sedimentation). Therefore, this highlights

the importance of incorporating dynamic processes when evaluating the impacts of NPs on organisms to gain a more accurate and realistic assessment of NPs toxicity.

Thirdly, we distinguished the main driver for the impacts of NPs and the mode of actions of the nanoparticulate form and the released ionic form. The results demonstrate that the toxic effects of AgNPs are dramatically underestimated if there is only a focus on the impacts of dissolved ionic forms from metallic NPs alone. Also, the findings facilitate the mechanistic understanding of interactions between NPs and biological systems.

Fourthly, we quantified the toxicokinetic parameters of dissolved versus particulate forms of Ag nanowires associated with different physicochemical properties. This information is valuable for facilitating the establishment of toxicokinetic models to predict the accumulation and toxicity of NPs in higher plants. Moreover, we demonstrated that it is key to assess the actual time-related process of particles and ions in their uptake and toxicity to organisms.

Finally, we carried out the chronic exposure of NPs under more realistic exposure scenarios, such as assessing the transfer and toxicity of NPs in a microcosm consisting of the soil-lettuce-rhizosphere bacterial community as well as in a simulated terrestrial food chain of lettuce to snails. Our results clearly showed an upwards transfer of NPs in the terrestrial ecosystem from soil to plants and to snails, and a downward impact on the soil rhizosphere bacterial community. This highlights the potential risks of NPs in the terrestrial ecosystem. Importantly, we did not observe any significant impact of AgNPs on the rhizosphere bacterial community in short-term exposure, but long-term exposure to a high concentration of AgNPs indeed altered the structure and composition of the rhizosphere bacterial community. This indicates the importance of taking the long-term application of nanoparticles into account to better understand the ecological risks of nanoparticles in terrestrial ecosystems. The confirmed trophic transfer of NPs along the food chain emphasizes the importance of considering trophic transfer as a potential pathway for exposure of terrestrial herbivores to nanoparticles, especially given the increasing likelihood of application of nanoparticles in agriculture and soil remediation.

Overall, the findings of this thesis highlight the importance of 1) taking the intrinsic

properties and exposure modes of the NPs into consideration for accurate assessment of their ecotoxicological impacts, 2) considering the long term time-resolved dynamics of organisms in response to nanoparticle exposure, and 3) investigating the accumulation and translocation of NPs in organisms for environmental risk assessment of NPs.

6.2.2 Implications for agriculture

The loss of global crop production induced by pests and diseases and the growing food requirements as a result of the burgeoning global population are the major challenges faced by the agricultural sector, especially in developing countries[2,15]. This encourages the application of nanotechnology in agriculture to increase crop production and prevent the loss of global crop production induced by pest and diseases. To date, several metallic NPs have been applied in agriculture as nano-fertilizer (e.g Cu-based nano-agrochemicals), nano-pesticide (e.g AgNPs) or nano-carrier for delivery of agrochemicals to improve the use efficiency and to enhance crop productivity[15,317]. However, the application of NPs in agriculture not only brings benefits (including increased crop production and decreased application dose of pesticides), but potentially also presents adverse effects on the function and stability of the terrestrial ecosystem. As revealed by our findings, the impacts of NPs on plants depend on the application conditions such as the application dose, exposure duration and application method, as well as on the physicochemical properties of NPs. For example, we have shown that nanowires and larger sized AgNPs are less toxic compared to nanospheres and smaller sized AgNPs. These findings exemplify the potential of enabling the industry to optimize the desired properties of AgNPs with the aim of reducing unwanted side effects within the environment whilst preserving their basic functionalities. This is an important step to achieve "green and clean" claims that are a common requirement for novel materials nowadays. In addition, the exposure pathway determines how and to what extent the NPs can enter and translocate inside plants due to the size limitations of the xylem and the phloem. Future design of environmentally friendly nano-agrochemicals should also include this information. Moreover, we observed the slow but continuing dissolution of AgNPs in soil over a period of 63 days. This information can provide sustained antimicrobial effects against plant pathogens. This implies that repeated applications

of AgNP are not needed, which likely diminishes the total Ag load applied. However, we observed a relatively high amount of Ag in plant roots and the long-term disruptions of the composition of the rhizosphere bacterial community by Ag. Further, we confirmed the trophic transfer of NPs from lettuce to snails and associated negative impacts on snails. The findings highlights the potential risk of NPs being transferred to humans through the supply of crops treated with nano-agrochemicals. All these negative findings call for more attention that should be paid to balance between the potential negative effects of nano-agrochemicals and their implications in agriculture before their field application. Collaborative research among ecotoxicologists, agriculturists, physicists, chemists, material scientists and biologists is needed, as well as between the scientific community and industry to develop environmentally-friendly, efficient, mass-produced and cost-effective nano-agrochemicals that can actually get the label "green and clean".

6.3 Future research in nanoecotoxicology

Based on my research I want to provide advice on key research areas which need to be addressed in future studies to move this research field forward. Three of these area relate to the development of better analytical techniques, and another three focus on improved and more realistic toxicity testing.

6.3.1 Development in analytical techniques

The adequate detection and characterization of NPs in environment and biota are important for the accurate and comprehensive risk assessment of NPs, this section therefore addresses current challenges in the analytical techniques of NPs and the necessity of developing advanced analytical techniques.

1) Knowing the actual NPs concentrations in environmental compartments is a key prerequisite for the effective environmental risk assessment of NPs. Unfortunately, the current methods for the accurate detection, identification and quantification of NPs in environmental samples are still not optimal. ICP-MS based techniques, such as single-particle ICP-MS are being developed for quantifying the concentration of non-soluble metal-based nanospheres (e.g., AuNPs and CeO_2NPs). The dynamic nature of nanomaterials in the environment makes the effective extraction from

environmental compartments (such as soil and sewage sludge) however a challenge. Moreover, many of the current extraction methods have the potential to modify NPs. Although the concentrations of some NPs in the environmental compartments were predicted with the help of mathematic modeling, these results need to be further validated with appropriate analytical techniques. Therefore, future research is needed to improve the methods for sample preparation and to extend more techniques to make them suited for the detection of NPs in the environment.

2) As stated in this thesis, the relative contribution of nanoparticulate and dissolved ions to the bioavailability of NPs is important to understanding the toxicity mechanism of NPs. Currently, the quantitative analysis of metallic NPs is usually focused on the metallic mass concentrations as quantified with the help of ICP-MS based techniques. In this thesis, we distinguished the relative contribution of particles and ions with the help of modeling based on the total metal concentration in plants exposed to NPs and on reference experiments with metal salts (referred to as dissolved ions). Directly determining the concentrations of the nanoparticulate form and the dissolved ions released from NPs in organisms is a great difficulty, as faced by environmental and analytical scientists. The sp-ICP-MS and stable isotope-based analytical techniques show great potential in this field. However, these approaches are still in their infancy in this field. Much more effort needs to be paid to optimizing the performance of these techniques and improving their sensitivity to measure NPs. Additionally, to use these two methods NPs need to be extracted first by digestion of the samples, which may modify the properties of the NPs. Similarly, NPs accumulated inside organisms may also undergo a series of dynamic transformations. Therefore, the development of new methods and techniques or the use of a combination of multiple techniques that will enable to quantify the *in-site* and real-time concentration of NPs in organisms is urgently needed.

3) In this thesis, we investigated the uptake and translocation of NP in plants and snails without considering their subcellular location and the potential speciation patterns inside organisms. Such information is very valuable for a better and comprehensive understanding of the internalization of NPs inside biota. Transmission electron microscopy, confocal laser scanning microscopy or

fluorescence microscopy have been used to track the subcellular location of dyed/labeled NPs in organisms. But there are important limitations to these methods, including detachment of dye/labels attached to the NPs, while some techniques are not suitable for undyed/labeled NPs. Microbeam X-ray fluorescence mapping (μ-XRF) and X-ray absorption near edge structure spectroscopy (μ-XANES) can be used to identify the chemical speciation of NPs in organisms. But the lateral resolution of most μ-XRF/μ-XAS beamlines in the world is above 1 μm or a few hundred nm[111]. The development of higher spatial resolution techniques is therefore needed to further advance our understanding of the subcellular fate of NPs in organisms.

6.3.2 NPs exposure

Even though the results presented in this thesis improve the understanding of the interactions of NPs with terrestrial biota to a certain extent and provide implications for risk assessment of NPs, there is still a long way to go to get a fully clear picture of nano-ecotoxicology. Therefore, based on the results of this thesis, I will propose several issues that deserve further investigation:

1) Although we conducted long-term experiments, the results reported in this thesis did not cover the full life cycle of plants and snails. As a result, we may underestimate or overestimate the impacts of NPs on biota. Also, the growth stages of the tested organisms play an important role in affecting the toxicity of NPs. Therefore, full life cycle studies of different plants and snails in response to NPs exposure are needed for future research, as this may give a more realistic evaluation of the real effects of NPs on biota.

2) We investigated the effects of the exposure pathway, the exposure concentration and time, and the physicochemical properties of NPs on their impacts. In addition, environmental conditions such as the pH, the NOM content, the ionic strength are also needed to be considered in assessing the environmental risks of NPs, and these properties are not specifically considered or modified in this thesis. In particular, we found that soil exposure of NPs to plants induced less toxicity compared to hydroponic exposure. The low bioavailability of metallic NPs in soil may be due to reduction of the transport of NPs, as affected by the characteristics of soil including

the pH, soil natural organic matter, the clay and mineral contents in soil, and the activity of soil microbes. To better understand the interactions between NPs and biota, further efforts should be devoted to studying how the environmental conditions influence the toxicity of NPs in plants and how soil components affect the behaviors of NPs in soil.

3) We confirmed the occurrence of mixture toxicity and trophic transfer of NPs along a simple two-trophic level food chain. The design of the experiments was focused on establishing and maintaining controlled conditions. In a natural ecosystem, the exposure conditions are more dynamic and transfer between organisms is likely to be more complex as well as due to the changing exposure conditions the bioavailable fraction of the NPs will change. Further mesocosm studies and even field research including more species and using environmentally relevant concentrations of NPs are therefore needed to properly simulate realistic exposure scenarios.


Sahara, Morocco, 2018
Photo by Yupeng
yupeng

Björkliden, Kiruna, Sweden, 2019

References

1. Feynman, R. P. There's Plenty of Room at the Bottom. *Eng. Sci.* **23**, 22–36 (1959).
2. Rai, P. K. *et al.* Nanoparticle-plant interaction: Implications in energy, environment, and agriculture. *Environ. Int.* **119**, 1–19 (2018).
3. Taniguchi N.; Arakawa, C.; Kobayashi, T. On the Basic concept of Nanotechnology. *Proc. Int. Conf. Prod. Eng.* (1974).
4. Bayda, S., Adeel, M., Tuccinardi, T., Cordani, M. & Rizzolio, F. The History of Nanoscience and Nanotechnology: From Chemical–Physical Applications to Nanomedicine. *Mol. 2020, Vol. 25, Page 112* **25**, 112 (2019).
5. National Nanotechnology Initiative. What is nanotechnology? Available at: https://www.nano.gov/nanotechnology-facts. (Accessed: 28th July 2021)
6. Hannah, W. & Thompson, P. B. Nanotechnology, risk and the environment: a review. *J. Environ. Monit.* **10**, 291–300 (2008).
7. Lauterwasser, C. *Opportunities and risks of Nanotechnologies Report in co-operation with the OECD International Futures Programme.* (2014).
8. Danish Consumer Council. *The Nanodatabase.*
9. *Global Nanotechnology Market (by Component and Applications), Funding & Investment, Patent Analysis and 27 Companies Profile & Recent Developments - Forecast to 2024.*
10. Roco, M. C. Overview:Affirmation of Nanotechnology between 2000 and 2030. in *Nanotechnology Commercialization:Manufacturing Processes and Products* 1–23 (John Wiley & Sons, Inc., 2017). doi:10.1002/9781119371762.ch1
11. The European Commission. *Assessing the environmental safety of manufactured nanomaterials.* (2017). doi:10.2779/690478
12. Camboni, M., Hanlon, J., García, R. P. & Floyd, P. *A State of Play Study of the market for so called 'Next Generation' Nanomaterials. European Chemicals Agency* (2019). doi:10.2823/242422
13. Dolez, P. I. Nanomaterials Definitions, Classifications, and Applications. in *Nanoengineering: Global Approaches to Health and Safety Issues* 3–40 (Elsevier, 2015). doi:10.1016/B978-0-444-62747-6.00001-4
14. Abbas, Q. *et al.* Environmental transformation and nano-toxicity of engineered nano-particles (ENPs) in aquatic and terrestrial organisms. *Crit. Rev. Environ. Sci. Technol.* **50**, 2523–2581 (2020).
15. Usman, M. *et al.* Nanotechnology in agriculture: Current status, challenges and future opportunities. *Science of the Total Environment* **721**, 137778 (2020).
16. Wang, Z., Zhang, L., Zhao, J. & Xing, B. Environmental processes and toxicity of metallic nanoparticles in aquatic systems as affected by natural organic matter. *Environmental Science: Nano* **3**, 240–255 (2016).
17. Tourinho, P. S. *et al.* Metal-based nanoparticles in soil: Fate, behavior, and

effects on soil invertebrates. *Environmental Toxicology and Chemistry* **31**, 1679–1692 (2012).

18. Piccinno, F., Gottschalk, F., Seeger, S. & Nowack, B. Industrial production quantities and uses of ten engineered nanomaterials in Europe and the world. *Journal of Nanoparticle Research* **14**, 1–11 (2012).
19. Keller, A. A. & Lazareva, A. Predicted Releases of Engineered Nanomaterials: From Global to Regional to Local. *Environ. Sci. Technol. Lett.* **1**, 65–70 (2013).
20. Pulit-Prociak, J. & Banach, M. Silver nanoparticles - A material of the future...? *Open Chem.* **14**, 76–91 (2016).
21. Singh, H. *et al.* Recent advances in the applications of nano-agrochemicals for sustainable agricultural development. *Environ. Sci. Process. Impacts* **23**, 213–239 (2021).
22. Kahru, A. & Dubourguier, H. C. From ecotoxicology to nanoecotoxicology. *Toxicology* **269**, 105–119 (2010).
23. Oberdörster, G. *et al.* Principles for characterizing the potential human health effects from exposure to nanomaterials: Elements of a screening strategy. *Particle and Fibre Toxicology* **2**, 1–35 (2005).
24. Abbas, Q. *et al.* Transformation pathways and fate of engineered nanoparticles (ENPs) in distinct interactive environmental compartments: A review. *Environment International* **138**, 105646 (2020).
25. Barros, D. *et al.* Proteomics and antioxidant enzymes reveal different mechanisms of toxicity induced by ionic and nanoparticulate silver in bacteria. *Environ. Sci. Nano* **6**, 1207–1218 (2019).
26. Zhai, Y. *et al.* Compositional and predicted functional dynamics of soil bacterial community in response to single pulse and repeated dosing of titanium dioxide nanoparticles. *NanoImpact* **16**, 100187 (2019).
27. Liu, H. *et al.* Toxicity responses of different organs of zebrafish (Danio rerio) to silver nanoparticles with different particle sizes and surface coatings. *Environ. Pollut.* 414–422 (2019). doi:10.1016/j.envpol.2018.12.034
28. Ye, N., Wang, Z., Wang, S. & Peijnenburg, W. J. G. M. Toxicity of mixtures of zinc oxide and graphene oxide nanoparticles to aquatic organisms of different trophic level: particles outperform dissolved ions. *Nanotoxicology* **12**, 423–438 (2018).
29. Navarro, E., Wagner, B., Odzak, N., Sigg, L. & Behra, R. Effects of Differently Coated Silver Nanoparticles on the Photosynthesis of Chlamydomonas reinhardtii. *Environ. Sci. Technol.* **49**, 8041–8047 (2015).
30. Kwak, J. Il & An, Y. J. The current state of the art in research on engineered nanomaterials and terrestrial environments: Different-scale approaches. *Environmental Research* **151**, 368–382 (2016).
31. Geitner, N. K. *et al.* Size-Based Differential Transport, Uptake, and Mass Distribution of Ceria (CeO2) Nanoparticles in Wetland Mesocosms. *Environ. Sci. Technol.* **52**, 9768–9776 (2018).

32. The risks of nanomaterial risk assessment. *Nature Nanotechnology* **15**, 163 (2020).

33. Bundschuh, M. *et al.* Nanoparticles in the environment: where do we come from, where do we go to? *Environmental Sciences Europe* **30**, 6 (2018).

34. Gardea-Torresdey, J. L., Rico, C. M. & White, J. C. Trophic transfer, transformation, and impact of engineered nanomaterials in terrestrial environments. *Environ. Sci. Technol.* **48**, 2526–2540 (2014).

35. Yan, A. & Chen, Z. Impacts of silver nanoparticles on plants: A focus on the phytotoxicity and underlying mechanism. *International Journal of Molecular Sciences* **20**, 1003 (2019).

36. Gunawan, C., Lim, M., Marquis, C. P. & Amal, R. Nanoparticle-protein corona complexes govern the biological fates and functions of nanoparticles. *J. Mater. Chem. B* **2**, 2060–2083 (2014).

37. Lynch, I. & Dawson, K. A. Protein-nanoparticle interactions. *Nano Today* **3**, 40–47 (2008).

38. Ivask, A. *et al.* Mechanisms of toxic action of Ag, ZnO and CuO nanoparticles to selected ecotoxicological test organisms and mammalian cells in vitro : A comparative review. *Nanotoxicology* **8**, 57–71 (2014).

39. Escorihuela, L., Martorell, B., Rallo, R. & Fernández, A. Toward computational and experimental characterisation for risk assessment of metal oxide nanoparticles. *Environmental Science: Nano* **5**, 2241–2251 (2018).

40. Hristozov, D. *et al.* Frameworks and tools for risk assessment of manufactured nanomaterials. *Environment International* **95**, 36–53 (2016).

41. Wiesner, M. R., Lowry, G. V., Alvarez, P., Dionysiou, D. & Biswas, P. Assessing the risks of manufactured nanomaterials. *Environmental Science and Technology* **40**, 4336–4345 (2006).

42. Gottschalk, F. & Nowack, B. The release of engineered nanomaterials to the environment. *J. Environ. Monit.* **13**, 1145–1155 (2011).

43. Mueller, N. C. & Nowack, B. Exposure modeling of engineered nanoparticles in the environment. *Environ. Sci. Technol.* **42**, 4447–4453 (2008).

44. Nowack, B. *et al.* The Flows of Engineered Nanomaterials from Production, Use, and Disposal to the Environment. in *Handbook of Environmental Chemistry* **48**, 209–231 (Springer, Cham, 2016).

45. Keller, A. A., McFerran, S., Lazareva, A. & Suh, S. Global life cycle releases of engineered nanomaterials. *J. Nanoparticle Res.* **15**, 1–17 (2013).

46. Fajardo, C. *et al.* Assessing the impact of zero-valent iron (ZVI) nanotechnology on soil microbial structure and functionality: A molecular approach. *Chemosphere* **86**, 802–808 (2012).

47. Servin, A. D. & White, J. C. Nanotechnology in agriculture: Next steps for understanding engineered nanoparticle exposure and risk. *NanoImpact* **1**, 9–12 (2016).

48. Chhipa, H. Nanofertilizers and nanopesticides for agriculture. *Environmental*

Chemistry Letters **15**, 15–22 (2017).

49. Del Real, A. E. P. *et al.* Fate of Ag-NPs in Sewage Sludge after Application on Agricultural Soils. *Environ. Sci. Technol.* **50**, 1759–1768 (2016).

50. Pan, B. & Xing, B. Applications and implications of manufactured nanoparticles in soils: a review. *Eur. J. Soil Sci.* **63**, 437–456 (2012).

51. Zhao, J., Lin, M., Wang, Z., Cao, X. & Xing, B. Engineered nanomaterials in the environment: Are they safe? *Critical Reviews in Environmental Science and Technology* **51**, 1443–1478 (2021).

52. Sun, T. Y., Gottschalk, F., Hungerbühler, K. & Nowack, B. Comprehensive probabilistic modelling of environmental emissions of engineered nanomaterials. *Environ. Pollut.* **185**, 69–76 (2014).

53. Amde, M., Liu, J. fu, Tan, Z. Q. & Bekana, D. Transformation and bioavailability of metal oxide nanoparticles in aquatic and terrestrial environments. A review. *Environmental Pollution* **230**, 250–267 (2017).

54. Kaegi, R. *et al.* Fate and transformation of silver nanoparticles in urban wastewater systems. *Water Res.* **47**, 3866–3877 (2013).

55. Tan, W., Peralta-Videa, J. R. & Gardea-Torresdey, J. L. Interaction of titanium dioxide nanoparticles with soil components and plants: Current knowledge and future research needs-a critical review. *Environmental Science: Nano* **5**, 257–278 (2018).

56. Pokhrel, L. R. & Dubey, B. Evaluation of developmental responses of two crop plants exposed to silver and zinc oxide nanoparticles. *Sci. Total Environ.* **452–453**, 321–332 (2013).

57. Zhang, L. & Wang, W. X. Dominant Role of Silver Ions in Silver Nanoparticle Toxicity to a Unicellular Alga: Evidence from Luminogen Imaging. *Environ. Sci. Technol.* **53**, 494–502 (2019).

58. Li, X. *et al.* Silver nanoparticle toxicity and association with the alga Euglena gracilis. *Environ. Sci. Nano* **2**, 594–602 (2015).

59. Visnapuu, M. *et al.* Dissolution of silver nanowires and nanospheres dictates their toxicity to escherichia coli. *Biomed Res. Int.* **2013**, (2013).

60. Zhang, Z. *et al.* Impact of copper nanoparticles and ionic copper exposure on wheat (Triticum aestivum L.) root morphology and antioxidant response. *Environ. Pollut.* **239**, 689–697 (2018).

61. Yin, L. *et al.* More than the ions: The effects of silver nanoparticles on lolium multiflorum. *Environ. Sci. Technol.* **45**, 2360–2367 (2011).

62. Yang, X., Pan, H., Wang, P. & Zhao, F. J. Particle-specific toxicity and bioavailability of cerium oxide (CeO2) nanoparticles to Arabidopsis thaliana. *J. Hazard. Mater.* **322**, 292–300 (2017).

63. Ko, K.-S., Koh, D.-C. & Kong, I. C. Toxicity Evaluation of Individual and Mixtures of Nanoparticles Based on Algal Chlorophyll Content and Cell Count. *Mater. 2018, Vol. 11, Page 121* **11**, 121 (2018).

64. Albanese, A. & Chan, W. C. W. Effect of gold nanoparticle aggregation on cell

uptake and toxicity. in *ACS Nano* **5**, 5478–5489 (American Chemical Society, 2011).

65. Cho, E. C., Zhang, Q. & Xia, Y. The effect of sedimentation and diffusion on cellular uptake of gold nanoparticles. *Nat. Nanotechnol.* **6**, 385–391 (2011).
66. Pauluhn, J. Pulmonary toxicity and fate of agglomerated 10 and 40 nm aluminum oxyhydroxides following 4-week inhalation exposure of rats: Toxic effects are determined by agglomerated, not primary particle size. *Toxicol. Sci.* **109**, 152–167 (2009).
67. Soto, K., Garza, K. M. & Murr, L. E. Cytotoxic effects of aggregated nanomaterials. *Acta Biomater.* **3**, 351–358 (2007).
68. Schwab, F. *et al.* Barriers, pathways and processes for uptake, translocation and accumulation of nanomaterials in plants – Critical review. *Nanotoxicology* **10**, 1–22 (2015).
69. Lv, J., Christie, P. & Zhang, S. Uptake, translocation, and transformation of metal-based nanoparticles in plants: recent advances and methodological challenges. *Environ. Sci. Nano* **6**, 41–59 (2019).
70. Sabo-Attwood, T. *et al.* Uptake, distribution and toxicity of gold nanoparticles in tobacco (Nicotiana xanthi) seedlings. *Nanotoxicology* **6**, 353–360 (2012).
71. Cvjetko, P. *et al.* Toxicity of silver ions and differently coated silver nanoparticles in Allium cepa roots. *Ecotoxicol. Environ. Saf.* **137**, 18–28 (2017).
72. Jiang, H. S., Qiu, X. N., Li, G. B., Li, W. & Yin, L. Y. Silver nanoparticles induced accumulation of reactive oxygen species and alteration of antioxidant systems in the aquatic plant Spirodela polyrhiza. *Environ. Toxicol. Chem.* **33**, 1398–1405 (2014).
73. Syu, Y. yu, Hung, J. H., Chen, J. C. & Chuang, H. wen. Impacts of size and shape of silver nanoparticles on Arabidopsis plant growth and gene expression. *Plant Physiol. Biochem.* **83**, 57–64 (2014).
74. Pedruzzi, D. P. *et al.* ZnO nanoparticles impact on the photosynthetic activity of Vicia faba: Effect of particle size and concentration. *NanoImpact* **19**, 100246 (2020).
75. Lv, Z. *et al.* Interaction of different-sized ZnO nanoparticles with maize (Zea mays): Accumulation, biotransformation and phytotoxicity. *Sci. Total Environ.* **796**, 148927 (2021).
76. Xiang, L. *et al.* Effects of the size and morphology of zinc oxide nanoparticles on the germination of Chinese cabbage seeds. *Environ. Sci. Pollut. Res.* **22**, 10452–10462 (2015).
77. Yusefi-Tanha, E., Fallah, S., Rostamnejadi, A. & Pokhrel, L. R. Particle size and concentration dependent toxicity of copper oxide nanoparticles (CuONPs) on seed yield and antioxidant defense system in soil grown soybean (Glycine max cv. Kowsar). *Sci. Total Environ.* **715**, 136994 (2020).
78. Gubbins, E. J., Batty, L. C. & Lead, J. R. Phytotoxicity of silver nanoparticles to Lemna minor L. *Environ. Pollut.* **159**, 1551–1559 (2011).

79. Thuesombat, P., Hannongbua, S., Akasit, S. & Chadchawan, S. Effect of silver nanoparticles on rice (Oryza sativa L. cv. KDML 105) seed germination and seedling growth. *Ecotoxicol. Environ. Saf.* **104**, 302–309 (2014).

80. Demir, E., Kaya, N. & Kaya, B. Genotoxic effects of zinc oxide and titanium dioxide nanoparticles on root meristem cells of allium cepa by comet assay. *Turkish J. Biol.* **38**, 31–39 (2014).

81. Majumdar, S. *et al.* Surface coating determines the response of soybean plants to cadmium sulfide quantum dots. *NanoImpact* **14**, 100151 (2019).

82. Torrent, L. *et al.* Uptake, translocation and ligand of silver in Lactuca sativa exposed to silver nanoparticles of different size, coatings and concentration. *J. Hazard. Mater.* **384**, 121201 (2020).

83. Perreault, F., Popovic, R. & Dewez, D. Different toxicity mechanisms between bare and polymer-coated copper oxide nanoparticles in Lemna gibba. *Environ. Pollut.* **185**, 219–227 (2014).

84. Zhang, P. *et al.* Shape-dependent transformation and translocation of ceria nanoparticles in cucumber plants. *Environ. Sci. Technol. Lett.* **4**, 380–385 (2017).

85. Gorka, D. E. & Liu, J. Effect of Direct Contact on the Phytotoxicity of Silver Nanomaterials. *Environ. Sci. Technol.* **50**, 10370–10376 (2016).

86. Gorka, D. E. *et al.* Reducing Environmental Toxicity of Silver Nanoparticles through Shape Control. *Environ. Sci. Technol.* **49**, 10093–10098 (2015).

87. Sohn, E. K. *et al.* Aquatic Toxicity Comparison of Silver Nanoparticles and Silver Nanowires. *Biomed Res. Int.* **2015**, 1–12 (2015).

88. Abdolahpur Monikh, F. *et al.* Do the joint effects of size, shape and ecocorona influence the attachment and physical eco(cyto)toxicity of nanoparticles to algae? *Nanotoxicology* **14**, 310–325 (2020).

89. Nam, S. H. & An, Y. J. Size- and shape-dependent toxicity of silver nanomaterials in green alga Chlorococcum infusionum. *Ecotoxicol. Environ. Saf.* **168**, 388–393 (2019).

90. Wang, P. *et al.* Silver sulfide nanoparticles (Ag2S-NPs) are taken up by plants and are phytotoxic. *Nanotoxicology* **9**, 1041–1049 (2015).

91. Zhai, Y. *et al.* Compositional alterations in soil bacterial communities exposed to TiO2 nanoparticles are not reflected in functional impacts. *Environ. Res.* **178**, 108713 (2019).

92. Stampoulis, D., Sinha, S. K. & White, J. C. Assay-dependent phytotoxicity of nanoparticles to plants. *Environ. Sci. Technol.* **43**, 9473–9479 (2009).

93. Jośko, I. *et al.* Long-term effect of ZnO and CuO nanoparticles on soil microbial community in different types of soil. *Geoderma* **352**, 204–212 (2019).

94. Dai, Y. *et al.* Interaction of CuO nanoparticles with plant cells: Internalization, oxidative stress, electron transport chain disruption, and toxicogenomic responses. *Environ. Sci. Nano* **5**, 2269–2281 (2018).

95. da Cruz, T. N. M. *et al.* A new glance on root-to-shoot in vivo zinc transport and time-dependent physiological effects of ZnSO4 and ZnO nanoparticles on plants. *Sci. Rep.* **9**, (2019).

96. Chen, X., O'Halloran, J. & Jansen, M. A. K. Time Matters: the Toxicity of Zinc Oxide Nanoparticles to Lemna minor L. Increases with Exposure Time. *Water. Air. Soil Pollut.* **229**, 1–10 (2018).

97. Aravantinou, A. F., Andreou, F. & Manariotis, I. D. Long-term toxicity of ZnO nanoparticles to Scenedesmus rubescens cultivated in different media. *Sci. Rep.* **7**, 1–11 (2017).

98. Schlich, K. *et al.* Long-term effects of three different silver sulfide nanomaterials, silver nitrate and bulk silver sulfide on soil microorganisms and plants. *Environ. Pollut.* **242**, 1850–1859 (2018).

99. Jeyasubramanian, K. *et al.* Enhancement in growth rate and productivity of spinach grown in hydroponics with iron oxide nanoparticles. *RSC Adv.* **6**, 15451–15459 (2016).

100. Deng, R. *et al.* Nanoparticle interactions with co-existing contaminants: joint toxicity, bioaccumulation and risk. *Nanotoxicology* **11**, 591–612 (2017).

101. Yu, R. *et al.* Toxicity of binary mixtures of metal oxide nanoparticles to Nitrosomonas europaea. *Chemosphere* **153**, 187–197 (2016).

102. Tong, T. *et al.* Combined Toxicity of Nano-ZnO and Nano-TiO2: From Single- to Multinanomaterial Systems. *Environ. Sci. Technol.* **49**, 8113–8123 (2015).

103. Tong, T. *et al.* Chemical interactions between nano-ZnO and nano-TiO2 in a natural aqueous medium. *Environ. Sci. Technol.* **48**, 7924–7932 (2014).

104. Huynh, K. A., McCaffery, J. M. & Chen, K. L. Heteroaggregation Reduces Antimicrobial Activity of Silver Nanoparticles: Evidence for Nanoparticle–Cell Proximity Effects. *Environ. Sci. Technol. Lett.* **1**, 361–366 (2014).

105. Jośko, I., Oleszczuk, P. & Skwarek, E. Toxicity of combined mixtures of nanoparticles to plants. *J. Hazard. Mater.* **331**, 200–209 (2017).

106. Singh, D. & Kumar, A. Impact of Irrigation Using Water Containing CuO and ZnO Nanoparticles on Spinach oleracea Grown in Soil Media. *Bull. Environ. Contam. Toxicol. 2016 974* **97**, 548–553 (2016).

107. Wang, Y., Cai, R. & Chen, C. The Nano–Bio Interactions of Nanomedicines: Understanding the Biochemical Driving Forces and Redox Reactions. *Acc. Chem. Res.* **52**, 1507–1518 (2019).

108. Qu, G. *et al.* Property-Activity Relationship of Black Phosphorus at the Nano-Bio Interface: From Molecules to Organisms. *Chemical Reviews* **120**, 2288–2346 (2020).

109. Ma, Y. *et al.* Phytotoxicity and biotransformation of La 2O 3 nanoparticles in a terrestrial plant cucumber (Cucumis sativus). *Nanotoxicology* **5**, 743–753 (2011).

110. Geisler-Lee, J. *et al.* Phytotoxicity, accumulation and transport of silver

nanoparticles by Arabidopsis thaliana. *Nanotoxicology* **7**, 323–337 (2013).

111. Lv, J., Christie, P. & Zhang, S. Uptake, translocation, and transformation of metal-based nanoparticles in plants: recent advances and methodological challenges. *Environmental Science: Nano* **6**, 41–59 (2019).

112. Nair, R. *et al.* Nanoparticulate material delivery to plants. *Plant Science* **179**, 154–163 (2010).

113. Li, L. *et al.* Effective uptake of submicrometre plastics by crop plants via a crack-entry mode. *Nat. Sustain.* **3**, 929–937 (2020).

114. Tripathi, D. K. *et al.* Uptake, Accumulation and Toxicity of Silver Nanoparticle in Autotrophic Plants, and Heterotrophic Microbes: A Concentric Review. *Front. Microbiol.* **08**, 7 (2017).

115. Judy, J. D. & Bertsch, P. M. Bioavailability, Toxicity, and Fate of Manufactured Nanomaterials in Terrestrial Ecosystems. in *Advances in Agronomy* **123**, 1–64 (Academic Press Inc., 2014).

116. Peng, C. *et al.* Bioavailability and translocation of metal oxide nanoparticles in the soil-rice plant system. *Sci. Total Environ.* **713**, 136662 (2020).

117. Zhang, Z. *et al.* Uptake and distribution of ceria nanoparticles in cucumber plants. *Metallomics* **3**, 816–822 (2011).

118. Salehi, H., Chehregani, A., Lucini, L., Majd, A. & Gholami, M. Morphological, proteomic and metabolomic insight into the effect of cerium dioxide nanoparticles to Phaseolus vulgaris L. under soil or foliar application. *Science of the Total Environment* **616–617**, 1540–1551 (2018).

119. Tripathi, D. K. *et al.* An overview on manufactured nanoparticles in plants: Uptake, translocation, accumulation and phytotoxicity. *Plant Physiology and Biochemistry* **110**, 2–12 (2017).

120. Liu, W. *et al.* Interactions of metal-based nanoparticles (Mbnps) and metal-oxide nanoparticles (monps) with crop plants: A critical review of research progress and prospects. *Environmental Reviews* **28**, 294–310 (2020).

121. Ghosh, M., Bandyopadhyay, M. & Mukherjee, A. Genotoxicity of titanium dioxide (TiO2) nanoparticles at two trophic levels: Plant and human lymphocytes. *Chemosphere* **81**, 1253–1262 (2010).

122. Ghosh, M., Ghosh, I., Godderis, L., Hoet, P. & Mukherjee, A. Genotoxicity of engineered nanoparticles in higher plants. *Mutation Research - Genetic Toxicology and Environmental Mutagenesis* **842**, 132–145 (2019).

123. Zhu, Y. *et al.* Nanomaterials and plants: Positive effects, toxicity and the remediation of metal and metalloid pollution in soil. *Sci. Total Environ.* **662**, 414–421 (2019).

124. Kaveh, R. *et al.* Changes in Arabidopsis thaliana gene expression in response to silver nanoparticles and silver ions. *Environ. Sci. Technol.* **47**, 10637–10644 (2013).

125. Rastogi, A. *et al.* Impact of Metal and Metal Oxide Nanoparticles on Plant: A Critical Review. *Front. Chem.* **5**, 78 (2017).

126. Milani, N. *et al.* Dissolution kinetics of macronutrient fertilizers coated with manufactured zinc oxide nanoparticles. *J. Agric. Food Chem.* **60**, 3991–3998 (2012).

127. Gogos, A., Knauer, K. & Bucheli, T. D. Nanomaterials in plant protection and fertilization: Current state, foreseen applications, and research priorities. *J. Agric. Food Chem.* **60**, 9781–9792 (2012).

128. Yuvaraj, M. & Subramanian, K. S. Controlled-release fertilizer of zinc encapsulated by a manganese hollow core shell. *Soil Sci. Plant Nutr.* **61**, 319–326 (2014).

129. Avellan, A. *et al.* Nanoparticle Size and Coating Chemistry Control Foliar Uptake Pathways, Translocation, and Leaf-to-Rhizosphere Transport in Wheat. *ACS Nano* **13**, 5291–5305 (2019).

130. Song, U. *et al.* Functional analyses of nanoparticle toxicity: A comparative study of the effects of TiO2 and Ag on tomatoes (Lycopersicon esculentum). *Ecotoxicol. Environ. Saf.* **93**, 60–67 (2013).

131. Chavalmane, S. *et al.* Mechanistic evaluation of translocation and physiological impact of titanium dioxide and zinc oxide nanoparticles on the tomato (Solanum lycopersicum L.) plant. *Metallomics* **7**, 1584–1594 (2015).

132. Ameen, F., Alsamhary, K., Alabdullatif, J. A. & ALNadhari, S. A review on metal-based nanoparticles and their toxicity to beneficial soil bacteria and fungi. *Ecotoxicol. Environ. Saf.* **213**, 112027 (2021).

133. Lewis, R. W., Bertsch, P. M. & McNear, D. H. Nanotoxicity of engineered nanomaterials (ENMs) to environmentally relevant beneficial soil bacteria – a critical review. *Nanotoxicology* **13**, 392–428 (2019).

134. Xu, C. *et al.* Distinctive effects of TiO2 and CuO nanoparticles on soil microbes and their community structures in flooded paddy soil. *Soil Biol. Biochem.* **86**, 24–33 (2015).

135. Simonin, M. & Richaume, A. Impact of engineered nanoparticles on the activity, abundance, and diversity of soil microbial communities: a review. *Environ. Sci. Pollut. Res. 2015 2218* **22**, 13710–13723 (2015).

136. Zhai, Y., Hunting, E. R., Wouters, M., Peijnenburg, W. J. G. M. & Vijver, M. G. Silver Nanoparticles, Ions, and Shape Governing Soil Microbial Functional Diversity: Nano Shapes Micro. *Front. Microbiol.* **7**, (2016).

137. Samarajeewa, A. D. *et al.* Effect of silver nano-particles on soil microbial growth, activity and community diversity in a sandy loam soil. *Environ. Pollut.* **220**, 504–513 (2017).

138. Zhang, X. *et al.* Assessing the Impacts of Cu(OH)2 Nanopesticide and Ionic Copper on the Soil Enzyme Activity and Bacterial Community. *ACS Appl. Mater. Interfaces* **68**, 3381 (2020).

139. Meier, M. J., Dodge, A. E., Samarajeewa, A. D. & Beaudette, L. A. Soil exposed to silver nanoparticles reveals significant changes in community structure and altered microbial transcriptional profiles. *Environ. Pollut.* **258**, 113816 (2020).

140. Philippot, L., Raaijmakers, J. M., Lemanceau, P. & Van Der Putten, W. H.

Going back to the roots: The microbial ecology of the rhizosphere. *Nature Reviews Microbiology* **11**, 789–799 (2013).

141. Zhang, R., Vivanco, J. M. & Shen, Q. The unseen rhizosphere root–soil–microbe interactions for crop production. *Current Opinion in Microbiology* **37**, 8–14 (2017).

142. Zhao, L. *et al.* Metabolomics reveals that engineered nanomaterial exposure in soil alters both soil rhizosphere metabolite profiles and maize metabolic pathways. *Environ. Sci. Nano* **6**, 1716–1727 (2019).

143. Zhao, M. *et al.* Root exudates drive soil-microbe-nutrient feedbacks in response to plant growth. *Plant Cell Environ.* **44**, 613–628 (2021).

144. Esitken, A. *et al.* Effects of plant growth promoting bacteria (PGPB) on yield, growth and nutrient contents of organically grown strawberry. *Sci. Hortic. (Amsterdam).* **124**, 62–66 (2010).

145. Dai, Y. *et al.* Uptake, Transport, and Transformation of CeO 2 Nanoparticles by Strawberry and Their Impact on the Rhizosphere Bacterial Community. *ACS Sustain. Chem. Eng. Eng.* **8**, 4792–4800 (2020).

146. Guan, X. *et al.* CuO Nanoparticles Alter the Rhizospheric Bacterial Community and Local Nitrogen Cycling for Wheat Grown in a Calcareous Soil. *Environ. Sci. Technol.* **54**, 8699–8709 (2020).

147. Avellan, A. *et al.* Critical Review: Role of Inorganic Nanoparticle Properties on Their Foliar Uptake and in Planta Translocation. *Environ. Sci. Technol.* (2021). doi:10.1021/acs.est.1c00178

148. Kibbey, T. C. G. & Strevett, K. A. The effect of nanoparticles on soil and rhizosphere bacteria and plant growth in lettuce seedlings. *Chemosphere* **221**, 703–707 (2019).

149. Sillen, W. M. A. *et al.* Effects of silver nanoparticles on soil microorganisms and maize biomass are linked in the rhizosphere. *Soil Biol. Biochem.* **91**, 14–22 (2015).

150. Caixeta, M. B. *et al.* Toxicity of engineered nanomaterials to aquatic and land snails: A scientometric and systematic review. *Chemosphere* **260**, 127654 (2020).

151. De Vaufleury, A. *et al.* How terrestrial snails can be used in risk assessment of soils. in *Environmental Toxicology and Chemistry* **25**, 797–806 (2006).

152. Baroudi, F., Al Alam, J., Fajloun, Z. & Millet, M. Snail as sentinel organism for monitoring the environmental pollution; a review. *Ecological Indicators* **113**, 106240 (2020).

153. Starnes, D. L. *et al.* Impact of sulfidation on the bioavailability and toxicity of silver nanoparticles to Caenorhabditis elegans. *Environ. Pollut.* **196**, 239–246 (2015).

154. Quadros, M. E. *et al.* Release of Silver from Nanotechnology-Based Consumer Products for Children. *Environ. Sci. Technol.* **47**, 8894–8901 (2013).

155. Benn, T., Cavanagh, B., Hristovski, K., Posner, J. D. & Westerhoff, P. The

release of nanosilver from consumer products used in the home. *J. Environ. Qual.* **39**, 1875–1882 (2010).

156. Yu, S. J., Yin, Y. G. & Liu, J. F. Silver nanoparticles in the environment. *Environmental Sciences: Processes and Impacts* **15**, 78–92 (2013).

157. Wang, P. *et al.* Silver Nanoparticles Entering Soils via the Wastewater-Sludge-Soil Pathway Pose Low Risk to Plants but Elevated Cl Concentrations Increase Ag Bioavailability. *Environ. Sci. Technol.* **50**, 8274–8281 (2016).

158. Li, M., Wang, P., Dang, F. & Zhou, D. M. The transformation and fate of silver nanoparticles in paddy soil: effects of soil organic matter and redox conditions. *Environ. Sci. Nano* **4**, 919–928 (2017).

159. Park, J. *et al.* Characterization of exposure to silver nanoparticles in a manufacturing facility. *J. Nanoparticle Res.* **11**, 1705–1712 (2009).

160. Holder, A. L. & Marr, L. C. Toxicity of silver nanoparticles at the air-liquid interface. *Biomed Res. Int.* **2013**, 328934 (2013).

161. Li, C.-C. C. *et al.* Effects of exposure pathways on the accumulation and phytotoxicity of silver nanoparticles in soybean and rice. *Nanotoxicology* **11**, 699–709 (2017).

162. Lian, J. *et al.* Foliar spray of TiO2 nanoparticles prevails over root application in reducing Cd accumulation and mitigating Cd-induced phytotoxicity in maize (Zea mays L.). *Chemosphere* **239**, 124794 (2020).

163. Navarro, E. *et al.* Toxicity of silver nanoparticles to Chlamydomonas reinhardtii. *Environ. Sci. Technol.* **42**, 8959–8964 (2008).

164. Tripathi, A. *et al.* Differential phytotoxic responses of silver nitrate (AgNO3) and silver nanoparticle (AgNps) in Cucumis sativus L. *Plant Gene* **11**, 255–264 (2017).

165. Li, X. *et al.* Silver nanoparticle toxicity and association with the alga Euglena gracilis. *Environ. Sci. Nano* **2**, 594–602 (2015).

166. Qian, H. *et al.* Comparison of the toxicity of silver nanoparticles and silver ions on the growth of terrestrial plant model Arabidopsis thaliana. *J. Environ. Sci. (China)* **25**, 1947–1956 (2013).

167. Raliya, R. *et al.* Quantitative Understanding of Nanoparticle Uptake in Watermelon Plants. *Frontiers in Plant Science* **7**, (2016).

168. Wang, W. N., Tarafdar, J. C. & Biswas, P. Nanoparticle synthesis and delivery by an aerosol route for watermelon plant foliar uptake. *J. Nanoparticle Res.* **15**, (2013).

169. Achari, G. A. & Kowshik, M. Recent Developments on Nanotechnology in Agriculture: Plant Mineral Nutrition, Health, and Interactions with Soil Microflora. *Journal of Agricultural and Food Chemistry* **66**, 8647–8661 (2018).

170. Poynton, H. C. *et al.* Differential gene expression in daphnia magna suggests distinct modes of action and bioavailability for Zno nanoparticles and Zn ions. *Environ. Sci. Technol.* **45**, 762–768 (2011).

171. Xiao, Y., Vijver, M. G. & Peijnenburg, W. J. G. M. Impact of water chemistry

on the behavior and fate of copper nanoparticles. *Environ. Pollut.* **234**, 684–691 (2018).

172. Arenas-Lago, D., Abdolahpur Monikh, F., Vijver, M. G. & Peijnenburg, W. J. G. M. Dissolution and aggregation kinetics of zero valent copper nanoparticles in (simulated) natural surface waters: Simultaneous effects of pH, NOM and ionic strength. *Chemosphere* **226**, 841–850 (2019).

173. Jiang, H. S. *et al.* Silver nanoparticles induced reactive oxygen species via photosynthetic energy transport imbalance in an aquatic plant. *Nanotoxicology* **11**, 157–167 (2017).

174. Ma, C. *et al.* Defense mechanisms and nutrient displacement in: Arabidopsis thaliana upon exposure to CeO2 and In2O3 nanoparticles. *Environ. Sci. Nano* **3**, 1369–1379 (2016).

175. Lichtenthaler, H. K. Chlorophylls and Carotenoids: Pigments of Photosynthetic Biomembranes. *Methods Enzymol.* **148**, 350–382 (1987).

176. Wang, A. & Luo, G. Quanititative relation between the reaction of hydroxylamine and superoxide anion radicals in plants. *Plant Physiol Commun* **6**, 55-57 (in Chinese) (1990).

177. Mosa, K. A. *et al.* Copper Nanoparticles Induced Genotoxicty, Oxidative Stress, and Changes in Superoxide Dismutase (SOD) Gene Expression in Cucumber (Cucumis sativus) Plants. *Front. Plant Sci.* **9**, (2018).

178. Kampfenkel, K., Van Montagu, M. & Inzé, D. Extraction and determination of ascorbate and dehydroascorbate from plant tissue. *Anal. Biochem.* **225**, 165–167 (1995).

179. Xia, Z., Xu, Z., Wei, Y. & Wang, M. Overexpression of the Maize Sulfite Oxidase Increases Sulfate and GSH Levels and Enhances Drought Tolerance in Transgenic Tobacco. *Front. Plant Sci.* **9**, (2018).

180. Liu, Y., Baas, J., Peijnenburg, W. J. G. M. & Vijver, M. G. Evaluating the Combined Toxicity of Cu and ZnO Nanoparticles: Utility of the Concept of Additivity and a Nested Experimental Design. *Environ. Sci. Technol.* **50**, 5328–5337 (2016).

181. Nanotechnology - Project on Emerging Nanotechnologies. Available at: http://www.nanotechproject.org/. (Accessed: 22nd July 2019)

182. Vance, M. E. *et al.* Nanotechnology in the real world: Redeveloping the nanomaterial consumer products inventory. *Beilstein J. Nanotechnol.* **6**, 1769–1780 (2015).

183. Song, L., Vijver, M. G. & Peijnenburg, W. J. G. M. Comparative toxicity of copper nanoparticles across three Lemnaceae species. *Sci. Total Environ.* **518–519**, 217–224 (2015).

184. Stegemeier, J. P. *et al.* Speciation Matters: Bioavailability of Silver and Silver Sulfide Nanoparticles to Alfalfa (Medicago sativa). *Environ. Sci. Technol.* **49**, 8451–8460 (2015).

185. Piccapietra, F., Allué, C. G., Sigg, L. & Behra, R. Intracellular silver accumulation in Chlamydomonas reinhardtii upon exposure to carbonate

coated silver nanoparticles and silver nitrate. *Environ. Sci. Technol.* **46**, 7390–7397 (2012).

186. Stegemeier, J. P., Colman, B. P., Schwab, F., Wiesner, M. R. & Lowry, G. V. Uptake and Distribution of Silver in the Aquatic Plant Landoltia punctata (Duckweed) Exposed to Silver and Silver Sulfide Nanoparticles. *Environ. Sci. Technol.* **51**, 4936–4943 (2017).

187. Yang, Q. *et al.* Uptake and Transformation of Silver Nanoparticles and Ions by Rice Plants Revealed by Dual Stable Isotope Tracing. *Environ. Sci. Technol.* **53**, 625–633 (2019).

188. Peng, X., Palma, S., Fisher, N. S. & Wong, S. S. Effect of morphology of ZnO nanostructures on their toxicity to marine algae. *Aquat. Toxicol.* **102**, 186–196 (2011).

189. Geisler-Lee, J. *et al.* Reproductive Toxicity and Life History Study of Silver Nanoparticle Effect, Uptake and Transport in Arabidopsis thaliana. *Nanomaterials* **4**, 301–318 (2014).

190. Wang, P. *et al.* Characterizing the uptake, accumulation and toxicity of silver sulfide nanoparticles in plants. *Environ. Sci. Nano* **4**, 448–460 (2017).

191. Silva, S., Ferreira de Oliveira, J. M. P., Dias, M. C., Silva, A. M. S. & Santos, C. Antioxidant mechanisms to counteract TiO2-nanoparticles toxicity in wheat leaves and roots are organ dependent. *J. Hazard. Mater.* **380**, 120889 (2019).

192. Wang, Z. *et al.* Xylem- and phloem-based transport of CuO nanoparticles in maize (Zea mays L.). *Environ. Sci. Technol.* **46**, 4434–4441 (2012).

193. Shahid, M. *et al.* Foliar heavy metal uptake, toxicity and detoxification in plants: A comparison of foliar and root metal uptake. *J. Hazard. Mater.* **325**, 36–58 (2016).

194. Wang, J. *et al.* Phytostimulation of poplars and Arabidopsis exposed to silver nanoparticles and Ag+ at sublethal concentrations. *Environ. Sci. Technol.* **47**, 5442–5449 (2013).

195. Musante, C. & White, J. C. Toxicity of silver and copper to Cucurbita pepo: Differential effects of nano and bulk-size particles. *Environ. Toxicol.* **27**, 510–517 (2012).

196. Wu, Y. X. & von Tiedemann, A. Impact of fungicides on active oxygen species and antioxidant enzymes in spring barley (Hordeum vulgare L.) exposed to ozone. *Environ. Pollut.* **116**, 37–47 (2002).

197. Stewart, R. R. C. & Bewley, J. D. Lipid Peroxidation Associated with Accelerated Aging of Soybean Axes. *Plant Physiol.* **65**, 245–248 (2008).

198. Hong, J. *et al.* Evidence of translocation and physiological impacts of foliar applied CeO2 nanoparticles on cucumber (Cucumis sativus) plants. *Environ. Sci. Technol.* **48**, 4376–4385 (2014).

199. Singh, R., Upadhyay, A. K. & Singh, D. P. Regulation of oxidative stress and mineral nutrient status by selenium in arsenic treated crop plant Oryza sativa. *Ecotoxicol. Environ. Saf.* **148**, 105–113 (2018).

200. BEUTLER, E., DURON, O. & KELLY, B. M. Improved method for the determination of blood glutathione. *J. Lab. Clin. Med.* **61**, 882–888 (1963).

201. Cattani, D. *et al.* Developmental exposure to glyphosate-based herbicide and depressive-like behavior in adult offspring: Implication of glutamate excitotoxicity and oxidative stress. *Toxicology* **387**, 67–80 (2017).

202. Nel, A. Toxic Potential of Materials at the Nanolevel. *Science (80-.).* **311**, 622–627 (2006).

203. Colvin, V. L. The potential environmental impact of engineered nanomaterials. *Nat. Biotechnol.* **21**, 1166–1170 (2003).

204. Tortella, G. R. *et al.* Silver nanoparticles: Toxicity in model organisms as an overview of its hazard for human health and the environment. *Journal of Hazardous Materials* **390**, 121974 (2020).

205. Guan, P. *et al.* Recent Progress in Silver Nanowires: Synthesis and Applications. *Nanosci. Nanotechnol. Lett.* **10**, 155–166 (2018).

206. Jones, R., Draheim, R. & Roldo, M. Silver Nanowires: Synthesis, Antibacterial Activity and Biomedical Applications. *Appl. Sci.* **8**, 673 (2018).

207. Hu, L., Kim, H. S., Lee, J. Y., Peumans, P. & Cui, Y. Scalable coating and properties of transparent, flexible, silver nanowire electrodes. *ACS Nano* **4**, 2955–2963 (2010).

208. Toybou, D., Celle, C., Aude-Garcia, C., Rabilloud, T. & Simonato, J.-P. A toxicology-informed, safer by design approach for the fabrication of transparent electrodes based on silver nanowires. *Environ. Sci. Nano* **6**, 684–694 (2019).

209. H. Müller, K. *et al.* PH-dependent toxicity of high aspect ratio ZnO nanowires in macrophages due to intracellular dissolution. *ACS Nano* **4**, 6767–6779 (2010).

210. George, S. *et al.* Surface defects on plate-shaped silver nanoparticles contribute to its hazard potential in a fish gill cell line and zebrafish embryos. *ACS Nano* **6**, 3745–3759 (2012).

211. Riviere, J. E. *et al.* Modeling gold nanoparticle biodistribution after arterial infusion into perfused tissue: effects of surface coating, size and protein corona. *Nanotoxicology* **12**, 1093–1112 (2018).

212. Ji, Z. *et al.* Designed synthesis of CeO 2 nanorods and nanowires for studying toxicological effects of high aspect ratio nanomaterials. *ACS Nano* **6**, 5366–5380 (2012).

213. Bianchi, M. G. *et al.* Length-dependent toxicity of TiO2 nanofibers: mitigation via shortening. *Nanotoxicology* **14**, 433–452 (2020).

214. Kuo, C. W., Lai, J. J., Wei, K. H. & Chen, P. Studies of surface-modified gold nanowires inside living cells. *Adv. Funct. Mater.* **17**, 3707–3714 (2007).

215. Park, E. J. *et al.* Comparison of the toxicity of aluminum oxide nanorods with different aspect ratio. *Arch. Toxicol.* **89**, 1771–1782 (2015).

216. Scanlan, L. D. *et al.* Silver nanowire exposure results in internalization and

toxicity to daphnia magna. *ACS Nano* **7**, 10681–10694 (2013).

217. Wang, F. *et al.* Length and diameter-dependent phagocytosis and cytotoxicity of long silver nanowires in macrophages. *Chemosphere* **237**, 124565 (2019).

218. Safi, M. *et al.* Interactions between Magnetic Nanowires and Living Cells: Uptake, Toxicity, and Degradation. *ACS Nano* **5**, 5354–5364 (2011).

219. Moon, J., Kwak, J. Il & An, Y. J. The effects of silver nanomaterial shape and size on toxicity to Caenorhabditis elegans in soil media. *Chemosphere* **215**, 50–56 (2019).

220. Qiu, Y. *et al.* Surface chemistry and aspect ratio mediated cellular uptake of Au nanorods. *Biomaterials* **31**, 7606–7619 (2010).

221. Wu, J., Wang, G., Vijver, M. G., Bosker, T. & Peijnenburg, W. J. G. M. Foliar versus root exposure of AgNPs to lettuce: Phytotoxicity, antioxidant responses and internal translocation. *Environ. Pollut.* **261**, 114117 (2020).

222. Chithrani, B. D., Ghazani, A. A. & Chan, W. C. W. Determining the size and shape dependence of gold nanoparticle uptake into mammalian cells. *Nano Lett.* **6**, 662–668 (2006).

223. Chae, Y. & An, Y. J. Toxicity and transfer of polyvinylpyrrolidone-coated silver nanowires in an aquatic food chain consisting of algae, water fleas, and zebrafish. *Aquat. Toxicol.* **173**, 94–104 (2016).

224. Fan, W., Lu, H. & Wang, W. X. Aging Influences on the Biokinetics of Functional TiO2 Nanoparticles with Different Surface Chemistries in Daphnia magna. *Environ. Sci. Technol.* **52**, 7901–7909 (2018).

225. Jiang, C., Castellon, B. T., Matson, C. W., Aiken, G. R. & Hsu-Kim, H. Relative Contributions of Copper Oxide Nanoparticles and Dissolved Copper to Cu Uptake Kinetics of Gulf Killifish (Fundulus grandis) Embryos. *Environ. Sci. Technol.* **51**, 1395–1404 (2017).

226. Shao, Z. & Wang, W. X. Biodynamics of Silver Nanoparticles in an Estuarine Oyster Revealed by 110mAgNP Tracing. *Environ. Sci. Technol.* **54**, 965–974 (2020).

227. Dang, F., Wang, Q., Cai, W., Zhou, D. & Xing, B. Uptake kinetics of silver nanoparticles by plant: relative importance of particles and dissolved ions. *Nanotoxicology* 1–13 (2020). doi:10.1080/17435390.2020.1735550

228. Zhai, Y., Hunting, E. R., Wouterse, M., Peijnenburg, W. J. G. M. & Vijver, M. G. Importance of exposure dynamics of metal-based nano-ZnO, -Cu and -Pb governing the metabolic potential of soil bacterial communities. *Ecotoxicol. Environ. Saf.* **145**, 349–358 (2017).

229. Butz, S. V., Pinckney, J. L., Apte, S. C. & Lead, J. R. Uptake and impact of silver nanoparticles on the growth of an estuarine dinoflagellate, Prorocentrum minimum. *NanoImpact* **15**, 100181 (2019).

230. Akter, M. *et al.* A systematic review on silver nanoparticles-induced cytotoxicity: Physicochemical properties and perspectives. *J. Adv. Res.* **9**, 1–16 (2018).

231. Li, X., Lenhart, J. J. & Walker, H. W. Aggregation kinetics and dissolution of coated silver nanoparticles. *Langmuir* **28**, 1095–1104 (2012).

232. Römer, I. *et al.* Aggregation and dispersion of silver nanoparticles in exposure media for aquatic toxicity tests. *J. Chromatogr. A* **1218**, 4226–4233 (2011).

233. Yang, X. *et al.* Mechanism of silver nanoparticle toxicity is dependent on dissolved silver and surface coating in caenorhabditis elegans. *Environ. Sci. Technol.* **46**, 1119–1127 (2012).

234. Nguyen, K. C. *et al.* Comparison of toxicity of uncoated and coated silver nanoparticles. *J. Phys. Conf. Ser.* **429**, 012025 (2013).

235. Miller, E. L., Nason, S. L., Karthikeyan, K. G. & Pedersen, J. A. Root Uptake of Pharmaceuticals and Personal Care Product Ingredients. *Environ. Sci. Technol.* **50**, 525–541 (2016).

236. Medina-Velo, I. A., Peralta-Videa, J. R. & Gardea-Torresdey, J. L. Assessing plant uptake and transport mechanisms of engineered nanomaterials from soil. *MRS Bull.* **42**, 379–383 (2017).

237. Song, M. M. *et al.* Cytotoxicity and cellular uptake of iron nanowires. *Biomaterials* **31**, 1509–1517 (2010).

238. Lowry, G. V., Avellan, A. & Gilbertson, L. M. Opportunities and challenges for nanotechnology in the agri-tech revolution. *Nat. Nanotechnol.* **14**, 517–522 (2019).

239. *Silver Nanoparticles Market Size | Global Industry Report, 2012-2022. Grand View Research, Inc.: San Francisco, CA* (2015).

240. Rui, M. *et al.* Phytotoxicity of Silver Nanoparticles to Peanut (Arachis hypogaea L.): Physiological Responses and Food Safety. *ACS Sustain. Chem. Eng.* **5**, 6557–6567 (2017).

241. Pu, S., Yan, C., Huang, H., Liu, S. & Deng, D. Toxicity of nano-CuO particles to maize and microbial community largely depends on its bioavailable fractions. *Environ. Pollut.* **255**, 113248 (2019).

242. Das, P. *et al.* Nano-based soil conditioners eradicate micronutrient deficiency: soil physicochemical properties and plant molecular responses. *Environ. Sci. Nano* (2021). doi:10.1039/d1en00551k

243. Gao, X. *et al.* Effect of Soil Organic Matter, Soil pH, and Moisture Content on Solubility and Dissolution Rate of CuO NPs in Soil. *Environ. Sci. Technol.* **53**, 4959–4967 (2019).

244. Jośko, I., Kusiak, M. & Oleszczuk, P. The chronic effects of CuO and ZnO nanoparticles on Eisenia fetida in relation to the bioavailability in aged soils. *Chemosphere* **266**, 128982 (2021).

245. Gao, X. *et al.* CuO Nanoparticle Dissolution and Toxicity to Wheat (Triticum aestivum) in Rhizosphere Soil. *Environ. Sci. Technol.* **52**, 2888–2897 (2018).

246. Zhang, H. *et al.* Silver Nanoparticles Alter Soil Microbial Community Compositions and Metabolite Profiles in Unplanted and Cucumber-Planted Soils. *Environ. Sci. Technol.* **54**, 3334–3342 (2020).

247. Ge, Y. *et al.* Soybean Plants Modify Metal Oxide Nanoparticle Effects on Soil Bacterial Communities. *Environ. Sci. Technol.* **48**, 13489–13496 (2014).

248. Gao, X., Spielman-Sun, E., Rodrigues, S. M., Casman, E. A. & Lowry, G. V. Time and Nanoparticle Concentration Affect the Extractability of Cu from CuO NP-Amended Soil. *Environ. Sci. Technol.* **51**, 2226–2234 (2017).

249. Zhang, W., Dan, Y., Shi, H. & Ma, X. Effects of Aging on the Fate and Bioavailability of Cerium Oxide Nanoparticles to Radish (Raphanus sativus L.) in Soil. *ACS Sustain. Chem. Eng.* **4**, 5424–5431 (2016).

250. Montes de Oca-Vásquez, G. *et al.* Environmentally relevant concentrations of silver nanoparticles diminish soil microbial biomass but do not alter enzyme activities or microbial diversity. *J. Hazard. Mater.* **391**, 122224 (2020).

251. Grün, A. L. *et al.* Impact of silver nanoparticles (AgNP) on soil microbial community depending on functionalization, concentration, exposure time, and soil texture. *Environ. Sci. Eur.* **31**, 1–22 (2019).

252. Schlich, K. & Hund-Rinke, K. Influence of soil properties on the effect of silver nanomaterials on microbial activity in five soils. *Environ. Pollut.* **196**, 321–330 (2015).

253. Wang, Z., Yue, L., Dhankher, O. P. & Xing, B. Nano-enabled improvements of growth and nutritional quality in food plants driven by rhizosphere processes. *Environment International* **142**, 105831 (2020).

254. Vitali, F. *et al.* Environmental pollution effects on plant microbiota: the case study of poplar bacterial-fungal response to silver nanoparticles. *Appl. Microbiol. Biotechnol. 2019 10319* **103**, 8215–8227 (2019).

255. Klein, C. L. *et al. NM-Series of Representative Manufactured Nanomaterials NM-300 Silver Characterisation, Stability, Homogeneity*. doi:10.2788/23079

256. Hui, J., O'Dell, Z. J., Rao, A. & Riley, K. R. In Situ Quantification of Silver Nanoparticle Dissolution Kinetics in Simulated Sweat Using Linear Sweep Stripping Voltammetry. *Environ. Sci. Technol.* (2019). doi:10.1021/acs.est.9b04151

257. Das, P. *et al.* Mechanism of toxicity and transformation of silver nanoparticles: Inclusive assessment in earthworm-microbe-soil-plant system. *Geoderma* **314**, 73–84 (2018).

258. Cruz, N. C. *et al.* Dissolution of Ag Nanoparticles in Agricultural Soils and Effects on Soil Exoenzyme Activities. *Environments* **8**, 22 (2021).

259. Molleman, B. & Hiemstra, T. Time, pH, and size dependency of silver nanoparticle dissolution: The road to equilibrium. *Environ. Sci. Nano* **4**, 1314–1327 (2017).

260. Adamczyk, Z., Oćwieja, M., Mrowiec, H., Walas, S. & Lupa, D. Oxidative dissolution of silver nanoparticles: A new theoretical approach. *J. Colloid Interface Sci.* **469**, 355–364 (2016).

261. Lowry, G. V. *et al.* Long-Term Transformation and Fate of Manufactured Ag Nanoparticles in a Simulated Large Scale Freshwater Emergent Wetland. *Environ. Sci. Technol.* **46**, 7027–7036 (2012).

262. Settimio, L. *et al.* Fate and lability of silver in soils: Effect of ageing. *Environ. Pollut.* **191**, 151–157 (2014).

263. Carbone, S. *et al.* Bioavailability and biological effect of engineered silver nanoparticles in a forest soil. *J. Hazard. Mater.* **280**, 89–96 (2014).

264. Li, N., Li, X., Shi, Z. Y., Fan, X. Y. & Zhou, Z. W. Bacterial communities, potential pathogens and antibiotic resistance genes of silver-loaded stainless steel pipe wall biofilm in domestic hot water system. *J. Water Process Eng.* **40**, 101935 (2021).

265. Zeng, X. Y., Li, S. W., Leng, Y. & Kang, X. H. Structural and functional responses of bacterial and fungal communities to multiple heavy metal exposure in arid loess. *Sci. Total Environ.* **723**, 138081 (2020).

266. Ge, Y., Schimel, J. P. & Holdena, P. A. Identification of soil bacteria susceptible to TiO2 and ZnO nanoparticles. *Appl. Environ. Microbiol.* **78**, 6749–6758 (2012).

267. Ward, N. L. *et al.* Three genomes from the phylum Acidobacteria provide insight into the lifestyles of these microorganisms in soils. *Appl. Environ. Microbiol.* **75**, 2046–2056 (2009).

268. Bergmann, F. *et al.* Genomic insights into the metabolic potential of the polycyclic aromatic hydrocarbon degrading sulfate-reducing Deltaproteobacterium N47. *Environ. Microbiol.* **13**, 1125–1137 (2011).

269. Zhai, Y. *et al.* Interaction between a nano-formulation of atrazine and rhizosphere bacterial communities: atrazine degradation and bacterial community alterations. *Environ. Sci. Nano* **7**, 3372–3384 (2020).

270. Soil Analysis: An Interpretation Manual - Google 图书. Available at: https://books.google.nl/books?hl=zh-CN&lr=&id=pWR1vUWbEhEC&oi=fnd&pg=PR5&dq=Soil+Analysis:+An+Interpretation+Manual&ots=a_w5lEm_ZA&sig=gcDEzbQZXqg0AlsgxdM8LMn-83M#v=onepage&q=Soil Analysis%3A An Interpretation Manual&f=false. (Accessed: 23rd October 2020)

271. Walkley, A. & Black, I. A. An examination of the degtjareff method for determining soil organic matter, and a proposed modification of the chromic acid titration method. *Soil Sci.* **37**, 29–38 (1934).

272. Hendershot, W. H. & Duquette, M. A Simple Barium Chloride Method for Determining Cation Exchange Capacity and Exchangeable Cations. *Soil Sci. Soc. Am. J.* **50**, 605–608 (1986).

273. Nowack, B. *et al.* Potential scenarios for nanomaterial release and subsequent alteration in the environment. *Environmental Toxicology and Chemistry* **31**, 50–59 (2012).

274. Hu, J. *et al.* TiO2 nanoparticle exposure on lettuce (: Lactuca sativa L.): Dose-dependent deterioration of nutritional quality. *Environ. Sci. Nano* **7**, 501–513 (2020).

275. Larue, C. *et al.* Innovative combination of spectroscopic techniques to reveal nanoparticle fate in a crop plant. *Spectrochim. Acta - Part B At. Spectrosc.* **119**,

17–24 (2016).

276. Servin, A. D. *et al.* Synchrotron micro-XRF and micro-XANES confirmation of the uptake and translocation of TiO2 nanoparticles in cucumber (Cucumis sativus) plants. *Environ. Sci. Technol.* **46**, 7637–7643 (2012).

277. Yang, J. *et al.* Alteration of Crop Yield and Quality of Wheat upon Exposure to Silver Nanoparticles in a Life Cycle Study. *J. Agric. Food Chem.* **66**, 2589–2597 (2018).

278. Servin, A. D. *et al.* Synchrotron verification of TiO2 accumulation in cucumber fruit: A possible pathway of TiO2 nanoparticle transfer from soil into the food chain. *Environ. Sci. Technol.* **47**, 11592–11598 (2013).

279. Du, W. *et al.* TiO2 and ZnO nanoparticles negatively affect wheat growth and soil enzyme activities in agricultural soil. *J. Environ. Monit.* **13**, 822–828 (2011).

280. Larue, C. *et al.* Accumulation, translocation and impact of TiO2 nanoparticles in wheat (Triticum aestivum spp.): Influence of diameter and crystal phase. *Sci. Total Environ.* **431**, 197–208 (2012).

281. Yan, N. & Wang, W. X. Novel Imaging of Silver Nanoparticle Uptake by a Unicellular Alga and Trophic Transfer to Daphnia magna. *Environ. Sci. Technol.* **55**, 5143–5151 (2021).

282. Chen, X., Zhu, Y., Yang, K., Zhu, L. & Lin, D. Nanoparticle TiO2 size and rutile content impact bioconcentration and biomagnification from algae to daphnia. *Environ. Pollut.* **247**, 421–430 (2019).

283. Zhu, X., Wang, J., Zhang, X., Chang, Y. & Chen, Y. Trophic transfer of TiO2 nanoparticles from daphnia to zebrafish in a simplified freshwater food chain. *Chemosphere* **79**, 928–933 (2010).

284. Judy, J. D., Unrine, J. M. & Bertsch, P. M. Evidence for biomagnification of gold nanoparticles within a terrestrial food chain. *Environ. Sci. Technol.* **45**, 776–781 (2011).

285. Judy, J. D., Unrine, J. M., Rao, W. & Bertsch, P. M. Bioaccumulation of gold nanomaterials by Manduca sexta through dietary uptake of surface contaminated plant tissue. *Environ. Sci. Technol.* **46**, 12672–12678 (2012).

286. Ma, Y. *et al.* Trophic Transfer and Transformation of CeO2 Nanoparticles along a Terrestrial Food Chain: Influence of Exposure Routes. *Environ. Sci. Technol.* **52**, 7921–7927 (2018).

287. Dai, Y. *et al.* Transfer and transformation of CeO2 NPs along a terrestrial trophic food chain. *Environ. Sci. Nano* **7**, 588–598 (2020).

288. Hawthorne, J. *et al.* Particle-Size Dependent Accumulation and Trophic Transfer of Cerium Oxide through a Terrestrial Food Chain. *Environ. Sci. Technol.* **48**, 13102–13109 (2014).

289. Majumdar, S. *et al.* Cerium Biomagnification in a Terrestrial Food Chain: Influence of Particle Size and Growth Stage. *Environ. Sci. Technol.* **50**, 6782–6792 (2016).

290. De La Torre Roche, R. *et al.* Terrestrial Trophic Transfer of Bulk and Nanoparticle La2O3 Does Not Depend on Particle Size. *Environ. Sci. Technol.* **49**, 11866–11874 (2015).

291. Servin, A. D. *et al.* Weathering in soil increases nanoparticle CuO bioaccumulation within a terrestrial food chain. *Nanotoxicology* **11**, 98–111 (2017).

292. Sharifan, H., Ma, X., Moore, J. M. C., Habib, M. R. & Evans, C. Zinc Oxide Nanoparticles Alleviated the Bioavailability of Cadmium and Lead and Changed the Uptake of Iron in Hydroponically Grown Lettuce (Lactuca sativa L. var. Longifolia). *ACS Sustain. Chem. Eng.* **7**, 16401–16409 (2019).

293. Sharifan, H., Wang, X. & Ma, X. Impact of nanoparticle surface charge and phosphate on the uptake of coexisting cerium oxide nanoparticles and cadmium by soybean (Glycine max. (L.) merr.). *Int. J. Phytoremediation* **22**, 305–312 (2020).

294. Liu, J. *et al.* TiO2 nanoparticles in irrigation water mitigate impacts of aged Ag nanoparticles on soil microorganisms, Arabidopsis thaliana plants, and Eisenia fetida earthworms. *Environ. Res.* **172**, 202–215 (2019).

295. Mtisi, M. & Gwenzi, W. Evaluation of the phytotoxicity of coal ash on lettuce (Lactuca sativa L.) germination, growth and metal uptake. *Ecotoxicol. Environ. Saf.* **170**, 750–762 (2019).

296. RASMUSSEN Kirsten; *et al. Titanium dioxide, NM-100, NM-101, NM-102, NM-103, NM-104, NM-105:: Characterisation and Physico-Chemical Properties.* (2014). doi:10.2788/79554

297. Dang, F. *et al.* Discerning the Sources of Silver Nanoparticle in a Terrestrial Food Chain by Stable Isotope Tracer Technique. *Environ. Sci. Technol.* **53**, 3802–3810 (2019).

298. Wu, J., Yu, Q., Bosker, T., Vijver, M. G. & Peijnenburg, W. J. G. M. Quantifying the relative contribution of particulate versus dissolved silver to toxicity and uptake kinetics of silver nanowires in lettuce: impact of size and coating. *Nanotoxicology* **14**, 1399–1414 (2020).

299. Unrine, J. M., Shoults-Wilson, W. A., Zhurbich, O., Bertsch, P. M. & Tsyusko, O. V. Trophic transfer of Au nanoparticles from soil along a simulated terrestrial food chain. *Environ. Sci. Technol.* **46**, 9753–9760 (2012).

300. Xiong, T. *et al.* Copper Oxide Nanoparticle Foliar Uptake, Phytotoxicity, and Consequences for Sustainable Urban Agriculture. *Environ. Sci. Technol.* **51**, 5242–5251 (2017).

301. Hartono, D., Lioe, B., Zhang, Y., Li, B. & Yu, J. Impacts of particulate matter (PM2.5) on the behavior of freshwater snail Parafossarulus striatulus. *Sci. Rep.* **7**, 1–8 (2017).

302. Silva, P. V. *et al.* Toxicokinetics of pristine and aged silver nanoparticles in: Physa acuta. *Environ. Sci. Nano* **7**, 3849–3868 (2020).

303. Schleh, C. *et al.* Size and surface charge of gold nanoparticles determine absorption across intestinal barriers and accumulation in secondary target

organs after oral administration. *Nanotoxicology* **6**, 36–46 (2012).

304. Dang, F., Huang, Y., Wang, Y., Zhou, D. & Xing, B. Transfer and toxicity of silver nanoparticles in the food chain. *Environ. Sci. Nano* (2021). doi:10.1039/D0EN01190H

305. Kaloyianni, M. *et al.* Magnetite nanoparticles effects on adverse responses of aquatic and terrestrial animal models. *J. Hazard. Mater.* **383**, 121204 (2020).

306. Song, Y. *et al.* Uptake and adverse effects of polyethylene terephthalate microplastics fibers on terrestrial snails (Achatina fulica) after soil exposure. *Environ. Pollut.* **250**, 447–455 (2019).

307. Chae, Y. & An, Y. J. Nanoplastic ingestion induces behavioral disorders in terrestrial snails: Trophic transfer effects: Via vascular plants. *Environ. Sci. Nano* **7**, 975–983 (2020).

308. Kwak, J. Il & An, Y. J. Trophic transfer of silver nanoparticles from earthworms disrupts the locomotion of springtails (Collembola). *J. Hazard. Mater.* **315**, 110–116 (2016).

309. Mehennaoui, K. *et al.* Gammarus fossarum (Crustacea, Amphipoda) as a model organism to study the effects of silver nanoparticles. *Sci. Total Environ.* **566–567**, 1649–1659 (2016).

310. da Costa Araújo, A. P. & Malafaia, G. Microplastic ingestion induces behavioral disorders in mice: A preliminary study on the trophic transfer effects via tadpoles and fish. *J. Hazard. Mater.* **401**, 123263 (2021).

311. Zou, X., Shi, J. & Zhang, H. Coexistence of silver and titanium dioxide nanoparticles: Enhancing or reducing environmental risks? *Aquat. Toxicol.* **154**, 168–175 (2014).

312. Haghighat, F., Kim, Y., Sourinejad, I., Yu, I. J. & Johari, S. A. Titanium dioxide nanoparticles affect the toxicity of silver nanoparticles in common carp (Cyprinus carpio). *Chemosphere* **262**, 127805 (2021).

313. Ma, T., Wang, M., Gong, S. & Tian, B. Impacts of Sediment Organic Matter Content and pH on Ecotoxicity of Coexposure of TiO2 Nanoparticles and Cadmium to Freshwater Snails Bellamya aeruginosa. *Arch. Environ. Contam. Toxicol.* **72**, 153–165 (2017).

314. Fan, W. H., Cui, M. M., Shi, Z. W., Tan, C. & Yang, X. P. Enhanced oxidative stress and physiological damage in daphnia magna by copper in the presence of Nano-TiO 2. *J. Nanomater.* **2012**, (2012).

315. Scheringer, M. Nanoecotoxicology: Environmental risks of nanomaterials. *Nature Nanotechnology* **3**, 322–323 (2008).

316. Savolainen, K. *et al. Nanosafety in Europe 2015–2025: Towards Safe and Sustainable Nanomaterials and Nanotechnology Innovations, Finnish Institute of Occupational Health.* (2013).

317. Athanassiou, C. G. *et al.* Nanoparticles for pest control: current status and future perspectives. *Journal of Pest Science* **91**, 1–15 (2018).


Dubrovnik, Croatia, 2021

Summary

The rapidly increasing commercial application of metallic nanoparticles (NPs) within products will inevitably enhance the amount of NPs being released into environment. A large part of the released NPs is expected to accumulate in soil, which results in an increasing concern about their negative impacts on soil ecosystems. Knowledge on the fate, accumulation and impacts of NPs on plants is critical for understanding the environmental risk of NPs in soil ecosystems. The majority of studies aiming to assess potential effects of NPs were performed at early growth stages under root exposure with a short exposure time, which does not capture the long-term responses of plants to NPs. Very limited studies were carried out to examine the impact of engineered nanomaterials on plants upon foliar exposure, even though most nano-enabled agrochemicals are recommended to be applied by foliar spraying, relying on the so-called leaf-contact application. It is known that the behavior of NPs during the exposure period is determined by dynamic processes such as aggregation, sedimentation and/or dissolution, which results in the effective exposure dose changing over time. Nonetheless, the majority of published research, reports on experimental knowledge obtained making use of static initial exposure concentrations to quantify the dose of NPs without considering the impacts of these dynamic processes on their effective dose. Moreover, the dissolution of metallic NPs leads to the co-presence of nanoparticulate and ionic forms of metals. Subsequently, the overall effects of NPs to biota may be induced by the nanoparticulates and/or the released ions. Despite numerous studies on investigating the impacts of metallic NPs on plants, it is still unknown if their toxicity originates from the nanoparticles themselves or is caused by the released ions. Furthermore, one of the big quests is related to whether NPs have the potential to transfer to higher-level consumers via food chains. In this thesis, we integrated the exposure routes and exposure dynamics of NPs to investigate the uptake, translocation and impacts of metallic NPs in plants upon long-term exposure. We furthermore investigated the long-term impacts of NPs on the rhizosphere soil bacterial community and the potential transfer and biomagnification within a food chain.

In chapter 2, we quantified the uptake, translocation, biodistribution of Ag and various phytotoxic endpoints in lettuce by exposing lettuce to AgNPs (nanosphere, NSs) suspensions following either foliar or root pathway for 15 days. We found that the exposure pathway significantly affects the uptake, translocation and phytotoxicity of AgNSs in lettuce. Root exposure to AgNPs induced more phytotoxicity than foliar exposure at the same exposure level as revealed by the enlarged biomass reduction of plants, higher oxidative stress, and alterations of the activities of enzymatic antioxidants in plants after root exposure. Also, the plants accumulated more Ag following root exposure to AgNPs as compared to foliar exposure to AgNPs at the same exposure level. Interestingly, the translocation of Ag inside the plants from the exposed part to the unexposed part is more efficient following foliar exposure than in case of root exposure, as revealed by the higher translocation factors for the foliar exposure scenarios. The differences observed for root exposure and foliar exposure are likely due to their different mechanisms associated with the uptake and translocation of NPs. NPs can be taken up through stomatal openings and/or across waxy cuticles and then transported to other parts of the plants through phloem loading mechanisms. For root uptake and translocation, NPs need to traverse across the cell walls and the epidermal layers and are further transported upwards via xylem loading mechanisms.

In chapter 3, we determined the impacts of size, length and coating of Ag nanowires(AgNWs) on the fate, accumulation and phytotoxicity of AgNPs in lettuces upon root exposure. Firstly, we found that the dissolution of AgNPs in the growth medium (Hoagland solution) was coating-dependent. The dissolution extent and dissolution rate constant of the uncoated AgNWs (HAR-AgNW: 39 nm diameter×8.4 μm length) were both higher compared to the PVP coated AgNWs (LAR-AgNW: 43 nm diameter×1.8 μm length, and MAR-AgNW: 65 nm diameter×4.4 μm length). Addtionnally, the phytotoxicity, uptake rate constants and bioaccumulation factors of the PVP-coated AgNWs (43 nm diameter×1.8 μm length) and the uncoated AgNWs (39 nm diameter×8.4 μm length) were similar, but both parameters were higher than those of the PVP-coated AgNWs with the larger

diameter (65 nm diameter×4.4 μm length). These findings imply that the diameter rather than the length and coating of the AgNWs predominantly determines their toxicity and Ag accumulation in plants. Further, taking together the results of chapters 2 and 3, we also found that the dissolution, accumulation and phytotoxicity of AgNPs in plants was shape-dependent. The AgNSs resulted in higher dissolution ability and phytotoxcity but in less Ag uptake by the root of plants as compared to exposure to AgNWs. Our results highlight that the intrinsic characteristics of NPs need to be taken into consideration in investigating the interactions between metallic NPs and plants.

According to the response addition model, we quantified the relative contribution of nanoparticulate forms ($NPs_{(particle)}$) and the released ionic forms ($NPs_{(ion)}$) to the overall phytotoxicity of AgNPs suspensions and Ag accumulation in plants. As revealed in chapters 2 and 3, particulate Ag was found to be the predominant driver/descriptor of the overall toxicity and Ag accumulation in the plants, accounted for more than 65% for the overall toxicity in all exposure scenarios regardless of the shape, size and coating of AgNPs. The relative contribution of $NPs_{(particle)}$ versus $NPs_{(ion)}$ to the overall effects was however influenced by the exposure concentration and the extent of dissolution of AgNPs. The contributions of dissolved ions to the overall toxicity of AgNSs and AgNWs showed an increasing tendency upon increasing exposure concentration. The differences in the contributions of the particulate and ionic forms to the overall toxicity may be reflected by their different modes of action as particulate toxicity is shown to originate from the accumulation of Ag in plants by blocking of internal trafficking, while ions toxicity is likely due to the induction of excess ROS production.

In Chapter 4 we further extended the knowledge on the interactions between AgNPs and biota by investigating the dissolution dynamics (the dissolved Ag concentrations determined as the DTPA-extractable Ag concentrations) and accumulation of AgNPs in a microcosm consisting of soil - lettuce - rhizosphere bacterial community. Our results revealed that the extractability of Ag in AgNPs amended soil was concentration-dependent and changed over time as a result of the continuous

dissolution and uptake of AgNPs by the plants. Additionally, the results with use of the Spearman correlation demonstrated that the amount of Ag accumulated in the plant root and the shoots was positively correlated with the DTPA-extracted amount of Ag in the soil. These results highlight the important role of the dissolution of AgNPs in the soil in influencing the overall Ag bioavailability of the NPs. Furthermore, the alterations in the structure and composition of the rhizosphere soil bacterial community were found to be exposure time-dependent. For the short-term exposure (7d), we did not observe any significant impact of AgNPs on the rhizosphere bacterial community regardless of exposure concentration. However, after long-term exposure (63 d) to 50 mg/kg AgNPs, the shifts of the bacterial community and a total of 16 significantly changed featured taxa were observed as compared to control. The alterations in the rhizosphere soil bacterial community were potentially associated with the abondance changes in the bacterial groups related to element (e.g., N and S) cycling and stress tolerance.

In chapter 5, we investigated the trophic transfer of single NPs and a mixture of AgNPs and TiO_2NPs from lettuce to snails and their associated impacts on snails. We found that both Ag and Ti could be transferred from lettuce leaves to snails with trophic transfer factors of 0.2 to 1.1 for Ag and 3.8 to 47 for Ti when lettuce was exposed to either Ag^+/AgNPs or TiO_2NPs via the root. Ionic Ag was found to be more readily assimilated and translocated into the other organs of snails than the particulate form. Moreover, the majority of Ag captured by the snails in the AgNPs-containing treatments was excreted via faeces, whereas more than 70% of Ti was distributed in the digestive gland of snails in the TiO_2NPs-containing treatments. In addition, the behavioral responses of snails to the trophic transfer of AgNPs and TiO_2NPs were different. Treatment of snails with TiO_2NPs contaminated leaves strongly affected their faeces excretion whereas AgNPs strongly affected the locomotion activity (expressed as the average BSS) of the snails. Furthermore, concurrent application of AgNPs and TiO_2NPs did not affect the bioaccumulation and biodistribution patterns of Ag or Ti in snails compared to the trophic transfer following exposure to AgNPs or TiO_2NPs alone. However, their co-exposure induced

a more severe inhibition of the growth and activity of snails than in the case of applying AgNPs or TiO_2NPs alone. Our results improve the understanding of the trophic transfer of a mixture of metallic NPs within terrestrial food chains, which is valuable for assessing their possible risks to the environment and to ecosystem health.

To conclude, the newly generated knowledge depicted in this thesis advances the understanding of: 1) the differences in accumulation and phytotoxicity of AgNPs upon foliar exposure and root exposure; 2) the specific characteristics of AgNPs which dominate their fate, bioavailability and phytotoxicity; 3) the Ag forms present in AgNPs suspensions that predominantly drive their impacts on green leafy plants; 4) different mode of actions of particulate and ionic Ag in inducing phytotoxicity; 5) long-term impacts of the dissolution dynamics of AgNPs on Ag accumulation in plants and the rhizosphere soil bacterial community; 6) the possibility of transfer of a mixture of multiple NPs within the food chain, as associated with increased potential risks to higher trophic level organisms. Furthermore, the results highlight that the intrinsic properties of the NPs and the long time-resolved dynamics of NPs exposure should be taken into consideration for accurate assessment of their ecotoxicological impacts in the soil ecosystem. Overall, our results improve the knowledge about the interaction of NPs with different terrestrial biota as well as the hazard evaluation of NPs exposure. Such information assists the development of "Safe by Design" of NPs, which can help to balance between the nanomaterials applications and their implications in the environment and in agriculture.

Samenvatting

De snel toenemende commerciële toepassing van metallische nanodeeltjes (NPs) in productenzal onvermijdelijk de ongewenste emissies van deze NPs richting het milieu vergroten. Naar verwachting zal een groot deel van de vrijgekomen NPs zich ophopen in de bodem, wat leidt tot een toenemende bezorgdheid over de negatieve effecten op de bodemecosystemen. Kennis over het gedrag, de accumulatie en de effecten van NPs in planten is van cruciaal belang voor het begrijpen van de risico's van NPs in het bodemecosysteem. De meeste effect-onderzoeken worden gedaan middels korte blootstelling, meestal met planten in een vroeg groeistadia waarbij de blootstelling via de wortels plaats vindt. Of dit inzage geeft over de lange termijnreacties van planten op NPs is dan een grote vraag. Er zijn weinig studies uitgevoerd naar de impact van gemanipuleerde nanomaterialen op planten via blootstelling van de bovengrondse delen, de zogenaamde blad-contact blootstelling. En dat terwijl de meeste nano-gebaseerde landbouwchemicaliën worden aanbevolen voor gebruik door bladbesproeiing.

Het is bekend dat NPs tijdens de blootstelling dynamische processen ondergaan, zoals aggregatie, sedimentatie en/of oplossen. Hierdoor verandert de effectieve blootstellingsdosis in de loop van de tijd. Desalniettemin rapporteert het merendeel van de gepubliceerde onderzoeksrapporten een experimentele blootstellingsdosis die is verkregen door gebruik te maken van een statische meting van de start concentratie, en waarbij in het beschrijven van de blootstelling van de NM de dynamische veranderingen van de effectieve dosis dus niet worden meegenomen. Het is in dit verband vooral belangrijk om rekening te houden met het feit dat metallische NPs in nano-suspensies langzaam oplossen. Dit leidt tot het gelijktijdig voorkomen van nanodeeltjes en ionische vormen van metalen. Beide vormen zullen aan de toxiciteit bijdragen.. Ondanks talrijke onderzoeken naar de effecten van metallische NM op planten, is het nog steeds onbekend of de toxiciteit afkomstig is van de nanodeeltjes zelf of wordt veroorzaakt door de vrijgekomen ionen. Bovendien is het de vraag of NPs het potentieel hebben zich door de voedselketen te bewegen om daardoor potentie te hebben om in consumenten terecht te komen. In dit proefschrift richten wij ons op het onderzoeken van de toxiciteit en accumulatie van metallische NM in

planten bij langdurige blootstelling, waarbij we de blootstellingsroutes en blootstellingsdynamiek van NPs integreren met het experimenteel bepalen van de opname, translocatie en fytotoxiciteit. Verder onderzochten we de lange-termijn effecten van NPs op de rhizosfeer-bodembacteriële gemeenschap en de mogelijke overdracht en biomagnificatie in de voedselketen.

In hoofdstuk 2 kwantificeerden we de opname, translocatie en biodistributie van Ag en verschillende fytotoxische eindpunten in de sla-plant. Hiervoor werd de sla-plant gedurende 15 dagen bloot gesteld aan AgNPs-suspensies via het blad danwel via de wortel. We ontdekten dat de blootstellingsroute de opname, translocatie en fytotoxiciteit van AgNPs in sla significant beïnvloedt. Blootstelling via de wortel veroorzaakte hogere fytotoxiteit, dan blootstelling via de bladeren. Dit bleek voornamelijk uit de verminderde biomassa van planten, hogere oxidatieve stress, en uit veranderingen van de activiteiten van enzymatische antioxidanten in planten. Ook accumuleerden de planten meer Ag na blootstelling via de wortels in vergelijking met blootstelling via de bovengrondse delen. Interessant is dat de translocatie van Ag in de planten van het blootgestelde deel naar het niet-blootgestelde deel efficiënter is na blootstelling aan het blad dan na blootstelling aan de wortels. Dit was te zien aan de hogere overdracht (transfer)factoren. De verschillen die zijn waargenomen voor blootstelling aan wortels en bladblootstelling zijn waarschijnlijk te wijten aan verschillende mechanismen die verband houden met de opname en translocatie van de nanodeeltjes. Nanodeeltjes kunnen worden opgenomen door stomatale openingen en/of de was-laag die planten beschermt tegen uitdrogen (de cuticula). De deeltjes passeren vervolgens via floëem-laadmechanismen naar andere delen van planten te worden getransporteerd. Voor wortelopname en translocatie moeten nanodeeltjes door de celwanden en de epidermale lagen migreren om verder omhoog te worden getransporteerd via xyleem laadmechanismen.

In hoofdstuk 3 hebben we de impact van vorm, grootte en coating bepaald op het gedrag, de accumulatie en fytotoxiciteit van AgNPs in sla. Hierbij is alleen gekeken naar de blootstelling via de wortels. Ten eerste vonden we dat het oplossen van AgNPs in het plantengroei medium (Hoagland-oplossing) afhankelijk was van de vorm en van de coating van de deeltjes. Het percentage ionen dat vrijkomt uit AgNPs

(ongeveer 30%) was veel hoger dan het percentage ionen dat vrijkwam uit alle geteste Ag-nanodraden (AgNW, <15%). De mate van oplossing en de oplossnelheid van de niet-gecoate AgNW (HAR-AgNW: 39 nm diameter x 8,4 μm lengte) waren beiden hoger in vergelijking met de met PVP gecoate AgNW (LAR-AgNW: 43 nm diameter × 1,8 μm lengte, en MAR-AgNW: 65 nm diameter x 4,4 μm lengte). Bovendien was de tijds-gewogen blootstellingsconcentratie van AgNW 2 tot 4,5 keer die van AgNPs wanneer ze een vergelijkbare vermindering van de biomassa van planten induceerden. Dat geeft aan dat AgNPs meer effect induceren dan AgNW. De opname en translocatie van AgNPs in planten waren ook vormafhankelijk. Blootstelling aan AgNW resulteert in meer Ag-opname door de wortel van planten, maar minder Ag-translocatie naar bovengrondse delen in vergelijking met blootstelling aan AgNPs. Verder waren de fytotoxiciteit, de opnamesnelheidsconstanten en de bioaccumulatiefactoren van het met PVP beklede AgNW (43 nm diameter × 1,8 μm lengte) en het niet-gecoate AgNW (39 nm diameter × 8,4 μm lengte) vergelijkbaar, maar beiden waren hoger dan die van de PVP-gecoate AgNW met de grotere diameter (65 nm diameter x 4,4 μm lengte). De bevindingen impliceren dat de diameter in plaats van de lengte en coating van de AgNW voornamelijk de toxiciteit en de Ag-accumulatie van nanodraden in planten bepaalt. Onze resultaten benadrukken dat de intrinsieke kenmerken van NPs in overweging moeten worden genomen bij het onderzoeken van de interacties tussen metalen NPs en planten.

Gebruikmakend van het respons-additie model hebben we de relatieve bijdrage gekwantificeerd van nanodeeltjesvormen (NPs(deeltje)) en de vrijgekomen ionen (NPs(ion)) aan de algehele fytotoxiciteit van AgNPs-suspensies en Ag-accumulatie in planten. Zoals de resultaten in hoofdstuk 2 en 3 onthullen, beschrijft het Ag-deeltje voor 65% de toxiciteit en Ag-accumulatie in de planten en het opgelost Ag dus 35% ongeacht de vorm, grootte en coating van AgNPs. Echter, de relatieve bijdrage van NPs(deeltje) versus NPs(ion) aan de totale effecten werd beïnvloed door de blootstellingsconcentratie en de mate van oplossen van AgNPs. We ontdekten dat de bijdrage van NPs(ion) aan de algehele effecten in AgNPs met een hoge oplosbaarheid hoger was dan in het geval van AgNW met een lage oplosbaarheid. De verschillen in de bijdragen van de deeltjesvorm en de ion-vorm aan de algehele toxiciteit kunnen worden weerspiegeld door hun verschillende werkingsmechanismen, waarvan is

aangetoond dat de deeltjestoxiciteit afkomstig is van de accumulatie van Ag in planten door interne blokkades, terwijl ionentoxiciteit waarschijnlijk te wijten is aan de inductie van overtollige ROS-productie.

In Hoofdstuk 4 hebben we de kennis over de interactie tussen biota en NPs verder uitgebreid door de oplosdynamiek (de opgeloste Ag-concentraties bepaald als de DTPA-extraheerbare Ag-concentraties) en accumulatie van AgNPs te onderzoeken middels een microkosmos bestaande uit een bodem-sla- -rhizosfeer-bacteriegemeenschap.. Onze resultaten lieten zien dat de extraheerbaarheid van Ag in bodem waaraan AgNPs waren toegevoegd, concentratie-afhankelijk was en in de loop van de tijd ook nog eens veranderde als gevolg van het continu oplossen en de continue opname van AgNPs door de planten. Bovendien toonden de resultaten aan, gebruikmakend van een Spearman-correlatie, dat de hoeveelheid Ag die zich ophoopte in de plantenwortel en de scheuten positief gecorreleerd was met de hoeveelheid DTPA-extraheerbaar Ag in de grond. Deze resultaten tonen de belangrijke rol van het oplossen van AgNPs in de bodem bij het beïnvloeden van hun biologische beschikbaarheid. Bovendien bleken de veranderingen in de structuur en samenstelling van de bacteriële gemeenschap in de rhizosfeer tijdsafhankelijk te zijn. Voor de korte-termijn blootstelling (7d) hebben we geen significante impact van AgNPs op de bacteriële gemeenschap van de rhizosfeer waargenomen, ongeacht de blootstellingsconcentratie. Echter, na langdurige blootstelling (63 dagen) aan 50 mg/kg AgNPs was de bacteriële gemeenschap veranderd ten opzichte van de controle gemeenschap; in totaal werden 16 significant veranderde taxa waargenomen. De veranderingen in de rhizosfeer-bodembacteriële gemeenschap waren mogelijk geassocieerd met de abondance-veranderingen in de bacteriegroepen die verband houden met element (bijvoorbeeld N en S) cycli en stresstolerantie.

In hoofdstuk 5 hebben we de trofische overdracht van AgNPs en TiO_2NPs en hun combinatie onderzocht. Hiervoor is sla blootgesteld en gevoerd aan slakken. We ontdekten dat zowel Ag als Ti konden worden overgedragen van slabladeren naar slakken met trofische overdrachtsfactoren van 0,2 tot 1,1 voor Ag en 3,8 tot 47 voor Ti wanneer sla werd blootgesteld aan Ag^+/AgNPs of TiO_2NP via de wortel. Ag in de vorm van het ion wordt gemakkelijker geassimileerd en verplaatst naar andere

organen van slakken dan de deeltjesvorm. Het grootste deel van het geassimileerde Ag werd door de slakken uitgescheiden via feces. Rond de 70 % van het aanwezige Ti werd terug gemeten in de spijsverteringsklier van slakken. De gedragsreacties van slakken op de trofische overdracht van AgNP en TiO_2NP verschilden. Behandeling van slakken met bladeren die met TiO_2NPs waren opgeladen had een sterke invloed op de uitscheiding van hun feces, terwijl AgNPs de voortbewegingsactiviteit van de slakken sterk beïnvloedde. De gelijktijdige toepassing van AgNP en TiO_2NP had geen invloed op de bioaccumulatie en biodistributiepatronen van Ag of Ti in slakken in vergelijking met de enkelvoudige blootstellingen. De mengsel blootstelling induceerde echter een sterkere remming van de groei en activiteit van slakken dan in het geval van toepassing van AgNP's of TiO_2NP alleen. Onze resultaten verbeteren het begrip van de trofische overdracht van het mengsel van metalen NPs binnen terrestrische voedselketens. Dit is uiterst waardevol voor het beoordelen van hun mogelijke risico's voor het milieu en de gezondheid van ecosystemen.

Concluderend bevordert de in dit proefschrift beschreven nieuwe kennis het begrip in 1) de verschillen in accumulatie en fytotoxiciteit van AgNPs via blad-contact blootstelling en wortelblootstelling; 2) de kenmerken van AgNPs die het lot, biologische beschikbaarheid en fytotoxiciteit van deze deeltjes domineren; 3) welke vormen van Ag in suspensies van AgNPs een invloed uitoefenen op groene bladplanten en de verschillende werkingsmechanismen van deeltjesvormig en ionisch Ag bij het induceren van fytotoxiciteit; 4) de lange-termijn effecten van de oplossingsdynamiek van AgNP op Ag-accumulatie in planten en effecten op de bacteriegemeenschap in de rhizosfeer; 5) de mogelijkheid van de overdracht van een mengsel van meerdere NP's via de voedselketen en de bijbehorende potentiële risico's naar organismen van een hoger trofisch niveau. Bovendien benadrukken de resultaten de intrinsieke eigenschappen van de NPs' die hierbij een rol spelen en is duidelijk geworden dat rekening gehouden dient te worden met dynamiek van de blootstelling van planten aan NPs-blootstelling om ook op langere tijdsschalen nauwkeurige beoordeling van hun ecotoxicologische effecten op het bodemecosysteem te kunnen uitvoeren. Over het algemeen verbeteren onze resultaten de kennis over de interacties tussen NPs en terrestrische biota, evenals de beoordeling van de risico's die voortkomen uit de blootstelling van terrestrische

ecosystemen aan NPs. Dergelijke informatie helpt bij de ontwikkeling van "Safe by Design" van NPs, die kunnen helpen om een evenwicht te vinden tussen de toepassingen van nanomaterialen en ongewenste implicaties voor het milieu en voor de landbouw.

结论

随着金属纳米材料商业应用的飞速发展，将不可避免的增加其被释放到环境中的含量，从而引发新的环境污染问题。据估计，释放到环境中的纳米金属颗粒会在土壤中大量累积，因此人们越来越关注纳米金属颗粒可能对土壤生态系统造成的潜在不利影响。研究纳米金属颗粒对植物的影响以及其在植物体内的归趋和富集对于理解纳米金属颗粒在土壤生态系统中的环境行为和风险至关重要。大部分已报道的关于纳米金属颗粒对植物的潜在影响是在植物早期生长阶段通过根系短期暴露进行的，这并不能准确捕捉到植物对纳米金属颗粒的长期反应。尽管大多数纳米农用化学品都推荐通过叶面喷洒施用（依赖于所谓的叶面接触施用，但是极少数的研究报道了叶面暴露于纳米颗粒对植物的影响。众所周知，释放到环境中的纳米金属颗粒可能发生多种动态迁移转化过程（例如溶解，团聚和沉降），这将导致纳米金属颗粒的有效暴露剂量会随时间变化。然而，大多数已发表的研究是基于纳米金属颗粒的静态初始暴露浓度来量化其对植物的效应，而没有考虑这些动态过程对其有效剂量的影响。此外，纳米金属颗粒的溶解会导致颗粒态金属和离子态金属的共存。这些共存的纳米颗粒和释放的离子都可能会对生物群造成影响。目前对于纳米金属材料的毒性是源自纳米粒子本身还是由释放的离子引起的，仍然未知。再者，目前对纳米金属颗粒是否会通过食物链转移给更高级别的消费者知之甚少。在本论文中，我们综合了纳米金属颗粒的暴露途径和暴露动力学，研究了长期暴露情况下纳米金属颗被植物吸收并迁移及其对植物生长的影响，并且我们进一步研究了纳米金属颗粒对根际土壤细菌群落的长期影响以及其在食物链内的潜在转移和生物放大作用。

在第 2 章中，我们将生菜通过其叶面或根暴露于纳米银球悬浮液中 15 天，对比了 银 被植物吸收后在其体内的迁移和生物分布并测定了植物生长的各种毒性指标。我们发现暴露途径显著影响了生菜中纳米银球的吸收、迁移和植物

毒性。通过测定植物生物量，植物体内氧化应激的程度以及酶促抗氧化剂活性的改变，证明了在相同的暴露水平下，根部暴露于 纳米银球比叶面暴露引起更强的植物毒性。此外，在相同暴露水平下，与叶面暴露于纳米银球相比，根部暴露于纳米银球后导致植物积累了更多的银。有趣的是，植物体内银从暴露部分到未暴露部分的迁移在叶面暴露条件下比根暴露的情况更有效。根暴露和叶面暴露于纳米银球后对植物造成的差异可能是由于不同暴露途径下纳米颗粒的吸收和迁移相关的机制不同。 叶面暴露下，纳米颗粒可以通过气孔开口和/或蜡质表皮吸收，然后通过韧皮部加载机制运输到植物的其他部分。对于根暴露，纳米颗粒需要穿过细胞壁和表皮层，并通过木质部加载机制进一步向上运输。

在第 3 章中，我们对比了纳米银线的粒径，长度和涂层对根暴露后生菜中纳米银的归宿、富集和植物毒性的影响。首先，我们发现纳米银线在霍格兰培养基中的溶解与涂层有关。PVP 包覆的纳米银线(43 nm 直径×1.8 μm 长度 和 65 nm 直径×4.4 μm 长度)显著减缓了未包覆的纳米银线(39 nm 直径×8.4 μm 长度)的溶解性能。此外，PVP 包覆的纳米银线(43 nm diameter×1.8 μm 长度)和未包覆的纳米银线(39 nm 直径×8.4 μm 长度)的植物毒性、银的植物吸收速率常数和生物蓄积因子相似，但均高于具有较大直径的包覆的纳米银线 (65 nm 直径×4.4 μm 长度)。这些发现意味着纳米银线的植物毒性及银在植物体内的富集主要与其直径有关而不是长度和涂层。此外，结合第 2 章和第 3 章的结果，我们发现 纳米银颗粒的溶解及其在植物中的吸收、富集和植物毒性还与形状有关。与暴露于纳米银线相比，纳米银球引起的颗粒溶解和植物毒性更强。我们的结果强调，在研究纳米金属颗粒与植物之间的相互作用时，需要考虑纳米材料的不同特征。

根据 RA 模型，我们量化了纳米颗粒($NPs_{(particle)}$)及其释放的金属离子($NPs_{(ion)}$)对观察到的植物毒性及银在植物体内富集的贡献。正如第 2 章和第 3 章所揭

示的那样，无论纳米银颗粒的粒径，涂层以及形状如何，颗粒态银被发现是总体植物毒性和银在植物中积累的主要驱动因子，其贡献在 65%以上。然而，$NPs_{(particle)}$ 和 $NPs_{(ion)}$ 对总体影响的贡献受暴露浓度和 纳米银颗粒溶解程度的影响。随着暴露浓度的增加，溶解的离子态银对纳米银球和纳米银线的总体毒性的贡献显示出增加的趋势。$NPs_{(particle)}$ 和 $NPs_{(ion)}$ 对纳米银颗粒的总体影响的贡献差异可能反映在它们不同的作用模式上，因为颗粒毒性是由植物体内富集的银颗粒通过阻断物质在植物体内的运输引起的，而离子毒性可能是由于诱导了过量的 ROS 在植物体内积累。

在第 4 章中，我们通过研究纳米银颗粒在土壤中的溶解动力学（溶解的银浓度为 DTPA 可提取的银浓度）及其对土壤 - 生菜 - 根际细菌群落组成的微观系统中的影响，进一步拓展了对纳米银颗粒与生物群之间相互作用的理解。我们的研究结果表明，在纳米银颗粒污染的土壤中银的可提取性随暴露浓度的增加而增加，并且由于纳米银颗粒在土壤中的持续溶解和植物对其的吸收而随时间变化。此外， Spearman 相关性的结果表明，银在植物中的积累与土壤中 DTPA 提取的银的含量呈正相关。这些结果强调了纳米银颗粒在土壤中的溶解在影响其整体银生物有效性的重要作用。此外，根际土壤细菌群落结构和组成的变化与纳米银颗粒暴露时间有关。对于短期暴露（7d），无论暴露浓度如何，我们都没有观察到 纳米银颗粒 对根际细菌群落的任何显著影响。然而，长期暴露于 50 mg/kg 纳米银颗粒后（63 天），与对照相比，细菌群落的组成发生了明显变化并且发现了 16 个显著改变的特征分类群。根际土壤细菌群落的变化可能与元素（例如 N 和 S）循环和胁迫耐受性相关的细菌群的丰度变化有关。

在第 5 章中，我们研究了纳米银颗粒，纳米二氧化钛颗粒以及它们的混合物在生菜-蜗牛食物链中的迁移及其对蜗牛的相关影响。我们发现，当生菜通过根部暴露于纳米银或纳米二氧化钛时，银和钛都可以从生菜叶子转移到蜗牛

体内，其中银的营养迁移因子为 0.2-1.1，钛的营养迁移因子为 3.8-47. 离子态的银相比颗粒态的银更容易被蜗牛吸收被转移到其它组织中。此外，在纳米银的处理组中，蜗牛捕获的大部分银是通过粪便排泄的; 而在纳米二氧化钛处理组中，超过 70%的钛分布在蜗牛的消化腺中。再者，纳米银和纳米二氧化钛的食物链迁移对蜗牛造成的影响不同。用纳米银污染的叶子饲养蜗牛严重影响了蜗牛的运动活性，而用纳米二氧化钛污染的叶子饲养蜗牛严重影响了它们的粪便排泄。最后，与单独暴露于纳米银或纳米二氧化钛相比，它们的混合暴露没有改变银或钛在蜗牛中的生物积累和生物分布模式，但是对蜗牛的生长和活动产生了更严重的抑制作用。我们的研究结果提高了对陆地食物链中纳米金属混合物的营养级间迁移的理解，这对于评估它们对环境和生态系统健康可能造成的风险很有价值。

综上所述，本论文中描述的新知识促进了对以下方面的理解：1）纳米银 在叶面和根部暴露后在植物中积累和植物毒性的差异； 2) 决定其归趋、生物利用度和植物毒性的纳米银颗粒 的具体特征； 3) 纳米银悬浮液中主要驱动它们对绿叶植物的影响的银形态； 4) 颗粒态和释放的离子态银在诱导植物毒性方面的不同作用方式； 5）纳米银在土壤中的溶解动力学对银在植物中富集和根际土壤细菌群落的长期影响； 6) 多种 纳米金属颗粒混合物在食物链中转移的可能性，这与更高营养级生物的潜在风险增加有关。此外，本文结果强调了应考虑纳米颗粒的内在特性和纳米颗粒的长时间动态暴露，以准确评估其对土壤生态系统的生态毒理学影响。总的来说，我们的结果提高了关于纳米颗粒与不同陆地生物群相互作用的知识以及纳米颗粒暴露的风险评估。这些信息有助于开发纳米材料的“safe by design”，这有助于平衡纳米材料的应用及其对环境和农业的影响。


Taormina, Sicily, Italy, 2021

Acknowledgments

Time flies, and my four-years PhD journey is about to come to an end. Undoubtedly, it was challenging but I fulfilled the task of finalizing this thesis. The skills I learned in the past four years will benefit me during the rest of my academic career and make me more confident to continue upcoming research projects independently. No matter what research I will do in the future, I will never forget these years of being accompanied by nanomaterials in Leiden.

I want to pay tribute to all the previous scientists and pioneers who have made contributions and sacrifices to the development of science and made the world more wonderful. I would also like to extend my deep gratitude to all those who have offered me a lot of help and support in the process of finalizing my thesis. First and foremost, my sincere gratitude and appreciation to my Promotors Prof. Dr. Willie Peijnenburg and Prof. Dr. Martina Vijver for their professional knowledge, patient and valuable guidance, encouragement, inspiration and continuous support of my PhD study. I also would like to thank my other supervisor, Dr. Thijs Bosker for all his contributions of time, energy, advice and inspiration, especially for the guidance on statistics and writing. It is very enjoyable and cheerful to accomplish my PhD under their supervision. Thanks for their support and trust, I had high freedom to do what I really want and what I am interested in. I could not have accomplished the thesis without their help and contributions. I also want to thank my supervisor in my Master's study, Prof. Dr. Zhanqiang Fang, who opened the door of the scientific world for me and inspired my interests in science.

I am grateful to the Chinese Scholarship Council for the financial support of my PhD study.

I am grateful to the members of the thesis committee: Prof. dr. A. Tukker, Prof. dr. N. de Voogd, Prof.dr. C.A.M. van Gestel, Prof.dr. S. Bonnet, Dr. K. Trimbos and Dr. Y. Zhai for their time and expertise in reviewing my thesis.

Many thanks to the colleagues from ecotox group, Daniel, Henrik, Marinda, Fazel, Bregje, Tom, Pim, Zhuang, Yujia, Qi, Guiying, Zhenyan, Yuchao for the valuable discussions in Ecotox meetings, and help and suggestions for lab work. I also want to

thank the secretaries and management team, and the PhD-committee for organising different kinds of meetings and workshops. Thanks to my co-authors for their help and suggestions. Thanks to my student Inge van Frankenhuijzen for the help with lab work. Thanks to Riccardo Mancinelli and Emily Didaskalou for sharing the climate room and ordering stuff for my lab work. Thanks to Rudo Verweij and Sipeng Zheng for the help with AAS and ICP-MS measurement. Thanks to my officemates Mingming, Liang, Natalya, Yucaho and Oscar. I would like to express my sincere appreciation to the Chinese Community in CML for their help, company, celebration of Chinese festivals together and traveling together, especially for the help of Beilun and Yi with snails collection.

I always feel really lucky to have so many excellent friends standing by my side all the time. Endless thanks to my chummy friends Qi Yu, Yujia, Guiyin, Zhongxiao, Juan Wang, Di Dong, Jianhong, Feibo, Chen Tang, Weilin, Chunbo, Yi Jin and Yuchao for their help and company in the Netherlands. I really enjoyed the great and deep talks about academics and life with them together, and I received too much care and energy from them. I also want to thank my great friends in China, Pingyi, Hong, Jinzhi, Keying, Ting, Yunqiang and Yi Chen for sharing happiness, success and depression. I know that our friendship will be endless and last forever. Special thanks to Jinbiao for all things those we had been through together. Sometimes, you have to believe your loss is a bless.

Last but not the least, I would like to express my sincere appreciation to my parents and family for their encouragement, unconditional love and support for every decision I have ever made. 感谢爸爸妈妈，外公外婆，爱你们！

感恩所有相遇！

“满怀希望就会所向披靡”

Juan Wu

September 2021, Leiden

Curriculum Vitae

Juan Wu was born on November 07th, 1991 in Yingtan, Jiangxi Province, China. She graduated from No.1 High School of Guixi in 2010. She started her Bachelor study in Environmental Sicence in Yan'an University from 2010 to 2014. Her Bachelor thesis was entitled "The Release of Zn and Mn from spent Zn-C Batteries by Using Ultrasound-assisted bioleaching". She continued her Master study in Environmental Science and Engineering in South China Normal University from 2014 to 2017 and was awarded the National Scholarship (1 %). During this period, she was supervised by Prof. Zhanqiang Fang. Her Master thesis was focused on "The effects of biochar-supported Ni/Fe particles on removal mechanism and bioavailability of PBDEs in contaminated soil and the related phytotoxicity". During her master study, she presented her research findings in the 11th and 12th International Symposium on POPs in Xi'an and Wuhan, and registered a patent named "The prepared methods of biochar-supported Ni/Fe composite particles and its in situ application to remedy polybrominated diphenyl ether contaminated soil". After her Master study, she was granted a scholarship by the Chinese Scholarship Council for a PhD study project, and started her PhD study in the Institute of Environmental Sciences in Leiden University in 2017 under the supervision of Prof. dr. Willie Peijnenburg, Prof. dr. Martina Vijver and Dr. Thijs Bosker. Her PhD research focused on the ecotoxicological impacts of metallic nanoparticles, with specific aims on the fate, accumulation and impact of nanoparticles in plants and the follow-up food chain transfer. During her PhD study, she presented her research in the Anniversary symposium of MilieuChemTox in Utrecht and supervised MSc student.

Publication list

1. **Wu, J.**; Bosker, T.; Vijver, M. G.; Peijnenburg, W. J. G. M (2021). Trophic transfer and toxicity of (mixtures of) Ag and TiO2 nanoparticles in the lettuce - terrestrial snails food chain. ***Environmental Science & Technology.*** In revision.

2. **Wu, J.**; Zhai, Y.; Liu, G.; Bosker, T.; Vijver, M. G.; Peijnenburg, W. J. G. M. (2021). The dissolution dynamics and accumulation of AgNPs in a microcosm consisting of soil -lettuce - rhizosphere bacterial community. ***ACS Sustainable Chemistry & Engineering.*** Accepted

3. **Wu, J.**; Zhai, Y.; Abdolahpur Monikh, F.; Arenas-Lago, D.; Grillo, R.; Vijver, M. G.; Peijnenburg, W. J. G. M. (2021). The differences between the effects of a nano-formulation and a conventional form of atrazine to lettuce: Physiological responses, defense mechanisms and nutrient displacement. ***Journal of Agricultural and Food Chemistry.*** Accepted, DOI: 10.1021/acs.jafc.1c01382.

4. **Wu, J.**; Yu, Q.; Bosker, T.; Vijver, M. G.; Peijnenburg, W. J. G. M. (2020). Quantifying the Relative Contribution of Particulate versus Dissolved Silver to Toxicity and Uptake Kinetics of Silver Nanowires in Lettuce: Impact of Size and Coating. ***Nanotoxicology.*** 14 (10), 1399–1414.

5. **Wu, J.**; Wang, G.; Vijver, M. G.; Bosker, T.; Peijnenburg, W. J. G. M. (2020). Foliar versus Root Exposure of AgNPs to Lettuce: Phytotoxicity, Antioxidant Responses and Internal Translocation. ***Environ. Pollut.,*** 261, 114117.

6. **Wu, J.**; Yi, Y.; Fang, Z.; Tsang, E. P. (2018). Effects of Biochar on Phytotoxicity and Translocation of Polybrominated Diphenyl Ethers in Ni/Fe Bimetallic Nanoparticle-Treated Soil. ***Environ. Sci. Pollut. Res.,*** 25 (3), 2570–2579.

7. **Wu, J.**; Yi, Y. Q.; Li, Y. Q.; Fang, Z.; Tsang, E. P. (2016). Excellently Reactive Ni/Fe Bimetallic Catalyst Supported by Biochar for the Remediation of Decabromodiphenyl Contaminated Soil: Reactivity, Mechanism, Pathways and Reducing Secondary Risks. ***Journal of Hazardous Materials,*** 320, 341–349.

8. **Wu, J.**; Xie, Y.; Fang, Z.; Cheng, W.; Tsang, P. E. (2016). Effects of Ni/Fe Bimetallic Nanoparticles on Phytotoxicity and Translocation of Polybrominated Diphenyl Ethers in Contaminated Soil. ***Chemosphere,*** 162, 235–242.

9. Xue, C.*; **Wu, J.***; Wang, K.; Yi, Y.; Fang, Z.; Cheng, W.; Fang, J. (2021). Effects of Different Types of Biochar on the Properties and Reactivity of Nano Zero-Valent Iron in Soil Remediation. ***Front. Environ. Sci. Eng.,*** 155 2021, 15 (5), 1–13.

10. Yi, Y.; **Wu, J.**; Tu, G.; Zhao, D.; Fang, Z.; Tsang, P. E. (2019). The Humic Acid Influenced the Behavior and Reactivity of Ni/Fe Nanoparticles in the Removal of Deca-Brominated Diphenyl Ether from Aqueous Solution. ***Environ. Sci. Pollut. Res.,*** 26 (10), 10136–10147.

11. Yi, Y.; **Wu, J.**; Wei, Y.; Fang, Z.; Gong, Y.; Zhao, D. (2018). Effects of Synthesis Conditions on Characteristics of Ni/Fe Nanoparticles and Their Application for Degradation of Decabrominated Diphenyl Ether. ***Water, Air, Soil Pollut.,*** 2293 2018, 229 (3), 1–10.

12. Qiao, Y.; **Wu, J.**; Xu, Y.; Fang, Z.; Zheng, L.; Cheng, W.; Tsang, E. P.; Fang, J.; Zhao, D. (2017). Remediation of Cadmium in Soil by Biochar-Supported Iron Phosphate Nanoparticles. ***Ecol. Eng.,*** 106, 515–522.

13. Yi, Y.; **Wu, J.**; Wei, Y.; Fang, Z.; Tsang, E. P. (2017). The Key Role of Biochar in the Rapid Removal of Decabromodiphenyl Ether from Aqueous Solution by Biochar-Supported Ni/Fe Bimetallic Nanoparticles. ***J. Nanoparticle Res.,*** 19 (7), 1–15.

14. Yi, Y.; **Wu, J.**; Fang, Z. (2017). Identification Influence Mechanism of Humic Acid in the Degradation of Decabromodiphenyl Ether by the BC@ Ni/Fe Nanoparticles. ***Acta Chimica Sinica -Chinese Edition.,*** 75 (6), 629-636.

15. Zhai, Y.; Abdolahpur Monikh, F.; **Wu, J.**; Grillo, R.; Arenas-Lago, D.; Darbha, G. K.; Vijver, M. G.; Peijnenburg, W. J. G. M. (2020). Interaction between a Nano-Formulation of Atrazine and Rhizosphere Bacterial Communities: Atrazine Degradation and Bacterial Community Alterations. ***Environ. Sci. Nano,*** 7 (11), 3372–3384.

16. Zhang, Z.; Fan, X.; Peijnenburg, W. J. G. M.; Zhang, M.; Sun, L.; Zhai, Y.; Yu, Q.; **Wu, J.**; Lu, T.; Qian, H. (2021). Alteration of Dominant Cyanobacteria in Different Bloom Periods Caused by Abiotic Factors and Species Interactions. ***J. Environ. Sci.,*** 99, 1–9.


Texel, The Netherlands, 2021